NATIONAL COOPERATIVE HIGHWAY RESEARCH PROGRAM

NCHRP Report 370

Performance of Epoxy-Coated Reinforcing Steel in Highway Bridges

Transportation Research Board
National Research Council

NCHRP Report 370

page 14

In the Conclusions, Item 5, the third sentence from the end should read as follows:

Because coating flexibility often varies inversely with this weight loss, coating with a low solvent-extraction weight loss could be brittle to the extent that fabrication of bars before coating, rather than after, becomes necessary.

NATIONAL COOPERATIVE HIGHWAY RESEARCH PROGRAM

Report 370

Performance of Epoxy-Coated Reinforcing Steel in Highway Bridges

KENNETH C. CLEAR
KCC INC.
Boston, VA
and
WILLIAM H. HARTT, JACK McINTYRE,
and SEUNG KYOUNG LEE
Florida Atlantic University
Boca Raton, FL

Subject Areas

Bridges, Other Structures, and Hydraulics and Hydrology
Materials and Construction
Maintenance

Research Sponsored by the American Association of State Highway and Transportation Officials in Cooperation with the Federal Highway Administration

TRANSPORTATION RESEARCH BOARD
NATIONAL RESEARCH COUNCIL

NATIONAL ACADEMY PRESS
Washington, D.C. 1995

NATIONAL COOPERATIVE HIGHWAY RESEARCH PROGRAM

Systematic, well-designed research provides the most effective approach to the solution of many problems facing highway administrators and engineers. Often, highway problems are of local interest and can best be studied by highway departments individually or in cooperation with their state universities and others. However, the accelerating growth of highway transportation develops increasingly complex problems of wide interest to highway authorities. These problems are best studied through a coordinated program of cooperative research.

In recognition of these needs, the highway administrators of the American Association of State Highway and Transportation Officials initiated in 1962 an objective national highway research program employing modern scientific techniques. This program is supported on a continuing basis by funds from participating member states of the Association and it receives the full cooperation and support of the Federal Highway Administration, United States Department of Transportation.

The Transportation Research Board of the National Research Council was requested by the Association to administer the research program because of the Board's recognized objectivity and understanding of modern research practices. The Board is uniquely suited for this purpose as it maintains an extensive committee structure from which authorities on any highway transportation subject may be drawn; it possesses avenues of communications and cooperation with federal, state and local governmental agencies, universities, and industry; its relationship to the National Research Council is an insurance of objectivity; it maintains a full-time research correlation staff of specialists in highway transportation matters to bring the findings of research directly to those who are in a position to use them.

The program is developed on the basis of research needs identified by chief administrators of the highway and transportation departments and by committees of AASHTO. Each year, specific areas of research needs to be included in the program are proposed to the National Research Council and the Board by the American Association of State Highway and Transportation Officials. Research projects to fulfill these needs are defined by the Board, and qualified research agencies are selected from those that have submitted proposals. Administration and surveillance of research contracts are the responsibilities of the National Research Council and the Transportation Research Board.

The needs for highway research are many, and the National Cooperative Highway Research Program can make significant contributions to the solution of highway transportation problems of mutual concern to many responsible groups. The program, however, is intended to complement rather than to substitute for or duplicate other highway research programs.

Note: The Transportation Research Board, the National Research Council, the Federal Highway Administration, the American Association of State Highway and Transportation Officials, and the individual states participating in the National Cooperative Highway Research Program do not endorse products or manufacturers. Trade or manufacturers names appear herein solely because they are considered essential to the object of this report.

NCHRP REPORT 370

Project 10-37 FY'91

ISSN 0077-5614

ISBN 0-309-05370-6

L. C. Catalog Card No. 94-62111

Price $31.00

NOTICE

The project that is the subject of this report was a part of the National Cooperative Highway Research Program conducted by the Transportation Research Board with the approval of the Governing Board of the National Research Council. Such approval reflects the Governing Board's judgment that the program concerned is of national importance and appropriate with respect to both the purposes and resources of the National Research Council.

The members of the technical committee selected to monitor this project and to review this report were chosen for recognized scholarly competence and with due consideration for the balance of disciplines appropriate to the project. The opinions and conclusions expressed or implied are those of the research agency that performed the research, and, while they have been accepted as appropriate by the technical committee, they are not necessarily those of the Transportation Research Board, the National Research Council, the American Association of State Highway and Transportation officials, or the Federal Highway Administration, U.S. Department of Transportation.

Each report is reviewed and accepted for publication by the technical committee according to procedures established and monitored by the Transportation Research Board Executive Committee and the Governing Board of the National Research Council.

Published reports of the

NATIONAL COOPERATIVE HIGHWAY RESEARCH PROGRAM

are available from:

Transportation Research Board
National Research Council
2101 Constitution Avenue, N.W.
Washington, D.C. 20418

Printed in the United States of America

FOREWORD

By Staff
Transportation Research Board

This report describes unsatisfactory corrosion performance of epoxy-coated reinforcing steel and makes recommendations for improvements to current practice and specifications. The research produced a review of the evolution of epoxy-coated reinforcing steel in concrete; commentary on the practices of manufacturing, handling, and installing epoxy-coated reinforcing steel; an assessment of field samples of existing bridges; and laboratory evaluations of testing techniques designed to predict long-term performance. Specification writers and materials, design, and construction engineers concerned with reinforced concrete structures will be interested in the findings from this research.

The highway industry has made extensive use of epoxy-coated reinforcing steel in bridges during the last 15 years. Many states now specify epoxy-coated bars as the preferred protective system to reduce corrosion-induced deterioration in concrete bridge decks. As an extension of the concept, epoxy-coated reinforcing steel has also been used in concrete substructure elements although there are differences in deck and substructure applications, especially in respect to the size of the reinforcing steel and the amount of fabrication (i.e., the amount of bending of the steel bar after the epoxy coating has been applied).

This NCHRP research was prompted because of extensive premature corrosion of epoxy-coated reinforcing steel that had occurred in various substructure members of bridges built in the Florida Keys. Corrosion was initially observed in areas that contained bent reinforcing steel bars, but later it was also found on straight bars. These deteriorating members were in the "splash zone" and, thus, were subjected to salt spray and cycles of wetting and drying. High air and water temperatures also contributed to an adverse environment. In addition, other—albeit isolated and limited—instances of unsatisfactory performance of epoxy-coated reinforcement had been noted. Given these instances, there was a need to examine the potential for corrosion of epoxy-coated reinforcing steel in all highway bridges under a variety of environmental conditions.

Accordingly, the firm Kenneth C. Clear, Inc. and its subcontractor, Florida Atlantic University, were selected by the National Cooperative Highway Research Program to determine the reasons for unsatisfactory corrosion performance of epoxy-coated reinforcing steel, to determine where it has occurred in highway bridges, and to make recommendations for improvements to current practice and specifications. The researchers have reviewed the history of the development, testing, and use of epoxy-coated reinforcement in concrete structures, assessed field samples of existing bridges in various locations in the United States and Canada, developed laboratory and field-testing techniques, and made predictions on the long-term performance of epoxy-coated reinforcement.

The reader should be aware that most of the specimens used in the laboratory evaluations of testing techniques will be maintained by Florida Atlantic University until summer 1996. Although some specimens have been destroyed and the findings included in this report, the NCHRP agreed with the researchers that it would be beneficial to extend the monitoring of the remaining laboratory specimens an additional 2 years.

CONTENTS

ACKNOWLEDGMENTS

The authors express their sincere gratitude to Dr. Qizhong Sheng, Mr. Siva Venugopalan, Mr. Ivan Mathew, Mr. Steve DiMattia, Mr. Paul Clear, and Mr. Sherwood Ellis who are former employees of Kenneth C. Clear, Inc. and to Mr. Peter Clark and Mr. Ron Simmons of Florida Atlantic University for valuable technical assistance in various aspects of this program.

PERFORMANCE OF EPOXY-COATED REINFORCING STEEL IN HIGHWAY BRIDGES

SUMMARY

Specification of epoxy-coated reinforcing steel (ECR) has for most of the last two decades been the fundamental means of corrosion control in the design of new concrete transportation structures that experience marine or deicing salt exposure. The reporting of corrosion-induced concrete deterioration of ECR bridge substructures in the Florida Keys in 1986 only 6 years after construction provided an initial indication that the long-term protection provided by this material may be less than was intended, and other instances of failure have since been documented. Within this context, the present project was undertaken to identify the cause(s) of unsatisfactory ECR performance and where it has occurred, and to make recommendations for improvements to current practice and specifications that deal with this technology.

It was found that the quality of the epoxy coatings on reinforcing steel is often inadequate in preventing corrosion promotors from migrating to the underlying steel surface. Also, the coatings can contain defects from the original manufacture and from subsequent handling; and the corrosion that begins at these sites spreads underneath the coating with time. This eventually leads to cracking and spalling of the concrete cover. The problem is compounded by the finding that existing specifications and standards pertaining to ECR are based on quality hallmarks that are not necessarily service performance based. A testing methodology termed AC Resistance Measurement was developed for assessing the quality of in-place bars at the construction site. However, because in most instances the quality of these bars is inadequate, it was concluded that epoxy-coated reinforcing steel technology, as this is presently being practiced, cannot be relied upon to provide long-term (50-plus years) corrosion protection to salt-contaminated concrete transportation structures. It is recommended that one or more alternative corrosion protection techniques be employed either in lieu of or in concert with ECR until that time when the long-term corrosion protection performance afforded by this material can be better assured.

CHAPTER 1

INTRODUCTION AND RESEARCH APPROACH

INTRODUCTION

Corrosion of steel in concrete has evolved over the past two decades to become the single most costly problem of its kind in the United States. Consequently, Federal Highway Administration (FHWA), National Institute of Standards and Technology (NIST), Concrete Reinforcing Steel Institute (CRSI), American Association of State Highway and Transportation Officials (AASHTO), American Society for Testing and Materials (ASTM), National Association of County Engineers (NACE) International, American Concrete Institute (ACI), and state transportation agencies have ongoing activities to reduce and eliminate damage to structures from this cause. Early research by NIST (*1*) and FHWA (*2*) indicated that, for the time frame of the experiments and the conditions studied, powdered epoxy-coated reinforcing steel (ECR) performed well in salt-contaminated concrete; and based upon these results, the North American highway community has made extensive use of epoxy-coated reinforcing steel in bridges during the past 15-plus years.

The first indication that there may be problems with the long-term protection afforded to steel in concrete by epoxy coatings arose in connection with deterioration of various substructure members of bridges in the Florida Keys that were built approximately 13 years ago and that exhibited initial distress after only 6 years (*3–6*). Corrosion was initially observed in areas that contained fabricated (bent) steel reinforcing bars, but eventually straight ECRs were found to be deteriorated also. These members are located in the "splash zone" and, thus, are subjected to salt spray and cycles of wetting and drying. Relatively high air and water temperatures also contribute to the adverse nature of the environment. Other instances of unsatisfactory performance of ECR have also been reported (*7*).

RESEARCH OBJECTIVE

NCHRP Project 10-37 was developed as a consequence of the premature failure of the epoxy-coated reinforcing steel substructure members in the Florida Keys, as noted above, and other occurrences, which have raised questions regarding the degree of long-term corrosion protection that is afforded to steel in concrete by this methodology. A large body of information is available regarding the science and technology of epoxy coatings; however, this has not been thoroughly adapted and applied in the case of corrosion protection for reinforcing steel and concrete construction. Specifically lacking are performance-based qualification and quality control tests that can be correlated with long-term service performance. The objectives of this research, predicated upon these points, are 1) to determine the reasons for unsatisfactory corrosion performance of epoxy-coated reinforcing steel, where this has occurred in highway bridges and 2) to make recommendations for improvements to current practice and specifications that deal with this technology.

RESEARCH APPROACH

The approach of the present program was to integrate expertise from the disciplines of 1) coating science and technology, 2) corrosion science and engineering, and 3) concrete and concrete highway construction and, using innovative yet proven experimental methodologies, to focus on questions associated with long-term corrosion protection afforded to concrete structures by epoxy-coated reinforcing steel. Also, it was intended that this effort complement and build upon ongoing and recently completed studies in this field (*7,8*) rather than duplicate them. Accomplishment of this has been based on the following tasks:

1. Task 1: State-of-knowledge definition and critical interpretation.
2. Task 2: Identification and development of techniques for evaluation of epoxy-coated reinforcing steel a) during production, b) at the construction site prior to concrete placement, c) in an existing structure, and d) based on samples obtained from structures and returned to the laboratory.
3. Task 3: Development of a work plan based on Tasks 1 and 2 that represents the best opportunity for accomplishing the project objectives.
4. Task 4: Performance of the Task 3 work plan, once approved.
5. Task 5: Preparation and submission of the final report.

CHAPTER 2

FINDINGS

STATE-OF-KNOWLEDGE DEFINITION AND CRITICAL INTERPRETATION

In the period leading up to this research, the instances where epoxy-coated reinforcing steel (ECR) had not performed satisfactorily were considered by many technical persons involved in this field to be isolated and attributable to some undefined variance or variances as may occur in any large construction project. This situation has changed dramatically during the $2\frac{1}{2}$ years that the present research has been ongoing (May 1991–January 1994) to the point where concerns and reservations regarding the ability of ECR to afford long-term corrosion protection to concrete structures—that is, to provide repair-free service for the design life (50-plus years)—now exist in the technical community. In addition to the examples cited above (*3–6*), these concerns and reservations have been based on 1) reexamination of specimens and test slabs from the early FHWA research programs, 2) evaluation of ECR samples acquired from field structures, and 3) results of recently completed research programs (*8,9*). However, the situation remains highly controversial with ECR proponents noting that no distress is apparent for many in-place structures and detractors contending that the epoxy coating on the reinforcing steel within these has at least partially debonded and, as such, does not provide the necessary corrosion protection and that extensive corrosion will result when a critical concentration of chlorides reaches the steel depth. As a consequence, the various parties involved—including producers and fabricators, trade organizations, professional societies involved with standards and recommended practices, and owners—are posing the following questions:

1. Does ECR provide long-term protection to steel in salt-contaminated concrete?
2. If ECR does provide long-term protection, what quality control improvements are required to eliminate those instances of corrosion damage which have occurred?
3. If ECR does not provide long-term protection, what practical quality improvements can be affected so that it will?

An inherent difficulty arises in any attempt to answer these questions, however, because there presently exists no accepted procedure for projecting long-term ECR performance based either on coating parameters (thickness and defect density, for example) or results from laboratory experiments or test yard exposures. Based on the critical literature evaluation that was performed during the initial phase of this project (see APPENDIX A), it was concluded that ECR technology, as practiced, cannot be relied on to provide long-term corrosion protection in corrosive environments such as may arise from application of deicing salts or marine exposure or both.

IDENTIFICATION AND DEVELOPMENT OF TECHNIQUES FOR EVALUATION OF EPOXY-COATED REINFORCING STEEL

Findings that contributed to accomplishment of Task 2 objectives were in most instances related to results from experimentation performed as a part of the Task 4 research. In this regard, the conduct of these two tasks was complementary and overlapping.

Epoxy-coated reinforcing steel specimens used in the laboratory portion of this study were from bar stock that was acquired from 11 different sources, three of which were foreign (United Kingdom, Germany, and Japan) and the remainder from North America. The coating for these was from four different suppliers with three different modifications being represented in one case. The bars were provided to the research team directly from the coating plant in all but one instance (the source T-bars), and shipment involved special packaging to avoid coating damage. As such, the bars were not subjected to potential distress that can arise from normal handling, storage, transportation, and placement practices. As will become apparent subsequently, these bars were of higher quality than if they had also experienced handling, transportation, storage, and placement practices that are typical of highway construction. The quantity and time of receipt of bars from the 11 sources were such that the testing of some was limited. This is reflected by the fact that none of the data comparisons presented herein include specimens from all sources.

Testing During Production

This facet of the program focused on incorporation of state-of-the-art corrosion science and coating science experimental techniques into the research. This approach is exemplified by the use of Electrochemical Impedance Spectroscopy (EIS) as a procedure for assessing coating quality and deterioration processes, in fact, this technology served as the cornerstone of present activities in these categories. As used here, EIS involved measuring the impedance of ECR specimens as a function of frequency of an alternating current electrical signal input and relating this impedance to coating properties. A tutorial, which provides background information regarding EIS and its interpre-

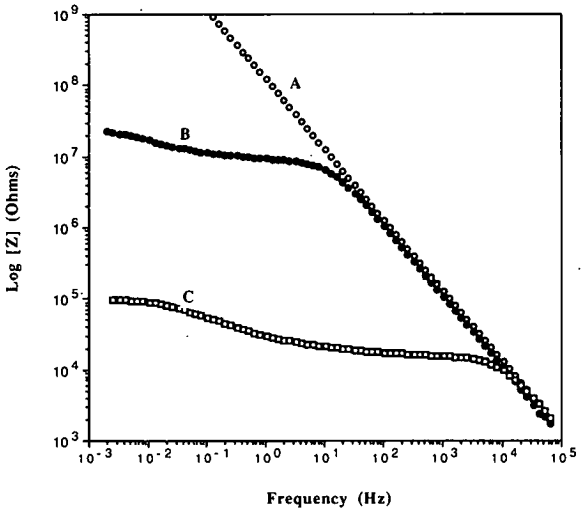

Figure 1. Typical EIS responses.

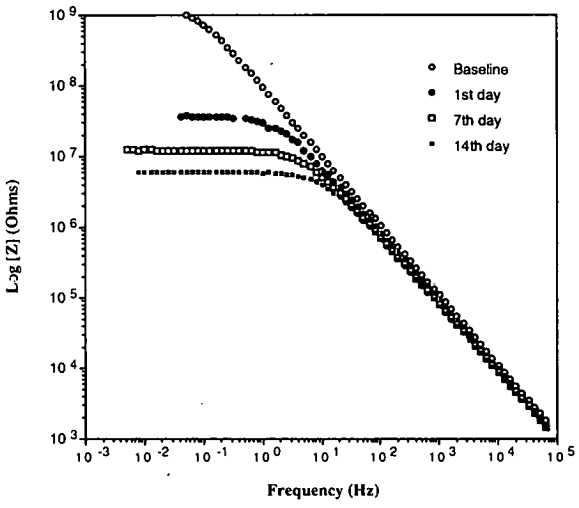

Figure 2. Example of change of EIS scans during distilled hot water test.

tation, is presented as APPENDIX B. Figure 1 schematically illustrates the results of several EIS scans as plots of impedance magnitude versus frequency (logarithmic coordinates). The curve labeled "A" is termed purely capacitive behavior and is indicative of a high-quality coating with no defects. The scans labeled "B" and "C," on the other hand, are indicative of intermediate and poor coating quality, respectively, in association with either coating defects or conductive paths through the coating, or both. These three scans could represent three different ECR specimens or the same specimen after three different exposure times. EIS instrumentation is relatively sophisticated and expensive, and data interpretation is complex. Consequently, the methodology involved must be simplified for field or in-plant applications so that it is useable by technical level individuals. How this can best be accomplished is addressed elsewhere in this report.

A hot water test (HWT) procedure (see APPENDIX C), which involves exposure of ECR specimens to either distilled water or a salt solution at 80°C with periodic acquisition of EIS data, was determined to be appropriate for in-plant ECR quality assessment. The procedure is also applicable to coating-quality assessment at downstream stages of the bar cycle prior to placement in forms. Figure 2 illustrates typical EIS scans performed upon an ECR specimen at four different times during a HWT and shows that impedance decreased with exposure duration. As projected above, the indicated change with time is indicative either of development of coating defects or of progressive establishment of conductive paths within the coating, or both. It is generally recognized that as long as the test temperature is at least 10°C or so below the glass transition temperature of the coating, as was the case here, the elevated temperature serves only to speed the degradation process and not to alter it. Because most of the impedance decrease occurred during the initial 24 hours of exposure, the time for an in-plant test might realistically be reduced to a single day.

Figure 3 presents 10 EIS scans after 24 hours exposure to distilled water at 80°C for ECR specimens from seven different

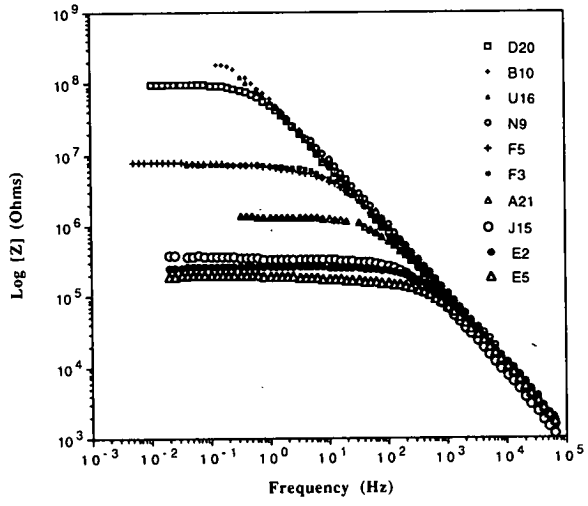

Figure 3. EIS scan plots obtained after 23 hours exposed to distilled water at 80°C.

producers. All of the specimens were initially defect free, as determined by conventional holiday detection, and exhibited purely capacitive EIS behavior. Data for specimens from the other four sources are not presented either because bar quantity limitations precluded testing or because defects on specimens were too numerous to permit preparation of defect free specimens. A range of quality is indicated by the results; for example, specimens from sources B, N, and U exhibited capacitive behavior, whereas the low-frequency impedance for E and J specimens was low. This illustrates that bars from the same source generally showed similar properties, but large differences often were evident between ones from different sources. Bars exhibiting other

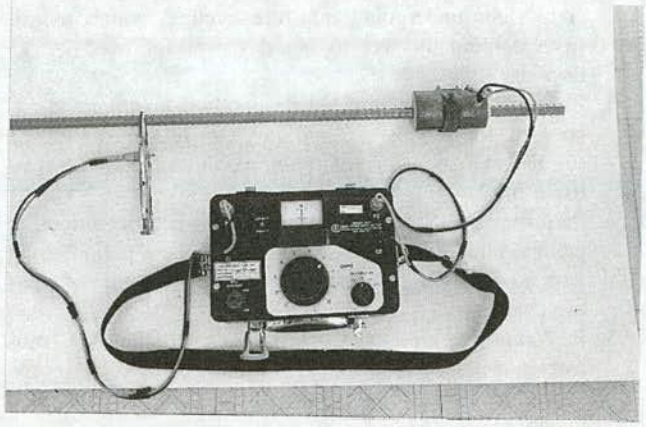

Figure 4. AC resistance equipment and test setup.

than capacitive behavior are unlikely to provide long-term corrosion protection, as explained subsequently.

The hot water test, which is prescribed by the German ECR standard (*10*), was evaluated within the context of the HWT/EIS methodology described above. This standard requires that the ECR coating not exhibit blisters after 7 days of hot distilled water exposure. Such a criterion was determined to lack sufficient sensitivity in its characterization of ECR quality in that it did not identify bars that were considered unlikely to perform satisfactorily in long-term service, as was possible using EIS in conjunction with the hot water soak.

Testing at the Construction Site Prior to Concrete Placement

Work in this area concentrated on the development of new procedures for rapid ECR quality assessment with respect to coating breaks. In this regard, a methodology termed alternating current (ac) resistance testing was developed for application to straight bars after placement and prior to concreting (see APPENDIX D). The procedure draws on past laboratory testing and the theory of EIS impedance measurements. Initial work involved the use of a pair of cylindrical moist sponge electrodes wrapped around the ECR at two different positions and measurement of resistance (impedance) between the electrodes at a frequency of 97.5 Hz. In the absence of significant defects, the measured value for this parameter should be dominated by impedance of the coating. Field tests showed that the procedure was useful but that coating quality could be overestimated when coating defects were present under one probe only. Therefore, the procedure was modified to involve one cylindrical moist sponge electrode only and direct electrical connection to the ECR. This test configuration is shown in Figure 4, and the procedure was determined to expediently provide information on the quality of ECR with respect to coating defects. The procedure can be used at any stage in the ECR life cycle prior to concreting but is particularly appropriate for characterizing bars after placement in forms and prior to concreting. Table 1 provides results from five bridges that were under construction in 1993, where the ratio of ECR-to-bare (uncoated) bar resistance was measured and compared to both visual observations and electrical defect testing. These data were taken on straight and bent bars tied-in-place. By comparing the individual straight bar data it was determined that ECRs with ac resistance ratios in excess of 2,000 corresponded to bars that were free of visible coating defects and that the ac resistance ratio range of 300 to 2,000 represented the transition from poor to good quality coated bars from the standpoint of coating defects. Unfortunately, only about 15 percent of the field ECRs studied exhibited ac resistance ratios in excess of 2,000. A field quality control test method based on this ac resistance measurement procedure is provided in APPENDIX D.

TABLE 1 Field ECR quality with respect to coating breaks

Structure	Percent < 300 AC Resist. Ratio	Percent < 2,000 AC Resist. Ratio	Percent with Coating Breaks	Percent with Visible Damage
Straight Bars:				
East. U.S. #1	45	80	88	83
East. U.S. #2	57	71	71	50
Canadian #1	40	75	70	45
East. U.S. #3	75	100	100	70
East. U.S. #4	90	100	100	95
Bent Bars:				
East U.S. #1	-	-	99	-
East. U.S. #2	-	-	90	-
Canadian #1	-	-	69	-
East. U.S. #3	-	-	97	-
East. U.S. #4	-	-	100	-

Follow-up laboratory development efforts defined an even simpler field quality control test that is applicable to both straight and bent bars. This method, which involves straightforward modifications to a commercially available, portable coating holiday detector, is rapid and of low cost. An audible "beep" results when the coated bars are of unacceptable quality, the latter being defined by calibration of the instrument with ac resistance ratio data. The equipment is pictured in Figure 5, and a test method is presented in APPENDIX D.

Testing in an Existing Structure

Multivector magnetometer instrumentation and procedures were employed in a feasibility study (see APPENDIX E) to assess if this technology, which is based on measurement of the magnetic field associated with an electrical (corrosion) current, can be used to detect ongoing corrosion upon ECR in concrete. The technique has been used successfully in the past to characterize corrosion on coated buried pipelines. The results were positive in that corrosion activity in laboratory-prepared concrete specimens that contained ECR with intentional coating defects was identified. Additional research is required, however, to modify the sensor coils from what is appropriate for buried pipeline dimensions to that which is optimum for ECR in concrete.

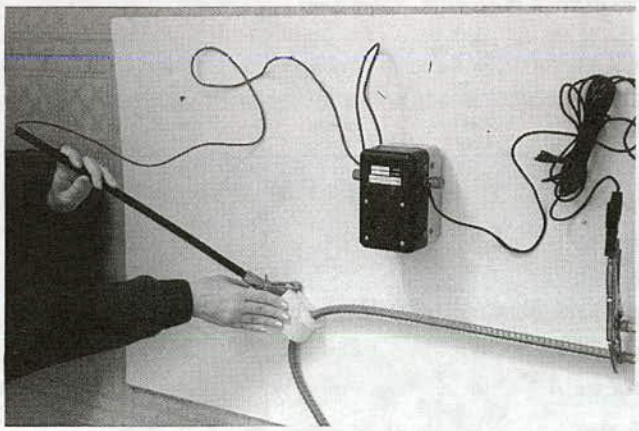

Figure 5. Modified holiday detector equipment and test setup for bent bars.

Testing Based on Samples Obtained from the Structure and Returned to the Laboratory

Procedures for detailed study of ECRs have been improved in recent years in response to the need to further study bar samples from field structures (*8,9*). Tests available include 1) coating hardness (pencil method); 2) coating thickness (magnetic gage and microscopic evaluation); 3) coating foam and underfilm contamination (microscopic analyses); 4) documentation of visibly mashed (reduced coating thickness) and bare areas; 5) reinforcing steel surface condition and anchor pattern determinations; 6) coating "knife" adhesion; 7) ECR laboratory ac resistance testing; 8) accelerated corrosion testing or ACT (*11*); and 9) chemical immersion testing (CIT). Completed and blank sample sheets for these tests are included as APPENDIX F and methods are described in Reference 9.

DEVELOPMENT OF A WORK PLAN

The approved work plan, which was submitted and approved in general accordance with the project timetable, consisted of the following sub-tasks: 1) Continuation of the HWT/EIS/adhesion testing and research that had been a part of Task 2. 2) Evaluation of epoxy-coated reinforcement from foreign sources. 3) Evaluation of the effect of exposure environment on performance of epoxy-coated reinforcement. 4) Evaluation of epoxy-coated reinforcement in the field.

Performance of the Work Plan

Activities in the first three categories listed above (Nos. 1-3) were performed in an integrated fashion and consisted of the following:

1. Obtaining and characterizing ECR from a total of 11 different producers, as described above.
2. Performing exposure tests on ECR specimens in a) distilled water and salt solutions at 80°C (described above); b) distilled water and salt solutions at ambient temperature (chemical immersion tests); and c) natural weathering concrete slabs undergoing moisture cycling, which ranged from continually wet to one-day wet followed by 13 days dry.
3. Exposing ECR specimens outdoors, both covered and uncovered, for periods of 2 and 4 months to simulate jobsite storage and inclusion of these specimens into the tests listed in (2).
4. Performing EIS and coating adhesion determinations at predetermined intervals during the exposure period along with a post test visual and microscopic evaluation of coating condition.
5. Performing Accelerated Corrosion Tests (ACT) and Chemical Immersion Tests (CIT) on bars from each of the sources and comparing results with evaluations conducted under (4).
6. Analyzing data to establish correlations, if possible, between a) initial bar properties, b) accelerated HWT results, c) exposure results for ECR in ambient temperature solutions (CIT), d) outdoor exposure results for ECR in concrete, and e) appearance and properties of ECR samples acquired from the field.

ECR CHARACTERIZATION

The as-received ECRs were characterized with regard to properties of the coating including thickness, defect density, hardness, solvent extraction weight loss and visual appearance with microscopic examination when necessary. It was determined from this that bars from five of the sources did not conform to the applicable specification with regard to defect density (*11*). Further, the coating on bars from two of the sources exhibited such a high defect density—many of which were visually apparent—that attempts to quantitatively characterize these were abandoned. Bars from the remaining six sources conformed to specification (*11*).

Hot Water Tests

Figure 3 presents examples of typical HWT results for bars from seven of the sources, as discussed above. The tests represented by these data involved bars without initially detectable defects, although in some cases defects developed during the test. In over 100 HWTs, only one instance of blistering was found in the case of ECR specimens that did not develop defects. On the other hand, blistering was common for specimens with defects. It is not clear at this time if the accelerated HWT and EIS measurements performed on ECR specimens containing initial defects are capable of distinguishing between good and bad coatings per se. Impedance measurements on these specimens (ones with initial defects) should reflect progression of corrosion at localized (defect) sites. Specimens containing controlled, intentional defects experienced attack at the exposed bare areas, which appeared similar to what occurred at the base of holidays, and the impedance response for these two specimen types (ones with intentional and naturally occurring coating defects) was nearly identical. The reduced impedance with exposure time of specimens without detectable defects is attributed to development of conductive pathways in the coating, as noted above. This does not always (or necessarily) portend poor service per-

formance but merely indicates that conductive pathways have developed; however, the presence of such pathways is a required precursor for localized coating breakdown.

Chemical Immersion Tests

For the ambient temperature exposure of ECRs to various solutions, including distilled water plus 3.5 w/o NaCl, simulated pore water and simulated pore water plus KCl, three types of EIS response were observed: (1) unchanged impedance, (2) development of finite coating pore resistance from initially capacitive behavior, and (3) modest impedance reduction with time from an initially intermediate or low impedance value. Figure 6 provides examples of each of these. The behavior illustrated by Figure 6c was consistent with development of holidays or localized rust spots (or both) during testing of an ECR with initially poor coating quality, as revealed by low impedance. The above three response categories are essentially the same as were determined to apply for ECR specimens exposed to the elevated temperature test environments (see Figure 3); however, in the latter case (HWT) less than 24 hours was required for a significant impedance decrease, compared to 2 months or more at ambient temperature. This correlation was noted only when the ECR specimen exhibited capacitive behavior prior to exposure (that is, for cases where the initial quality of the coating was high) and was not evident when bare areas or holidays were present. For the case of ECR with no initially detectable defects, 1 day of hot water exposure was apparently equivalent to 60 to 120 days at ambient temperature, and the EIS response for each was consistent with a common factor (progressive reduction in pore resistance in association with development of conductive pathways) being mostly responsible for the impedance drop with time.

Concrete Test Slabs

The test yard portion of the program involved 152 ECRs from six sources embedded in 76 chloride-contaminated concrete slabs in addition to 12 baseline slabs with bare (uncoated) bars. EIS scans were performed on selected slabs at 0, 4, 6, and 8 months of exposure. Of the ECRs examined after 4 months, 54 (approximately one-third) showed an overall reduction in impedance, while the remainder exhibited a slight to moderate impedance increase. This latter observation is not presently understood; however, buildup of corrosion products, which block active sites or deactivation of corrosion sites because of changes in the local concrete environment, could have been responsible. Figure 7 presents typical impedance plots that exemplify "good," "intermediate," and "poor" coating protectiveness, respectively. Only several of the bars exhibited initially capacitive behavior, which is indicative of a lack of conductive pathways and no coating defects. This suggests either that it is difficult to avoid coating damage in the fabrication of even laboratory concrete specimens or that defects developed early in the program prior to the initial EIS scan. Also, the increased surface area for the concrete slab bars compared to the laboratory test specimens may have been a factor, because the probability of a coating defect being present increases in proportion to surface area. No

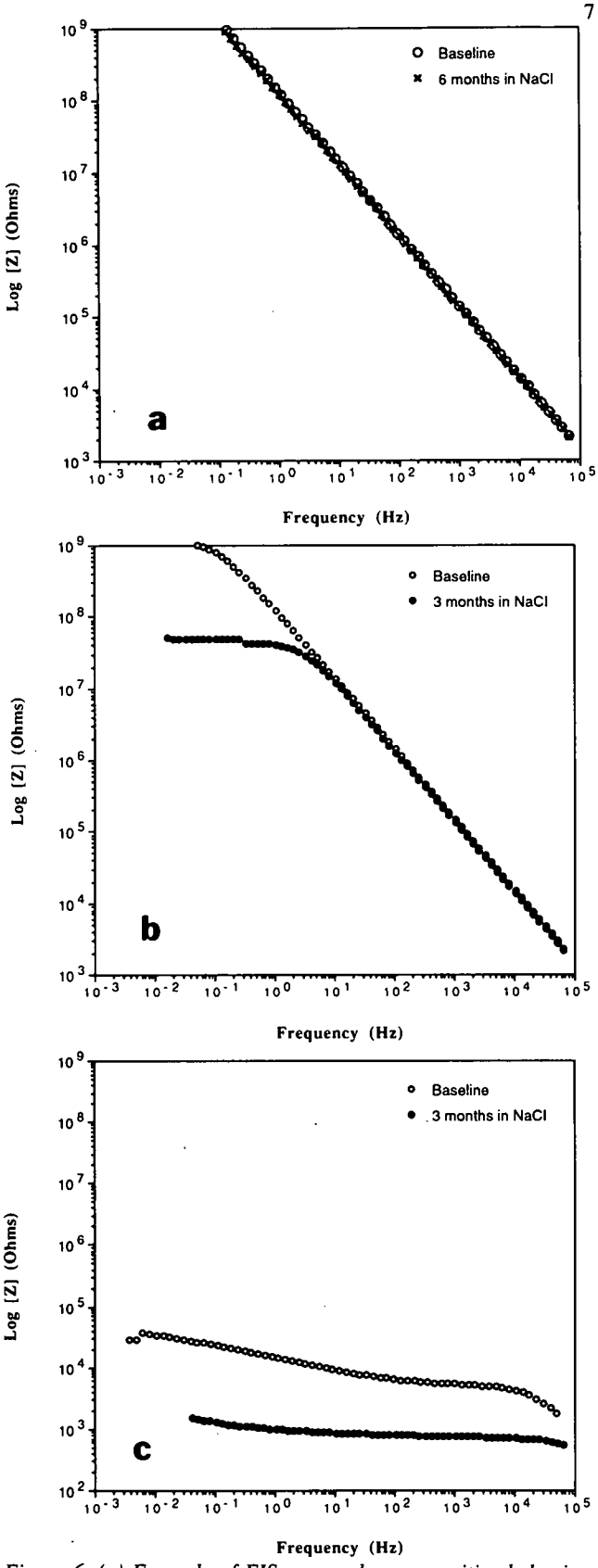

Figure 6. (a) Example of EIS scans where capacitive behavior was retained. (b) Example of an ECR that exhibited reduced pore resistance with exposure time. (c) Example of modest impedance reduction as typically occurred for coatings that were of low initial impedance.

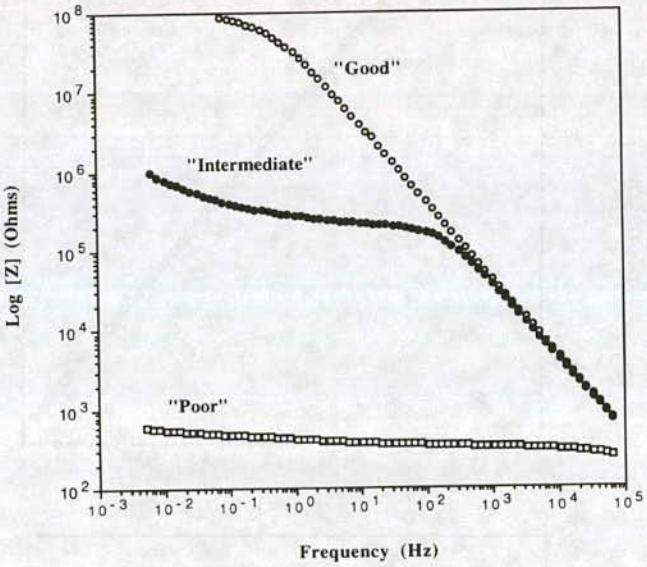

Figure 7. Typical EIS response of ECRs in test slabs.

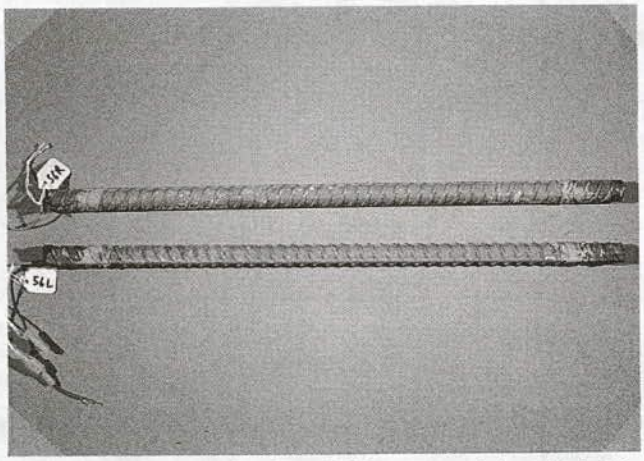

Figure 8. Photograph of two ECRs recovered from Slab 56. ECR (56L), which shows corrosion, exhibited low impedance with high macrocell current (30μA).

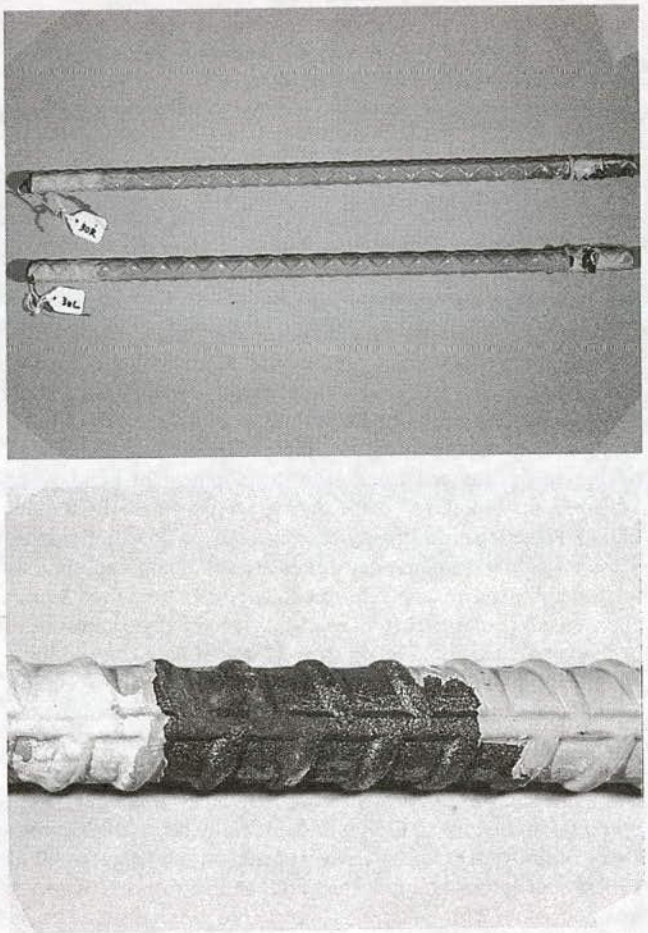

Figure 9. (Top) Photograph of the two ECRs recovered from Slab 30. ECR (30R) performed well with negligible macrocell current and relatively high impedance. (Bottom) Close-up of debonded area of a poorly performed ECR. Bright substrate next to rust area at left indicates cathodic disbondment.

influence of the different wet-dry cycles that were employed on coating response was apparent.

At the end of 10 months exposure, eight of the slabs were autopsied and the bars recovered and examined. Figure 8 is a photograph of a bar from a slab that exhibited relatively low impedance and high macrocell current. Corrosion has progressed on this to a significant degree, particularly when the relatively short exposure duration (10 months) is considered. The general appearance of bars from slabs for which there was little or no indication of corrosion—as suggested by high impedance and low macrocell current—was excellent, as shown by the typical example in Figure 9 (top). Bars with intermediate impedance behavior did not exhibit extensive deterioration; however, one or more defects was present on each of these and in several instances these bars exhibited localized attack at the defect(s) and cathodic disbonding for up to approximately 1 in. (2.5 cm) away from defects. An example of this is illustrated by Figure 9 (bottom). Progressive corrosion beginning at the defect and working its way underneath the coating was apparent. A debonded coating such as this cannot be expected to afford corrosion protection in the long term. A ranking from good to bad of the ECR in the slab specimens according to impedance measurements, macrocell current, and visual appearance was A,D,U > N,J > T. (Note: Because of material quantity limitations on acquisition schedule, slab specimen fabrication included ECR from only 6 of the 11 sources).

There was a general similarity between impedance measurements for each of the three types of exposure with one day of HWT being equivalent to several months of ambient temperature exposure either in an aqueous solution or in chloride contaminated concrete. Comparison of corroded ECR field samples, as reported in reference 9, revealed similarity between the appearance of these and the bar in Figure 8. This is consistent with an identical process(es) having been involved in both instances.

Based on the above findings, it is apparent that in the case of all three types of tests (HWT and ambient temperature exposure

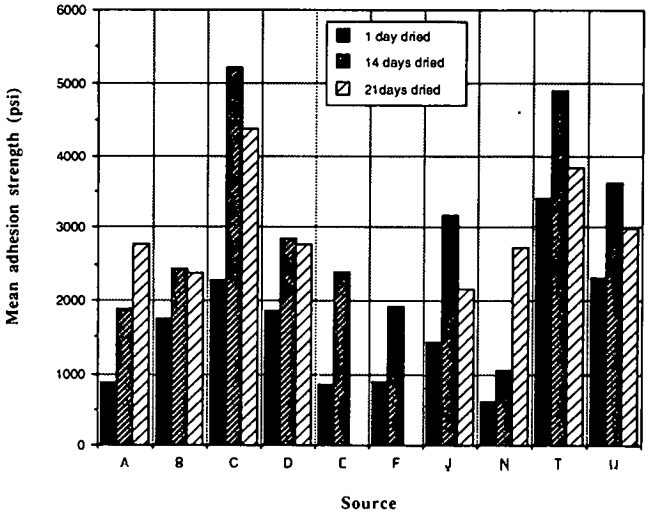

Figure 10. Average adhesion strength of different source ECRs after 14-day 80 C DW HWT.

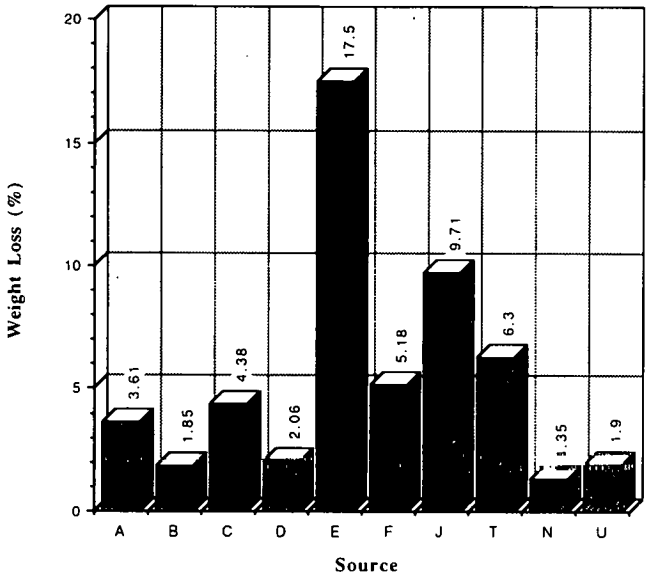

Figure 11. Weight loss of epoxy coatings after 1-week solvent extraction test.

in aqueous solutions and in salty concrete) bars that did not contain defects initially often developed defects during exposure. This indicates that presently practiced defect-detection procedures do not necessarily identify all defects or areas that are potentially predisposed to breakdown.

COATING ADHESION

In addition to the procedures described above, coating adhesion was also measured for the ECR, both as-received and at the termination of the various exposures. In the former case (as-received), the adhesion was sufficiently high for bars from all 11 sources that coatings invariably failed cohesively rather than at the coating-metal interface, and the bond strength could only be estimated as having been greater than 9300 psi (64 MPa). Wet adhesion loss was confirmed to have occurred for each of the three types of exposure, however. Subsequent adhesion strength of the coating apparently depended on, first, the amount of underfilm corrosion that occurred during the exposure period and, second, the drying period, as suggested by Figure 10. (Note: There was inadequate stock available for ECR from one source and so the data here are limited to bars from the remaining 10 sources).

While a correlation was found between HWT/EIS and slab exposure results, as discussed above, the situation with regard to adhesion was not as clear. Thus, specimens from most sources that retained high impedance during exposure also exhibited relatively high adhesion upon post exposure drying. In other instances, however, the opposite was apparent (low impedance but high adhesion); and it was concluded that development of conductive pathways and presence of coating defects did not, in and of itself, preclude good adhesion. Specific aspects of these experiments and results are discussed in detail in APPENDIX H.

ATMOSPHERIC EXPOSURE OF ECR

ECR specimens from two sources were exposed outdoors for periods of 2 and 4 months to simulate job site storage. Some of these bars were shielded from ultraviolet radiation and others unshielded. All exposures were in south Florida — some at a marine site and others several miles inland. Post exposure HWT/EIS and adhesion measurements failed to reveal any indication of coating degradation for specimens exposed for 2 months. Degradation was apparent for bars exposed for 4 months, however, as reflected by reduced adhesion; and holidays and rust spots were evident. Also, the average 0.1 Hz frequency impedance after 2 months was 8×10^8 Ohms, whereas after 4 months it was 2×10^7 Ohms or 40 times lower. The degradation appeared to be independent of exposure site (coastal versus inland). Also, bar appearance and HWT/EIS performance were the same irrespective of whether or not the specimens were shielded from ultraviolet radiation. ECR specimens that were atmospherically exposed for 4 months and subsequently included in the test yard concrete slab specimens exhibited relatively active corrosion potentials and high macrocell currents.

FOREIGN SOURCE ECR

Despite the fact that ECRs from the United Kingdom, Germany, and Japan are fabricated according to a stricter standard, and specialists from these countries consider their bars to be of better quality than U.S. ones, the results of the present HWT, ambient aqueous exposures, and concrete specimen experiments (because of delayed acquisition only one foreign source bar was included in this last class of experiments) did not indicate this to be the case. In general, the quality of these foreign-source ECRs was comparable with the better and intermediate bars from domestic sources. For example, in the ranking according to EIS and adhesion response discussed above, the F and U specimens were foreign sources.

ECR PROPERTIES AND ACCELERATED TEST PERFORMANCE

Figure 11 plots coating weight loss, as determined by the solvent extraction technique, for samples from 10 ECR sources

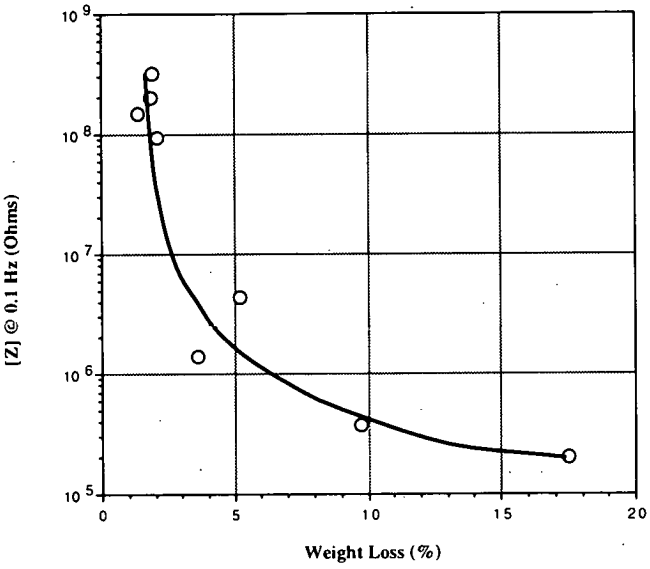

Figure 12. Relationship between solvent-extraction weight loss and [Z] at 0.1 Hz after 1 day in distilled hot water test for ECRs from eight sources.

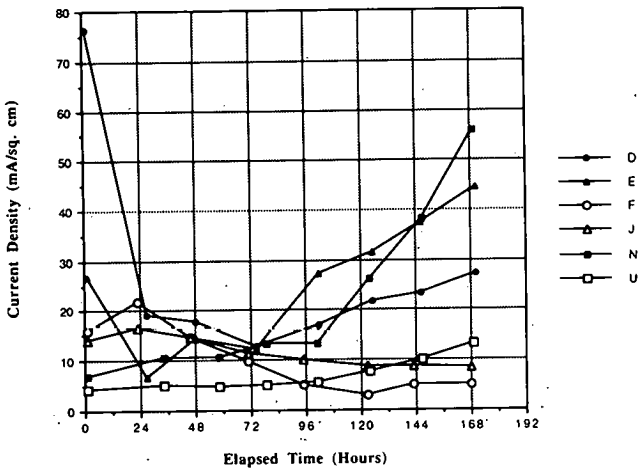

Figure 13. Results of ACT with ECRs from six sources.

and shows that this varied from 1.9 to 17.5 percent. This parameter (coating weight loss) is expected to be proportional to the amount of soluble filler in the coating and to vary inversely with the degree of cure (*12,13*). Thus, the higher the weight loss of a particular coating, the more porous and permeable it is likely to become in service. Correspondingly, Figure 12 plots 24-hour impedance magnitude (frequency 0.1 Hz) for the experiments represented in Figure 3 as a function of solvent extraction weight loss and shows an inverse proportionality between the two. This result is consistent with the fact that conductive pathways are more likely to develop in coatings containing relatively high amounts of soluble, unpolmerized components that dissolve upon exposure or ones with a lesser degree of cure (or both). A possible source of scatter for the data in Figure 12 is development of coating defects during the HWT. This would contribute to reduced impedance but, of course, would not influence coating weight loss. Little, if any correlation was disclosed between accelerated test results and any of the other bar or coating properties that were evaluated (coating thickness and uniformity, hardness, defect density, type of deformations, and visual and microscopic appearance).

ACCELERATED CORROSION TEST

Figure 13 presents current density versus time data for Accelerated Corrosion Testing (ACT) that was performed on bars from six sources (see APPENDIX G for methodology). The relative performance ranking for these (best to worst based on measured current density) was F > U > J > D > N > E. Comparison with results from the HWT and slab exposures (Table 2) reveals a general lack of correlation. Thus, some bars that exhibited either high adhesion or high impedance (or both) performed poorly in the ACT and visa versa. Also, there was no correlation in this test between current density and the extent of coating delamination at either the anode or the cathode (see also APPENDIX H).

TABLE 2a Ranking of ECR sources in different types of tests

Type of Test	Ranking		
	Good	Intermediate	Poor
DW HWT/EIS (Capacitive)	U, D, B, N	> F, A >	J, E
DW HWT/EIS (As received)	U, B, N > D > F > A > J, E > T, C		
Concrete Slabs	A, D, U	> N, J >	T
ACT	F > U > J > D > N > E		

TABLE 2b Evaluation of each ECR source in different types of tests

Source	Ranking			
	DW HWT/EIS (Capacitive)	DW HWT/EIS (As received)	Concrete Slabs	ACT
A	I	I	G	G
B	G	G	-	G
C	-	P	-	-
D	G	G/I	G	I/P
E	P	P/I	-	P
F	I	I	-	G/I
J	P	P/I	I	I
N	G	G	I	P
T	-	P	P	-
U	G	G	G	I

* Note: G; Good
I; Intermediate
P; Poor

CHAPTER 3

INTERPRETATION, APPRAISAL, AND APPLICATION

INTERPRETATION

The quality of the ECR that was acquired and employed in this research was highly variable and, depending upon source or, presumably, production variables at a particular source, did not necessarily conform to the applicable specifications. Nonetheless, the quality of most, if not all, of these bars was determined to be better than what is invariably being realized as an in-place product for highway construction. Failure to meet specification does not, in and of itself, mean that ECR will not provide corrosion protection in service. Alternately, that ECR conforms to existing specifications does not guarantee good corrosion protection, since these standards are not performance based. Bars from the foreign sources investigated did not offer any particular advantage over domestically produced ones that were of relatively good quality (that is, those without defects and which exhibited initially capacitive EIS behavior). Also, no distinction was apparent among the four different types of coating that were represented; however, because of the lack of control of coating application variables, this does not necessarily mean that differences did not exist.

Two aspects of ECR, the protectiveness of the coating per se and the ability of the coating to maintain protection in the presence of defects, are projected as important with regard to long-term corrosion performance. Identification of solvent extraction weight loss as the coating property with which accelerated test and concrete exposure results best correlated is considered an important step toward understanding the cause-effect aspect of coating performance. Coating weight loss as determined by solvent extraction should, in turn, be determined by the formulation and by the temperature-time history during application. Some bars in the present study that exhibited initially capacitive behavior, as determined by EIS, and did not contain coating defects performed well in all phases of the test program (HWT, ambient temperature aqueous exposures and chloride contaminated concrete exposures), whereas others developed coating defects and corrosion in association with these defects during testing. The former have the potential for providing good corrosion resistance in service, but the latter do not. Bars with low initial impedance or with defects invariably performed poorly during these same exposures; and it was concluded that these also are likely to perform poorly in service. This is of particular significance in view of the finding that only 15 percent of the in-place ECRs on the five bridges being built in 1993, which were examined as a part of the field portion of this study, exhibited ac resistance ratios in excess of 2,000 (indicative of a coating with an acceptably low density and/or size of defects) and 60 percent had ratios below 300 (indicative of a poor quality coating). Holiday detection according to procedures that are commonly practiced in industry either did not reveal all coating defects or did not disclose sites that were predisposed for breakdown, or both.

The mechanism whereby ECR specimens fail invariably involves underfilm corrosion as a consequence of migration of reactants (water and oxygen and, to a lesser extent, chlorides) through the concrete and coating to the steel substrate. This, in turn, is facilitated by the presence of conductive pathways within the coating, as influenced by the degree of cross-linking and, perhaps, dissolution of soluble fillers. Any factor that reduces reactant transport distance, such as presence of burrs on the steel prior to coating thickness, either locally or globally, may reduce the initiation time for underfilm corrosion. Adhesion loss, as has been noted for ECR samples acquired from bridge structures (*9*), is indicative of water having migrated through the coating. In addition to the above, when coating defects are present, loss of protection is enhanced by cathodic disbondment in association with anodic activity at the defect, the latter occurring once a critical chloride concentration is reached and by production of hydroxides at cathodic sites along the coating-metal interface which leads to irreversible adhesion loss. The underfilm corrosion cell that results from either cathodic disbondment or wet adhesion loss serves essentially as a crevice and promotes electrolyte acidification and enhanced corrosion rates according to established mechanisms (*14*).

Any specification or accelerated test that is to accurately project service performance of ECR must be based on and address how the above processes (migration of reactants through the coating, disbondment of the coating, and resultant underfilm corrosion) are influenced by coating and bar properties. In the present study, the 24-hour HWT impedance of ECR specimens without initial coating defects varied inversely with solvent extraction weight loss of the coating (Figure 12), and this same impedance correlated also with ECR performance to-date of the chloride-contaminated concrete slabs (Table 2) in instances where this comparison could be made. Once longer-term data are available from the concrete specimens, development of a quantitative ECR property-accelerated test performance-concrete exposure performance relationship should be possible.

The observation that cathodic disbondment occurred at defects in poor and intermediate coatings implies that this process plays an important role in ECR deterioration. The occurrence of cathodic disbondment creates the opportunity for underfilm corrosion, as explained above. Consequently, if long-term corrosion protection is to be afforded to ECR in salt contaminated concrete, the coating must remain defect free or be capable of resisting cathodic disbondment in the presence of defects.

Presently the Accelerated Corrosion Test (ACT) and the Chemical Immersion Test (CIT) are prescribed (*11*) as methods

for ECR quality assessment. The latter procedure was incorporated into the present program via the ambient temperature aqueous exposures, and on the basis of the good correlations that were found between results of these and those for the HWT and the chloride contaminated concrete exposures, it was concluded that the CIT reflected service-relevant ECR failure processes. However, because this test lasts a minimum of 45 days, it is not appropriate as a short-term quality control measure. Also, the acceptance criteria based on the CIT, as presently stated, are subjective and bear no known correlation with service performance. It was concluded that the ACT does not adequately represent the coating failure mechanism(s) such as wet adhesion loss or cathodic disbondment or rate controlling steps (oxygen diffusion through the coating or concrete) thereof that are relevant under less adverse, more realistic exposure conditions. Another difficulty associated with this test is the lack of control on the extent of polarization at the cathode and anode. This results because the procedure involves using a general power supply as the source of polarization. Consequently, the potential for each electrode is not controlled; and this makes it difficult to compare results from different tests. Replacing the conventional power supply with a potentiostat would obviate this problem. The electrolyte employed in the present tests was a simulated pore water with KCl solution. This was judged from CIT results (see APPENDIX H) to be more severe than the NaCl solution recommended by the existing standard (*11*) and to be more representative of the environment of interest.

CHAPTER 4

CONCLUSIONS AND SUGGESTED RESEARCH

CONCLUSIONS

1. Epoxy-coating reinforcing steel (ECR) has been widely employed as the primary means of corrosion protection for concrete highway construction in North America during the past 15-plus years. However, ECR technology, as practiced, cannot be relied on to provide long-term (50-plus years) corrosion protection to concrete transportation structures exposed to corrosive environments (e.g., from application of deicing salts and marine exposure) for the intended service life.
2. ECR technology is presently in a dynamic state; and industry and owner response to recently expressed reservations regarding ECR performance has been such that various procedures associated with this technology, including materials, production, inspection, quality control, and handling/storage/placement methods, are being reevaluated. However, if ECR is to serve as the primary means for achieving a repair-free service life for concrete transportation structures exposed to a corrosive environment, then improvements in practices, procedures, and quality control for each step in the process from bar fabrication to concrete placement are necessary. To be effective, however, such "improvements" must have a beneficial impact upon the deterioration process(es) or the rate controlling step thereof, or both. Ultimately, the corrosion problems that can be associated with ECR must be understood and appreciated and a spirit of cooperation must exist among all parties involved.
3. Weight loss of ECR coatings in association with solvent extraction and electrochemical impedance spectroscopy in association with hot water exposure are appropriate methodologies for formulation qualification and for routine quality control assessment in a production plant.
4. A correlation exists between coating weight loss in association with solvent extraction and ECR specimen impedance after 1 day of hot water exposure. Also, this impedance correlated with ECR performance in longer-term test yard exposures that involved concrete slabs. With further research and analysis, it should be possible to establish a quantitative relationship between coating quality, as exists at the time of bar fabrication or at construction, accelerated test results and long-term performance in service and, relatedly, to establishment of a performance-based specification.
5. The highest quality bars evaluated within this program; that is, those ones without defects with a low solvent-extraction weight loss for the coating and those which exhibited capacitive behavior as determined by EIS, may perform satisfactorily in concrete highway structure service. However, presently practiced techniques for production, storage, handling, transporting, and placement do not provide an in-place product of the necessary quality. A criterion that includes low solvent-extraction weight loss is recommended for qualification of a specific coating formulation for ECR service. Because coating flexibility often varies inversely with this weight loss, coating with a low solvent-extraction weight loss could be brittle to the extent that fabrication of bars after coating, rather than before, becomes necessary. Quantitative coating impedance measurements, performed in association with accelerated hot water testing, and solvent-extraction weight loss determinations should be routinely made in association with ECR production as quality control measures. A frequency of 0.1 Hz appears to be optimum for this type of impedance measurement.
6. A maximum of 2 months outdoor storage, irrespective of whether or not the ECR is covered, is recommended.
7. The inspection procedures, including holiday detection, and quality control methods that are presently used fail to identify ECR that will not provide satisfactory corrosion protection in highway structure service. A quality control requirement based on 1) in-place coating impedance and 2) in-place defect density of bars, rather than on the density that exists at the production plant, is required.
8. Until several years ago, most ECR specifications permitted up to 2.0 percent of the area of bars in the field to exhibit visible coating breaks. To place this in perspective, as many as 3,100 pinhead-size bare areas were permitted on a 10-ft long No. 4 bar. After the initial field failure on ECR structures was reported, FHWA recommended that the visible bare area maximum be reduced to 0.25 percent. This, in turn, is equivalent to 390 pinhead size visible bare areas per 10-ft No. 4 bar. More recently, a maximum allowable bare area of 0.0006 percent has been recommended (*15*). In this case, less than one pinhead-size bare area would be permitted on 10 feet of the same type bar. The results of the present study take these past recommendations one step further by indicating that long-term corrosion protection in salt-contaminated concrete requires that the coating not develop conductive pathways and that the ECR be defect free. This level of ECR quality cannot be achieved by a specification that simply requires patching either all visible defects or defects identified by conventional holiday detection. The desired result from the standpoint of coating breaks, as these exist just prior to concrete placement, can be realized by the ac resistance ratio test

or the modified holiday detector test (or both) that were developed in this project; and these should be adopted as ECR quality control and acceptance processes at the construction site. An acceptance criterion is recommended where ac resistance testing be performed on a statistically significant number of bars in the structure of interest immediately prior to concreting and that 90 percent of these exhibit a resistance ratio in excess of 2,000 and that all ratios exceed 300. However, the level of effort required to provide in-place ECR of this quality is impractical for a field construction setting. One solution is to follow the lead of other applications where nonmaintained coatings are intended to provide long-term corrosion protection (buried pipelines, for example) and employ other protective systems, either in lieu of or in concert with ECR. Another alternative is to develop coating systems that, in ECR service, exhibit high resistance to cathodic disbondment and underfilm corrosion in association with defects. In this latter case, the more achievable requirement that 90 percent of the ac resistance ratios (measured on field bars immediately prior to concreting) be in excess of 300 and that 100 percent exceed 100 may be appropriate.

9. Loss of bond between reinforcing steel and concrete as a consequence of corrosion could eventually affect the structural integrity of concrete that has been fabricated using ECR. Recent research has shown that coating adhesion loss per se does not damage the bond/pullout strength of ECR because the bar deformations alone are integrally responsible for this bond (see Figure A-11 from APPENDIX A and related discussion). However, coating breakdown and corrosion on ECR often initiates at deformations (see, for example, Figures A-6 and A-7). Thus, corrosion of the deformations is greater than for the bar overall; and so as localized metal wastage occurs at these sites, bond could be lost. This may compromise integrity of ECR structures prior to occurrence of significant or widespread cracking and spalling.

FURTHER RESEARCH

Recommendations for further research are listed as follows:

1. Continue exposure and monitoring of the remaining 68 concrete test slabs containing ECR.
2. Conduct experiments to further investigate the importance of solvent-extraction weight loss as a performance relevant ECR property. Tests should include the following tasks: a) Confirm the appropriateness of solvent-extraction weight loss as a quality control parameter in association with ECR production. b) Determine the interrelationship between solvent-extraction weight loss and the ECR temperature-time history during the coating application period. This should identify the optimum conditions for application of a particular coating. c) Identify a maximum acceptable solvent-extraction weight loss for coatings of interest and of any fabrication limitation(s) if the coating is relatively brittle. d) Develop an ECR coating qualification criterion based on solvent-extraction weight loss.
3. Develop specifications for impedance-measurement instrumentation at a single or several defined frequencies for ECR quality assessment in lieu of EIS instrumentation and complete frequency spectrum scans.
4. Development of new coating systems or application techniques, or combinations thereof, that provide improved long-term ECR corrosion resistance in the presence of defects (resistance to cathodic disbondment and underfilm corrosion).
5. Determine if a chloride threshold exists for ECR corrosion.
6. Based on results from Nos. 1–5 above, develop a quantitative relationship between a) ECR properties (solvent extraction weight loss); b) HWT impedance/adhesion data; and c) ECR performance in chloride-contaminated concrete. The product of this effort should serve as a predictive model of ECR performance from accelerated test data; and a final quality control test procedure should result.
7. Perform a test yard exposure program on salt-contaminated concrete specimens to more comprehensively define the relationship between impedance (resistance) of in-place ECR using field instrumentation and expected service performance.
8. Investigate and develop improved instrumentation that will identify coating holidays and also areas that are predisposed for breakdown upon exposure.
9. Investigate the effect of ECR corrosion, as this is likely to occur at bar deformations, on the residual bond strength of reinforced concrete.

REFERENCES

1. CLIFTON, J.R., BEEGHLY, H.F. and MATHEY, R.G., "Nonmetallic Coatings for Reinforcing Bars," *Report No. FHWA-RD-74-18,* PB No. 236424, Federal Highway Administration, Washington, D.C. (Feb. 1974).
2. CLEAR, K.C. and VIRMANI, Y.P., "Corrosion of Non-Specification Epoxy-Coated Rebars in Salty Concrete," *Paper No. 114* presented at CORROSION/83 (April 18–22, 1983), Anaheim, CA.
3. GUSTAFSON, D.P., "Epoxy Update," *Civil Engineering,* Vol. 58, No. 10, pp. 38–41 (1988).
4. POWERS, R.G. and KESSLER, R., "Corrosion Evaluation of Substructure, Long Key Bridge," *Corrosion Report No. 87-9A,* Florida Department of Transportation, Gainsville, FL (1987).
5. POWERS, R.G., "Corrosion of Epoxy-Coated Rebar, Keys Segmental Bridges Monroe County," *Report No. 88-8A,* Florida Department of Transportation, Gainesville, FL (Aug. 1988).
6. ZAYED, A.M. and SAGUES, A.A., "Corrosion of Epoxy-Coated Reinforcing Steel in Concrete," *Paper No. 386* presented at CORROSION/89, April 21, 1989, New Orleans, LA.
7. "Performance of Epoxy-Coated Reinforcing Steel in Highway Bridges," Interim Report, NCHRP Project 10-37 prepared by K.C. Clear, Inc. and Florida Atlantic University, available from NCHRP (Feb. 1993).
8. "Effectiveness of Epoxy-Coated Reinforcing Steel," Final Report submitted to Concrete Reinforcing Steel Institute by K.C. Clear, Inc. (Dec. 1991).
9. "Effectiveness of Epoxy-Coated Reinforcing Steel," Final Report submitted to Canadian Strategic Highway Research Program by K.C. Clear, Inc. (Dec. 1992).
10. German ECR Standard Test No. 103, German Federal Office of Road Building (GFORB) (1990).
11. Standard Specification for "Epoxy-Coated Reinforcing Steel Bars," ASTM A775M-86, *ASTM Annual Book of Standards,* American Society for Testing and Materials, Philadelphia, PA.
12. TEMPLE, T.G. and COULSON, K.E.W., "The Use of Differential Scanning Calorimetry To Determine Coating Cure," *Materials Performance,* Vol. 24, No. 11 (1985) pp. 17–21.
13. NEAL, D., "Fusion-Bonded Epoxy Coatings — Cure and Glass Transition Temperatures," *Materials Performance,* Vol. 32, No. 2 (1993), pp. 49–52.
14. JONES, D.A., *Principles and Prevention of Corrosion,* Macmillan, New York, NY (1992), pp. 208–222.
15. PFEIFER, D.W., LANDGREN, J.R., and KRAUSS, P.D., "CRSI Performance Research: Epoxy Coated Reinforcing Steel," Final Report submitted to CRSI by Wiss, Janney, Elstner Associates, Inc. (June 1992).

APPENDIX A

STATE OF KNOWLEDGE, DEFINITION, AND CRITICAL INTERPRETATION (TASK 1)

BACKGROUND

Corrosion of steel in concrete has evolved over the past two decades to become the single most costly problem of its type in the United States. Consequently, FHWA, the State Transportation Agencies, NBS (now NIST), CRSI, FBCA, C-SHRP, AASHTO, ASTM, NACE International (formerly NACE), ACI, and the private sector (*1*) have ongoing activities to reduce and eliminate damage to structures from this cause. While the alkaline nature of the cement paste in concrete (pH of 12.5 or greater) facilitates formation and maintenance of a protective, passive film and low corrosion rate, carbonation or chloride intrusion can compromise this situation and, in the presence of moisture and oxygen, cause the corrosion rate to become unacceptably high (*2*). This leads to the accumulation of solid corrosion products in the cement pore space near the embedded steel-concrete interface which, in turn, gives rise to tensile stresses in the concrete and finally to concrete cracking and spalling.

Carbonation, which involves the reaction of cement constituents with atmospheric carbon dioxide to yield carbonates, reduces the pH to the range 8.5–9.5 at which embedded steel is no longer passive. In sound, dense concrete with adequate cover, as should be typical of modern highway structures with acceptable quality control during construction, carbonation is not expected to reach the embedded steel depth within the design life; and so relatively little attention is generally focused upon this phenomenon. The situation is different, however, in the case of chlorides, as may result from either deicing salts or marine exposure (or both), where no significant pH change accompanies accumulation of this species; but, instead, direct reaction of Cl^- with the steel surface leads to loss of passivity. While numerous variables associated with the concrete and exposure conditions may influence the chloride concentration and cause loss of passivity, several prominent historical research activities have concluded that as little as 0.025–0.033 percent Cl^- (concrete weight basis) may result in local loss of passivity (*3,4*). Related experiments involving simulated cement pore water electrolytes have indicated that the chloride/hydroxyl ion ration $[Cl^-]/[OH^-]$ is the critical parameter with which compromise of passivity best correlates (*5*).

Numerous factors influence corrosion of embedded steel in concrete, including 1) type of exposure, 2) inherent cement alkalinity, 3) concrete permeability, and 4) concrete resistivity. Parameters in the initial category include a) temperature; b) concentration of deleterious species (Cl^-, for example), as well as oxygen and water; and c) wet-dry cycling. Concrete permeability (item 3) is important as it governs the transport rate of influential species (Cl^-, O_2, and H_2O) to the steel-concrete interface, whereas item 4 (resistivity) is critical with regard to functioning of the electrochemical cell(s), particularly when anodes and cathodes exist on a macroscopic scale, as is typically the case for bridge components.

Corrosion Prevention

A number of materials, techniques, and procedures have been identified that reduce or eliminate corrosion of steel in concrete. These may be categorized as either mechanical or electrochemical, according to the manner in which they function. A major difficulty often associated with these is the relatively short time period over which a corrosion mitigation alternative might be qualified based upon research and testing results (several years maximum) compared to the design life of monumental structures (75 years, for example). Thus, there is no accelerated evaluation procedure in which the technical community can be fully confident for predicting long-term performance; and some uncertainty is invariably associated with accepting a corrosion prevention alternative, as opposed to retaining it in an "experimental" or "development" category for extended time periods. At the same time bridges must continue to be built, and so materials selection and design decisions must be made based upon available information and results.

Mechanical techniques for reducing or eliminating embedded steel corrosion are based upon a physical barrier to chloride, oxygen, or water intrusion. Electrochemical methods, on the other hand, involve a supplementary electrochemical cell in addition to the naturally occurring one with the embedded steel as cathode. The resultant potential and current are intended either to electrochemically migrate chlorides from this electrode (electrochemical chloride removal (*6,7*) or to polarize the metal to a more negative potential where corrosion rate is low or nil (cathodic protection (*8*).

The electrochemical category also include inhibitors, which when admixed into fresh concrete or combined with standard deicing salts, can prevent or minimize the action of corrosion cells (*9*). The mechanical category includes the use of admixtures such as high-range water reducers, fly ash, or silica fume (*10,11*); and this results in improvements in concrete mix design and placement procedures to produce less permeable concrete with higher electrical resistivity. Also included in this category are sealers and membranes (*12*) used to prevent ingress of water and chloride ions into the concrete and epoxy-coated reinforcing steel to isolate the steel from the aggressive environment.

Epoxy-Coated Reinforcing Steel

In the case of epoxy-coated reinforcing steel, early research performed by the NBS (now NIST) and FHWA indicated that

reinforcing bars coated with select powdered epoxies using an electrostatic spray process after bar cleaning performed well in salt-contaminated concrete (*13*). An evaluation of various epoxy products resulted in the selection of the three most promising powders for use in coating reinforcing steel. Such coated rebars were shown to be resistant to corrosion, and so early age deterioration of the surrounding concrete due to the pressures generated by expansive corrosion products is minimized.

Epoxy resins are thermosetting plastics belonging to the polyaddition plastics family and are reported to have good long-term durability in concrete and to be resistant to solvents, chemicals, and water (*14*). Epoxy resins also have desirable mechanical properties such as high ductility, small shrinkage upon polymerization and good heat resistance (*15*). Further, test results indicate that the oxygen and chloride ion permeabilities of defect-free epoxy coatings of significant thickness (e.g., 7 mils) are very low, even in a worst case exposure (*13,14,16,*). Epoxy coatings are, on the other hand, permeable to moisture (water), and it has been known for years (although not highlighted within the highway community) that the adhesion of epoxy-based coatings to steel is greatly reduced after exposure to moisture (*17*). Thus, the primary advantage afforded by a defect-free epoxy coating of adequate thickness is that it acts as a barrier that prevents chloride ions and oxygen from reaching the steel surface. Also, by increasing the electrical resistance between neighboring coated steel locations, such coatings reduce the magnitude of macroscopic corrosion cells that have been responsible for extensive early bridge deck deterioration (*18*).

Because the protective ability of epoxy coatings is based on preventing aggressive materials from contacting the steel surface, effective corrosion control necessitates that the coating integrity be maintained. Therefore, one of the most important factors governing the performance of epoxy-coated bars is appropriate quality control during coating application and subsequent handling. ASTM specifications A775 and D3963, AASHTO Specification M284 and CRSIEDR No. 19 provide stringent guidelines to be followed during coating application and subsequent handling and storage of the bars.

For more than a decade, epoxy-coated reinforcing steel in concert with higher quality concrete and deeper cover have, for the most part, been effective in reducing or preventing chloride-induced corrosion distress in bridges and other concrete structures. In the early to mid-1980s it was believed that the additional initial structure cost of employing this technology was expected to be recovered because of reduced downstream maintenance expenses, thus rendering this approach economically justifiable (*19*). By 1975, 10 U.S. State highway departments had constructed bridge decks with epoxy-coated bars; and during the next decade the use of this product became widely adopted by highway agencies with freeze-thaw climates or coastline exposures (or both). Widespread acceptance of this technology is exemplified by the fact that most state highway agencies today use epoxy-coated bars in their bridges (*20*).

In Canada, Ontario standardized use of epoxy-coated steel for the top mat of bridge decks, curbs, and lane barrier walls in 1978, and in 1981, epoxy-coated rebars were specified for some substructure components. Other provinces and agencies have also used epoxy-coated reinforcing steel.

More recently, several investigators have performed field inspections and laboratory studies, which led them to question the use of ECR as a realistic strategy for mitigating corrosion damage to concrete structures (see subsequent sections). On the other hand, there exists the opinion that epoxy-coated reinforcing steel provides a viable, long-term option for protection of concrete structures (*21*) and that the reports of corrosion problems with this material are isolated and a consequence of some yet unidentified impropriety associated with the coating or coated bar. Alternately, others consider that the corrosion failures observed to-date are indicative of a generic shortcoming of this technology as it is presently practiced and that additional premature failures will occur as structures continue to age (*22*). The problem associated with proving or disproving the former view is a classical one in that the researcher can predict what will transpire beyond the time of an experiment only by extrapolation and projection. Thus, the fact that no corrosion or corrosion failure occurs within say 1 year or even 20 years does not mean that breakdown would not take place if the experiment had lasted an additional day. A similar rationale applies to the latter view (that ECR technology as practiced is inadequate) in that failure of a limited number of systems does not in and of itself mean that problems are pervasive. What can be done, however, is to acquire information from experiments and exposures that have been performed and attempt to establish trends and correlations upon which prediction of failure properties and performance can be projected with an acceptable degree of confidence. It is within this context that a review of previous research regarding this topic has been prepared and critically evaluated, as presented below.

REVIEW OF RELEVANT INVESTIGATIONS

Results Indicative of Good Performance

It has been concluded by the investigators in a relatively large number of projects that epoxy-coated reinforcing steel in concrete provides good or excellent long-term corrosion protection. For example, a 3-year investigation of epoxy-coated reinforcing steel by Wiss, Janney, Elstner, Associates (*23*) consisted of two laboratory programs. The first involved slab specimens subjected to 48 weeks of "Southern Exposure" per *NCHRP Report 244,* with measurement of macrocell current and half cell potential. Situations of only the top mat coated and both mats coated were studied. The year-long follow-on work (second study) involved the testing of full-size reinforced concrete columns and beams subjected to cyclic saltwater exposure. Normal production epoxy-coated rebars were used with coating thickness typically averaging from 8 to 10 mils. About half the bars contained no holidays and the other contained one or two holidays per foot (bars with more than 2 holidays per foot were discarded). The findings showed that epoxy-coated reinforcing steel was superior to uncoated rebar in minimizing corrosion, even with 1 in. of cover, poor quality concrete (w/c = 0.51), and chloride levels around the rebar, which were 20 times that required to induce corrosion of uncoated rebar. The authors stated that no corrosion activity developed on the coated rebars, that holidays premarked on the bars did not develop any corrosion, and that specimens with coated bars developed very high internal electrical resistances (bar-to-bar or mat-to-mat) due to the properties of the epoxy-coating. The uncoated controls with 1-in. cover, on the other hand, exhibited high corrosion rates.

In October 1979, the Florida Department of Transportation (DOT) began an investigation of different types of reinforced

concrete piles at Matanzas Inlet on the east coast of Florida. The initial report in July 1982 (*24*) indicated that no change had occurred on any of the piles; but potential measurements in the tidal area showed active corrosion after about 5 months for both the uncoated and the epoxy-coated (Scotchkote 213) specimens. It was noted that along the length of the piles, the potential differences were much greater for the uncoated rebar piles than for the piles with epoxy-coated rebar; that is, macrocells were apparently not present in the epoxy-coated case. Each pile was 6 in. by 6 in. by 10 ft and incorporated four number 4 reinforcing bars held in place by insulated chairs. Placement of the piles, in October 1979, was done by jetting to 5 ft. It was reported that at least one of the piles with uncoated rebar exhibited corrosion induced distress after 4 years. In the fall of 1988, the piles were examined in the field, and select piles were removed and autopsied in the Florida DOT laboratories (*25*). The pile with uncoated rebar showed severe corrosion damage and advanced corrosion of the embedded steel with corrosion products having migrated into the surrounding concrete. The pile with epoxy-coated rebar, on the other hand, showed no corrosion induced distress, even at cross-section cracks caused by removal damage. The epoxy-coated rebar was in excellent condition with a small amount of corrosion at a holiday only. This corrosion had not migrated beneath the coating (that is, no undercutting) and was judged insignificant. Microscopic evaluation revealed that the coating exhibited excessive foam (*26*), which is indicative of an excessive application temperature.

Results from Non-North American Programs

While there has been extensive use of epoxy-coated reinforcing steel in the United States and to a lesser extent in Canada, only limited usage and study have occurred in Europe and the Far East. As one example, a Finnish study (*15*) involved testing of European powdered epoxy-coated rebars, some of which contained deliberate defects, placed in poor quality concrete with and without calcium chloride. Single bar and tube specimens, some of which were cracked, were subjected to partial immersion in synthetic seawater during both curing and subsequent exposure. Sound epoxy coatings exhibited only light corrosion, and it was projected that these gave good protection even in the aggressive environment. Uncoated bars, on the other hand, were badly corroded. Some corrosion in the area around defects was noted, and it was concluded that defects considerably compromised any protectiveness afforded by the coating. Similarly, a study involving columns exposed in the sea in Norway (*27*) showed good performance of epoxy-coated rebar, as measured by the current demand of an external cathodic protection system. The columns, which were exposed in three zones (submerged, tidal, and atmospheric), were loaded in three-point bending to 35–70 percent of yield in the most highly stressed layer of reinforcement. After three years, the authors concluded "*. . .the magnitude of the polarization current is reduced by more than 90 percent when the reinforcing steel is coated with Scotchkote 213 compared to the values recorded for bare steel. This shows that the Scotchkote 213 fusion-bonded epoxy coating acts as an effective barrier against the oxygen diffusion to the reinforcing steel.*" The epoxy-coated rebar used in this study is referred to only as "standard U.S.," and no other property data were provided.

A Japanese study (*28*) involved the 3-year exposure of loaded (bar tensile stress of 20 kg/mm^2 or 28,440 psi) concrete columns to a marine tidal zone environment. The specimens are precracked. Concrete cover over the fusion bonded epoxy-coated and the uncoated reinforcement varied from 0.8 to 2.8 in. (2 to 7 cm). The epoxy coating thickness on the coated bars varied from 4 to 12 mils (100–300 μm). During the 3-year exposure all the epoxy-coated deformed bars were free from rust, whereas the uncoated bars were corroded, with rust covering 9 to 50 percent of their surfaces. Another phase of this study involved repeated immersion in 60°C sea water for 6 hours followed by atmospheric exposure for 6 hours. After 2 years, the uncoated bars from the specimens with 0.8 and 1.6 in. (2 and 4 cm) of cover were almost completely covered with red rust, while those from the specimens with 2.8 in. (7 cm) of cover had about 75 percent red rust coverage. The epoxy-coated rebars, regardless of cover depth and coating thickness, all showed red rust coverage of 0.1 percent or less. The bars coated to a thickness of four mils (100 μm) exhibited a few small blisters but remained unpitted. Those with coating thicknesses of 8 and 12 mils (200–300 μm) were described as follows "*. . .the film was wholesome even after 24 months, irrespective of the depth of cover, with all its gloss, adhesive strength, scoring hardness (5H) and peeling hardness (6H) remaining unchanged from initial values.*" The authors state that the fusion-bonded epoxy film used on the bars was chosen because of its good performance in a series of preliminary screening tests. They did not, however, identify the powder used.

Roper (*29*) investigated the conjoint influences of sea water exposure and fatigue stressing upon beams with both Australian and American coated and uncoated reinforcing steel. He stated that, "*although epoxy-coated bars lead to improved fatigue endurance of the concrete beams in the presence of seawater, corrosion of areas of the bars adjacent to the lugs has been observed after the test,*" and concluded that, "*doubt must be held as to the long-term efficiency of the epoxy coating due to general corrosion at the lug base.*" There were no data within his paper concerning the source of epoxy-coated rebar, the coating material, its thickness, whether or not the bars met specifications or other information on coating quality. After failure, it was noted that, in addition to the corrosion at some lugs, attack appeared to be advancing under the epoxy coating. Microscopic examination did not reveal flaws at the lugs. It was hypothesized that the fluctuating load in the marine environment caused the formation of small access paths through the epoxy coating at the rib bases (high stress points), and the epoxy underwent creep because of its viscoelastic properties. This resulted in perforation of the epoxy cover; and once chloride access to the steel occurred, corrosion was rapid and undercutting of the epoxy coating took place. Roper (*29*) also noted that the adhesion characteristics of the epoxy coating were greatly reduced in the presence of water and stated that, "*evidence available from this series of experiments suggests that water and chloride ions may have moved considerable distances along the concrete-epoxy bar interface. . .*"

FHWA Programs

Several extensive studies addressing the protection afforded to reinforcing steel in concrete by epoxy coatings have been

performed by the Federal Highway Administration (*18,19,30–33*). These involved exposing slabs to a deicing salt environment where the rate of salt application and, hence, the rate of chloride uptake in the concrete was accelerated compared to what occurs for bridge decks, but all other factors were typical of actual service. Variables that were incorporated into the programs included the influence of 1) bare versus coated steel, 2) type of coating, 3) exposure duration, 4) specification versus nonspecification coatings, 5) presence of coating damage and 6) one versus both mats coated. In the first of these programs, a series of slabs was fabricated in 1974 that contained both uncoated and coated reinforcing steel with the latter consisting of either Scotchkote 202 or Flintflex 6080, the materials employed for the first bridge deck constructed with epoxy-coated reinforcing steel. The coated rebars were of varying quality, although the coater stated that all met specifications, and were defined as either specification (two or less holidays per foot), or nonspecification (more than two holidays per foot) bars. The slabs were non-air entrained, and various amounts of deliberate coating damage were provided to simulate what was considered likely to occur in the field. After curing, the slabs were subjected to daily applications of a 3 percent salt solution on the top surface during the summer months for 4 years. Subsequently, the slabs experienced only natural weathering at the FHWA outdoor exposure facility in northern Virginia. Freeze-thaw damage became severe after several years on some of the slabs, and this has complicated evaluation. Although bottom rebars were included, tests showed that they were not tied electrically to the top mat rebar. Additionally, the testing indicated that in most cases the various top mat rebars also were not electrically interconnected.

The uncoated rebar slabs exhibited cracking after 0.7 year exposure; and severe corrosion and section loss was apparent after 7 years. The first cracking and delamination of epoxy-coated rebar slabs was documented in 1978 or after about 4.2 years of exposure in association with the nonspecification Flintflex 6080 coated bars. However, the results of this research indicated that even nonspecification epoxy-coated bars provided enhanced corrosion protection compared to black (uncoated) steel (*18,19,30*). Subsequent autopsies performed after 7 years exposure revealed significant corrosion and undercutting of the coating on these nonspecification bars (*31*), and the 1979 FHWA progress report (*30*) stated:

> In summary, the slab studies indicate that even epoxy-coated reinforcing steel, which was poorly coated and badly damaged, is highly superior to black steel. Time to corrosion-induced cracking will be extended at least about 5 times. However, the slab studies also show that corrosion of the poorly coated rebar will eventually lead to at least isolated instances of corrosion induced distress. Additional exposure time and screening studies are needed to define the magnitude of the distress and to relate specific types of coating damage to distress.

The rationale associated with the conclusion that epoxy-coated reinforcing steel provides a corrosion life extension that is at least five times greater than that for bare steel is considered particularly important and is discussed in greater detail in a subsequent section of this Appendix.

A follow-on study was performed after 7 years (1981) upon these slab specimens, but the results were never reported. This study involved demolition of four slabs and examination of the embedded steel and coating. KCC INC obtained and analyzed

Figure A-1. Fall 1981 condition of top rebar. FHWA 1974 Slab 14-Flintflex 6080 coating with excessive holidays, spliced bars and bare bar ends.

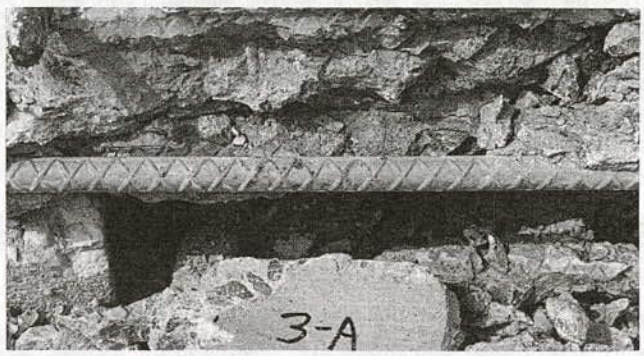

Figure A-2. Fall 1981 condition of top rebar. FHWA 1974 Slab 3—Scotchkote 202 coating meeting specifications, no deliberate damage.

these data and photographs. Figure A-1 shows the condition of the top mat reinforcing in the Flintflex 6080 coated rebar slab number 14 case, which was characterized by excessive holidays (more than 25 per foot), spliced bars and uncoated bar ends (total bare area of approximately 1.1 percent). Note the severe corrosion and the appearance of undercutting. There were numerous cracks in the concrete that extended from the rebar trace, and the coating was easily removed from more than half of the coated rebar area using a knife. While Flintflex 6080 was prequalified for highway application, subsequent evaluation has shown that this coating developed a high holiday density and might be inappropriate for this type of service.

Figure A-2 shows the top rebar that was coated to specifications (no more than two holidays per foot) using Scotchkote 202. These bars did not have any visible coating damage and the ends were coated. No cracks were found in the concrete extending from the rebar traces, and only light spotty rust staining was present at a few locations. Little, if any, undercutting was observed. Figure A-3 is a photograph of the top rebar in slab 8, which was coated to specifications with Scotchkote 202. In this case, the bar coating had 1 in. (2.54 cm) bare areas on

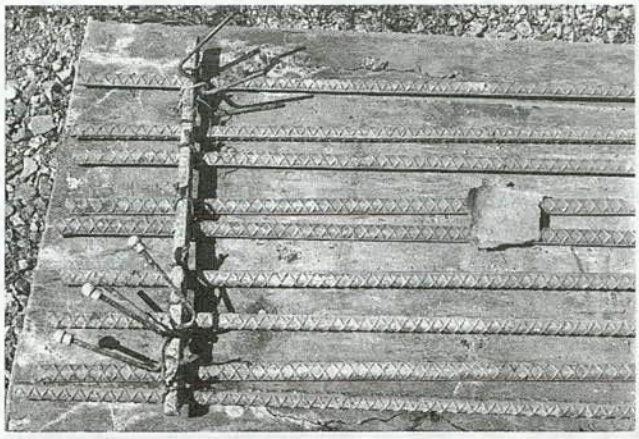

Figure A-3. Fall 1981 condition of top rebar. FHWA 1974 Slab 8—Scotchkote 202 coating to specifications 1-in.-wide bare ridges on 6-in. centers, bare bar ends.

Figure A-4. Fall 1981 condition of top rebar. FHWA 1974 Slab 16—Scotchkote 202 coating with excessive holidays and bare bar ends.

6 in. (15.2 cm) centers to simulate field damage, and the bar ends were uncoated. This rebar was found to be in excellent condition with most of the bare areas showing slight corrosion damage, and no undercutting was apparent. Figure A-4 shows a photograph of the top rebar in slab 16 (Scotchkote 202), which had excessive holidays (more than 25 per foot) and bare bar ends. It exhibited greater corrosion damage than the slabs in Figures A-2 and A-3 but much less damage than exhibited by slab 14 (see Figure A-1). A small amount of undercutting was noticed. The lower rebar in this slab is an uncoated bottom mat that had been positioned along one edge, and it exhibited much more corrosion than the coated steel. However, the concrete around the uncoated bar had become chloride contaminated due to salt solution runoff during rainy weather.

After about 7 years exposure (1981) corrosion-induced cracking was confirmed on coated rebar slabs that initially had bare areas and in some cases excessive holidays, in addition to the case cited above. Upon autopsying, disbondment and undercutting were seen for bars coated with Scotchkote 202 and Flintflex 6080. Although data were scarce, Scotchkote coated bars with excessive holidays and no bare areas were in better condition than those with bare areas of 1.1 and 7.2 percent of the bar surface. Only light corrosion and no undercutting were apparent on the Scotchkote 202 coated bars that originally had two or less holidays per foot and no bare areas.

Sixteen years after exposure (1990) all slabs were badly cracked (probably due to both freeze-thaw and corrosion damage) except for the two remaining ones that contained bars without deliberate coating damage, two or less holidays per foot and zero bare areas. These slabs exhibited only slight cracking, which could have been freeze-thaw related. Thirty-four cores were extracted and analyzed from eight slabs. The bars from all slabs with deliberate coating damage or bare bar ends (or both) were severely corroded; and the epoxy coating was cracked, blistered, brittle and debonded. Concrete cracking as a consequence of corrosion was judged to have occurred. Less corrosion was seen on the rebars from the Scotchkote 202 slab, which had too many holidays to measure but no bare areas, although the coating had lost adhesion on all bars; and corrosion-induced cracking on this slab was also likely. The bars from the low holiday (two or less per foot of rebar) coated rebar slabs with no bare areas exhibited only light or spotty corrosion, but the coating bond (adhesion) was poor on all of the bars (dry knife adhesion of 5 on a scale of 1 to 5 with 5 indicating complete adhesion loss). It would appear that these bars (low holidays and no bare areas) were after 16 years exposure experiencing the early stages of corrosion failure. The data collected from this evaluation along with a description of the corrosion state and the coating adhesion characteristics of the bars for each core were presented in the Interim Report for this project. It is noteworthy that the most negative half cell potential measured on the epoxy-coated rebar slabs was –845 mV CSE (copper sulfate electrode) and that seven of the eight slabs studied exhibited half cell potentials more negative than –600 mV (CSE). Only the slab with no bare areas and two or less holidays per foot in both mats had more positive potentials, where the most negative value was –543 mV (CSE).

In another FHWA study, which was initiated in 1974, specification bars also outperformed nonspecification ones. This investigation involved partial immersion of over 100 reinforced (single rebar) beams in a saturated sodium chloride solution (*30*). After 80 months of testing only 5 percent of the beams with specification epoxy-coated rebars (two holidays per foot or less and up to 2 percent visible damage area) showed cracking, whereas 49 percent of the beams with nonspecification bars (greater than 25 holidays per foot or greater than 2 percent visible bare area, or both) showed cracking. All beams with uncoated steel were cracked after only 34 months exposure. During autopsy of select beams in 1981, it was noted that all the uncoated specimens were much more severely corroded than the coated rebars, that all Flintflex 6080 coated rebars were more badly corroded than those coated with Scotchkote 202, that the specification Scotchkote 202 bars exhibited the least corrosion with no undercutting at deliberately damaged areas, and that all the coatings could be removed with varying degrees of ease with a knife when first removed from the concrete (that is, when they were in a wet state). The ease of removal did not, however, correlate with corrosion damage. Further, the dry coating on the upper portion of each bar, which had not been in concrete, could not be removed easily with a knife in any case.

In 1980 the FHWA initiated a second investigation of nonspecification epoxy-coated rebar in slab-type specimens (*32*). The bars in this case were coated with Scotchkote 213 and were

certified by the producer to meet specification with the exception of coating thickness, which was requested to be excessive by FHWA. However, the bars were stored outdoors for 3 years prior to slab fabrication and after that time were found to have holidays in excess of 25 per foot. In the time-to-corrosion studies, these bars were referred to as "nonspecification," based on the excessive coating thickness, failure in the bend test in which poor coating adhesion was noted, and the holiday/bare area evaluation after outdoor exposure prior to concrete placement. However, since field bars are not normally checked for holidays and small bare areas and are not subjected to bend testing subsequent to outdoor exposure prior to concreting, these bars may not have differed greatly from many field epoxy-coated rebars, even after additional damage of less than 1 percent of the surface area was purposely created for some of the specimens. The mix design included 15 lbs (6.8 kg) of chloride as NaCl per cubic yard (0.76 m^3) of concrete placed about the top mat reinforcing steel but with no intentional chlorides added to the concrete placed about the bottom mat. Exposure was at the FHWA outdoor test facility in northern Virginia and involved salt water ponding for the initial 1.5 months followed by exposure to natural weathering only. In some instances, the bottom bars were epoxy-coated and in others they were bare. All top mat rebars were electrically continuous and connected externally to the bottom mat rebar to allow measurement of mat-to-mat macrocell current. Half-cell potentials, AC resistance, temperature, macrocell current, and visual appearance were monitored. Consistent with results from other experiments the control slabs with uncoated reinforcing steel cracked first, as was predicted from the macrocell current measurements (typically 1.8 mA/ft^2 of top mat rebar). At about this same time (1981), the epoxy-coated rebar slabs exhibited macrocell currents that were only 1.9–7.3 percent of those on the uncoated rebar, and mat-to-mat AC resistances on the coated rebar slabs were 3.4–8.4 times higher than for the slabs with uncoated reinforcing steel. Cracking of slabs with epoxy-coated rebar was first noted in 1987, and by 1989 all the coated rebar slabs were badly cracked as a result of corrosion. There was no significant difference in the time-to-cracking of the slabs with 1) epoxy-coated rebars in one mat compared to both and 2) intentionally damaged bars compared to ones without intentional damage. An autopsy performed on one of these slabs after 9 years (1989) showed significant corrosion of the top mat reinforcing and undercutting of the epoxy coating (*33*). Photographs taken by FHWA during this autopsy are presented in Figure A-5. Tests by KCC INC showed that the coating on a bottom mat rebar of this slab was easily removed using a knife when the coating was wet and after it had dried. It was reported that a deliquescent liquid of low pH (less than 1) was present on the corroded coated bars. This was apparently similar to what has been observed for corroding ECR in the Florida substructures, as discussed below.

Evaluation of Field Structures

Structures Indicating Good Performance. Investigations of epoxy-coated rebar bridge decks have been conducted in Maryland, Minnesota, Virginia, and Pennsylvania (*34–37*). These studies did not provide unequivocal results due to the early age of the structures at the time of evaluation and the low chloride levels in the concrete. The Virginia study (*36*) evaluated two poor quality epoxy-coated rebar bridge decks. After 7 years the corrosion potentials were relatively positive, and chloride contamination levels were below the threshold except in an area with several transverse cracks that had probably formed when the bridge deck was placed. In this area, the rebar level chlorides averaged 2.6 lbs Cl^-/yd^3 (1.5 kg/m^3). No delaminations were detected even in the cracked area. A Pennsylvania study by Weyers and Cady (*37*) involved 22 concrete bridge decks, half with uncoated rebar and half with epoxy-coated rebar, which had been in service approximately 10 years. All decks were visually inspected and four (two with each type rebar) were evaluated in-depth. Forty percent of the visually examined uncoated rebar decks showed signs of corrosion damage, as did one of the two uncoated decks, which was examined in detail and which had 3 percent delamination. None of the epoxy-coated rebar decks showed any signs of corrosion induced distress, and the two studied in-depth showed no delamination even though the rebar chloride levels were high over much of the deck areas.

The Pennsylvania Department of Transportation study (*38*) involved detailed examination of four epoxy-coated rebar decks and visual examination and rating of 32 others as part of a large effort that evaluated all protective systems. On average, epoxy-coated bars received from cores were rated to be in excellent condition (no corrosion) for all decks studied, even though the water-soluble chloride content surrounding the bars was high in many instances (3.3 to 11.7 lbs Cl^-/yd^3). At least one coated rebar was found, however, that showed some corrosion; and a coating defect was identified as the cause. Coating thickness varied from 4.2 to 12.5 mils and averaged 9.2 mils. A survey indicated that epoxy-coated reinforcing steel in both mats was the preferred new deck protection system of 10 of the 11 Districts in the State. The overall average age of the epoxy-coated rebar decks was 7.7 years and for the four decks investigated in detail 10–12 years. The estimated life of the epoxy-coated rebar decks by the Districts ranged from 20 to 50 years and averaged 39 years.

A field study of two 9-year-old concrete bridge barrier walls in Canada also provided positive results (*39*). This study indicated that both rebars with epoxy coatings (Scotchkote 214) meeting specified requirements and a rebar with the coating damaged performed satisfactorily with only superficial corrosion activity observed on the latter. There was no evidence of pitting or of corrosion activity under the coating (undercutting) in the area adjacent to damage. Coating thicknesses were generally in the range of 5 to 9 mils with a few readings below 5 mils. There was no indication of debonding between the steel and the coating in any of the samples. However, isolated examples of poor bonding between the epoxy and the ribs were found on all bars by prying off the coating with a knife. Chloride analyses indicated that these epoxy-coated rebars had been in a corrosive environment for a number of years. A barrier wall of the same age constructed with uncoated steel exhibited high corrosion rates, and both visual inspection and coring confirmed significant corrosion.The performance comparison between epoxy-coated reinforcement and uncoated reinforcement subjected to similar exposure conditions indicated that there was substantially reduced corrosion activity on the former (epoxy-coated) compared to the latter (uncoated).

Field Structures Indicative of Poor Performance. In contrast to the numerous field performance studies that have reported

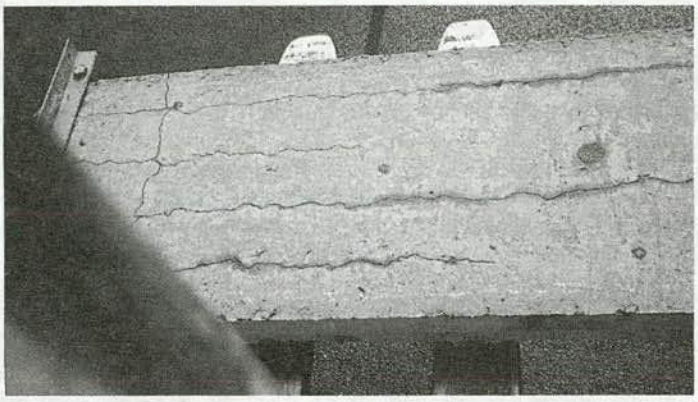

Figure A-5. FHWA September 1989 autopsy of non-spec epoxy-coated rebar Slab 235 (see time to corrosion, Volume 5 Report).

positive performance of epoxy-coated reinforcing steel in concrete, recent instances of corrosion problems or failures in Florida, Oregon, and New York have raised important questions regarding long-term performance and the role of different factors or variables that influence the effectiveness of this corrosion mitigation technique. In particular, progressive cracking and spalling of marine exposed bridge substructures in the Florida Keys after only 6 to 9 years of service has been reported (*20,40–43*). The damage affected approximately one-third of the epoxy-coated bent rebars in three major bridges (Seven Mile, Long Key, and the Niles Channel bridges). Locations showing distress had an average of 2 in. of concrete cover over the rebar, although in some instances the initial chloride content of the concrete was high. Both bent and straight bars showed corrosion, typically in the region extending from 2 to 6 ft (0.6 to 1.8 m) above the high water line. Advanced stages of damage involved severe pitting and accumulation of corrosion products between the epoxy and the remaining metal as well as corrosion products in direct contact with the concrete. A chloride rich liquid of pH ~ 5.5 between the epoxy and the steel was frequently observed in newly exposed rebar, even when the surrounding concrete was relatively dry. Soundings made under these conditions indicated extensive delamination of the concrete, which was demonstrated by easy removal with a hammer. In areas of severe corrosion, the coating was completely debonded, and in less severe cases of deterioration, the coating could still be easily removed.

The underlying metal appeared dull and slightly darkened. Disbondment of this type has been observed in portions of the substructure above the regions of greatest damage, as well as in the substructure of other south, central and west Florida bridges constructed with epoxy-coated reinforcing steel and with 7 to 11 years of service. The Florida DOT concluded that epoxy-coated bars in the marine substructure applications were more susceptible to corrosion than bare steel and that coating quality, while a possible contributory factor, was not the primary cause (*42*). Others disagree and believe that poor coating quality or field damage (or both) or possibly an influence of Florida aggregates was the primary cause of the problems, and the importance of surface preparation and other aspects of quality control on the performance of epoxy-coated reinforcing steel has recently been stressed (*44*). It has been suggested that an imperfection in the coating may cause a small anode-large cathode situation, which could result in more severe local attack than in the case of uncoated steel and that this may be accompanied by accelerated underfilm attack leading to disbondment (*45*) or to loss of adhesion from cathodic disbondment. It is important to note that the deteriorated bars from the Florida Keys bridges were similar in appearance to the failed nonspecification bars taken from FHWA outdoor exposure specimens in 1981 and again in 1989 (*30,31,33*). The FHWA specimens were from slabs exposed to a northern deicing salt environment, suggesting that the type of failure encountered in the Florida substructures was not unique to that particular exposure situation.

Particularly noteworthy with regard to field structure ECR performance are results from the recently completed C-SHRP (Canadian Strategic Highway Research Program), where epoxy-coated reinforcing steel from 19 field structures in Canada and the northern U.S. that were constructed between 1974 and 1988 were evaluated (*46*). This research extended beyond the normal visual inspection of recovered bars in that both qualitative and quantitative examinations were performed to characterize the coating, including determination of 1) thickness; 2) holiday, bare area, and mashed area densities; 3) underfilm contamination; 4) percent foam; 5) steel anchor pattern; 6) coating hardness; 7) coating adhesion; and 8) coating electrical resistance. Cover over and chloride concentration at the ECR depth were also considered. Additionally, an Accelerated Corrosion Test (ACT) and Chemical Immersion Test (CIT) were performed to project future coating performance.

It was determined that the visual appearance of the ECRs was generally good except for samples from cracked cores where the structure was more than 8 years old. In this case, corrosion varied from minor staining only at the crack to significant attack and complete debonding, both at the crack and in the surrounding areas. In general, the coating thickness, anchor pattern, percent foam and hardness for bars recovered from field cores were within specification limits. On the other hand, the holiday and bare area densities were high in that 79 percent of the samples had more than two holidays per foot and 94 percent had three or more bare areas per foot. This indicated either that the bars were of poor initial quality or that coating defects occurred during the service exposure. Correspondingly, dry-knife adhesion for approximately one-half of the bars was "moderate" to "poor." In most cases these were from the older structures. AC resistance determinations for the bars were highly variable and ranged from 1.0 to greater than 50,000 kOhms/ft^2. These translated to an AC resistance ratio (resistance of the coated bar divided by that for an uncoated bar of equal size) of 2.0 to 100,000. The median, however, was 130, which is less than the 300 minimum recommended by the NBS as a part of the original ECR research. Generally, low AC resistances and resistance ratios were associated with corroded bars, bars with high holiday and bare area densities or ones with poor bonding.

Data obtained for 44 bars that were part of the ACT and CIT tests indicated, based upon posttest visual appearance, AC resistance changes, debonding and loss of coating adhesion, that all were adversely affected to varying degrees by the testing and none exhibited behavior indicative of high quality coating. It was concluded that, even though no corrosion induced distress was apparent on many of the nine structures represented in the program, the protective properties of the coatings were poor. The fact that chloride concentration at the ECR depth was below threshold for a number of the structures was cited as a reason for the lack of corrosion. It was projected that these ECRs will not afford protection once the threshold chloride concentration is reached and for this reason that these coatings will not be effective in providing long-term corrosion protection to reinforcing steel in salt contaminated concrete.

In addition to the substructure members of the three large Florida Keys bridges (which showed concrete distress in spite of epoxy-coated reinforcing steel after about 6 to 10 years of service), several other structures have been reported to be exhibiting corrosion induced concrete damage or severe corrosion of the epoxy-coated reinforcing steel, or both. These are listed and briefly discussed below:

1. A New York bridge deck constructed in the mid-1970s with epoxy-coated reinforcing steel (Flintflex 6080), a recognized poor quality coating, was reported in 1990 to be exhibiting widespread delamination and spalling and severe corrosion of the epoxy-coated reinforcing steel.
2. A northern U.S. parking deck constructed in 1982 with epoxy-coated reinforcing steel is exhibiting delamination and spalling of the concrete in lower cover areas (about 0.5 in.). The design cover was 1.5 in. The water soluble chloride levels from deicing salt in this structure were high (2.5 to 23.5 lbs chloride per cubic yard at the 0 to 1 in. level and 0.8 to 13.7 lbs per cubic yard at the 1 to 2 in. level). The spalling and delamination was first noted after 8 winters of service.

3 and 4. The epoxy-coated reinforcing steel near the expansion dams on two bridge decks in Ontario (Madawaska River Bridge, Site 29-191, and Ford Drive/QEW interchange, Site 10-284) was recently examined during replacement of the dams. This area of the decks was not waterproofed and severe corrosion of the epoxy-coated reinforcing steel was noted in both instances. The Ontario Ministry of Transportation is presently evaluating these structures and bars.

5. An Ontario noise barrier wall, Keele Street and Highway 401 westbound, which has been in service since 1981 was found to exhibit corrosion-induced concrete cracking, rust staining, and spalling after 10 years of service. The precast concrete panels contain a single ECR with low cover (about 0.5 in.) and are subject to deicing salt spray.
6. Another New York bridge deck located in the Albany area and constructed in 1981 was found to contain badly corroded ECRs and to exhibit horizontal cracking that is typi-

cal of corrosion induced delamination. Concrete cover over the ECR varied from 2.0 to 2.4 in. Four of the seven cores taken from this structure in 1990 after 9 years of service were found to be broken into three or four pieces with the ECR at the center.

7. A single Oregon marine test pile was recovered and autopsied after 9 years of exposure. Laboratory examination revealed corroded areas on two of the #4 and several of the #3 hoop bars, while other bars showed no distress. It was reported that there was no visible concrete damage, but active half-cell potentials were recorded in the splash zone region. Low coating thickness was noted.
8. Evaluation of existing epoxy coated reinforcing steel was performed on a 9-year-old coastal bridge in Georgia (*47*). This revealed locations of complete loss of coating bond in spite of the fact that the cover was 5–7 in. Although no cracking or spalling distress was apparent, the steel recovered from two of the six cores that were obtained exhibited corrosion. It was recommended that a phasing out of the use of epoxy-coated reinforcement on bridge decks and marine environment concrete be considered.

Non-FHWA Laboratory and Test Yard Studies

Florida Programs. Several laboratory investigations have been performed to determine the cause(s) of corrosion damage to substructures in Florida (*41,48,49*). Concern was initially focused upon bent bar stirrups because damage was first noticed here and because it has been suggested that when coated bars are fabricated into the required shape there may be some loss of bond between the epoxy-coating and the steel at the outer radius of the bend. Alternately, coating fissures or holidays have been reported to develop at these locations.

Zayed and Sagues (*41,50*) studied the corrosion behavior of epoxy-coated reinforcing steel in concrete exposed to a simulated marine environment. Bent and straight #7 coated and bare rebars were cast into concrete specimens of water-cement ratio 0.5 and after curing were partially immersed in 3.5 percent NaCl such that the apex of the bend was at the water line. Bars from two suppliers were included, both of which contained holidays with these being more dense in one case than the other; and some of the specimens were precracked. It was noted that fabrication resulted in reduced coating adherence, as measured by peel-off with a knife, and increased numbers of holidays and cracks at the outer radius of the bends. Bars coated after fabrication were also included. Intentional coating distress was also included for some of the bars. In general, the data indicated that corrosion was initiated at about the same time for both the coated and uncoated specimens, but corrosion rates of coated bars were about ten times less than for the uncoated ones. The data also revealed significant differences between bars from each of the two suppliers. A follow-on report (*50*) concluded that after 680 days of exposure, "fabrication of epoxy-coated rebar to diameters typical of construction practice tends to cause minute cracking and extensive disbondment of the epoxy cover." It was noted that fabrication defects tended to shorten the time for corrosion initiation, that bars fabricated after coating corroded more severely than straight bars or bars coated after fabrication and that the estimated corrosion rate of the uncoated rebars was an order of magnitude higher than for the epoxy-coated rebars that were fabricated after coating. Appearance of the fabricated bars (bending after coating), which were autopsied after 680 days, showed 1) a darkening of the steel beneath delaminated areas, 2) low pH development in corroded areas, 3) presence of corrosion products in local areas near the epoxy-concrete interface, and 4) small blisters in the coating. Conversely, results from a New York DOT study revealed that not all bent bars exhibited cracking and debonding of the coating (Scotchkote 213). This investigation involved bars from four sources; and coating disruptions, which occurred at the base of deformations on the outside radius, were limited to large #11 bars compared to #3 and #5, as revealed by knife-peel and microscopic examination.

Factors other than fabrication were also addressed by Sagues and coworkers (*41,43,48,50*). Foremost from these studies was the tendency for anodic and cathodic disbonding in various solutions, including limewater, 3.5 percent NaCl and saturated limewater with 3.5 percent NaCl (*48,50*). One study (*51*) involved extensive testing of bars from eight U.S. suppliers from which the following conclusion were reached:

1. Considerable differences were found in the amount of disbonding for the various products. Disbonded coatings eventually enhanced corrosion by promoting the formation of metal-coating crevices where anodic actions are facilitated and additional surface area for cathodic reactions is available.
2. Sodium hydroxide solutions were found to cause significant cathodic disbondment in ECR in the absence of chloride ions, consistent with observations of disbondment in the field when this anion is not present. Laboratory tests upon simulated piling specimens containing ECR confirmed that virtually complete disbondment can take place at cathodic sites where no significant levels of chlorides are present.
3. Delaminations indicative of cathodic disbondment occurred after freely corroding and cathodically polarized exposure to a 3.5 percent NaCl solution. Pitting with little disbondment occurred under anodic polarization.
4. Pitting and delamination occurred in $Ca(OH)_2$ solution under anodic polarization. The corrosion morphology was similar to attack observed on damaged structures. Extensive debonding did not result from cathodic polarization.
5. Prior corrosion in NaCl solution, which was intended to simulate marine jobsite storage, was found to promote anodic disbondment in simulated chloride contaminated concrete environments.
6. Corrosion macrocell action was confirmed as a failure mechanism in simulated marine pilings containing surface damaged ECR. Corrosion of the bars before placement was an aggravating factor at early test times. However, after prolonged exposure even the material without prior corrosion sustained increased corrosion macrocell activity.
7. Field deterioration was interpreted as a combination of several factors, including a) exposure of the bars to a severe marine environment during construction, b) damage from handling and fabrication, and c) occurrence of macrocells.
8. An analytical model was developed for corrosion prediction in substructure members with corroding ECR. This was based upon results from the simulated piling tests combined with field measurements of concrete resistivity. The model was used for estimating the effect of concrete resistivity, piling height and rebar condition on corrosion severity in typical bridge substructures. The results confirmed that the relatively short times

to detrimental corrosion in the field (6–10 years) are consistent with the mechanisms of corrosion advanced in the study.

KCC INC Long-Term Exposure Studies. KCC INC has maintained a long-term exposure program that started in 1982 (*52*) to study straight, specification Scotchkote 214 epoxy-coated reinforcing steel. Findings were reported through 1991 (*22*), and some of the slabs have been studied under the present program. In addition to the epoxy-coated bars both galvanized and uncoated reinforcing steel bars, which met the applicable 1982 ASTM and AASHTO specifications, were procured and cast into concrete slabs using one ready mix truckload of bridge deck quality concrete (water-cement ratio 0.42 by weight). The epoxy-coated rebars were obtained directly from the coater; and so they were not subjected to normal handling, transportation, or jobsite exposure prior to concreting. No intentional coating defects were introduced. The slabs were 1 ft by 2 ft by 6 in. and contained two mats of reinforcing steel with 1 in. of concrete cover over the top mat rebar. Some slabs contained the same type of rebar (epoxy-coated, galvanized or bare) in both mats, while for others the top mat was epoxy-coated or galvanized but the bottom one was uncoated rebar. After curing, the slabs were subjected to 3.1 years of ponding 3 days a week with a 3 percent NaCl solution and 4 days of natural weathering (solution removed). The salt ponding was terminated in December 1985, because more than 10 lbs per cubic yard of chloride was present at the top rebar level; and subsequently the slabs were subjected to natural weathering only. As of June 1991 the salted slabs with uncoated rebar and those with galvanized rebar exhibited corrosion induced cracking, while the ones with epoxy-coated reinforcing steel were uncracked.

Surveys in the fall of 1991 identified the presence of hairline cracks of length 2–12 in. on five of the six salted epoxy-coated rebar slabs. Most of these were aligned with the top mat reinforcing, but no cracking was detected on the unsalted epoxy-coated reinforcing steel slab. In February 1992, one-half of one of the cracked epoxy-coated rebar slabs (epoxy-coated rebar in the top mat only) was removed from test and autopsied. Prior to this, the macrocell corrosion current was 0.026 mA/ft^2, the most negative top mat half cell potential was −166 mV (CSE) and the mat-to-mat AC resistance was 475 Ohms. In contrast, the initial mat-to-mat resistance for this slab after curing was 539 Ohms, whereas the corresponding value for uncoated rebar slabs averaged 22 Ohms. Although this 1992 data would not normally be considered particularly bad with respect to ongoing corrosion, the autopsy revealed significant corrosion of specification epoxy-coated rebar 2. The coating on this bar had blistered, exhibited cracked areas, was disbonded or easily removed and exhibited a pH on the coating underside of 4.5–5; and corrosion of the epoxy-coated rebar was apparent. Figure A-6 presents photographs of 1) the slab surface before autopsy, 2) the trace of rebar 2 in the concrete, and 3) a blistered and cracked portion of the epoxy-coated rebar. Interestingly, epoxy-coated rebar 1, which was from the same production lot as rebar 2, showed no significant corrosion or other deterioration. The coating on this bar was tightly adhered and flexible; and when the coating was removed, the metal substrate appeared clean and shiny. It was projected that the epoxy-coated rebar slabs were, in 1992 (10 years or exposure), experiencing the early stages of corrosion failure.

CRSI-Sponsored Research. In this program, which was also performed by KCC INC., both bent and straight epoxy-coated reinforcing steel bars, produced by eight different U.S. suppliers in 1988, were incorporated into test slabs and exposed and evaluated for 3-plus years. All bars except those from one supplier met specification, and the coating on most was of very high quality (many had zero holidays and bare areas). No intentional defects were introduced. All suppliers knew that the bars would be used for research purposes; and none were subjected to normal handling, transportation, or field storage. Twenty variables, including comparison with uncoated rebar, coating thickness, bend speed and temperature, patching of the outer bend radius, coating before and after fabrication, and bend diameter were addressed. Sixty slabs (three per variable), each of which contained a macrocell with the straight top mat and with the bent top mat rebar, were cast. Concrete cover over the top mat rebar was 1 in. in all instances, and the water-cement ratio was 0.47 by weight. All bottom mat rebars were uncoated, and the bottom-to-top rebar surface area ratio was 1.7 for the case of #5 top mat rebars and 1.9 for the #4 case. Forty slabs (two per variable) were subjected sequentially to:

1. 1.35 years of Southern Exposure cycling (a weekly cycle consisting of 4 days ponding with 15 percent NaCl at room temperature followed by 3 days unponded at 100°F and ultraviolet light). (See *NCHRP Report 244.*)
2. 0.4 to 0.9 years of continuous tap water ponding at 70 °F with the bottom surface exposed to laboratory air.
3. 1.3 years of natural weathering outdoors in Sterling, VA.

It was concluded from the Southern Exposure cycling that a net drying had occurred, as evidenced by an increase with time of the AC resistance between mats. In contrast, slabs stored outdoors typically maintained a relatively constant temperature corrected mat-to-mat resistance. It was concluded from this that the Southern Exposure probably does not reflect a typical real world condition and that testing according to such a protocol may yield misleadingly optimistic ECR performance results. At the end of Southern Exposure testing, the slabs did have high chloride concentrations (greater than 10 lbs/yd^3) at the rebar level, and so the subsequent continuous tap water ponding provided a high moisture content, thereby facilitating accelerated corrosion.

The remaining 20 slabs (one per variable) were exposed to natural weathering but without salt water ponding exposure. For all slabs, half-cell potential, mat-to-mat AC resistance, and macrocell current of the embedded rebars were monitored throughout the exposure.

Corrosion-induced cracking of the uncoated rebar control slabs was noted at 1.3 years in association with macrocell current densities in the range of 1.5 mA/ft^2 of top rebar surface area. At the end of Southern Exposure cycling (1.35 years), no rust staining or cracking was apparent on any of the epoxy-coated rebar specimens with 74 percent of these exhibiting what conventionally has been assumed to be a negligible macrocell current density (less than 0.01 mA/ft^2 of total bar surface area). Autopsies performed on selected slabs showed only a few, small, isolated areas of corrosion and blistering on the ECRs. In these areas, the coating was poorly bonded and brittle, but elsewhere it was well adhered.

However, during tap water ponding, the macrocell current on a majority of the epoxy-coated specimens increased and approached values typical of the uncoated rebar slabs. Correspond-

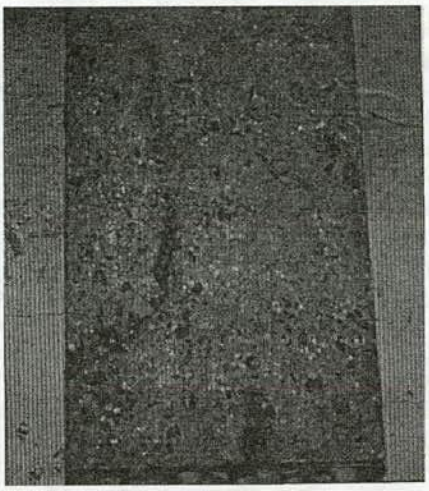

Cracked Slab Surface Before Autopsy

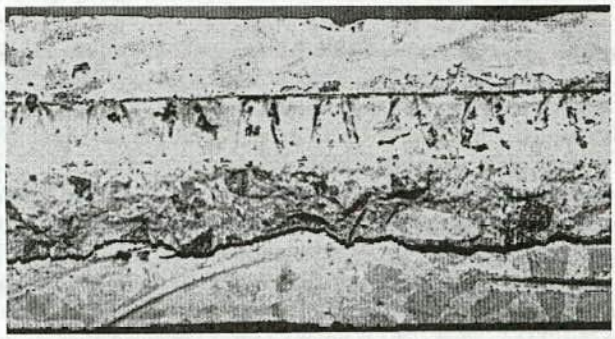

Trace of ECR #2

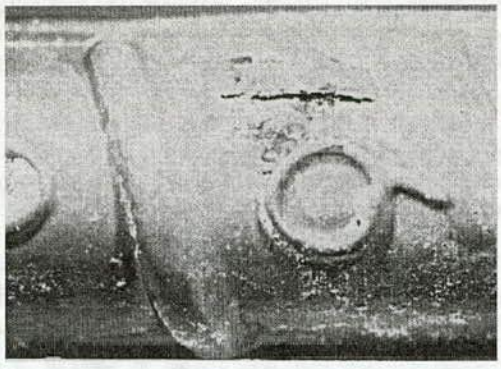

ECR #2 with Crack in Coating

Closeup of the Trace of ECR #2 with Rust

Closeup of Crack in ECR #2

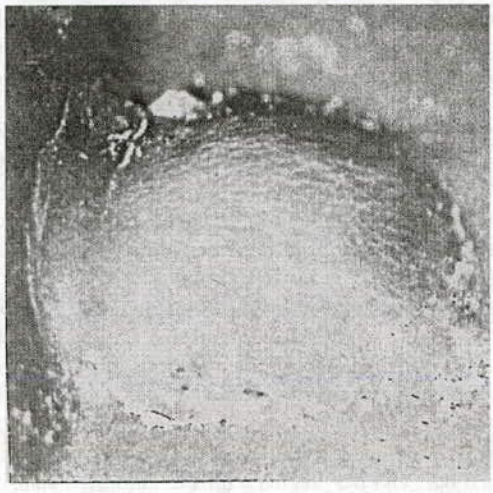

Closeup of Blister in ECR #2

Figure A-6. Feb '92 autopsy of KCC INC epoxy-coated rebar long-term exposure Slab 6.

ingly, mat-to-mat AC resistances decreased, in some instances by greater than an order-of-magnitude. These observations indicated that for these slabs the epoxy-coating was no longer providing adequate corrosion protection, and the high corrosion rates continued or increased on many of the specimens when they were transferred to outdoor exposure. Statistical analyses of the data indicated that coating thickness, bent versus straight bar, coating before or after fabrication, bend speed, and bend temperature had no significant effect upon the ECR performance. Generally, both the bent and straight bars from five of the sources performed poorly, while those from two sources performed well (no salted slabs from one source remained after Southern Exposure). It was concluded that maintenance of a high electrical resistance was essential and that some yet unidentified property of the coated bars from the latter two versus the former five sources was responsible.

Concrete cracking over the top mat epoxy-coated rebar occurred on three slabs at 2.6 years exposure (January 1991), and 42 percent of these slabs were cracked over both bent and straight bars by 3.0 years exposure. Seventy-six percent of the epoxy-coated rebar specimens exhibited macrocell currents in excess of 0.01 mA/ft^2, 68 percent in excess of 0.1 mA/ft^2 and 24 percent above 1 mA/ft^2. The highest macrocell corrosion current density recorded for an epoxy-coated rebar specimen was 2.8 mA/ft^2, in comparison to a maximum for the bare bar slabs of 3.9 mA/ft^2. An autopsy of three slabs in mid-1991 confirmed severe corrosion on bars from two of the high current/low resistance specimens but no corrosion for a low current/high resistance one.

High corrosion rates continued, and additional slabs exhibited corrosion induced cracking. In February 1992, two additional specimens were broken open as a part of the present project. Both were cast with very high-quality epoxy-coated rebars that exhibited no significant holidays or bare areas. Figure A-7 presents photographs of the concrete and coated rebars from these after 3.25 years of exposure. The concrete was cracked and delaminated, the corrosion severe and the coating was brittle, blistered, cracked, and debonded in many areas on both the straight and bent bars. A black deposit was apparent beneath the coating, and pH for this was in the range 5–6.

Epoxy-coated rebars in slabs that were subjected to outdoor exposure only (no salt) did not experience loss of insulative properties, as measured by mat-to-mat resistance, or exhibit any macrocell corrosion, rust staining or concrete cracking. No studies of coating adhesion have been performed upon ECRs from these slabs.

It was initially concluded from this research that the Southern Exposure was not sufficiently aggressive for evaluating ECR because of its drying effect on the concrete and that damage to the epoxy-coating protective properties was a consequence of the continuous ponding phase of the experiments. As a part of the recently completed C-SHRP (*45*), however, AC resistance of retained bars and bars recovered from autopsied slabs subsequent to the Southern Exposure was measured. Values for the former were indicative of a quality protective coating (resistance ratio for 10 of the 11 bars tested exceeded 2,400), while this was not the case for the latter (70 percent had resistance ratios below 300). It was concluded that the epoxy-coating had been compromised by the Southern Exposure, although severe corrosion activity did not take place during this time because moisture content of the concrete was low. On the other hand, the presence of moisture from the continuous tap water ponding established conditions that were conducive for corrosion.

In fall 1991, approximately one-half of these slabs and many of the retained bars were transferred to Wiss, Janney, Elstner, Associates, Inc (WJE) for further evaluation under CRSI sponsorship. WJE concluded that the KCC INC. measurements underestimated holidays and bare areas and that the macrocell current data for the slabs correlated with coating defect densities (*53*). However, Clear (*46*) has rejected this explanation on the basis that 1) the WJE measurements included data from the bar ends (not embedded in concrete) where the density of defects was high, 2) the measurements were made on retained bars whereas KCC INC used the best bars for casting into the concrete specimens and 3) an increase in defect density with time may have occurred for the bent bars.

Epoxy-Coated Reinforcing Steel Specifications

Review and Commentary. The applicable AASHTO, ASTM, draft NACE, and OPSS specifications define what has become more or less standard in the United States and Canada, although it is expected that these documents will experience revision and change with time. The situation is less well defined in Europe, however, where acceptance of ECR has been more deliberate and the technology has been approached with greater caution and skepticism than in the United States. Some European countries (Norway and Denmark) have adapted ASTM A775 (*54*), while others (Germany, Great Britain, and Switzerland) have developed their own specifications; the Germans and Swiss having worked in concert. In the Netherlands, research, which could serve as the basis for development of a specification, has recently been concluded by TNO (Dutch Paint Research Institute), and a specification has been recommended. This, however, is not significantly different from the British document. Where separate specifications have been developed, the promoters of these national standards point out that they are more strict than the ASTM counterpart (*55*). The European situation is undoubtedly a dynamic one in view of the EC requirement for commonality. Based upon the information acquired, distinctions between ASTM A775, BS7295, and GFORB upon which the Europeans focus are listed below (note: BS7295 is the British specification, "Fusion Bonded Epoxy-Coated Carbon Steel Bars for the Reinforcement of Concrete" and GFORB refers to the draft standard, "Guidelines for the Use of Epoxy-Resin Coated Steel Reinforcements," published by the German Federal Office of Road Building in January 1990):

A. Profile/Amplitude: Not specified by ASTM A775, qualitatively specified by ASTM D3963 and AASHTO M284, quantitatively specified by draft NACE spec. (1.5 to 4 mils). BS7295 specifies 50–70 microns (1.3–1.8 mils) and GFORB references the ISO 8503 comparator.

B. Surface Preparation: ASTM references SSPC SP10, BS7295 references BS2451, and GFORB references DIN 55928. The ASTM and GFORB are thought to be essentially the same, whereas the British consider their requirement superior.

C. Coating Thickness: ASTM requires 90 percent at 5 to 12 mils with no specified min/max. BS7295 lists 6 to 10 mils for 95% and 5 to 12 mils for 100%. GFORB specifies 5 to 12 mils with min. of 3 and max. of 12 mils.

Delam in N2-SE1

Delam in N7-SE2

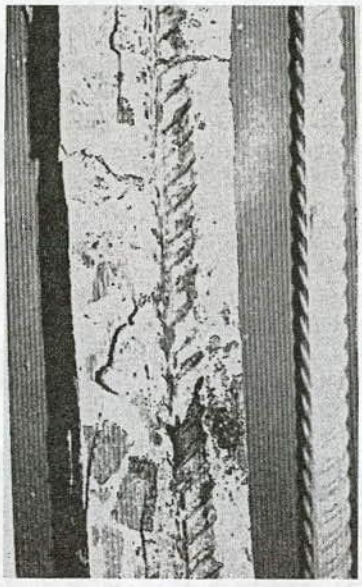

Straight Bar & Trace N2-SE1

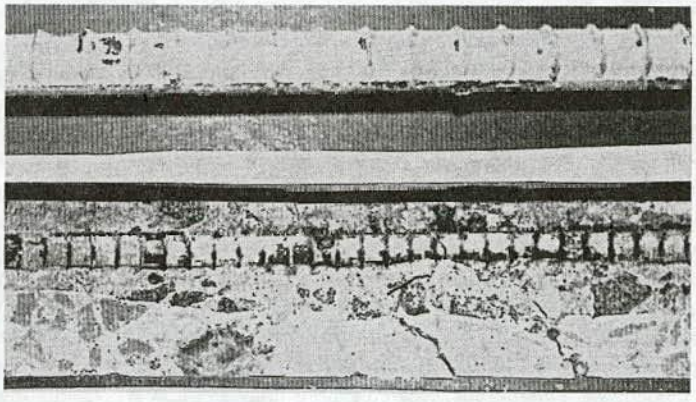

Left Straight Bar & Trace N7-SE2

Typical Cracking of Coating N2-SE1

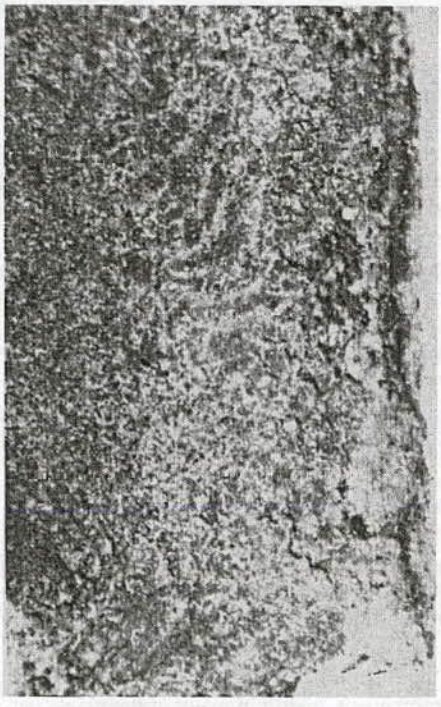

Underside of Epoxy from Bent Bar N7-SE2

Figure A-7. Autopsy findings—specification epoxy-coated rebars after 3.25 years of exposure to intermittent saltwater ponding, tap water ponding, and outdoor exposure.

D. Surface Defects: ASTM states that bare areas up to $0.09in^2$ and up to 2 percent of bar area are acceptable. BS7295 lists $0.016in^2$ as an upper limit with no more than four defects per bar length (length unspecified), while GFORB has $0.04in^2$ and 0.5 percent.

E. Cure of Coating: GFORB specifies Differential Scanning Calorimetry and Infra Red Spectroscopy to determine extent of cure.

F. Coating Material Tests (Prequalification): These include a) chemical resistance, b) applied voltage, c) chloride permeability, d) abrasion resistance, e) impact resistance, and f) hardness and are generally similar between the three specifications, although GFORB does not address d) or f). However, the German testing includes preliminary, quality assurance and external monitoring, where the latter involves a separate contract subject to GFORB approval.

European ECR projects are not emerging in concert with the availability of the respective national standards, the foremost example being the 4-mile-long Great Belt Tunnel in Denmark. While ASTM A775 was the applicable document for this activity, design and construction incorporated elaborate quality control and coating techniques based upon a modern fluidized bed dipping plant that handled blasted and preheated prefabricated reinforcing cages 1.3 x 5.4 x 13.7 ft in size (*56*).

This and related indications suggest that much of the European community considers ASTM A775 insufficient and U.S. ECR practice inadequate. The present research team is unaware, however, of any long-term service experience that permits calibration of the different specification criteria, which the Europeans have developed, and of any correlation of these with service experience or projected service performance. Thus, each specification incorporates generally recognized hallmark coating integrity tests and adapts its own emphasis and parameter limits, often with a degree of apparent arbitrariness, according to knowledge at the time of authorship and perception of the writers. On this basis, the different opinions regarding what is required to achieve acceptable ECR performance, as reflected by specification distinction, should not be surprising and are a natural consequence of the differences between U.S. and European practice and the approach of each to public construction. Also, there appears to be a tendency in the European national codes to "make ours better" (that is, more strict). The critical questions are, however, what are the important parameters for assuring long-term ECR corrosion resistance in concrete and what are the parametric specification requirements to achieve this.

CRSI Coater Certification Program and Proposed Specifications. In June 1991, the research team requested and received a copy of "CRSI's Voluntary Certification Program for Fusion Bonded Epoxy Coating Applicator Plants" (*57*). An update was provided in August 1991 (*58*). In the attachment to a February 1992 letter, CRSI notes ". . . that CRSI's independent inspection agency for the Plant Certification Program has observed significant improvements in quality in many of the plants participating in the CRSI Certification Program"; and that "Industry support for CRSI's voluntary quality control program is strong. CRSI has certified nine plants since the program was launched in June 1991, and has a number of applications pending" (*59*).

The certification program is a detailed and extensive one and involves quality control guidelines, commentary, test procedures, rating scales and checklists covering the following: Handling and Storage of Uncoated Bars, Surface Preparation, Heating, Storage and Handling of Powder, Powder Application, Curing, Continuity of Coating, Thickness Measurement, Bend Tests, and Handling and Storage of Epoxy-Coated Bars.

The document was reviewed in detail and the tests used therein were compared to those performed in the C-SHRP and the present NCHRP efforts, as summarized in Table A-1. It is notable that the certification process relies solely on measurements of present condition "in air" and does not include any tests aimed at predicting performance of the bars in concrete. Of those certification tests applicable to coated bars that had already passed the bend test, only a single test is used in the program (chloride on cleaned bar surface) but not used in the C-SHRP and NCHRP programs. However, several methods are used in the C-SHRP and NCHRP programs but not in the certification program. These include pencil hardness, through-film and underside coating foam evaluations, dry knife adhesion tests, AC resistance tests, the accelerated corrosion test, and the chemical immersion test.

It is concluded that the CRSI certification program in its present form does not include sufficient tests to ensure that the epoxy coating will not disbond from the steel substrate when exposed to a concrete environment.

Also, CRSI (*59*) and others have recently proposed several specification changes to NACE, ASTM, and AASHTO, including:

1. Increasing the minimum coating thickness to 7 mils;
2. Requiring repair of all visible damage;
3. Making the bend test more severe; and
4. Further quantifying the required anchor pattern after cleaning (1.5 to 4 mils as determined by replica tape measurements).

It is notable that in the KCC INC bent bar studies the bars with a desired coating thickness of 6 mils performed no differently than those with an intended thickness of 9 or 12 mils; that straight bars performed almost as poorly as bent bars; and that many bars either with no visible damage or with no more than two holidays per foot performed poorly. Although results of the bend test may relate to adhesion of coating to the steel in a qualitative way, they are not necessarily relevant to long-term coating adhesion in the alkaline concrete environment. Thus, it is concluded that these proposed specification changes are not sufficient to assure significantly improved performance of ECR/concrete members in adverse environments.

The above programs, voluntary certification of coating plants, and improved specifications are valuable additions to the quality assurance process for ECR; and the individuals and organizations involved should be commended. Unfortunately, at present it is believed that the programs are not measuring the properties that have been found to be the most important determinants of performance and, thus, neither the certification program nor the proposed specifications can be expected to yield ECRs that provide long-term corrosion protection to concrete members in adverse environments. Once other tests, especially adhesion tests that simulate long-term exposure in concrete, are available, correlated with long-term performance and subjected to round-robin testing, their adoption in both of these programs should be considered. It is notable that the CRSI program recognizes the need

Table A-1. CRSI volume certification program for coating plant: quality control item conducted by KCC INC and CRSI program

Quality Control Items	KCC INC Measurement	Required by CRSI Certification Program
HANDLING AND STORAGE OF UNCOATED REINFORCING STEEL BARS		
1. Contaminants (Visual)	Yes (When coating removed)	Yes
2. Surface Defects (Visual)	N/A	Yes
SURFACE PREPARATION		
1. Blast Cleaning:		
Visual Check	Yes	Yes
Copper Sulfate Test	Yes (Backside of Coating)	Yes (On Rebar Surface)
Detection of Chloride	No	Yes
Backside Contamination	Yes (Backside of Coating)	Yes (Backside of Tape)
2. Anchor Pattern:		
Replicate Tape	Yes	Yes
Profilometer	Yes (Perthometer)	Yes
3. Abrasive Contamination:		
Oil Contamination	N/A	Yes
Detection of Chloride	N/A	Yes
Sieve Analysis	N/A	Yes
HEATING		
1. Bar Temperature	N/A	Yes
STORAGE AND HANDLING OF POWDER		
1. Powder Temperature	N/A	Yes
2. Shelf Life	N/A	Yes
3. Powder Certification	N/A	Yes
POWDER APPLICATION		
1. Cleaning/Coating Application Interval	N/A	Yes
2. Spray Application	N/A	Yes
3. Air Supply	N/A	Yes
CURING		
1. Gel Time	N/A	Yes
2. Time-to-Quench Requirements	N/A	Yes
3. Pencil Hardness	Yes	No
CONTINUITY OF COATING		
1. Holiday (67 1/2 Volt DC Detector)	Yes	Yes
THICKNESS MEASUREMENT		
1. Magnetic Gauge	Yes	Yes
ADHESION TESTS		
1. Bend Test	N/A	Yes
2. Dry Knife Adhesion	Yes	No
HANDLING AND STORAGE OF EPOXY COATED BARS		
1. Coating Abrasion (Coating Damage)	Yes	Yes
2. Exposure to Moisture	N/A	Yes
3. Rejected Coated Material	N/A	Yes
PREDICTING PERFORMANCE IN SALTY CONCRETE		
1. Accelerated Corrosion Test	Yes	No
2. Chemical Immersion Test	Yes	No
3. Rapid Macrocell Test	Yes	No

for updating as the technology changes and has made provisions for modifying the program when appropriate (*57,59*).

Epoxy-Coated Reinforcing Steel Test Methods

Overview of Failure Mechanisms: Test methods for epoxy coatings on steel have existed for some time; but for ECR these are relatively new and, in fact, continue to evolve. Prior to considering the appropriateness of various test methods for epoxy-coatings and ECR, it is important that probable failure mechanisms be reviewed. Only by doing this can the relevancy of the phenomenon or property being measured to coating integrity be established. In this regard, epoxy-coatings provide protec-

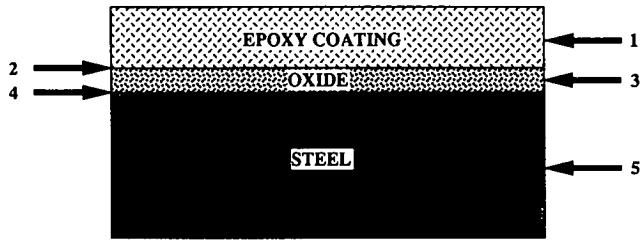

Figure A-8. Potential failure sites on epoxy-coated steel: 1- Epoxy; 2- Epoxy/Oxide Interface; 3- Oxide; 4- Oxide/Steel Interface; and 5- Steel.

tion by acting as a physical barrier that prevents or slows down the arrival of corrodents to the coating/steel interface. Failure of organic coating systems can be attributed to several phenomena, including 1) mechanical damage, 2) cathodic disbondment, 3) anodic undermining, 4) blistering, and 5) wet adhesion loss. Ultimate failure can take place in five localized areas, as shown by the schematic in Figure A-8. In most cases, failure is the result of anodic activity under the coating, which leads to the destruction of the coating-to-steel bond or production of hydroxides at cathodic regions, which dissolves the oxide film or reacts with the coating/oxide bond (or both). Also contributing is wet adhesion loss. This occurs when the coating is displaced from the substrate by a thin layer of water. Although wet adhesion loss is often recoverable, it may become permanent in the presence of a stress that can arise from applied loads, through substrate deformations or by build-up of underfilm corrosion products. Each of these possibilities can reduce or destroy the coating/metal bond. In addition, wet adhesion loss can set up the necessary conditions for local cell action or facilitate the formation of osmotic blisters. Each of the above scenarios can ultimately lead to degradation of the coating system (*60*).

The German and Swiss ECR research communities have placed emphasis on hot water testing (HWT) as a quality and performance indicator. Such an approach has a historical basis both within ASTM, per recommended practices C870-86 and C868-85, and elsewhere with specific applicability to epoxy coatings (for example, the buried pipeline industry). The procedure involves immersion of samples in hot water at, for example, 90°C or a temperature that is at least 10°C below the glass transition temperature of the epoxy. High osmotic pressures result in rapid vapor migration to the coating-steel interface and blister formation at locations of poor adhesion. As such, the procedure is an indicator of adhesion loss. The test is considered particularly relevant to service performance, because adhesion is a fundamental property upon which coating integrity and substrate protection from corrosion are projected to depend in most cases. The criterion for classifying a particular coating or specimen as being of acceptable quality is that no blistering occur within 7 to 10 days. Experiments by the present research team have judged this criterion to be inadequate for the coatings and ECRs evaluated; and more quantitative criteria are recommended based upon parameters inherent to electrochemical impedance spectroscopy (EIS) and adhesion testing, as described below. The present project team considers, however, that the HWT has utility with regard to the goals of NCHRP 10-37; and Task 2 and Task 4 experiments have accordingly been based upon this technology (see Chapter 3). To repeat, no correlations presently exist whereby HWT results, or results from any other accelerated test for that matter, can be directly correlated with service performance. However, the present research team is investigating the utility of accelerated tests for prediction of service performance and quality control.

EIS has evolved over the past several decades from a corrosion science laboratory technique to the point where it is now finding applicability in corrosion engineering. The procedure involves making impedance measurements as a function of frequency and is particularly applicable to coated systems such as ECR since the influence of coating resistance, which can cloud or invalidate direct current measurements, is easily separable from other electrochemical properties of the system. The resultant impedance plots can provide both mechanistic information and performance indications such as significance of defects and electrolyte take-up by the coating. Sagues and co-workers (*61–63*) have successfully used EIS in laboratory ECR experiments involved intentionally damaged bars and were able to project corrosion rate from the data and to confirm a macrocell model using specimens that simulated pilings on Florida Keys bridges, as briefly reviewed above (see the section titled, "Florida Programs"). EIS is a complex technology, however, which involves sophisticated instrumentation and interpretation complexities; and it is unrealistic to consider that it can be developed into a practical field tool within a single project.

Adhesion strength is another property that would be determined in conjunction with hot water testing. Measurement of coating adhesion is difficult because of the absence of simple methods whereby the force necessary to separate a coating from its substrate can be applied. In effect, the measurement of the adhesive strength of a coating is much like determining the cohesive force holding a material together, in which case conventional tensile testing can be used. Any mechanically induced separation between coating and substrate involves energy input to the system. This energy consists of 1) the energy to create new surfaces, 2) the energy absorbed during plastic deformation of the metal, and 3) the energy absorbed during plastic flow of the viscoelastic material (coating). Material failure or coating adhesion loss could ideally be quantitatively evaluated utilizing first principles by employing Fracture Mechanics. However, the fundamentals of Fracture Mechanics are not well established for this particular application (coating adhesion failure), and so scientists and engineers typically use empirically developed adhesion tests. A number of such methods are available, including abrasion, impact, cross-cutting, mandrel, shearing, knife cutting, centrifugal, deceleration, tensile, and blister tests. However, only the last five are capable of providing quantitative or semi-quantitative test results. An overview of these tests is provided by Asbeck (*64*). Of these, knife cutting is the easiest to employ. This involves forcing a sharp blade along the interface between a coating and a substrate. The hand-held versions provide only semi-quantitative ratings and can be subject to operator error and variability. However, the reliability and accuracy of this technique are enhanced by employing an instrumented version, such as the Hesiometer, which can provide results in absolute units. The tensile test was considered by the present research team as most appropriate, and it is this methodology that has been adopted for development as a method to measure adhesion strength. Tensile testing provides quantitative results that permit easy comparison of different coating systems, coating suppliers,

coating applicators and different environmental conditions. This procedure has been combined with hot water immersion. Observations made during continuous ponding of CRSI slabs (*22*) and the recent work of Sagues (*65*) suggest that either wet adhesion or cathodic disbondment (or both) are major contributors to ECR failure. Therefore, developing techniques to measure coating adhesion as a function of various environmental parameters were part of the NCHRP 10-37 project team's efforts. Development of a reliable adhesion test will serve two purposes. First, it will assist in understanding mechanism(s) of failure and, second, it should lead to the establishment of a potentially new quality control test. A complete description of the tensile adhesion test procedure and preliminary results are presented in Appendix G and are discussed in Appendix H. The objective of conducting adhesion tests as a part of the present program was to better characterize the properties of ECR before placement, to distinguish differences among the various coaters and to assist in elucidation of the mechanism(s) of ECR failure, particularly at early times of exposure.

FEASIBILITY OF HYBRIDIZED CORROSION PREVENTION METHODOLOGIES FOR ECR

The possibility that epoxy-coating of reinforcing steel cannot be relied upon to provide long-term protection of bridge decks from corrosion leads to the consideration that an additional corrosion mitigation technique or techniques be used in conjunction with ECR. Cathodic protection (CP) is presently recognized as a proven technology for reducing or arresting ongoing corrosion on existing structures; and a corrosion inhibitor (calcium nitrite in particular) is known to accomplish the same result when admixed with concrete in association with new construction. Each of these alternatives is discussed below.

Cathodic Protection

This corrosion prevention methodology is widely used in concert with epoxy coatings in the gas transmission pipeline industry. After identifying distress with ECRs in salty concrete in the field and in laboratory and outdoor exposure specimens, the Florida Department of Transportation and KCC INC initiated independent tests and trials on the use of CP to control corrosion of ECR in concrete.

The Florida Department of Transportation has developed a method of corrosion control for deteriorating epoxy-coated rebar substructures, which involves flame or arc spraying of a sacrificial zinc anode coating on the surface of the affected members after delamination removal and cleaning. The initial trials have been in place for over 2 years and are performing well with adequate current distribution and polarization of the embedded reinforcement (*66,67*). A program based upon this methodology is now being implemented on the Florida Keys substructures containing ECR that exhibit concrete distress.

Tests were conducted to determine the feasibility of cathodic protection of epoxy-coated reinforcing steel in concrete and to define means of electrically connecting epoxy-coated rebars to allow corrosion monitoring and the application of cathodic protection (*68*). The major points addressed were 1) the ability to adequately polarize corroding epoxy-coated rebars in salt contaminated field concrete, 2) the effect of a bottom uncoated rebar mat, 3) the ability to adequately polarize epoxy-coated rebar and the current requirements associated with this polarization, and 4) the means for interconnecting rebars when spot welding is deemed unacceptable for structural reasons.

To address the question concerning adequate polarization of epoxy-coated rebars in salt-contaminated field concrete, a portion of the Ontario Noise Barrier Wall panels (*46*) was studied. Four wall sections, 1 to 2 ft long by 8 in. wide and 2 in. thick, were fitted with a conductive paint cathodic protection anode; and the system was powered to protect the single embedded epoxy-coated rebar. Two of the specimens were from storage panels (no field exposure), one was from the top panel of the field wall, and another was a portion of the bottom field wall panel. Half-cell potentials were monitored at two locations per specimen. After collecting static data, the CP system was activated on November 13, 1991, at KCC INC laboratories. Though the desired current density was 0.25 mA TRMS (true root mean square) per square foot of rebar, difficulty was experienced in maintaining this value, apparently because circuit resistances varied depending upon moisture content of the concrete; and the resultant current densities ranged from 0.047 to 1.427 mA TRMS/ft^2 and averaged about 0.30 mA TRMS/ft^2. The data (instant-off potentials and magnitude of depolarization) collected immediately after and 1 month after power application indicated that the epoxy-coated reinforcing steel was readily polarized and fully protected. Values for the individual specimens and monitoring locations were presented in the Appendix of the Interim Report (*69*). Polarization and depolarization were lowest on the bottom field panel wall section, which is consistent with this concrete having the highest chloride level and the most ECR corrosion.

After three months of CP, the epoxy-coated rebar was removed from one of the storage panel sections and compared to a bar removed from another section of the same panel which had not been subject to cathodic protection. No adverse effects of the cathodic protection were noted.

Epoxy-coated reinforcing bars have been extensively employed historically in decks with uncoated rebar bottom mats. To study this situation, slabs with two mats of reinforcing steel were cathodically protected. One slab had epoxy-coated reinforcing steel in both mats with the top steel undergoing the early stages of deterioration. A second slab with this same type of epoxy-coated rebar had an uncoated rebar bottom mat, while a third had badly corroding epoxy-coated straight rebar in the top mat and uncoated rebar in the bottom. A fourth slab had a badly corroded bent epoxy-coated rebar in the top mat and straight uncoated rebar in the bottom. All slabs were heavily chloride contaminated in the area surrounding the top rebar with essentially chloride free concrete about the bottom one. These slabs had been tested in previous KCC INC work on epoxy-coated rebar without CP. Slabs 1 and 2 were 1- by 2-ft long-term outdoor exposure specimens, and slabs 3 and 4 were from a bent bar specimen, which was cut in half (*22*). Macrocell corrosion current densities prior to the application of cathodic protection were as follows (top rebar anodic);

Slab 1—Epoxy Both Mats	= 0.0027 mA/ft^2
Slab 2—Epoxy Top Only	= 0.0042 mA/ft^2
Slab 3—Epoxy Bent, Top Only	= 0.835 mA/ft^2
Slab 4—Epoxy Straight, Top Only	= 0.156 mA/ft^2

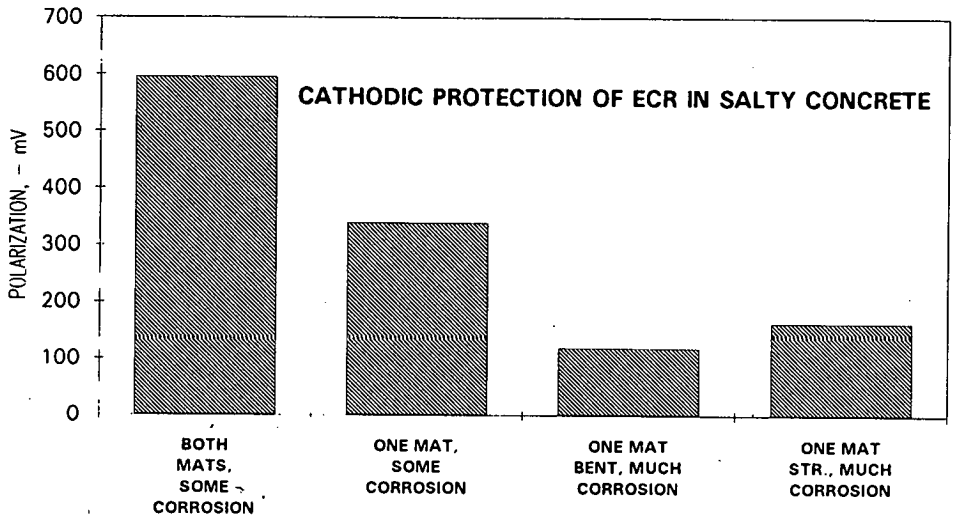

Figure A-9. Polarization at 1 mA/sq. ft. of rebar.

In all cases the cathodic protection anode was installed on the top slab surface, and the top and bottom mats remained interconnected. The CP systems for slabs 1 and 2 were activated in October 1991; and those for slabs 3 and 4 were activated in mid-November 1991. The slabs were initially powered at the KCC INC outdoor exposure facility, moved into the laboratory to allow continued testing during the winter of 1991–92, and subsequently returned to the outdoor test facility. Testing continues today. While in the laboratory they were subjected to a weekly wet-dry cycle by covering them with wet burlap and plastic for three days each week. After a short period at 0.5 mA TRMS/ft^2 of total rebar, all systems were adjusted to 1 mA/ft^2. Cathodic protection system voltages were in the range 1.5 to 3.5 volts to maintain the constant current. Half cell potentials were monitored at three to five locations per slab, including via wells drilled close to the top mat rebar. On all four slabs, the corrosion macrocell was reversed by the cathodic protection, thus indicating that the top mat rebar had been cathodically polarized, rather than being anodic and corroding as was the case prior to CP. Polarization (7 days for slab 1 and 24 hours for the other slabs) exceeded -100 mV at all sites monitored. Average values are presented in Figure A-9, and the data through December 1991 were listed in the Appendix of the Interim Report (*69*). Note that the polarization was greatest for the slab with epoxy-coated rebar in both mats and least for the slab exhibiting the highest corrosion rate (bent top mat epoxy-coated rebar, uncoated bottom rebar). Figure A-10 presents the percent of the total cathodic protection current received by the top mat epoxy-coated rebar in each slab. Note that more current was received by the uncoated rebar in the bottom mat for slabs 2 to 4 than in the case of the epoxy-coated bottom mat rebar in slab 1. However, this did not create difficulties in protecting the top mat rebar in any of the slabs. Depolarization at all measurement locations on all slabs exceeded 100 mV (average 24 hour depolarizations varied from 160 to 842 mV).

The specimens continue to be monitored. After 2 years of cathodic protection, the CP voltages to provide 1 mA/sq. ft. (11 mA/sq. m.) of TRMS current range from 3.5 to 4.8 volts. A detailed nondestructive evaluation performed in October 1993 (2 years of CP) found that current distribution and polarization/depolarization characteristics were unchanged from those reported in Figures A-9 and A-10. The average 48-hour depolarizations were as follows:

Slab 1, Both Mats ECR, Some Initial Corrosion = 705 mV
Slab 2, Top Mat Straight ECR, Some Initial Corrosion = 466 mV
Slab 3, Top Mat Bent ECR, Much Initial Corrosion = 195 mV
Slab 4, Top Mat Straight ECR, Much Initial Corrosion = 254 mV

Companion ECR control slabs without CP exhibited progressive rust staining, cracking and delamination during the 2-year test period. No additional cracking, rust staining, or delamination occurred on the ECR slabs, which were under cathodic protection.

As noted in earlier sections, ECR appears to be subject to naturally occurring adhesion loss after prolonged (2 to 10 year) exposure to a moist concrete environment. This knowledge has raised questions concerning the effect of adhesion loss on the structural performance characteristics of ECR. If ECR is susceptible to cathodic disbondment under normal exposure conditions, it is logical to assume that cathodic protection could accelerate coating disbondment. But, will that lead to bond/pullout problems in existing structures? A research effort was conducted at KCC INC to address this question. The effort involved casting of bond test specimens, application of various levels of cathodic protection (including none) over a period of time, and the performance of bond/pullout tests (*70*). The bond test specimen configuration was similar to that used in other studies (*71,72*) with the exception that #5 bars (both epoxy coated and uncoated) were used instead of #4 reinforcing bars. The epoxy coating on the ECRs was Scotchkote 213. Variables included:

Non-Salty Concrete, Uncoated Rebar, and No CP
Non-Salty Concrete, ECR, and No CP
Salty Concrete, ECR, and No CP
Salty Concrete, ECR, and 50 Amp-hr/sq. ft. (540 Amp-hr/sq. m.) CP

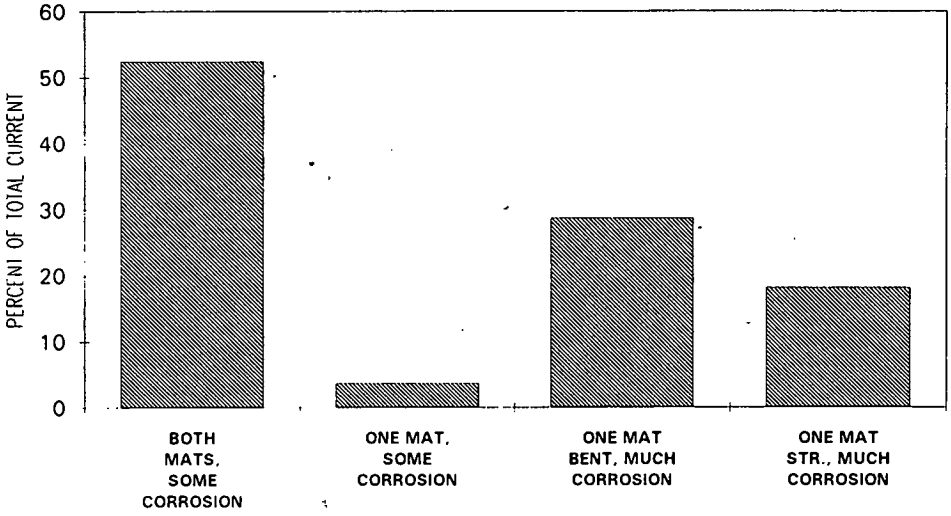

Figure A-10. Percent of current to top mat rebar.

Salty Concrete, ECR, and 100 Amp-hr/sq. ft. (1,080 Amp-hr/sq. m.) CP

A minimum of three specimens represented each variable. Figure A-11 presents the average findings with respect to ultimate stress, loaded end slip and free end slip for each variable. Conclusions of this research were as follows:

1. Based upon these studies and the references, it would appear that the application of cathodic protection simply accelerated the naturally occurring ECR coating/steel substrate adhesion loss phenomenon. But, most importantly, the loss of coating adhesion and the passage of currents equivalent to about 12 years of cathodic protection had no significant effect on the bond/pullout strength between the concrete and the ECR.
2. This work also has significance with respect to ECR field structures that have poorly adhering coatings and to others that may develop poor coating adhesion in the future. The data indicate that, although the poor adhesion may lead to accelerated corrosion in salty concrete, it will not cause structural performance problems.

The above data indicate that cathodic protection is feasible for electrically interconnected epoxy-coated rebars in concrete structures, even when uncoated rebar is also present. Also indicated is that protection can be achieved at current densities at or below those commonly used on uncoated rebar structures. The current requirements should be lowest on structures where all the rebar is epoxy-coated and the epoxy-coated rebar is not yet experiencing high corrosion rates.

The choice of CP can be affected by a number of structure factors such as the ability to withstand additional dead loading and the possible presence of reactive aggregates. These factors, however, must be considered regardless of whether the rebar is epoxy coated or is uncoated. The reader is referred to Reference 73.

Field studies on decks have indicated that in only about half the cases were the epoxy-coated rebars electrically continuous (*74*). Therefore, it is necessary to electrically interconnect the rebars in many structures as part of the cathodic protection installation. This can be done by trenching and spot welding a small size rebar to the epoxy-coated ones, provided the welding does not significantly effect the structural properties of the bars. If strength reduction from welding is a concern, an alternative is the FHWA conductive polymer grout (a pourable polymer mortar with calcined fluid petroleum coke as aggregate), which has been used successfully in several field projects involving uncoated rebar. On these existing structures a 2- to 4-in.-wide trench was excavated such that at least 50 percent of the circumference of each bar was exposed. Then the trench concrete and rebars were sandblasted, a steel tie wire was placed perpendicular to the bars, and both the wire and the rebars were surrounded to at least $\frac{1}{2}$-in. depth with the conductive polymer grout. Such systems have been under cathodic protection for over 4 years and have performed well.

An electrical resistance welding technique is also available for interconnecting uncoated rebars in new as well as existing structures (*75*). KCC INC investigated use of this technique in the C-SHRP study (*46*) and found that strong connections that were resistant to failure could be made using $\frac{1}{8}$-in. mild steel wire if the epoxy coating was removed at two spots (about 0.5 by 0.15 in. each and spaced 1.75 in. apart) per bar. One bare area was used as the ground and the other as the weld location. The coating was easily removed using a ball rasp attached to a hand-held rotary drill. If cathodic protection is to be applied within several months of making the connections, it is probably not necessary to coat the tie wire or the weld areas. However, if a longer time will elapse, coating is recommended.

Two bridge decks in Connecticut contain epoxy-coated rebar and cathodic protection systems (*76*). Bridge No. 1242 (22,000 sq ft) on U.S. Route 229 over I-84 at Southington was rehabilitated using ECR and cathodic protection. The top half of the deck concrete, including the original uncoated rebar, was removed and replaced with ECR and a bonded concrete overlay. The bottom rebar is the original uncoated steel and the surrounding concrete is believed to be salt contaminated. The cathodic protection anode is Elgard $\frac{1}{2}$ in. titanium ribbon with a precious metal oxide catalyst and was positioned vertically underneath the top

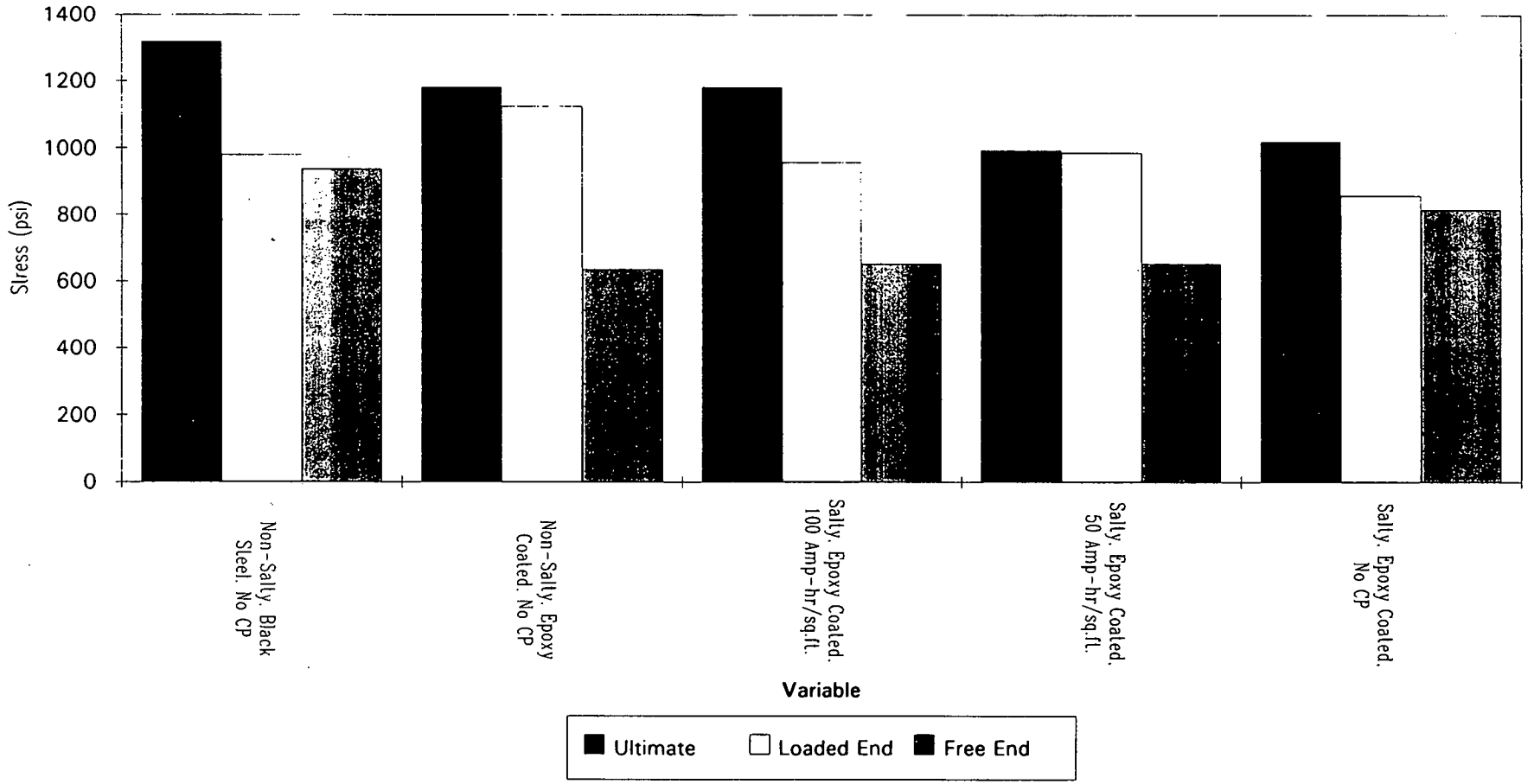

Figure A-11. Electrical resistance welding used for interconnecting epoxy-coated bars.

mat at 12 in. on center with slotted ribbon fasteners. Rebar continuity was provided by grinding away the epoxy coating at laps and cross-overs and using double wrapped bare wire ties. Ten CP zones were included and the system was activated in January 1990, at a current density in the range of 0.4–0.5 mA/ft^2 of concrete surface.

Bridge No. 242 on I-95 over the Lieutenant River in Old Lyme is 14,000 sq ft in size and involves an entire new superstructure with ECR in both the top and bottom mats. Elgard ribbon and Raychem Ferex 100 anodes are positioned between the top and bottom mats of steel. Rebar continuity was established in a manner similar to that for Bridge No. 1242, except that uncoated rebar was substituted around the perimeter of each span. The deck underwent significant cracking after construction. The State then elected to install a waterproof membrane; and consequently the CP system was never activated.

Calcium Nitrite. The results of studies on the ability of a calcium nitrite corrosion inhibiting admixture to reduce macrocell corrosion of epoxy-coated reinforcing steel have recently been reported (*77,78*). Concrete beams similar to those defined in ASTM G109 were fabricated with ECR as the top rebar and uncoated bars for the bottom. The concrete surrounding the top rebar included 15 lbs Cl^- per cubic yard as NaCl. The ECR was obtained in 1992 from a commercial supplier who confirmed that it met all requirements of ASTM A775. The bars were not subjected to outdoor exposure by the researchers, were handled with great care, and no deliberate damage was induced. Four different amounts of Darex Corrosion Inhibitor by W.R. Grace (calcium nitrite), 0, 4.5, 6.0 and 9.0 gallons per cubic yard, were employed. The beams were fabricated, fog room cured, and then exposed outdoors on above ground racks in Virginia. Four macrocell beams for each inhibitor concentration were tested.

Results though the initial 1.5 years of testing are summarized in Figure A-12. The data indicate that calcium nitrite was effective in minimizing macrocell corrosion of ECR in the presence of large amounts of chloride. The concrete containing calcium nitrite exhibited average macrocell corrosion cumulative current densities, which were only 3 to 12 percent of those with ECR only. This equates to a corrosion reduction in the range of 8 to 30 times. During the entire test program each individual specimen with calcium nitrite exhibited corrosion currents less than the lowest value for beams with ECR only (that is, ones with no calcium nitrite). This testing is continuing.

DISCUSSION AND CRITICAL EVALUATION

The present research team considers that certain points and conclusions from the above state-of-the-art definition and commentary are particularly noteworthy and significant. Consequently, these are presented separately in the discussion below.

Significance of Macrocell Current Measurements

It is generally recognized that an important factor in the corrosion of bare reinforcing steel in bridge deck applications is occurrence of macrocells established between the upper and lower steel mats. Such cells occur as a consequence of the upper mat becoming depassivated from the high chloride concentration which typically accumulates in the top concrete, while chloride accumulation about the bottom steel is delayed and this material remains passive. An important indicator of rebar corrosion for concrete slabs employed in research and testing has been measurement of the macrocell current. Such measurements have also been employed in studies of ECR corrosion, and the significance of macrocell current in the case of epoxy-coated reinforcing steel has been considered to be essentially the same as for bare steel.

As a part of the KCC INC long-term exposure studies described above, macrocell current for slabs with both bare and epoxy-coated reinforcing steel was measured; and the mA-year/ft^2 for occurrence of hairline cracking was calculated. The results indicated that the total charge passed at the time of hairline cracking for uncoated rebar slabs was about 3.5 times greater than for slabs with ECR in the top mat only and 24 times greater than when both mats were epoxy-coated. For the case of bare bars, such data are typically reported as a current density relative to the top mat surface area. This same procedure was used here also for calculating the above ratios in the case of ECR; however, in all probability, the current concentrates at defects and bare areas of the coating. The observation that the net charge transferred in association with cracking of the three slab types was different indicates either that different amounts of corrosion were required or that macrocell current was not an accurate indicator of corrosion phenomena in the ECR case. Interestingly, the slabs with ECR in one mat only and the ones with ECR in both mats cracked at about the same time, despite the sevenfold difference in charge transferred for the two. This suggests that there was no apparent advantage in coating the bottom mat. It is projected that the responsible failure mechanism involved progressive coating disbondment and underfilm corrosion that led to cracking of the epoxy coating, as discussed above. It is thought that this process was not enhanced by presence of a macrocell, and presumably the macrocell current was low as this disbondment and underfilm corrosion occurred. One or more macrocells can be present also upon a single mat; however, normal instrumentation techniques do not permit measurement of the current associated with these. The possible presence of macrocells upon the upper mat is not thought to be a requisite for initiation of ECR corrosion. Once the coating was compromised, however, macrocell current increased as this cell provided an additional driving force for corrosion of the upper mat. Such a rationale is consistent with the difference in macrocell current noted above for bare versus epoxy-coated reinforcing steel slabs; and it is concluded that, while occurrence of a high macrocell current in an ECR slab is indicative of corrosion, the absence of such current does not necessarily mean that corrosion is not ongoing.

Accelerated Testing and Life Prediction

The questions and uncertainties that naturally arise with regard to predicting the long-term integrity of a material system such as epoxy-coated reinforcing steel in concrete based upon short-term, accelerated testing were addressed previously. Although standards have been developed and continue to evolve, they have been established without the benefit of laboratory or test yard data of a time frame that approaches a realistic design life or from which long-term service performance can logically be

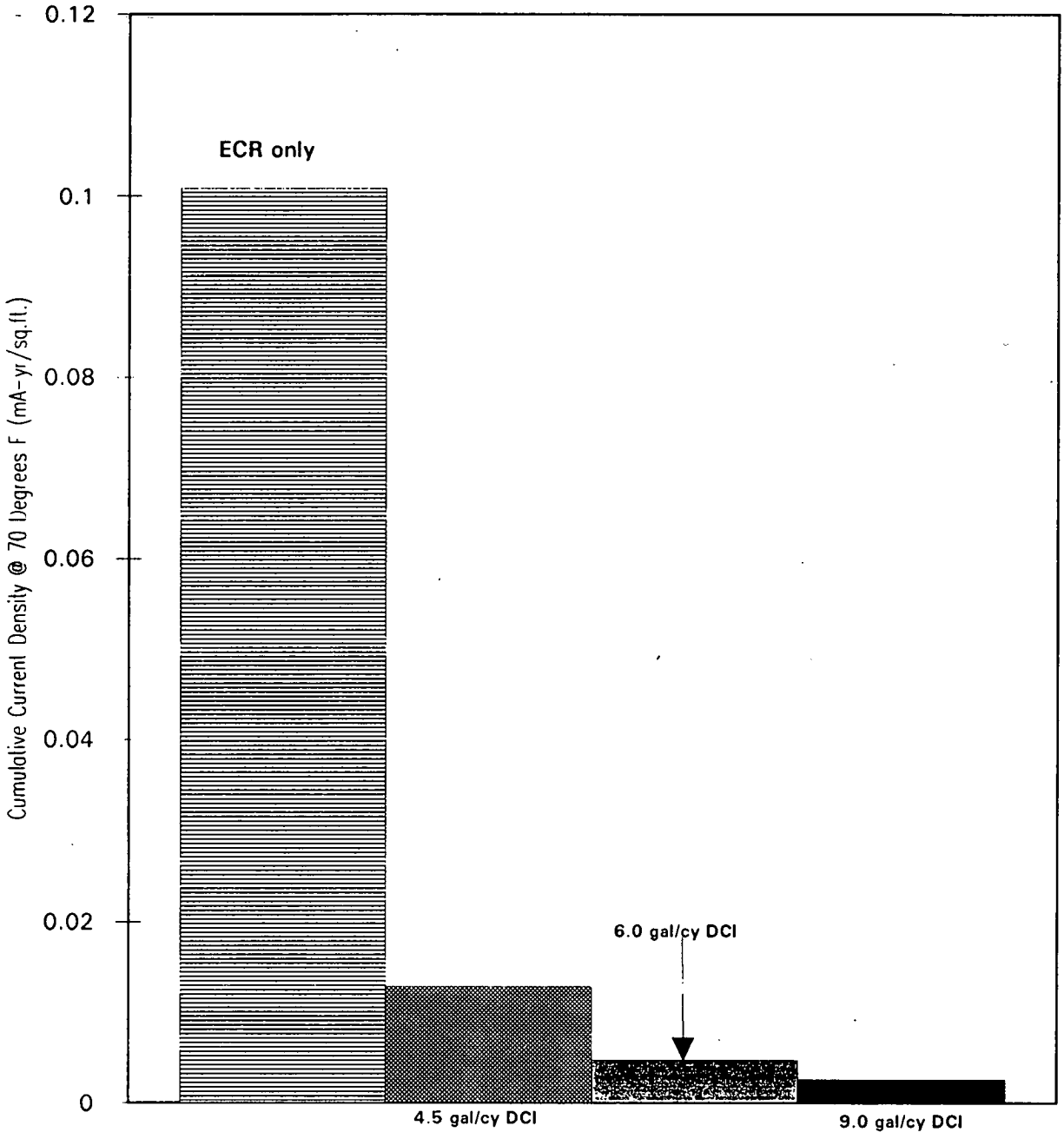

Figure A-12. Effect of calcium nitrite addition on macrocell current density.

projected. Also, controversy remains regarding the specific mechanism of ECR corrosion failure and of the specific influence of important variables. Uncertainty regarding ECR performance will remain until more information regarding this topic becomes available.

One quantitative correlation between corrosion testing results and anticipated long-term service performance has been made, however, based upon the time-to-cracking studies by FHWA and KCC INC, which were discussed earlier. Listed in Table A-2 are results from these programs for concrete slab specimens with both bare and epoxy-coated reinforcing steel. If these data are evaluated according to the original procedure employed by FHWA (*30*) as discussed previously, where time-to-cracking for ECR specimens was divided by the corresponding life for bare bars, then their original projection that life for the former exceeds that of the latter by more than a factor of five is confirmed. It is considered, however, that this rationale was in error and that subtraction rather than division of the respective times-to-cracking is the correct approach. On this basis, a life extension for ECR compared to bare bar slabs of 6 to 8 years is projected. It is important to recognize that the exposures upon which this analysis is based were accelerated only with respect to the rate of salt ingress, and otherwise the tests are considered similar to what a bridge deck with 1 in. of cover constructed at the indi-

TABLE A-2.
Times-to-cracking for different slab types

TYPE OF SLAB SPECIMEN	TIME TO INITIAL CRACKING (years)[1]	TIME TO SEVERE CRACKING (years)[2]
Uncoated rebar both mats	1.3	1.5
ECR, top mat only	9	8
ECR, both mats	9	8

[1]Research by KCC INC reported in references 46 and 52.

[2]FHWA research program initiated in 1980.

cated times in northern Virginia should experience. Note also that there was no difference in time-to-cracking for slabs with coated bars in both mats compared to those with ECR at the top level only.

Deck Cracking and Epoxy-Coated Reinforcing Steel

Cracking of concrete in bridge and parking decks constructed with epoxy-coated reinforcing steel has become a concern in recent years. At a 1987 American Concrete Institute Workshop (*79*), the participants noted that, "From the viewpoint of both researchers and field engineers, observations were made that new bridge decks with epoxy-coated reinforcing bars have been developing an excessive amount of deep cracks during the early stages of curing." They concluded that this may be an interactive effect resulting partly from the higher cement content and lower water-cement ratio of the concrete, greater cover over the reinforcing steel, and the lower "in and out" bond strength (transfer of tensile thrust into the reinforcing bar at cracks and out away from cracks) of epoxy-coated bars to the matrix (*80,81*). Severe early age cracking of Canadian parking decks constructed with epoxy-coated reinforcing steel has also been reported. Parking decks are often more slender and flexible than bridge decks. The bays are typically 30–40 ft wide, and dynamic loadings are relatively high. In one structure, the rate of development of new cracking was 10,000 lineal ft per year. Portions of the discussion in a June 1989 report by G. G. Litvan (*81*) are given below:

> The documented case histories leave little doubt that suspended slabs of parking garages are prone to excessive cracking if constructed with epoxy-coated reinforcing steel.
> The cause of the excessive cracking is not known. It appears to be reasonable to accept the hypothesis that it is related to decreased adhesion between the epoxy-coated steel and the concrete matrix compared to that existing between bare steel and concrete. Whereas the bond between the two steel types (bare and epoxy-coated) varies in the range of 10 to 15 percent, differences exist in the nature of the interaction. Thus, the bare system is characterized by significant adhesion, whereas for the epoxy-coated one adhesion plays a minor role and the bond is mainly mechanical. The cured, mature systems reinforced with bare or coated steel have essentially similar mechanical properties; and so far these aspects have not been investigated by the researchers. There may well be differences in the nature of the responses of the system during setting when considerable shrinkage takes place.
> There is no indication that the cracking of concrete is caused by the corrosion of the steel or that the epoxy coating is not protecting the steel from corrosion. The decks were only 1 to 7 years old when studied, and a detailed coring and ECR analysis program was not included. The excessive cracking, however, will accelerate the ingress of water and chlorides into the deck; and if appropriate measures are not implemented, corrosion of the lower mat (uncoated steel) is to be expected in time.
> The unavoidable conclusion is that in conformity to the CAN/CSA S413 Standard requirement, the installation of a waterproofing membrane is essential.

Although the purpose of this effort is not to determine the causes of cracking (another NCHRP effort is addressing this issue), the fact that significant cracking has been documented on ECR bridges and parking decks must be considered because of its effect on corrosion-induced deterioration. It is notable that significant cracking was found on many of the ECR bridge decks studied in the CRSI and C-SHRP programs and that ECR corrosion was common at the cracks on the structures that were more than 8 years old. This is a potential problem area the nature of which must be characterized in detail if ECR is to be used as the primary protective system on decks.

REFERENCES

1. STAFFORD, R.T., "Epoxy Coated Rebar," *Parking* (March-April 1985), p. 39.
2. SLATER, J.E., Corrosion of Metals in Association with Concrete, *ASTM STP 818,* Am. Soc. for Test. and Matls., Philadelphia, PA (1983), pp. 16–22.
3. SPELLMAN, D.S. and STRATFULL, R.F., "Concrete Variables and Corrosion Testing," *Highway Research Record No. 423* (1963), p. 27.
4. CLEAR, K.C., "Time-to-Corrosion of Reinforcing Steel in Concrete Slabs," *FHWA-RD-76-70,* Federal Highway Administration, Washington, D.C. (1976).
5. HAUSMANN, D.A., *Materials Protection,* Vol. 8(10) (1969), p. 23.
6. MORRISON, G.L., et al., "Chloride Removal and Monomer Impregnation of Bridge Deck Concrete by Electro-Osmosis," Kansas DOT, *FHWA Report No. FHWA-KS-RD 74-1,* (April 1976).
7. LANKARD, D.R., et al., "Development of Electrochemical Techniques for Removal of Chlorides from Concrete Bridge Decks," Battelle Columbus Laboratories, *FHWA Rept. No. DOT-FH-11-9026* (June 1978).
8. STRATFULL, R.F., "Experimental Cathodic Protection of a Bridge Deck," *Transportation Research Record No. 500* (1974).
9. HARTT, W.H. and ROSENBERG, A.M., "The Influence of $Ca(NO_2)_2$ Concentration upon Seawater Corrosion of Reinforcing Steel in Concrete," in Performance of Concrete in Marine Environment, *ACI Pub. SP-65* (1980), p. 609.
10. WHITING, D. and SCHMITT, J., "Durability of In-Place Concrete Containing High-Range Water-Reducing Admixtures," *NCHRP Report 296* (Sept. 1987).
11. BERKE, N.S. and SUNDBERG, K.M., "The Effects of Admixtures and Concrete Mix Designs on Long-Term Concrete Durability in Chloride Environments," *Paper No. 386,* CORROSION/89, April 17–21, 1989, New Orleans, LA.
12. PFEIFER, D.W. and SCALI, M.J., "Concrete Sealers for Protection of Bridge Structures," *NCHRP Report 244* (Dec. 1981).
13. CLIFTON, J.R., BEEHGLY, H.F., and MATHEY, R.G., "Nonmetallic Coatings for Concrete Reinforcing Bars," *Report No. FHWA-RD-74-18,* Federal Highway Administration, Washington, DC (Feb. 1974). PB No. 236424.
14. PIKE, R.G., "Nonmetallic Coatings for Concrete Reinforcing Bars," *Public Roads,* Vol. 37, No. 5 (June 1973), pp. 185–197.
15. SALPARANTA, L., "Epoxy-Coated Concrete Reinforcements," Finland Technical Research Center, *Research Reports VTT-RR-525-88* (March 1988), p. 17.
16. BEEGHLY, H.F., et al., "Nonmetallic Coatings for Concrete Reinforcing Bars," Coating Materials, Washington, DC, National Bureau of Standards, *NBS Technical Note 768,* (1973) p. 36.
17. LEE, H. and NEVILLE, K., *Handbook of Epoxy Resins,* New York: McGraw-Hill, Inc. (1967).
18. CLEAR, K.C. and VIRMANI, Y.P., "Corrosion of Non-Specification Epoxy-Coated Rebars in Salty Concrete," *Paper No. 114,* CORROSION/83, April 1983, Anaheim, CA.
19. CLEAR, K.C., "Cost Effective Rigid Concrete Construction and Rehabilitation in Adverse Environments," Federal Highway Administration, FCP Annual Progress Report, Year Ending September 30, 1981, Project No. 4K.
20. GUSTAFSON, D. P., "Epoxy Update," *Civil Engineering,* Vol. 58(10) (1988), pp. 38–41.
21. EDGELL, T. W. and RIEMENSCHNEIDER, J.A., "Specification and Research of Fusion Bonded Epoxy Coating Technology," *Paper No. 203,* CORROSION/92, April 27–May 1, 1992, Nashville, TN.
22. KENNETH C. CLEAR, INC., "Effectiveness of Epoxy-Coated Reinforcing Steel," Final Report, Concrete Reinforcing Steel Institute (CRSI) (Dec. 1991).
23. PFEIFER, D.W., LANGREN, J.R., and ZOOB, A., "Protective Systems for New Prestressed and Substructure Concrete," Wiss, Janney, Elstner Associates, Inc., *Report FHWA/RD-86/193* (April 1987), 133 pp.
24. BROWN, R.P. and POORE, T.G., "Two Years of Corrosion Monitoring of Reinforced Concrete Piles at Matanzas Inlet," Interim Report, *Report No. 82-1,* Florida Department of Transportation (July 1982).
25. EDGELL, T.W. and RIEMENSCHNEIDER, J.A., "Epoxy-Coated Reinforcing Steel Performance in Marine Exposure—A Nine-Year Observation," Pipeline & Construction Specialty Markets, 3M Austin Center, 130-4N-07.
26. POWERS, R.G., Florida DOT, Office of Materials and Research, Gainesville, FL 32601, unpublished research.
27. ESPELID, B. and NILSEN, N., "A Field Study of the Corrosion Behavior on Dynamically Loaded Marine Concrete Structures," Concrete in Marine Environment, Proceedings, 2nd International Conference, St. Andrews by-the-Sea, Canada (1988), Editor, V. M. Malhorta, ACI SP-109, pp. 85–104.
28. J. SATAKE, ET AL., "Long-Term Corrosion Resistance of Epoxy-Coated Reinforcing Bars," Chapter 21, *Corrosion of Reinforcement in Concrete Construction,* Ellis Harwood Ltd., U.K. (1983).
29. ROPER, H., "Investigations of Corrosion, Fatigue and Corrosion Fatigue of Concrete Reinforcement," *Paper No. 169,* CORROSION/83, Anaheim, CA, April 18–22, 1983, 12 pp.
30. CLEAR, K.C., FCP Annual Progress Report—Year Ending September 30, 1978, Project 4B "Eliminate Premature Deterioration of Portland Cement Concrete," Federal Highway Administration (April 1979), pp. 38–40.
31. Unpublished FHWA data and photographs by Clear, Virmani and Jones (1981).
32. VIRMANI, Y.P., CLEAR, K.C. and PASKO, T.J., "Time-to-Corrosion of Reinforcing Steel in Concrete Slabs, Vol. 5: Calcium Nitrite Admixture or Epoxy-Coated Reinforcing Bars as Corrosion Protection Systems," *Report No. FHWA-RD-83-012,* Federal Highway Administration, Washington, DC (Sept. 1983).
33. Unpublished FHWA data and photographs by Virmani (1989).
34. MANJAL, S.K., "Evaluation of Epoxy-Coated Reinforcing

Steel Bridge Decks," *Report No. FHWA-MD-82-03,* Maryland State Highway Administration, Brooklandville (March 1981).

35. HAGEN, M.G., "Bridge Deck Deterioration and Restoration—Final Report," *Report No. FHWA-MN-RD-82-01,* Minnesota Department of Transportation, St. Paul (Nov. 1982).
36. MCKEEL, W.T., Jr., "Evaluation of Epoxy-Coated Reinforcing Steel, Milestone Report," *HPR Study No. 79,* Virginia Highway and Transportation Research Council, Charlottesville (July 1984):
37. WEYERS, R.E. and CADY, P.D., "Deterioration of Concrete Bridge Decks from Corrosion of Reinforcing Steel," *Concrete International,* Vol. 9(1) (1989).
38. MALASHESKIE, G.J. ET AL., "Bridge Deck Protective Systems," Final Report, Dept. of Trans., Commonwealth of Pennsylvania, *FHWA-PA-88-001-85-17* (July 1988).
39. HEDEDAL, P. and MANNING, D.G., "Field Investigation of Epoxy-Coated Reinforcing Steel," *MTO Report MAT-89-02,* Ontario Ministry of Transportation (Dec. 1989).
40. POWERS, R. and KESSLER, R., "Corrosion Evaluation of Substructure, Long Key Bridge," *Corrosion Report No. 87-9A,* Florida Department of Transportation, Gainesville, FL (1987).
41. ZAYED, A.M. and SAGUES, A.A., "Corrosion of Epoxy-Coated Reinforcing Steel in Concrete," *Paper No. 386* CORROSION/89, April 17–21, 1989, New Orleans, LA.
42. POWERS, R. "Corrosion of Epoxy-Coated Rebar, Keys Segmental Bridges Monroe County," *Corrosion Report No. 88-8A,* Florida Department of Transportation, Gainesville, FL (Aug. 1988).
43. ZAYED, A.M., SAGUES, A.A., and POWERS, R.G. "Corrosion of Epoxy-Coated Reinforcing Steel in Concrete," *Paper No. 379* at CORROSION/89, New Orleans, LA. April 17–21, 1989.
44. READ, J.A., "FBECR: The Need for Correct Specification and Quality Control," *CONCRETE,* Vol. 23(8) (Sept. 1989), pp. 23–27.
45. ROMANO, D.C., "Preliminary Investigation of Epoxy-Coated Reinforcing Steel Disbondment; Cause and Effects," Florida Department of Transportation, Materials Office, Gainesville, FL (Nov. 1988).
46. CLEAR, K.C., "Effectiveness of Epoxy Coated Reinforcing Steel," Final Report, Canadian Strategic Highway Research Program, Ottawa, Canada (Dec. 1992).
47. GRIGGS, R.D., "Use of Epoxy Coated Concrete Reinforcement Steel in Georgia Highway Construction and a Limited Field Evaluation of the Performance of Epoxy Coated Reinforcement Steel as Corrosion Protection System in Coastal Georgia Bridge Construction," Report submitted to the Office of Materials and Research, Georgia Department of Transportation (Feb. 1993).
48. SAGUES, A.A. and POWERS, R.G., "Effect of Concrete Environment on the Corrosion Performance of Epoxy-Coated Reinforcing Steel," *Paper No. 311,* CORROSION/90, Bally's Hotel, Las Vegas, NV, April 23–27, 1990, pp. 15.
49. SOHANGHPURWALA, A.A. and CLEAR, K.C., "Effectiveness of Epoxy Coatings in Minimizing Corrosion of Reinforcing Steel in Concrete," presented at Transportation Research Board Annual Meeting, Washington, DC (Jan. 1990).
50. SAGUES, A.A. and ZAYED, A.M., "Corrosion of Epoxy-Coated Reinforcing Steel, Phase II," University of South Florida for Florida Department of Transportation (Dec. 1989).
51. SAGUES, A.A., "Mechanism of Corrosion of Epoxy-Coated Reinforcing Steel in Concrete," Final Report, Florida Department of Transportation *Report No. FL/DOT/RMC/0543-3296,* University of South Florida, Tampa (April 1991).
52. SCANNELL, W.T. and CLEAR, K.C., "Long-Term Outdoor Exposure Evaluation of Concrete Slabs Containing Epoxy Coated Reinforcing Steel," presented at Transportation Research Board Annual Meeting, Washington, DC (Jan. 1990).
53. PFEIFER, D.W. and LANDGREN, J.R., and KRAUSS, P.D., "CRSI Performance Research: Epoxy Coated Reinforcing Steel," Final Report submitted to CRSI by Wiss, Janney Elstner Associates, Inc. (June 1992).
54. Standard Specification for "Epoxy-Coated Reinforcing Steel Bars," ASTM A775M-86, *ASTM Annual Book of Standards,* American Society for Testing and Materials, Philadelphia, PA (1986).
55. SCHIESSL, P. and RENTER, C., "Coated Reinforcing Steel Development Applications in Europe," *Paper No. 556* CORROSION/91, March 11–15, 1991, Cincinnati, OH.
56. ECOB, C.R., KING, E.S., ROSTAM, S., and VINCENTSEN, L.J., "Epoxy-Coated Reinforcement Cages in Precast Concrete Segmental Tunnel Linings: Durability," in *Corrosion of Reinforcement in Concrete,* Ed. C. L. Page, K. W. J. Treadway, and P. B. Bamforth, Society of Chemical Industry, London (1990), p. 550.
57. "Concrete Reinforcing Steel Institute Epoxy Coating Plant Certification Program," Theodore L. Neff, P.E. Administrator (June 11, 1991).
58. NEFF, T.L., "CRSI Plant Certification Program for Epoxy Coating Applicators—Manual Revisions," Letter to Mr. Kenneth C. Clear (Aug. 1991).
59. NEFF, T.L., Letter to Specifiers of Corrosion Protective Systems with attachments entitled "CRSI Comments on Kenneth C. Clear's January 10, 1992, Letter to Clients and Associates," and "Effectiveness of Epoxy-Coated Reinforcing Steel" by Kenneth C. Clear of KCC INC (Feb. 1992).
60. LEIDHEISER, Jr., H., *Corrosion,* Vol. 38 (1982) p. 374.
61. ZAYED, A.M. and SAGUES, A., *Corrosion Science,* Vol. 46 (1990) pp. 1025–1044.
62. SAGUES, A. and ZAYES, A.M., *Corrosion,* Vol. 47 (1991) pp. 852–858.
63. SAGUES, A., PEREZ-DURAN, H.M., and POWERS, R.G., *Corrosion,* Vol. 47 (1991), pp. 884–893.
64. ASBECK, W.K., "Measuring the Adhesion of Coatings," *Journal of Paint Tech.,* Vol. 43 (1971), p. 84.
65. SAGUES, A.A., Private Communication (Oct. 1991).
66. KESSLER, R. and POWERS, R., "Zinc Metallizing for Galvanic Cathodic Protection of Steel Reinforced Concrete in a Marine Environment," *Paper No. 324,* CORROSION/90, National Association of Corrosion Engineers, Houston, TX (1990).
67. SAGUES, A. and POWERS, R., "Low-Cost Sprayed Zinc Galvanic Anode for Control of Corrosion of Reinforcing Steel in Marine Bridge Substructures," Contract No. SHRP-88-IDO24, 3rd Quarterly Report (October 12, 1991).
68. CLEAR, K.C., "Feasibility of Cathodic Protection of Epoxy Coated Reinforcing Steel in Concrete," Final Report, Cana-

dian Strategic Highway Research Program, Ottawa, Canada (Dec. 1992).

69. KCC INC and Florida Atlantic University, "NCHRP 10-37, Performance of Epoxy Coated Reinforcing Steel in Highway Bridges," Interim Report, National Cooperative Highway Research Program, Washington, DC (April 1992; revised Feb. 1993).
70. CLEAR, K.C., "Effect of Cathodic Protection on Bond/Pull-out Characteristics of Epoxy Coated Reinforcing Steel in Concrete," Kenneth C. Clear, Inc., Boston, Virginia (Oct. 1993).
71. VRABLE, J.B., "Cathodic Protection for Reinforced Concrete Bridge Decks—Laboratory Phase," *NCHRP Report 180,* National Cooperative Highway Research Program, Washington, DC (1977).
72. BENNETT, J., SCHUE, T.J., CLEAR, K.C., LANKARD, D.L., HARTT, W. H., and SWIATT, W. J., "Electrochemical Chloride Removal and Protection of Concrete Bridge Components: Laboratory Studies," *Report SHRP-S-657,* Strategic Highway Research Program, Washington, DC (1993).
73. BENNETT, J.E., BARTHOLOMEW, J.J., BUSHMAN, J.B., CLEAR, K.C., KAMP, R.N. and SWIAT, W.J., "Cathodic Protection of Concrete Bridges: A Manual of Practice," Strategic Highway Research Program Report SHRP-S-372 (1993).
74. CLEAR, K.C., "FCP Annual Progress Report—Year Ending September 30, 1980—Project 4K," Federal Highway Administration, Washington, DC (1980).
75. "Procedure for Using Elgard Resistance Spot Welder for Continuity Bonding," by Elgard Corporation.
76. DAILY, S.F., Elgard Corporation Letter to Mr. K.C. Clear (March 24, 1992).
77. "Effect of DCI on Macrocell Corrosion of Epoxy-Coated Reinforcing Steel," Kenneth C. Clear, Inc. (April 1992).
78. CLEAR, K.C., "Effect of Select Concrete Admixtures on Corrosion of Epoxy Coated Reinforcing Steel in Salty Concrete," Kenneth C. Clear, Inc., Boston, VA, (Dec. 1993).
79. American Concrete Institute Workshop on Epoxy-Coated Reinforcement, *Concrete International,* Vol. 10, 1988, pp. 80–84.
80. LITVAN, G.G., "Deterioration of Parking Structures," *ACI SP 126-17,* Vol. 1, V. M. Malhotra, Ed.
81. LITVAN, G.G., "Investigation of the Performance of Parking Garage Decks Constructed with Epoxy-Coated Reinforcing Steel," National Research Council, Canada, Report No. CR-5493/5517/5518/5519.5 (June 30, 1989).

APPENDIX B

ELECTROCHEMICAL IMPEDANCE SPECTROSCOPY BASICS

BACKGROUND

A number of techniques have been developed in recent years in an attempt to understand the nature of the processes responsible for organic coating failures in aggressive environments. The common objective of these is to predict the useful lifetime of coatings from results of short duration experiments and to aid in elucidating mechanistic information. Accurate assessment using conventional dc electrical and electrochemical techniques to predict the lifetime of a coating and/or determine quantitative corrosion rate data is often difficult because of the characteristic insulating properties of most coating systems; in this case, the large ohmic drop that typically exists across the electrolyte/coating/metal interphases generally dominates the electrical response of the system and introduces errors when attempting to calculate meaningful corrosion rate data. Electrochemical impedance spectroscopy (EIS) techniques overcome this difficulty, because a separation of the individual contributing factors related to coating water uptake, coating conductance and interfacial attack can be obtained, provided a large frequency range is scanned and the relaxation times of the individual reactions are sufficiently different. In comparison, AC resistance measurements give an overall impedance for a system at a single frequency, whereas EIS provides impedance information over a broad frequency range. Hence, EIS is capable of providing a more complete picture concerning the protective properties of coatings. For example, the following information is often available from EIS measurements: 1) percent moisture uptake by the coating; 2) extent of conductive pore development; and 3) time at which interfacial attack first occurs.

The EIS technique has been used successfully by others to study the deterioration of coated metals (1-5). In general, coatings that have overall impedance values greater than 10^8 Ω/cm^2 usually exhibit excellent corrosion resistance, while coatings with values between 10^6-10^8 Ω/cm^2 show intermediate behavior and coatings with values below 10^6 Ω/cm^2 behave poorly (6,7). Therefore, coatings that maintain overall high impedance values for the course of the experiment will in high probability perform well in service.

EIS TECHNIQUE

EIS is a steady-state technique that is capable of assessing relaxation phenomena over a broad range of frequencies and of providing information about the change in the electrical properties of a metal or coated metal as a function of time. The response of a linear system to a perturbation of arbitrary form is given by

$$Z(f) = V(t)/I(t), \qquad [1]$$

where Z is the frequency dependent impedance of the system and V(t) and I(t) are a time-dependent voltage and current, respectively (2). The equation for a steady-state sinusoidal voltage perturbation, V(t), is

$$V(t) = V_o \sin \omega t, \qquad [2]$$

where ω is $2\pi f$. The response of the system to this perturbation is

$$I(t) = I_o \sin (\omega t + \phi), \qquad [3]$$

where ϕ is the phase angle (shift). Equation [1] holds true for impedances provided the system is linear, remains stable over time of the measurement, and causality is obeyed (that is, the observed system response is due entirely to the perturbation) (8). The impedance, $Z(j\omega)$, is a vector quantity and, as such, is a complex number containing both magnitude and phase information. This value, when obtained over a wide frequency range, contains all the information that can be used to characterize a coating system by purely electrical methods. The impedance is commonly expressed in terms of a complex number according to

$$Z(j\omega) = Z' - jZ'', \qquad [4]$$

where $j = \sqrt{-1}$ and Z' and Z'' are frequency-dependent real numbers, which represent the resistive and reactive (capacitive) components of the system. These impedance values are related to the magnitude and phase by

$$|Z(j\omega)| = [Z'^2 + Z''^2]^{1/2} \qquad [5]$$

and

$$\tan (\phi) = - Z''/Z'. \qquad [6]$$

The most common methods of displaying impedance data include (1) the Nyquist plot ($-Z''$ vs Z'); and (2) Bode magnitude ($\log |Z|$ vs $\log \omega$) and Bode phase angle ($\log \phi$ vs $\log \omega$) plots. Excellent reviews on the fundamentals of the EIS technique are provided by Macdonald (8), McKubre (9) and Silverman (10).

BASIC INTERPRETATION

A review of impedance plot methods is given by Walter (11). Impedance data are generally presented in two basic formats: Bode and complex plane plots. The Bode format involves plotting $\log |Z|$ versus $\log \omega$ ($\omega = 2\pi f$) and phase angle shift (ϕ) versus $\log \omega$. The complex plane format (also commonly referred to as the Nyquist plot) involves plotting $-jZ''$ on the ordinate and Z' on the abscissa.

Attempts to interpret impedance spectra usually begin with the selection of electrical analog models to aid in representing the behavior of the system. This approach is sometimes cumbersome because of the infinite number of analog circuits that provide good fit to the data. However, only a limited number of resistor, capacitor and inductor (and Warburg term, a diffusional impedance) combinations can be used to represent meaningful electrochemical behavior. For example, the response of a coated metal to applied ac signals at early times of immersion is, in general, dominated by the electrical properties of the polymer (dielectric response) in which the impedance response is characterized by an ω^{-1} frequency dependence and an overall high system impedance, see Figure B-1. A coating that displays capacitive behavior over the entire frequency range is considered, at least at the time of measurement, to exhibit good corrosion resistance. A coating that absorbs water but otherwise remains intact will show a small shift in the Bode magnitude plot in a direction indicated by Figure B-2.

Conductive pathways may develop through a coating with increasing time of exposure. Representative Bode plots for this behavior are given in Figure B-3. Curve 2 in this figure is indicative of a coating that is conductive due to the establishment of solution filled pores. If this behavior occurs within the first few days of exposure, it could be reflective of a porous coating that may perform poorly in service. This is especially true if the frequency-independent resistance at low frequencies decreases noticeably with time as illustrated in Figure B-4. Although a

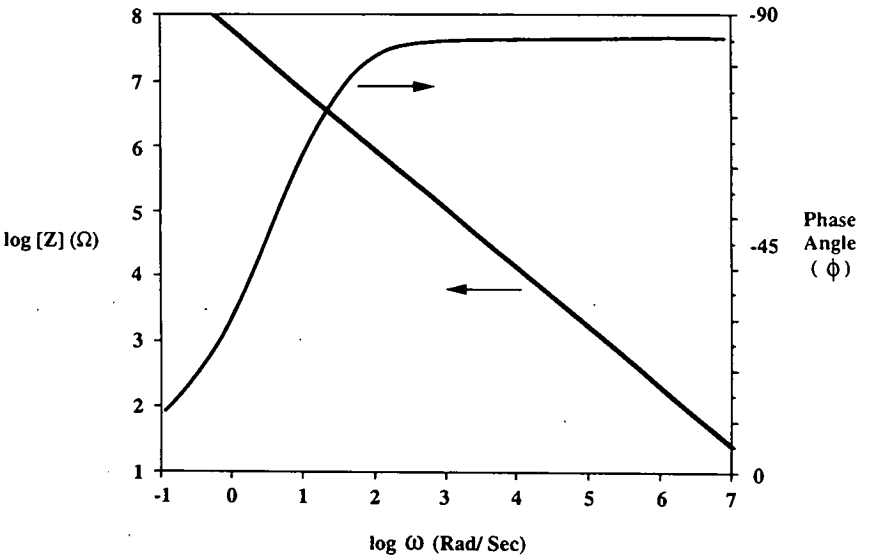

Figure B-1. Bode Plots for Coated Steel Exhibiting Good Corrosion Resistance.

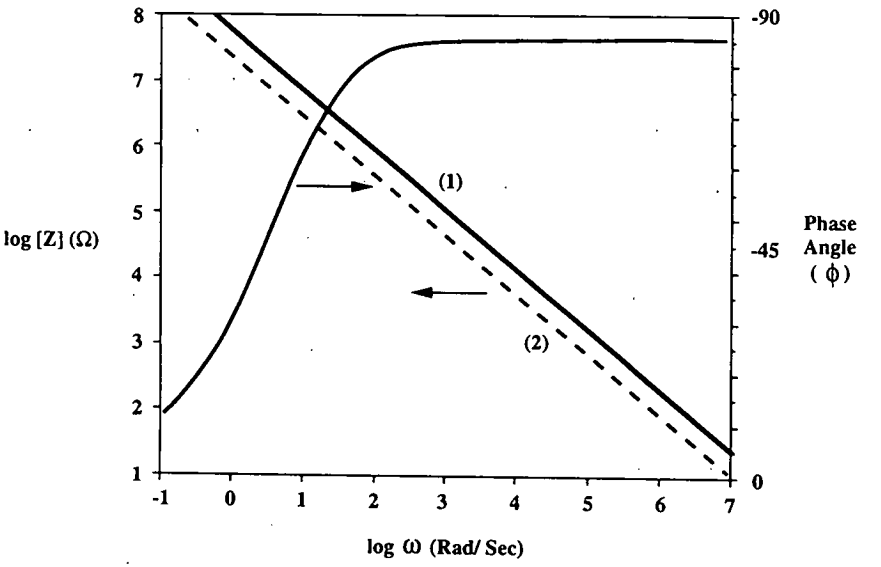

Figure B-2. Bode Plots for Coated Steel Exhibiting Good Protective Properties: (1) t_o=0; (2) at some time t_1 where $t_1 > t_o$.

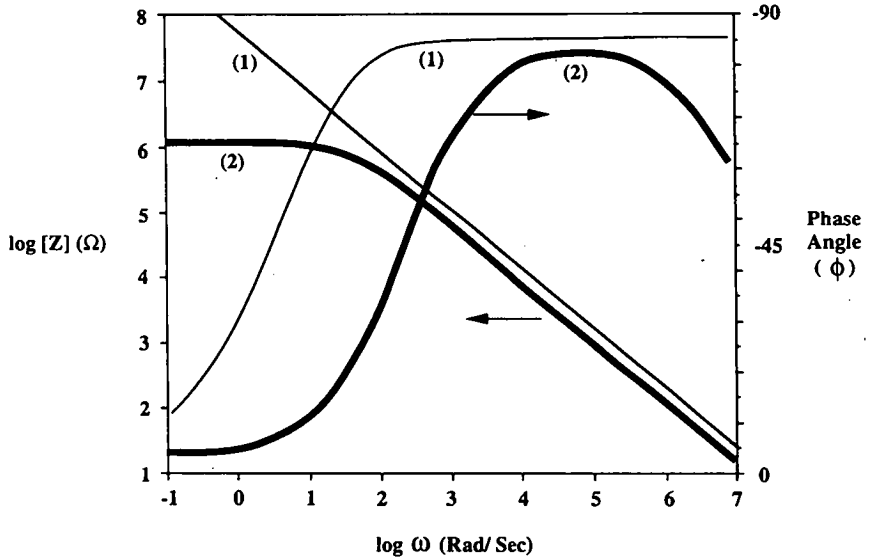

Figure B-3. Bode Plots for Coated Steel: (1) at t_o=0; (2) at t_1 where $t_1 > t_o$.

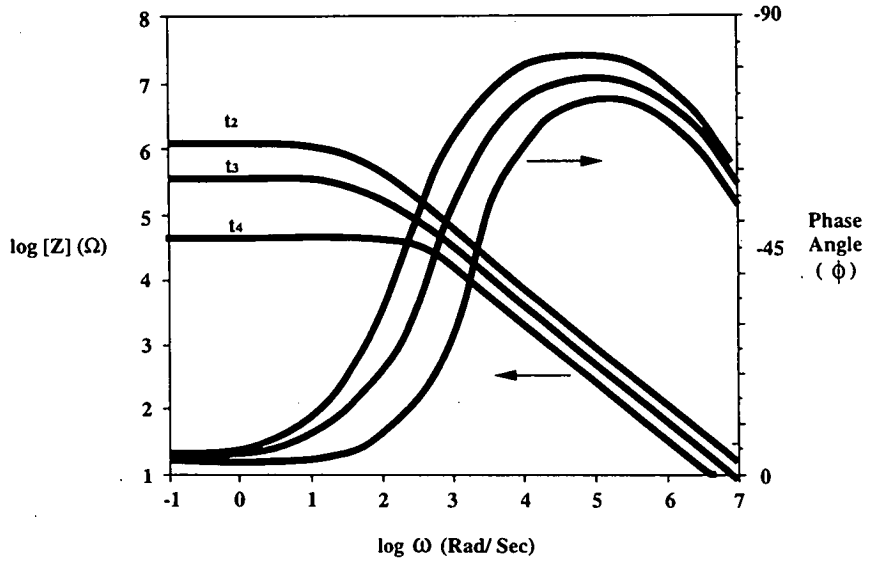

Figure B-4. Bode Plots for Coated Steel. Curves Show Progressive Decrease Pore Solution Resistance with Increasing Time of Exposure where $t_4 > t_3 > t_2$.

coating may exhibit this trend with time, it does not necessarily portend coating failure. It is possible for some good coatings to develop conductive pathways at early times and still provide reliable protection. However, the existence of such pathways is a necessary condition for coating breakdown and corrosion at the coating/metal interface.

Interfacial breakdown is indicated by the appearance of a second, low frequency time constant, an example being provided in Figure B-5. The development of a frequency independent impedance below about 1 Hz is related to corrosion of the metal substrate. This is known as the charge transfer resistance, R_{ct}, which can be used directly to calculate a corrosion rate. When this type of response occurs, ultimate coating failure is likely.

Two common equivalent circuit analogs that have been used by others to model the behavior of organic coating systems are shown in Figure B-6. Model I represents a parallel combination of impedance components for the coating and the coating/substrate interface. In this model, C_{dl} is not a true double-layer capacitance because the physical conditions are much different than one would find for a bare (oxide covered) metal exposed to a bulk electrolyte; therefore, this circuit element is usually treated as a pseudo capacitance. In model II, W is the Warburg impedance which represents a non-conventional circuit element that takes into account the influence of diffusion on the corrosion process. A number of curve fitting routines

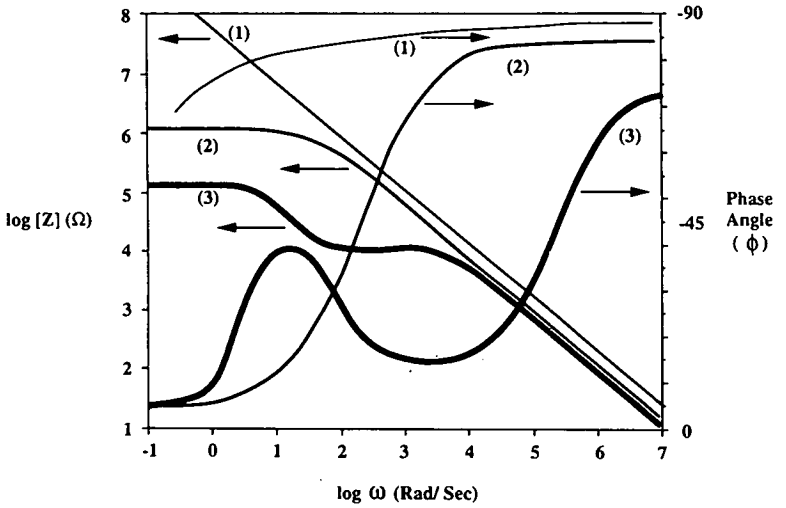

Figure B-5. Bode Plots for Coated Steel. Curve (1) Shows Response at t_e=0, Curve (2) Indicates Development of Conductive Pores, Water Absorption and Curve (3) Represents a System Experiencing Corrosion at the Coating/Steel Interface.

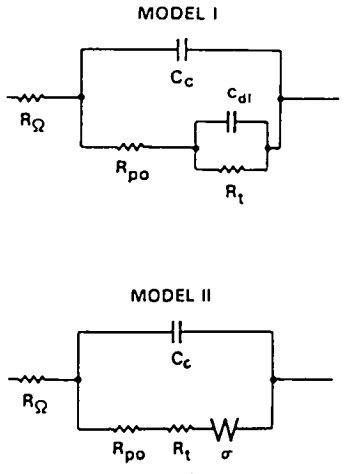

Figure B-6. Equivalent Circuit Analogs for Modeling Behavior of Organic Coating Systems, where R_Ω is the Bulk Solution Resistance, C_c is the Coating Capacitance, R_{po} is the Coating Pore Resistance, C_{dl} is the Pseudo Capacitance at the Coating/Substrate Interface, R_t is the Charge Transfer Resistance and W is the Warburg Diffusional Impedance.

have been used for data analysis in order to check the validity of a given model. A common approach is to use a complex nonlinear least squares regression technique.

Reviews on EIS data analysis are provided by Macdonald (12,13), Kendig et al. (14) and Macdonald (15).

REFERENCES

1. Mansfeld, F. and Kendig, M. W., "Electrochemical Impedance Tests for Protective Coatings," ASTM STP 866, Ed. Haynes and Baboian, 1985, p. 122.
2. Kendig, M. W., Allen, A. T., Jeanjaquet, S. L. and Mansfeld, F., "The Application of Impedance Spectroscopy to the Evaluation of Corrosion Protection by Inhibitors and Polymer Coatings," CORROSION/85, Paper # 74 (NACE International: Houston, TX, 1985).
3. Kendig, M. and Scully, J. R., "Basic Aspects of the Application of Electrochemical Impedance for the Life Prediction of Organic Coatings on Metals," CORROSION/89, Paper # 32 (NACE International: Houston, TX 1989).
4. Scully, J. C., "Evaluation of Organic Coating Deterioration and Substrate Corrosion in Seawater Using Electrochemical Impedance Measurements," CORROSION/86, Paper # 222 (NACE International: Houston, TX, 1986).
5. Kendig, M. W., Mansfeld, F. and Tsai, S., Corr. Sci. 23(4), 317 (1983).
6. Bacon, R. C., Smith, J. J. and Rugg, R. M., Ind. Eng. Chem. 40(1), 161 (1948).
7. Leidheiser, Jr., H., "Electrical and Electrochemical Measurements as Predictors of Corrosion at Metal-Organic Coating Interface," in Corrosion Control by Coatings, Ed: H. Leidheiser (Science Press: Princeton, NJ, 1979), p. 143.
8. Macdonald, D. D., "The Advantages and Pitfalls of Electrochemical Impedance Spectroscopy," CORROSION/89, Paper # 30 (NACE International: Houston, TX, 1989).
9. McKubre, M. C., "Techniques for AC Impedance Measurements in Corrosion Systems," CORROSION/87, Paper # 480 (NACE International: Houston, TX, 1987).
10. Silverman, D. C., "Electrochemical Impedance Technique: A Practical Tool for Corrosion Prediction," CORROSION/87, Paper # 269 (NACE International: Houston, TX, 1987).
11. Walter, G. W., Corr. Sci. 26(9), 681 (1986).
12. Macdonald, D. D., "Theoretical Analysis of Electrochemical Impedance," CORROSION/87, Paper # 479 (NACE International: Houston, TX, 1987).
13. Macdonald, D. D., Electrochim. Acta 35(10), 1509, (1990).
14. Kendig, M. W., Meyer, E. M., Lindberg, G. and Mansfeld, F., Corr. Sci. 23(9), 1007 (1983).

15. Macdonald, J. R., "Data Analysis," in Impedance Spectroscopy: Emphasizing Solid Materials and Systems, Ed: J.R. Macdonald (John Wiley & Sons, Inc. New York, NY, 1987), p. 173.

APPENDIX C

PROCEDURE FOR CONDUCTING HOT WATER/ELECTROCHEMICAL IMPEDANCE/ADHESION TESTING

SCOPE

This test method describes a procedure for estimating the corrosion performance of epoxy-coated rebar (ECR) by immersion in hot aqueous environments.

REFERENCE DOCUMENTS

1. ASTM Standards:

A 775/775M-86	Epoxy-Coated Reinforcing Steel Bars
G 12-83	Nondestructive Measurements of Film Thickness of Pipeline Coatings on Steel
G 62-85	Holiday Detection in Pipeline Coatings
D 4541-85	Pull-Off Strength of Coatings Using Portable Adhesion Testers
D 610-85	Evaluating Degree of Rusting on Painted Steel Surfaces
D 714-81	Evaluating Degree of Blistering of Paints
D 1193	Reagent Water

SIGNIFICANCE AND USE

1. This test method provides a means of rapid prediction of the corrosion performance of epoxy-coated rebars.

2. Good performance in this test does not necessarily mean that adequate long-term performance in concrete can be expected from the rebar tested. Other tests are also necessary. However, failure in these tests would be indicative of pending poor service performance.

3. This test provides a reliable method to identify poorly coated rebar in terms of holidays that are not always evident from conventional detection methods.

APPARATUS

1. The required equipment for conducting this procedure includes a temperature controlled bath preferably capable of multi-specimen immersion, electrochemical impedance measuring instrumentation and adhesion pull-off tester.

2. Schematics of the adhesion pull-off instrumentation and aluminum pull-stubs are shown in Figure C-1.

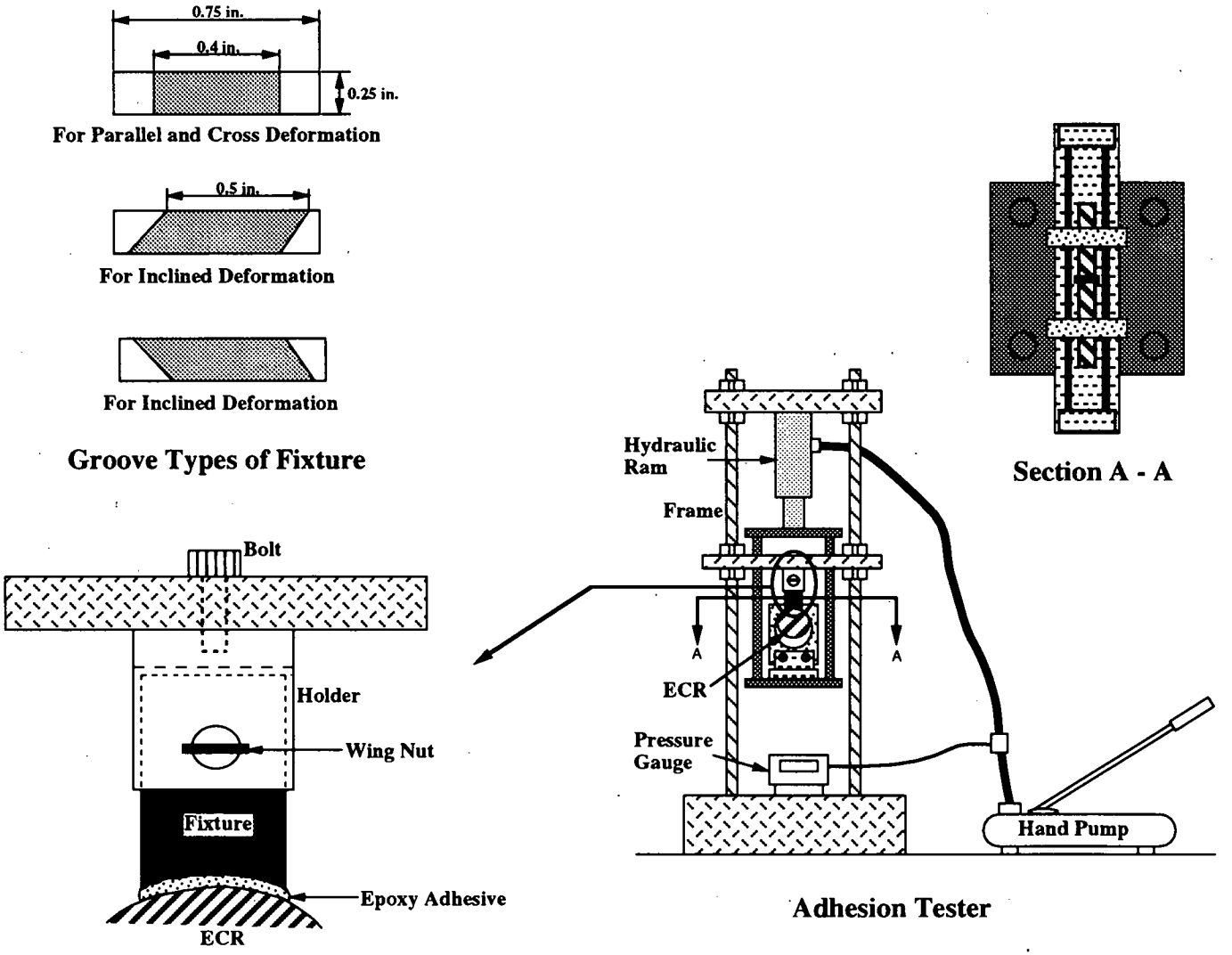

Figure C-1. Schematic of Adhesion Testing System.

REAGENTS AND MATERIALS

1. Epoxy-coated reinforcing steel specimens (see ASTM A 775/775M-86) of desired size and quality.

2. Distilled water should conform to Type IV or better according to ASTM D1193.

3. Reagent grade sodium chloride for preparation of aqueous sodium chloride solutions.

4. Room temperature curing (two-part) epoxy mounting material.

5. Plastic end caps, at least two to three times the diameter of the ECR, for mounting the test specimen.

6. Silver/silver chloride reference electrode.

7. Noble metal, mesh auxiliary electrodes (for example, titanium, platinum or niobium).

8. Thermometer for monitoring of bath temperature.

9. Glass exposure cells (for example, tall form beakers) capable of holding a minimum of one (1) liter of test solution.

10. Structural adhesive with minimum tensile peel strength of 70 lb/in (75°F) and an overlap shear strength of 4500 psi (75°F).

PREPARATION OF ECR TEST SPECIMENS

ECR Test Specimens:

1. Cut ECR specimens into lengths of 6 to 8 inches (15.25 to 20.5 cm).

2. Drill and tap one end of the ECR specimen and attach an electrical lead wire using an appropriately sized screw.

3. Seal both ends of the specimen using a room temperature curing (two-part) epoxy. Place the end opposite to end with electrical connection in plastic cap and fill with epoxy resin. Refer to Figure C-2.

4. Allow epoxy to cure according to the manufacturer's specifications.

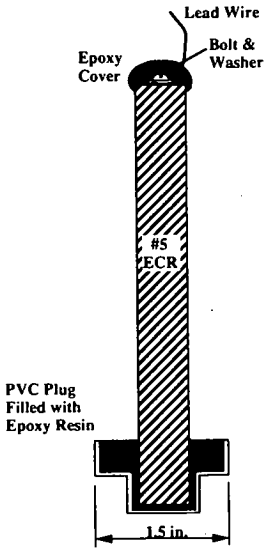

Figure C-2. Schematic of ECR Specimen.

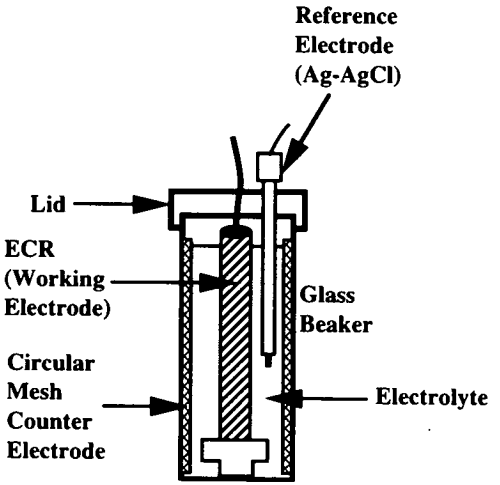

Figure C-3. Schematic of Immersion Test Cell.

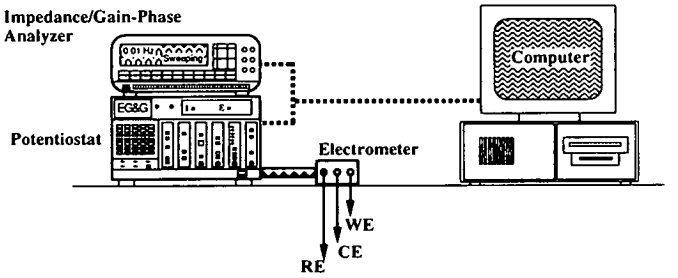

Figure C-4. Schematic of Electrochemical Impedance Instrumentation.

TEST PROCEDURES

Preliminary Characterization of ECR Specimens:

1. Determine number of coating holidays for each ECR specimen following procedures of ASTM G 62-85.

2. Determine coating thicknesses for each ECR on ribs, lugs and areas between lugs. A minimum of three measurements should be made at each location and the average recorded. Follow procedures as outlined in ASTM G 12-83.

3. Perform visual characterization using a low power stereomicroscope or equivalent to identify mashed, bare and cracked areas of the coating.

4. If desired, coat bare areas and holidays with epoxy patching material. Patching shall be done in accordance with manufacturer's recommendations.

Procedures Prior to Elevated Temperature Immersion:

1. Place ECR specimen into immersion test cell and fill with room temperature tap water. Immersion cell should be configured with a noble metal auxiliary electrode that is placed circumferentially around the ECR specimen. Refer to Figure C-3.

2. Run baseline electrochemical impedance scan for each ECR specimen according to procedures outlined in the following section.

Electrochemical Impedance Spectroscopy Test Procedures:

1. A schematic of typical electrochemical impedance instrumentation is illustrated in Figure C-4.

2. This system consists of a gain phase analyzer, a potentiostat and computer interface. Experimental control and data acquisition are accomplished with commercially available software.

3. Position ECR in immersion cell so that the mesh auxiliary electrode is located around the inner circumference of the cell and the reference electrode is placed between the auxiliary electrode and the ECR specimen at about mid specimen height. Refer to Figure C-3.

4. The following parameters are provided as a guide; actual parameters may vary with specimen type, environment and limitations of the electrochemical impedance testing instrumentation:

Amplitude:	100 mV[1]
Wave Form:	sine wave
Frequency Range:	65kHz → 10mHz (or 1 mHz)
Reference:	Ag/AgCl, or Ag/AgCl + capacitively coupled Pt wire for low conductivity environment
Auxiliary:	expanded commercially pure titanium or catalyzed titanium mesh

Elevated Temperature Immersion Test Procedures:

1. Set immersion bath temperature to the desired level (for example, 80°C).[2] Verify that temperature of immersion bath is stable before starting test.

2. Place ECR specimens into immersion test cell and fill cell with the desired test solution (for example, distilled water or 3.5 weight percent sodium chloride solution) to a level just below the top of the ECR specimen. Immersion test cells should be fitted with a cover plate to prevent evaporative water loss. Monitor water level of individual immersion cells and add distilled water as required for replenishment.

[1] Perturbation amplitude can be lowered for ECR specimens that contain defects, that is, those specimens that exhibit low impedances.
[2] Maximum temperature is 20°C below the glass transition temperature of the epoxy coating.

3. Insert immersion test cell (with ECR specimen) into temperature controlled bath. Refer to Figure C-5.

4. Test duration should be 14 days.

5. Run electrochemical impedance scans at intervals of 1, 3, 7 and 14 days.[3]

6. Monitor ECR specimens on a daily basis for blister formation following guidelines as set forth in ASTM D 714-81 and for rusting as specified in ASTM D 610-85.

7. After running the final electrochemical impedance scan, remove ECR specimens from the elevated temperature bath. Conduct final visual examination of test specimens and determine number of holidays according to procedures noted in the first item under Test Procedures section.

[3] Limit electrochemical impedance scans to two (2) hours in order to avoid instability problems that might occur during the data acquisition period. This can be especially problematic during the first 24 hours of immersion, during which time the electrochemical system undergoes the most change. Instability problems are often characterized by discontinuities in the impedance diagrams at low frequencies.

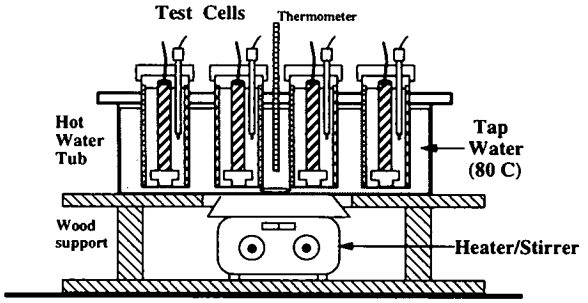

Figure C-5. Schematic of Hot Water Test Apparatus.

Adhesion Test Procedures:

1. The adhesion test procedure is summarized below:

   1) Remove ECR specimen from the immersion test cell;

   2) Dry ECR surface using clean lab tissues;

   3) Determine area between deformations on ECR to be tested;

   4) To improve adhesion between the epoxy coating and the aluminum pull-stub, roughen the ECR coating with abrasive paper;

   5) Roughen contact surface of aluminum pull-stub[4];

   6) Remove all dirt and oils on both contact surfaces with ethanol;

   7) Place aluminum pull-stub into adhesive mounting fixture. This fixture ensures that a proper gap and alignment is maintained between the ECR and the loading fixture (refer to Figure C-1);

   8) Apply adhesive to ECR specimen surface and to the concave side of the aluminum pull-stub;

   9) Allow adhesive to cure according manufacturer's specifications;

   10) Remove excess adhesive before final cure using a clean, dry cloth;

   11) Remove ECR with attached aluminum pull-stub and score the coating around outside edge of the aluminum pull-stub. Ensure that this scribe cuts completely through the coating;

   12) Install ECR with attached pull-stub into tensile testing machine or equivalent;

   13) Check alignment of the fixture within the grips;

[4] Note that the aluminum pull-stub geometry will vary according to the deformation pattern of the reinforcing steel.

14) Select appropriate cross-head speed (for example, 0.2 inches per minute) and start test;

15) Record maximum load at time of failure; and

16) Test is complete when the epoxy coating is detached.

2. Three (3) locations along the bar length should be selected randomly per specimen. Avoid locations of obvious damage such as corrosion or blisters.

3. The nominal adhesion strength of the epoxy coating is obtained by dividing the maximum applied force by the projected area of the concave surface of the aluminum pull-stub.

REPORTING REQUIREMENTS

The report shall include:

1. Source and size of the ECR test specimen.

2. Full detail of the ECR specimen characterization prior to elevated temperature testing.

3. Individual electrochemical impedance plots.

4. Adhesion strength values in pounds per inch and Pascals. Documentation of percent of coating detachment from reinforcing steel specimen.

APPENDIX D

JOBSITE QUALITY CONTROL OF ECR COATING BREAKS

INTRODUCTION

One factor defining the corrosion resistance of epoxy coated reinforcing steel is the number and size of coating breaks. Coating breaks (visible and invisible) cause the electrical resistance of epoxy coating reinforcing steel to decrease significantly (1-4). A very small amount of damage causes large reductions in resistance, and a log-log plot of resistance versus coating break area (i.e. bare area) is approximately linear. The original NBS (now NIST) report on ECR stated "Resistance measurements are probably more reliable indicators than potential measurements, since the resistance values are primarily dependent on the integrity of the coating films" (1). A laboratory AC resistance test was utilized to evaluate field ECRs extracted from cores and reported in Reference 2. Also, this subject is discussed in detail in Reference 3, section 3.13, in which ECRs were soaked in various solutions and the resistance was monitored. This report states:

"...the following percentage of damaged coating area would create a 90 percent loss in resistance after 30 days.

Tap water	0.0018 percent
Deionized water	0.0020 percent
3 percent NaCl	0.0004 percent"

"These striking parallels illustrate the extreme value of this test method in evaluating the holiday and resistance quality of coated bars, as well as its potential corrosion performance."

"When the percentage of exposed steel was in the 0.1 to 1 percent range, the reduction in resistance from the 1,000,000 ohm perfect bar was essentially 100 percent."

"The data in Fig. 3.13z indicate that the maintenance of a high electrical resistance between 200,000 and 1,000,000 ohms required a low holiday count per foot of less than 3, with an estimated percentage of exposed steel area less than 0.0006 percent."

The laboratory test methods utilized in Reference 3 involved soaking for time periods up to 30 days and it was noted that "changes in resistance occur with time as specimens are immersed in tap water, deionized water and salt solutions. These variations in resistance generally are greatest during the first day of immersion". However, from the resistance versus time plots in Reference 3 and the results of the many AC resistance tests performed by KCC INC after 3 minutes and 3 or 4 days of immersion (2,5), it is obvious that for all practical purposes, a measurement made shortly after immersion will provide an excellent indicator of coating breaks.

When dealing with only a single bar size or source, or a single test setup, it is possible to report only resistance values and draw conclusions from these data. However, for situations involving differing bar sizes, test methods or solutions, the calculation and use of an AC resistance ratio (resistance of the test bar (ECR) divided

by the resistance of an uncoated bar of equal size) provides better comparative information (1-4). Most agree that, as a minimum, an AC resistance ratio in excess of 300 is required.

WORK PLAN

OBJECTIVES:

1. To develop a field test method to define the AC resistance ratio of ECRs prior to concrete placement.
2. To utilize the test method and visual examination to define the quality of ECRs being used in North America today.
3. To develop a quick, low cost field quality control test for ECR coating breaks.

The work plan involved the following subtasks:

PHASE I

1. Definition of an AC resistance ratio test procedure involving "wrap-around" secondary electrodes and a portable AC resistance meter.
2. Laboratory testing of the method to define practicality and to confirm the inverse relationship between macrocell corrosion of ECR and the AC resistance ratio.
3. Trial uses in the field, followed by field testing of ECR on eight bridge structures in 1992 and 1993.

PHASE II

4. Modifications, as required based upon the Phase I experiences, and additional laboratory testing of the final test using very high quality ECRs with visible coating breaks of known size.
5. Data analyses to define the AC resistance ratio which corresponds to minimal visually discernible coating breaks.
6. Definition and confirmation testing of a quick, low cost field test for ECR coating breaks (i.e. for routine quality control and acceptance testing in the field).

PROCEDURES AND FINDINGS - PHASE I

The initial test setup involved the use of two copper pipes, which were cut in half longitudinally and filled with cellulose sponge, as the test probes; a soil resistance meter; and leadwires. Thus, the measurement is made from probe to probe and no direct contact with the ECR is necessary. This test setup is shown in Figure D-1. The probes were constructed in two different lengths, 4-inches long and 12-inches long. The longer probe has the advantage of a larger test area, but cannot be used in situations where crossing bars are tied in place at intervals of less than 13 inches. To provide for easy use, hinges were attached to one side of each split pipe and Velcro™ closures were placed on the other side. Soapy water was used as the contact medium. Probe schematics are presented in Figure D-2.

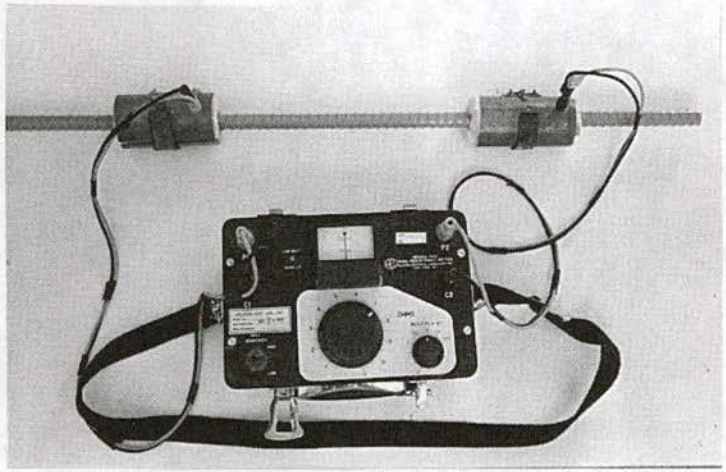

4-inch Probes.

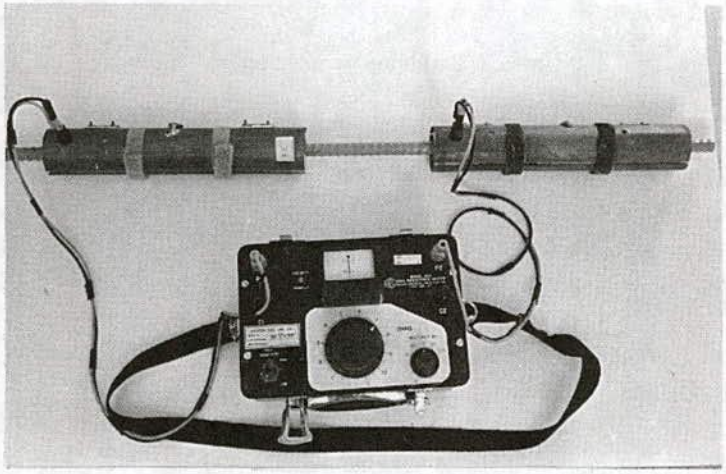

12-inch Probes.

Figure D-1. Double Probe AC Resistance Test.

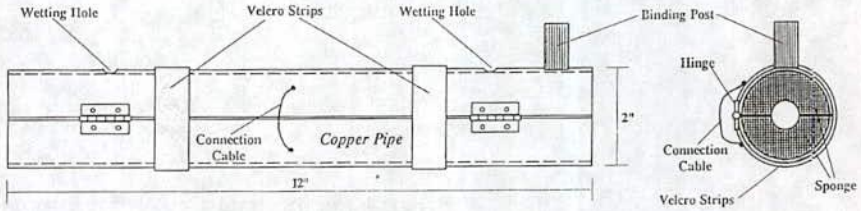

12-inch AC Resistance Probe

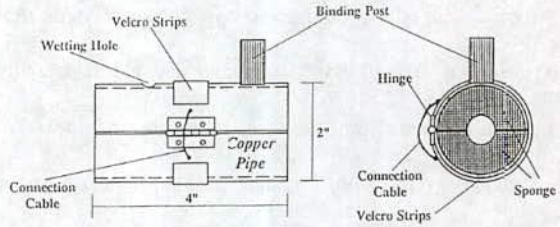

4-inch AC Resistance Probe

Figure D-2. Probe Schematic.

Reinforced concrete beams of the type defined in ASTM G109 had previously been cast using a single #5 ECR as the top bar and two uncoated reinforcing bars as the bottom reinforcement. The concrete surrounding the bottom reinforcement was essentially salt-free while that surrounding the ECR contained 15 lbs Cl⁻/cy admixed as NaCl. Both concretes had a water-cement ratio of 0.50. The ECRs for these beams were obtained from coaters, jobsites and a commercial supplier. Two beams with uncoated reinforcing in the top mat were also cast. After moist curing, the top and bottom bars were connected externally using a precision resistor and a switch, and the beams were exposed on above-ground racks in Sterling, Virginia. The macrocell corrosion current flow was periodically monitored as the voltage drop across the precision resistor. Additionally, the AC resistance between the top and bottom rebar mats were monitored periodically. Additional detail on these beams and the resulting data were presented in the interim report (4). Companion retained bars from twelve bar lots were tested for AC resistance ratio using the proposed field test (4-inch probes).

Table D-1 provides summary data on the AC resistance ratios defined by the double probe version of the new test as well as the average AC resistance ratios and the macrocell current densities defined for the beams. The data have been sorted by increasing macrocell current density.

Table D-1. Field QC Test vs Macrocell Beam Data

ECR Source	New Test AC Resistance Ratio	Average Beam AC Resistance Ratio	Average Beam Macrocell Current Density mA/sq. ft.
Jobsite Can 2	>6377	442	0.000
Coater Can 4	928	4559	0.000
Coater US4	>6377	1538	0.001
Jobsite US 1	986	51	0.010
Coater US 3	>6377	377	0.010
Coater Can 3	96	20	0.030
Jobsite Can 1	84	6	0.070
Coater Can 5	61	28	0.074
Coater US 2	133	45	0.077
US Supplier 1-1	13	3	0.493
US Supplier 1-2	10	5	0.493
Jobsite US 2	45	2	0.694

Inspection of these data indicates that the AC resistance ratios correlate well with macrocell corrosion current density, with low AC resistance ratios corresponding to high corrosion. The new test provided reasonable estimates of the corrosion occurring in the beams, especially when one notes that the new test was run on companion bars rather than the actual bars used in the beams.

To study the reproducibility of the test, uncoated rebars were tested by a single operator on four separate days using both double 4-inch and double 12-inch probes and a single lot of "soapy water". The data presented in Table D-2 indicate that the test is quite reproducible, with the range for #5 bars varying from 450 to 460 ohms with the 4-inch probes and 130 to 150 ohms with the 12-inch probes.

To provide initial data on the quality of ECR being provided commercially in 1992, fifty six-foot long ECRs were purchased from a commercial U.S. supplier who certified that the bars met all requirements of ASTM A775. The results of the double probe tests on these bars are presented in Table D-3, and indicate that the bars are poor quality with respect to coating breaks. With the 4-inch probes, the median AC resistance ratio was 14 and only 14 percent of the bars exhibited AC resistance ratios in excess of 300. With the 12 inch probes, the median AC resistance ratio was 12 and only 2 percent (1 in 50) of the bars exhibited an AC resistance ratio in excess of 300. Twelve other ECRs from jobsites in four US states were also tested in 1992

Table D-2. AC Resistance Test for Field QC Data Summary for Uncoated Rebar - June 18, 1992.

BAR SIZE	BAR CODE	4" probe AC RESISTANCE ohms	12" probe AC RESISTANCE ohms
June 15,1992			
#6	A	440	110
#5	A	455	130
#5	B	450	135
#5	I-C-SHRP-25	450	
#5	N1-S7-A	455	
	Average (#5)	453	133
	Minimum (#5)	450	130
	Maximum (#5)	455	135
June 16,1992			
#6	A	410	115
#5	A	455	135
#5	B	450	135
#5	I-C-SHRP-25	455	
#5	N1-S7-A	450	
	Average (#5)	453	135
	Minimum (#5)	450	135
	Maximum (#5)	455	135
June 17,1992			
#6	A	410	120
#5	A	455	130
#5	B	460	135
#5	I-C-SHRP-25	460	
#5	N1-S7-A	450	
	Average (#5)	456	133
	Minimum (#5)	450	130
	Maximum (#5)	460	135
June 18,1992			
#5	A	460	140
#5	B	450	140
#5	C	460	150
#5	D	450	140
#5	I-C-SHRP-25	455	
#5	N1-S7-A	455	
#5	N1-S7-B	460	
	Average	456	143
	Minimum	450	140
	Maximum	460	150

Table D-3. AC Resistance Ratio Test Findings ECR Certified Commercial Supplier as Complying with ASTM A775 - June 1992.

SOURCE	BAR #	4" Probe AC RESISTANCE RATIO	12" Probe AC RESISTANCE RATIO
ECRs Obtained from U.S. ECR Supplier			
TS1	1	7	8
TS1	2	9	7
TS1	3	4	4
TS1	4	5	5
TS1	5	18	27
TS1	6	5	5
TS1	7	39	13
TS1	8	10	12
TS1	9	> 2,423	2,336
TS1	10	12	8
TS1	11	9	9
TS1	12	6	6
TS1	13	19	18
TS1	14	8	5
TS1	15	174	55
TS1	16	6	5
TS1	17	14	17
TS1	18	26	8
TS1	19	1,564	51
TS1	20	6	6
TS1	21	> 2,423	88
TS1	22	19	36
TS1	23	11	12
TS1	24	40	43
TS1	25	46	5
TS1	26	6	6
TS1	27	19	18
TS1	28	7	14
TS1	29	3	3
TS1	30	18	45
TS1	31	33	66
TS1	32	9	12
TS1	33	> 2,423	39
TS1	34	7	8
TS1	35	11	18
TS1	36	24	15
TS1	37	40	42
TS1	38	6	8
TS1	39	13	7
TS1	40	112	40
TS1	41	15	11
TS1	42	> 2,423	47
TS1	43	4	5
TS1	44	441	60
TS1	45	4	4
TS1	46	> 2,423	28
TS1	47	21	19
TS1	48	11	26
TS1	49	6	4
TS1	50	119	288
Median		14	12
% > 300		14%	2%
Maximum		> 2,423	2,336
Minimum		3	3

using both 4-inch and 12-inch probes. For the 4-inch probes, the resistance ratios ranged from 1 to 114. For the 12-inch probes, the resistance ratios varied from 3 to 107. Thus, the bars from all four jobsites yielded resistance ratios below the desired 300 minimum, indicating that they were poor quality with respect to coating breaks.

The ECRs for one bridge deck and one bridge substructure being constructed in 1992 in the eastern U.S. were field tested. The testing was performed using double 4-inch probes on both bars stored at the jobsite and tied-in-place bars. The ECR portion beneath each probe was carefully examined (mirrors were used for the underside examination), and rated as being visibly damaged or undamaged. The findings are presented in Tables D-4 and D-5 and are summarized below:

Property	**Jobsite Storage**	**Tied-in-Place**
Median Resist. Ratio	391	306
Minimum Resist. Ratio	28	11
Maximum Resist. Ratio	> 6,857	> 8,148
Percent < 300 Ratio	36	47
Percent w/ Visible Damage	40	66

Although the ECRs used in these decks are better quality than the jobsite and commercial bars tested earlier, about one-third of the jobsite bars and one-half of the bars which were tied in place exhibited AC resistance ratios less than 300. Also,

Table D-4. Field Epoxy Coated Straight Rebar Testing 1992 Double 4-inch Probes Bars in Jobsite Storage.

Test No.	Bar Size	AC Resist. Ratio	Visual	Count
12	5	28	VD	1
8	5	32	VD	2
10	5	43	VD	3
14	5	43	VD	4
13	5	48	VD	5
11	5	113	VD	6
9	5	143	NVD	7
21	5	148	VD	8
7	5	152	VD	9
15	5	313	NVD	10
22	5	330	VD	11
5	5	378	VD	12
23	5	391	NVD	13
19	5	396	NVD	14
18	5	448	NVD	15
24	5	739	NVD	16
2	4	1,357	NVD	17
6	5	1,522	NVD	18
4	4	1,571	NVD	19
3	4	3,143	NVD	20
16	5	4,783	NVD	21
17	4	4,783	NVD	22
20	5	4,783	NVD	23
25	5	4,783	NVD	24
1	4	6,857	NVD	25
Median Ratio =		391		
Percent < 300 =		36		
Percent with Visible Damage =		40		

Table D-5. Field Epoxy Coated Straight Rebar Testing 1992 Double 4-inch Probes Bars-in-Place: U.S. Decks.

Test No.	Bar Size	AC Resist Ratio	Visual	Count
15	5	11	VD	1
13	5	21	VD	2
2	5	32	VD	3
18	5	42	VD	4
3	5	48	VD	5
1	5	50	VD	6
9	5	67	VD	7
4	5	81	VD	8
16	5	85	NVD	9
27	5	94	VD	10
23	5	125	VD	11
11	5	126	VD	12
12	5	141	NVD	13
22	5	271	VD	14
26	5	294	VD	15
5	5	304	VD	16
20	4	307	NVD	17
8	5	311	VD	18
21	5	369	VD	19
29	5	400	VD	20
32	5	438	VD	21
28	5	494	VD	22
7	5	496	VD	23
25	5	500	VD	24
24	5	656	NVD	25
6	5	3,481	NVD	26
14	5	4,000	NVD	27
30	5	6,875	NVD	28
31	5	6,875	NVD	29
19	4	7,857	NVD	30
10	7	8,148	NVD	31
17	5	8,148	NVD	32
Median Ratio =		306		
Percent < 300 =		47		
Percent with Visible Damage =			66	

these data appear to indicate that the process of installing the bars in-place resulted in significant damage. For the tied-in-place bars, two-thirds exhibited visible damage, while "only" 40 percent of the bars in jobsite storage exhibited such damage.

A third US field structure was studied in 1992 to quantify the amount of damage exhibited by the ECR. The ECR used in this deck was by far the highest quality bar encountered in the field efforts. There were locations on many bars where no coating breaks were detectable, either visually or with an 80,000 ohm holiday detector. Such was not the case on any of the other structures studied to date. Because of this, a special study was performed to evaluate the double probe AC resistance test technique and the specific amount of visible bare area was defined.

Nine double probe AC resistance measurements were made at locations in which one of the probes was placed in an area free of visible coating breaks and the other was placed in a damaged area. In six of the nine cases, the resistance measured exceeded 1.1 million ohms in spite of the fact that the visible coating breaks beneath one probe varied from 0.010 to 0.031 percent. These tests showed that in many cases where one probe is placed in an area free of visible coating breaks, the result (i.e. the probe to probe resistance measurement) does not reflect the presence of breaks beneath the other probe. This shortcoming of the double probe test is of little significance on badly damaged ECR since coating breaks are most often present beneath both probes. However, in the case of high quality bars, the quality can be overestimated. For this reason, all other AC resistance work in this study utilized

only a single probe and a direct contact was made to each test ECR using needle-nosed vise grips. This test setup is shown in Figure D-3. Such a means of contact proved to be easily implemented, but it does result in the need to patch the connection location. For cases when at least one coating break exists under each probe, data obtained by the double probe method and that obtained by the single probe method can be directly compared when both are presented as resistance ratios.

The bars on the above referenced deck, after being tied-in-place, were carefully examined at 80 locations and the size of each coating break was estimated using a comparative visual scale in which twenty four breaks of known area were presented. The percentage visible bare area was then calculated as one hundred times the sum of all the estimated bare areas divided by the surface area of the portion of each bar examined. The bare areas varied from 0.000 to 0.302 percent, with an average of 0.034 percent and a median of 0.011 percent. Even on this deck, with the highest quality bar studied thus far, only 25 percent of the locations met the 0.0006 percent or less recommendation of Reference 3, and 50 percent of the locations studied had visible bare areas exceeding 0.010 percent (i.e. about 17 times the 0.0006 maximum recommended by Reference 3).

Four U.S. and one Canadian bridge decks were evaluated in the summer and fall of 1993 using the single AC resistance probe (4-inch) technique and visual examination on straight bars, and electrical coating break ("holiday") detection on both straight and bent bars. The detailed visual examination technique described

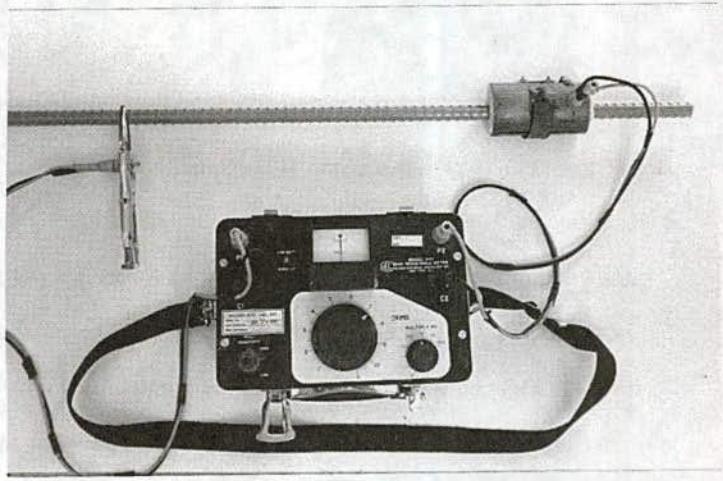

AC Resistance Ratio Test.

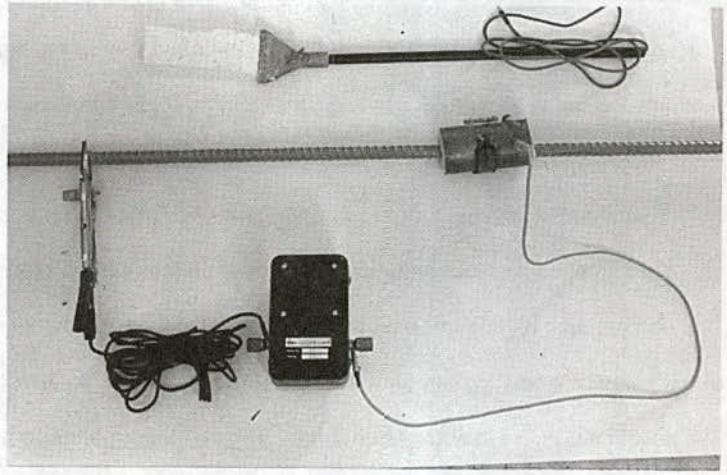

Modified Holiday Detector Test.

Figure D-3. Single Probe Test Setups.

above proved to be too time consuming for field use. Therefore, on these bridges, the surface beneath each probe was merely closely examined (mirrors were used for the underside) and designated as having "visible defects (VD)" or "no visible defects (NVD)". For the straight bars, 14 to 40 locations were examined for each structure as time and weather allowed. Fifteen bent bars were examined for each structure and each bar was divided into six two-inch segments on or near the bend for a total of 90 test locations, except for Eastern U.S. structure #2 on which only five bent bars were tested at 30 locations. Each bent bar segment was tested separately by tightly wrapping a 2-inch wide by 6-inch long by 2-inch thick damp sponge around it. The sponge contained minimal free water to prevent water runoff onto other areas of the bar. The sponge was connected to a nonmetallic wand which was connected to one terminal of an 80,000 ohm holiday detector, and the ECR was grounded to the other terminal. Straight bar coating break detection was accomplished by connecting one terminal of an 80,000 ohm holiday detector directly to the 4-inch probe and the other terminal directly to the ECR (via the vise grips).

All the ECRs were coated with a "green colored" epoxy during 1993. The bars for the Canadian structure involved the use of a primer prior to coating application, while the U.S. bars did not. The Canadian bars were metric bar designation No. 15 (16 mm diameter) but for convenience are noted in Tables D-6 and D-7 as #5 bars (the closest U.S. bar number). The resulting data are tabulated in

Table D-6. Field Epoxy Coated Straight Rebar Quality Control Testing.

Test No.	Bar Size	AC Resist. Ratio	Coating Break Y or N	Visual	Count
49	5	8	Y	VD	1
25	5	11	Y	VD	2
106	5	13	Y	VD	3
48	5	15	Y	VD	4
102	5	15	Y	VD	5
107	5	16	Y	VD	6
52	5	20	Y	VD	7
56	5	24	Y	VD	8
83	5	25	Y	VD	9
100	7	29	Y	VD	10
65	5	29	Y	VD	11
114	5	31	Y	VD	12
72	5	32	Y	VD	13
84	5	33	Y	VD	14
8	5	34	Y	VD	15
57	5	38	Y	VD	16
85	5	39	Y	VD	17
55	5	40	Y	VD	18
9	5	40	Y	VD	19
78	4	43	Y	NVD	20
108	5	45	Y	VD	21
96	7	48	Y	VD	22
104	5	50	Y	VD	23
15	5	53	Y	VD	24
110	5	56	Y	VD	25
11	5	64	Y	VD	26
50	5	65	Y	VD	27
53	5	67	Y	VD	28
88	5	69	Y	VD	29
98	7	70	Y	VD	30
71	5	74	Y	VD	31
105	5	75	Y	VD	32
112	5	75	Y	VD	33
70	5	75	Y	VD	34
47	5	76	Y	VD	35
69	5	90	Y	VD	36
82	5	94	Y	VD	37
68	5	94	Y	VD	38
64	5	103	Y	VD	39
39	7	107	Y	VD	40
43	7	107	Y	VD	41
74	5	112	Y	VD	42
45	5	113	Y	NVD	43
37	5	118	Y	VD	44
101	7	118	Y	NVD	45
109	5	122	Y	VD	46
6	5	126	Y	VD	47
87	5	127	Y	VD	48
14	5	131	Y	VD	49
31	5	132	Y	VD	50
20	5	133	Y	VD	51
41	7	144	Y	VD	52
66	5	145	Y	NVD	53
27	5	147	Y	VD	54
42	7	159	Y	VD	55
95	7	161	Y	VD	56
38	7	163	Y	VD	57
97	7	185	Y	VD	58
7	5	189	Y	VD	59
94	5	204	Y	VD	60

Table D-6 (continued)

Test No.	Bar Size	AC Resist. Ratio	Coating Break Y or N	Visual	Count
61	5	217	Y	VD	61
51	5	218	Y	VD	62
21	4	220	Y	NVD	63
16	5	226	Y	VD	64
111	5	235	Y	VD	65
29	5	236	Y	VD	66
32	5	245	Y	NVD	67
26	5	273	Y	VD	68
60	5	319	Y	VD	69
44	7	336	Y	NVD	70
92	5	347	Y	NVD	71
103	5	364	Y	VD	72
113	5	388	Y	NVD	73
59	5	391	Y	VD	74
40	7	397	Y	NVD	75
46	5	397	Y	NVD	76
75	5	420	Y	VD	77
3	5	453	Y	VD	78
63	5	464	Y	VD	79
99	7	470	Y	NVD	80
54	5	475	Y	NVD	81
34	5	500	Y	VD	82
76	5	507	Y	NVD	83
10	5	516	Y	VD	84
89	5	551	Y	NVD	85
18	5	629	Y	VD	86
91	5	694	Y	VD	87
19	5	969	Y	NVD	88
67	5	1014	Y	VD	89
35	5	1091	Y	NVD	90
33	5	1182	Y	NVD	91
17	5	1195	Y	NVD	92
93	5	1224	N	NVD	93
77	5	1304	Y	VD	94
73	5	1449	Y	VD	95
79	5	1515	Y	NVD	96
23	4	1767	Y	VD	97
12	5	2264	N	NVD	98
36	5	3364	N	NVD	99
58	4	3768	Y	VD	100
86	5	4490	N	NVD	101
90	5	4490	N	NVD	102
2	5	4528	N	NVD	103
28	5	5000	N	NVD	104
30	5	5000	N	NVD	105
81	4	5152	N	NVD	106
24	4	5400	N	NVD	107
13	5	6289	N	NVD	108
80	4	6667	N	NVD	109
22	5	7333	N	NVD	110
5	5	7547	N	VD	111
4	5	11321	Y	VD	112
1	4	13836	Y	NVD	113
62	5	15942	N	VD	114

Median Resist. Ratio 174

Overall Percent with Visible Damage = 70%
Overall Percent with Coating Breaks = 87%

Table D-7. Field Coating Break Detection on Bent Bars.

Test No.	Bar Size & Bend Degrees	Number of Locations showing Coating Breaks	Test No.	Bar Size & Bend Degrees	Number of Locations showing Coating Breaks	Test No.	Bar Size & Bend Degrees	Number of Locations showing Coating Breaks
Job: Eastern U. S. Bridge Deck #1: Tested September 15, 1993								
1	5/180	6	6	5/180	6	11	5/180	6
2	5/180	6	7	5/180	6	12	5/180	6
3	5/180	6	8	5/180	6	13	5/180	6
4	5/180	5	9	5/180	6	14	5/180	6
5	5/180	6	10	5/180	6	15	5/180	6
Overall Percent of Bend Sections with Coating Breaks: 98.9%								
Job: Eastern U. S. Bridge Deck #2: Tested September 27, 1993								
1	5/180	3	3	5/180	6	5	5/180	6
2	4/90	6	4	5/180	6			
Overall Percent of Bend Sections with Coating Breaks: 90.0%								
Job: Canadian Bridge Deck #1: Tested September 29, 1993								
1	5/90	6	6	5/120	0	11	5/90	5
2	5/90	6	7	5/45	6	12	5/45	6
3	5/90	3	8	5/45	6	13	5/90	6
4	5/90	0	9	5/45	2	14	5/90	6
5	5/120	6	10	5/45	0	15	5/45	4
Overall Percent of Bend Sections with Coating Breaks: 68.9%								
Job: Eastern U. S. Bridge Deck #3: Tested October 13, 1993								
1	7/180	6	6	7/180	6	11	7/180	6
2	7/180	5	7	7/180	5	12	7/180	6
3	7/180	6	8	7/180	6	13	7/180	6
4	7/180	6	9	7/180	6	14	7/180	6
5	7/180	5	10	7/180	6	15	7/180	6
Overall Percent of Bend Sections with Coating Breaks: 98.7%								
Job: Eastern U. S. Bridge Deck #4: Tested October 20, 1993								
1	5/180	6	6	5/180	6	11	5/180	6
2	5/180	6	7	5/180	6	12	5/180	6
3	5/180	6	8	5/180	6	13	5/180	6
4	5/180	6	9	5/180	6	14	5/180	6
5	5/180	6	10	5/180	6	15	5/180	6
Overall Percent of Bend Sections with Coating Breaks: 100.0%								
All Decks: Overall Percent of Bend Sections with Coating Breaks: 83.8%								

Note: Each Bar Segment = 1 foot; Hand Detector with 2" Wide Sponge, placed at 6 Locations per Foot of Bend.
Comments: Bars tied-in-place ready for concrete placement.

Table D-6 for straight bars (sorted by resistance ratio) and Table D-7 for bent bars, and are summarized below by structure.

Structure	Percent < 300 AC Resist. Ratio	Percent < 2000 AC Resist. Ratio	Percent with Coating Breaks	Percent with Visible Damage
Straight Bars:				
East. U.S. #1	45	80	88	83
East. U.S. #2	57	71	71	50
Canadian #1	40	75	70	45
East. U.S. #3	75	100	100	70
East. U.S. #4	90	100	100	95
Bent Bars:				
East. U.S. #1	-	-	99	-
East. U.S. #2	-	-	90	-
Canadian #1	-	-	69	-
East. U.S. #3	-	-	97	-
East. U.S. #4	-	-	100	-

The straight bar data tabulation in Table D-6 was sorted by AC resistance ratio to allow comparison of the AC resistance and visual damage data for the purposes of defining a resistance ratio above which visual damage will be rare. From the data in the table, the following can be noted:

- 33 percent of all measurements yielded AC resistance ratios of 100 or less. These are poor quality bars, and as expected ninety-seven percent of these were also identified as exhibiting visual damage and 100 percent exhibited coating breaks as defined by an 80,000 ohm holiday detector.
- 60 percent of all measurements yielded AC resistance ratios less than 300. These are also poor quality bars. Ninety-one percent were identified as also exhibiting visible damage and 100 percent exhibited coating breaks as defined with an 80,000 ohm holiday detector.
- The AC resistance ratio "zone" of 300 to 2000 appears to be the transition area between good and marginal quality bars with respect to excessive coating breaks. About half of the bars with ratios in that range exhibited visible coating breaks and half did not. However, 97 percent of the bars in this range exhibited coating breaks as defined by the 80,000 ohm holiday detector. Since the 4-inch probe represents only one-third of a foot, these data indicate that the coating break rate on 97 percent of the bars equaled or exceeded 3 per foot (specifications

typically allow no more than 2 per foot at the plant). 85 percent of the field ECRs had AC resistance ratios less than 2,000.

- Fifteen percent of the bars exhibited AC resistance ratios greater than 2,000. Of these, 76 percent exhibited no visual damage and 82 percent showed no coating breaks according to the 80,000 ohm holiday detector.
- Overall, 70 percent of these straight field ECRs exhibited visual damage and 87 percent exhibited coating breaks as identified by the 80,000 ohm holiday detector. The median resistance ratio was 174.

The bent bar data presented in Table D-7 indicate that the bent bars were of about the same poor quality as the straight bars. For the bent bars, 91 percent of the bar segments indicated coating breaks using the 80,000 ohm holiday detector. Since the 2-inch sponge covered only one-sixth of a foot, these data indicate that the coating break rate on 91 percent of the bars equaled or exceeded 6 per foot (specifications typically allow no more than 2 per foot at the coating plant).

In addition to the above tests, the straight bars were tested at 81 additional locations on each deck using the 80,000 ohm electrical coating break detector and the 4-inch probe, except for Eastern U.S. Deck #2 where only 45 additional locations were tested. The results were as follows:

Eastern U.S. #1 = 96 percent with Coating Breaks

Eastern U.S. #2 = 82 percent with Coating Breaks

Canadian #1 = 67 percent with Coating Breaks

Eastern U.S. #3 = 73 percent with Coating Breaks

Eastern U.S. #4 = 100 percent with Coating Breaks

Overall, 84 percent of these straight bars exhibited coating breaks as defined by the 80,000 ohm holiday detector. Since the 4-inch probe represents only one-third of a foot, these data indicate that the coating break rate on 84 percent of the field bars equaled or exceeded 3 per foot (specifications typically allow no more than 2 per foot at the plant).

PROCEDURES AND FINDINGS - PHASE II

Phase I dealt primarily with AC resistance ratios, and uncoated bar measurements were made during each laboratory or field measurement of ECR (using the same equipment and solutions). As a result, variations in solution or contact resistances were compensated by the test technique. However, since one of the goals of Phase II was to define a simpler test, knowledge was needed on the factors affecting the resistance measurement itself. Toward this end, a laboratory evaluation was performed.

All Phase II work involved the use of a single probe (4-inch or 12-inch) and direct connection to the reinforcing steel. Very high quality #5 epoxy coated rebars were procured directly from a U.S. coater and used in this testing. Each bar was carefully tested with the 80,000 ohm holiday detector and a small 0.5 inch wide sponge and all holidays were marked on the bars prior to their use. Laboratory tests were performed to examine the effect of various factors on test results. It was known that the AC resistance measured was dependent upon: (1) the contact resistance between the probe and the solution; (2) the solution resistivity and path; and (3) the contact resistance between the probe and the bar. But the relative importance of each of these was not known.

The soapy water solution used in Phase I consisted of tap water to which a small amount of liquid dish soap had been added. Its resistivity was about 2,000 ohm-cm and typical resistance readings for uncoated bars were in the range of 120 ohms for a 12-inch probe and 350 ohms for a 4-inch probe when the sponges were saturated with this solution. On high quality epoxy coated rebars without coating breaks, the 12-inch probe typically yielded resistances in excess of 500,000 ohms and the 4-inch probe read in excess of 1.1 million ohms. It had been noticed in Phase I that the uncoated rebar measurements were somewhat variable from field site to field site and therefore, it was deemed appropriate to examine the effects of various parameters on the resistance measurement.

The copper probes oxidize somewhat with use, with the result being a dark film on the surfaces. Measurements were made at six locations on several #5 uncoated bars with the probes which had been in use for over one year, and then the measurements were repeated after the probes had been thoroughly cleaned. In all cases the re-measured resistances varied by only 1 ohm or less. Similar measurements on the high quality ECRs found no change in measured resistance. These data indicate that the contact resistance between the probe inner surface and the wet sponges was a minor component of the overall measurement.

The uncoated bars used in the above test contained surface mil scale and some rust. They were then thoroughly cleaned to near white metal by heavy wire brushing, and the tests were repeated. The resistances measured on the cleaned bars were, in all cases, 1 to 2 ohms less than those measured on the uncleaned bars, indicating that uncoated bar cleanliness was not a dominant factor in the measurement.

The wetness level of the sponges was then examined, with three levels of wetness studied (damp only, partially saturated, and totally saturated). With the 12-inch probe on a cleaned, uncoated bar, the probe with damp sponges indicated a resistance of 230 ohms, the partially saturated sponges yielded 160 ohms and the totally saturated sponges yielded 120 ohms. Such a variation is significant, and therefore, all future probe testing involved the use of totally saturated sponges.

The effect of wetting agent resistivity was examined using uncoated bars and solutions of three resistivities (2000, 800 and 80 ohm-cm). The solution resistivity

had a significant influence on the resistances measured on uncoated bars. For example, the 12-inch probe on the uncoated bar (saturated sponges) read 120 ohms with the 2000 ohm-cm solution, about 40 ohms with the 800 ohm-cm solution and about 4 ohms with the 80 ohm-cm solution. The degree of sponge wetness had little effect on ECRs without coating breaks. However, on ECRs with small defects, the defects could be missed when the probe sponges were not saturated.

Thus, the primary factors affecting the resistance measurement using the copper probes on uncoated bars and ECRs with defects are the degree of wetness of the sponges and the solution resistivity. Future testing was standardized by using sponges which had been totally saturated with the 80 ohm-cm solution. The solution was made by adding 100 grams of Cascade™ dishwasher powdered detergent to one gallon of tap water.

Three electrodes were used in the testing: 4-inch split copper probe, 12-inch split copper probe, and 2-inch wide by 2-inch thick by 6-inch long cellulose sponge attached to a nonmetallic wand with leadwire. The copper probes were constructed in our laboratory per Figure D-2 and the nonmetallic wand with leadwire was the standard contact medium for a commercially available holiday detector.

From examination of past laboratory and field data, it was noted that visible coating breaks correspond to an AC resistance of about 2,500 ohms with either probe. This was confirmed by testing two holiday-free ECRs onto which a barely visible single 1/64-inch diameter coating break was created, thus yielding a bare area of 0.0024 percent beneath a 4-inch probe. The measured resistances were in excess of 1.1 million ohms prior to the break and 2,675 and 2,300 ohms after the break was created. The 80,000 ohm holiday detector with the wand and sponge saturated with the 80 ohm-cm solution detected no breaks on the original bar, but identified the 1/64-inch diameter hole on each bar. The detector was then modified by adjusting the internal potentiometer such that it would detect breaks at a resistance of about 2,000 ohms or less only. This was accomplished simply by placing a 2,200 ohm resistor between the leads and slowly adjusting the pot until the beeping sound ceased. Proper operation was then checked by replacing the 2,200 ohm resistor with 1,500 and 3,300 ohm resistors. The detector "beeped" with the 1,500 ohm resistor in the circuit, but did not "beep" with the 3,300 ohm resistor in the circuit. With this simple modification, the commercially available 80,000 ohm "holiday" detector became a 2,000 ohm "field coating break" detector. As a cross-check, the 2,000 ohm detector was used to retest several of the as-received ECRs at locations which previously had been identified as locations with invisible holidays by the 80,000 ohm detector. Individual invisible holidays were not detected at any of the 6 test sites. However, at one location at which more than 10 holidays existed together in a 2-inch wide area on a longitudinal ridge, the 2,000 ohm detector with the 2-inch wide saturated sponge "beeped". This detection was considered desirable since that area of the bar was outside the allowable production specification of 2 or less holidays per foot. The

more than 10 invisible holidays at that location would be at least as detrimental as a single small visible bare area.

For follow-up testing, six ECRs were selected which exhibited no coating breaks as indicated by the 80,000 ohm holiday detector. The coating thickness averaged 8.5 mils with a range of 6.7 to 10.4 mils for 12 measurements. The bars were then tested using the 4-inch and 12-inch probes, the location of each probe being marked on each bar; and each visible bare area was tested using the 2,000 ohm field break detector with wand and sponge and separately with the detector attached directly to the 4-inch probe. In all instances the sponges were saturated with 80 ohm-cm solution prior to each test. After these tests, coating breaks were created by drilling through the coating using a 1/32-inch drill bit at select locations (one beneath each 4-inch probe and three beneath each 12-inch probe) to yield a coating break area of 0.010 percent. The bars were then retested. The coating breaks were then increased to a total of 0.156 percent beneath each probe and retests were performed. Finally, the coating break area was increased to 0.312 percent beneath each probe and retests were again performed. These coating break percentages were selected because they represent the range of visible coating breaks commonly encountered in "real world" ECRs which were tied-in-place in bridge structures. The resulting data for the 4-inch and 12-inch probes are presented in Table D-8 as raw resistances and Table D-9 as resistance ratios (ECR resistance divided by resistance of uncoated rebar of equal size), and are discussed below.

Table D-8. AC Resistances of #5 Epoxy Coated Reinforcing Steel.

12-inch Probe

ECR # & Position	Undamaged Resistance, ohms	0.01% Damage Resistance, ohms	0.16% Damage Resistance, ohms	0.31% Damage Resistance, ohms
9L	560,000	740	445	150
9R	675,000	310	350	94
7L	485,000	280	160	77
7R	630,000	1,800	345	60
5L	910,000	785	350	89
5R	1,100,000	490	580	83
Average	726,667	734	372	92
Median	652,500	615	350	86
Minimum	485,000	280	160	60
Maximum	1,100,000	1,800	580	150

Note: Uncoated #5 Rebar averaged 2.2 ohms.

4-inch Probe

ECR # & Position	Undamaged Resistance, ohms	0.01% Damage Resistance, ohms	0.16% Damage Resistance, ohms	0.31% Damage Resistance, ohms
9L	>1,100,000	1,600	500	310
9R	>1,100,000	930	410	195
7L	>1,100,000	1,850	360	180
7R	>1,100,000	850	385	255
5L	>1,100,000	850	430	210
5R	>1,100,000	1,400	350	215
Average	>1,100,000	1,247	406	228
Median	>1,100,000	1,165	398	213
Minimum	>1,100,000	850	350	180
Maximum	>1,100,000	1,850	500	310

Note: Uncoated #5 Rebar averaged 5.7 ohms.

Table D-9. AC Resistance Ratios of #5 Epoxy Coated Reinforcing Steel.

12-inch Probe

ECR # & Position	Undamaged Resistance Ratio	0.01% Damage Resistance Ratio	0.16% Damage Resistance Ratio	0.31% Damage Resistance Ratio
9L	254,545	336	202	68
9R	306,818	141	159	43
7L	220,455	127	73	35
7R	286,364	818	157	27
5L	413,636	357	159	40
5R	500,000	223	264	38
Average	330,303	334	169	42
Median	296,591	280	159	39
Minimum	220,455	127	73	27
Maximum	500,000	818	264	68

Note: Uncoated #5 Rebar averaged 2.2 ohms.

4-inch Probe

ECR # & Position	Undamaged Resistance Ratio	0.01% Damage Resistance Ratio	0.16% Damage Resistance Ratio	0.31% Damage Resistance Ratio
9L	>193,000	281	88	54
9R	>193,000	163	72	34
7L	>193,000	325	63	32
7R	>193,000	149	68	45
5L	>193,000	149	75	37
5R	>193,000	246	61	38
Average	>193,000	219	71	40
Median	>193,000	204	70	37
Minimum	>193,000	149	61	32
Maximum	>193,000	325	88	54

Note: Uncoated #5 Rebar averaged 5.7 ohms.

12-inch Probe:

- For the undamaged, holiday-free ECRs, the resistances averaged over 700,000 ohms with a range 485,000 to 1,100,000 ohms. These resistances correspond to resistance ratios in excess of 200,000.
- 0.01 percent damage caused the resistance average to be reduced to 734 ohms (i.e. by 99.9 percent), with a range of 280 to 1,800 ohms. The resistance ratio averaged 334 with a range of 127 to 818.
- 0.16 percent damage caused the average resistance to be further reduced to 372 ohms, and the average AC resistance ratio to be 169.
- 0.31 percent damage yielded an average resistance of 92 ohms and an average AC resistance ratio of 42.

4-inch Probe:

- For the undamaged, holiday free ECRs, the resistances all read greater than 1.1 million ohms. This corresponds to resistance ratios in excess of 193,000.
- 0.01 percent damage caused the resistance average to be reduced to 1,247 ohms (i.e. by 99.9 percent), with a range of 850 to 1,850 ohms. The resistance ratio averaged 219 with a range of 149 to 325. The 2,000 ohm coating break detector identified all the damaged areas when connected to the 4-inch probe.

- 0.16 percent damage caused the average resistance to be further reduced to 406 ohms, and the average AC resistance ratio to be 71.
- 0.31 percent damage yielded an average resistance of 228 ohms and an average AC resistance ratio of 40.

2,000 ohm Field Break Detector:

- The 2,000 ohm detector found no flaws on any of the original undamaged bars. Such was the case both when the detector was connected to the 4-inch probe and when the bar was contacted with the portable 2-inch wide sponge connected to the nonmetallic wand. However, it detected all damage purposely created on all bars. The 2-inch wide sponge did not require complete saturation for break detection provided it was squeezed tightly to the ECR using hand pressure. However, the sponges in the 4-inch probe required complete saturation for detection of the smaller breaks.

The effect of uncoated bar size and manufacturer was studied by making 4-inch and 12-inch probe measurements on #3 thru #8 uncoated bars from two sources. The results, presented in Table D-10, indicate a range of 4.7 to 8.4 ohms for the 4-inch probe on the various bars, and a range of 2.1 to 4.0 for the 12-inch probe on

Table D-10. AC Resistances of Uncoated Bars.

Bar Size & Test #	AC Resistance, ohms 4" Probe	12" Probe
3-A	8.1	3.2
3-B	8.4	4.0
4-A	6.2	2.6
4-B	6.3	2.7
5-A	5.8	2.2
5-B	5.5	2.3
6-A	5.4	2.1
6-B	5.4	2.2
7-A	4.8	1.8
7-B	4.7	2.0
8-A	4.8	1.7
8-B	4.7	2.1

these same bars. In most instances, the larger bars yielded the lower resistances. For a given bar size, there was little difference between the resistances measured on bars from the different manufacturers.

DISCUSSION, CONCLUSIONS AND RECOMMENDATIONS

This testing indicated that the epoxy coated reinforcing steel being supplied and installed on five randomly selected North American bridge decks in 1993 was indeed poor quality with respect to coating breaks. If these data are representative of all North American ECR, they project that regardless of the evaluation method (i.e. visual, AC resistance ratio, or electrical coating break detection) more than half (and perhaps more than 85 percent) of the ECRs being installed in 1993 had excessive coating breaks. Straight bars were not much better than bent bars. The data in the State of the Art Appendix and the Introduction to this Appendix clearly show that bars of that quality will not provide the desired long-term performance in severe deicing salt and marine environments when used in conventional concretes with 2 to 3 inches of concrete cover.

The median AC resistance ratio for straight bars tested on North American bridge decks being constructed in 1993 was 174. Interestingly, in laboratory studies (2) of ECRs from cores from 19 highway structures in North America which were 3 to 16 years old, the median AC resistance ratio was 130. Thus, both these efforts yielded similar results, and indicated that most of the field ECRs had many coating breaks.

Recent specification changes have required that all visible coating breaks be repaired in the field prior to concrete placement. However, visual examination is time consuming, tedious and dependent on human skill and the use of mirrors. The field data on the 1993 bridge decks shows the inadequacy of repairing "visual" damage in that most of those data were obtained immediately before concreting after all required patching had been completed. And yet, 70 percent of the test locations still exhibited visual damage. Electrical testing on the other hand has been shown to be a viable means of identifying poor quality bars in the field.

AC resistance testing of field ECRs and visual examination in this effort indicate that minimal coating damage corresponds with AC resistance ratios in excess of 2,000. Only 15 percent of the field bars tested in 1993 had ratios in excess of 2,000. ECRs with AC resistance ratios less than 300 almost always exhibited visible damage. Those with ratios between 300 and 2,000 exhibited visible damage about half the time, and visible and/or excessive invisible damage 97 percent of the time. Since the 4-inch probe used in these tests represents only one-third of a foot, these data indicate that the coating break rate on 97 percent of the bars equaled or exceeded 3 per foot. Specifications typically allow no more than 2 invisible holidays per foot at the plant, and as noted in the Introduction, recent work has recommended that this be applied to field bars as well (3). Although this transition range (300 to 2,000

resistance ratios) may at first glance seem large, when one considers the fact that holiday-free ECRs exhibit ratios in excess of 193,000, a better perspective results. A ratio of 2,000 represents a 99.0 percent drop from the ratio for a holiday-free bar, and a ratio of 300 represents a 99.8 per reduction.

It is concluded that the single probe (4-inch or 12-inch) AC resistance ratio test procedure used herein is an excellent means of defining the quality of field ECR with respect to coating breaks. A test method is included as Attachment 1. Equipment for the AC resistance ratio test method is commercially available, except for the copper probe which can easily be constructed. The overall equipment cost should be in the range of $1,000.

The AC resistance ratio test has proven to be fieldworthy and can be used by a trained technician for field quality control and ECR acceptance prior to concrete placement. From a technical standpoint, it is the preferred field test for coating breaks on straight ECRs and it is recommended that Attachment 1 be adopted as an ECR acceptance tool. At least 90 percent of the measurements should yield AC resistance ratios in excess of 2,000 and 100 percent of the measurements should exceed a ratio of 300. If lesser resistance ratios are determined, then either coating repairs can be made or the ECR rejected. If the decision is to repair, then AC resistance measurements and ratio calculations shall be repeated for a statistically significant sampling.

There remains a need to test bent bars, and there will undoubtedly be instances in which an even lower cost and simpler field test is needed for straight ECRs. For this reason, a "yes or no" electrical coating break field test has also been defined. This test involves modification of a commercially available 80,000 ohm holiday detector by adjustment of the circuit board potentiometer such that the resistance detection limit is reduced to 2,000 ohms. The detector will then provide an audible "beep" when coating breaks create a situation in which the AC resistance ratio falls below about 250 to 425. The detector can be used with either a 4-inch copper probe which is wrapped around straight bar or with a portable wand with a 2-inch wide sponge attached to it for bent bar. Testing of uncoated rebar of the same size is not required, and the test equipment, except for the 4-inch probe which is easily constructed, is commercially available at a cost of under $300. A test method is provided as Attachment 2. All tests performed upon a statistically significant sampling shall **not** indicate an audible "beep" response. If failures occur, then either coating repairs can be made or the ECR rejected. If the decision is to repair, then the testing of a statistically significant sampling shall be repeated. The wetting solution specified in the test method must be used during this testing.

A resistance ratio range is given for this test because a correction is not being made for bar size. A lower detection limit (i.e. resistance ratio in the range of 250 to 425 rather than 2,000) was provided for the audible coating break detector to account for field variations affecting the resistances measured. If the user desires to apply the

more technically correct AC resistance ratio limit of 2,000, such can be accomplished simply by adjusting the potentiometer in the detector to provide an audible signal at a resistance value of about 9,400 ohms (rather than the 2,000 ohms defined above). This will result in detection using the 4-inch probe at AC resistance ratios below 1,160 to 2,000 depending upon bar size.

It is concluded that the 2,000 ohm electrical coating break tester described above is a quick, low cost means of inspecting both straight and bent ECRs in the field. It is recommended that this technique be used for ECR acceptance purposes immediately prior to concrete placement, when the AC resistance ratio test (Attachment 1) cannot be used. If any tests for a statistically significant sampling indicate excessive coating breaks (i.e. the detector "beeps"), the epoxy coated reinforcing steel should either be repaired or rejected as explained previously.

REFERENCES

1. Clifton, J. R., Beehgly, H. F. and Mathey, R. G., "Nonmetallic Coatings for Concrete Reinforcing Bars," Report No. FHWA-RD-74-18, Federal Highway Administration, Washington, D.C., Feb. 1994, PB No. 236424.
2. Clear, K. C., "Effectiveness of Epoxy Coated Reinforcing Steel," Final Report, Canadian Strategic Highway Research Program, Ottawa, Canada, December 1992.
3. Pfeifer, D. W., Landgren, J. R. and Krauss, P. D., "CRSI Performance Research: Epoxy Coated Reinforcing Steel", Final Report, Concrete Reinforcing Steel Institute, Schaumburg, Illinois, June 1992.
4. KCC INC and Florida Atlantic University, "NCHRP 10-37, Performance of Epoxy Coated Reinforcing Steel in Highway Bridges", Interim Report, National Cooperative Highway Research Program, April 1992 (revised February 1993).
5. Kenneth C. Clear, Inc., "Effectiveness of Epoxy-Coated Reinforcing Steel", Interim Report, Concrete Reinforcing Steel Institute, January 1991, p. 4-149.

Attachment 1

PROCEDURE FOR CONDUCTING AC RESISTANCE RATIO TESTING OF STRAIGHT EPOXY COATED REINFORCING STEEL

1. SCOPE
   - 1.1 This test method describes a procedure for evaluating the coating quality, with respect to coating breaks, of straight epoxy coated reinforcing steel (ECR) in the field by measuring the AC resistance and comparing that resistance to the resistance of an otherwise equal uncoated reinforcing bar.
   - 1.2 The values stated in inch-pound units are to be regarded as standard. The SI units in parentheses are provided for information.

2. REFERENCED DOCUMENTS
   - 2.1 NCHRP 10-37 Final Report, "Performance of Epoxy Coated Reinforcing Steel in Highway Bridges, Appendix D: Jobsite Quality Control of Coating Breaks".

3. SIGNIFICANCE AND USE
   - 3.1 This test method provides a reliable means of rapidly evaluating the quality of epoxy-coated reinforcing steel (rebar) before concrete placement.
   - 3.2 At least 90 percent of all tests for a statistically significant sampling shall yield AC resistance ratios in excess of 2,000 and 100 percent of the tests shall yield ratios in excess of 300. An AC resistance ratio higher than 2,000 does not in itself ensure that adequate long-term performance in a corrosive environment can be expected from the ECR represented by the testing. Other tests are also necessary. However, an AC resistance ratio lower than 2,000 indicates a good probability that the test rebar will perform poorly in a corrosive environment.

4. APPARATUS
   - 4.1 *AC Resistance Test Probes* - The AC resistance test probes shall be constructed as shown in Figure 1 using copper pipe. The sponge used shall be pure cellulose sponge or its equivalent. The 4-inch (10 cm) probe is standard. One such probe is required. Use of a 12-inch (30 cm) probe is optional.
   - 4.2 *Soil Resistance Meter and Leadwires* - A soil resistance meter, Nilsson 400™ (Nilsson Electrical Laboratory, Inc., 111 Eighth Avenue, New York, N.Y. 10011; 212-675-7944) or its equivalent, and 4 insulated #18 AWG leadwires (at least 6 feet (1.8 meters) long) with alligator clips are required for testing.
   - 4.3 *Grounding Device* - Two needle-nosed vise grips or equivalent for attaching the resistance meter ground lead to the reinforcing steel (through the epoxy coating).

5. REAGENTS AND MATERIALS
   - 5.1 *Wetting Solution* - Soapy water having an electric resistivity of 70 to 90 ohm-cm at 73°F (23°C). This solution can be made by adding 100 grams of Cascade™ powdered dishwasher detergent to 1 gallon (3.8 liters) of tap water.
   - 5.2 *Epoxy Patching Material* - Two component field liquid patching material compatible with the epoxy coating on the reinforcing steel and inert in concrete, as recommended by the coating manufacturer.

6. TEST SAMPLES
   - 6.1 ECR for the AC resistance test shall be sampled randomly using an applicable standard method.
   - 6.2 Twenty (20) or more ECR samples shall be tested for each batch of ECR represented.

7. TEST PROCEDURES
   - 7.0 Completely saturate the probe sponges by immersing them in a container filled with the wetting solution specified in Section 5.1. Remove the sponges and place one inside each probe half without compressing them.
   - 7.1 For each test, randomly select a location on the test ECR (between crossing bars if the ECRs are already tied in place). Place the lower half of the open probe on the underside of the ECR at the test location. Ensure that the sponge in the probe is in complete contact with the ECR to be tested, and that the ECR is centered in the probe sponge.
   - 7.2 Close the probe and tighten it with Velcro™ strips, allowing excess wetting solution to drain away from the test bar.
   - 7.3 Ensure that the ECR surface on both sides of the probe is dry.
   - 7.4 Attach needle-nosed vise grips to the test ECR at least two inches (5 cm) away from the probe. Use sufficient pressure to ensure that the epoxy coating is penetrated and the vise grip directly contacts the steel beneath the coating. If in doubt, install a second vise grip on the same bar and measure the resistance between the two using the soil resistance meter in accordance with the manufacturer's instructions. The resistance should be less than 0.1 ohm.
   - 7.5 Connect pins C1 and P1 of the soil resistance meter to the binding post on the probe and pins C2 & P2 to the vise grip. Determine the AC resistance in accordance with the meter manufacturer's instructions.

7.6 If the reading is unstable, engage the resistance meter for 10 seconds, null it and record the measured resistance.

7.7 Remove the vise grip and patch the epoxy coating using the patching material specified in Section 5.2 in accordance with the manufacturer's instructions. Use a mirror to ensure that the patching is adequate on the back side of bars which are tied-in-place.

7.8 Repeat the above steps on all other ECRs and perform three tests at different locations on a black (uncoated) rebar which is the same size as that of the test ECR. Determine the average AC resistance of the three tests on the black rebar and round it to the nearest 0.1 ohms.

Note: Totally resaturate the sponges between each test. The uncoated rebar should be at least two feet (60 cm) long, but does not need to be from the same manufacturer or lot as the coated rebars. It may be covered with mill scale and light rust, but should not be heavily rusted. It is suggested that the first uncoated rebar test be performed prior to the start of ECR testing, the second be performed after half of the ECRs are tested and that the third be performed after completion of the ECR testing.

7.9 Divide the AC resistance of each test ECR by the average AC resistance of the black rebars to define the AC resistance ratio for each test ECR. Round the result to the nearest whole number.

REPORTING REQUIREMENTS

8.1 The report shall include:

8.1.1 *Temperature* - The estimated air temperature at the time of the measurements shall be reported.

8.1.2 *Results* - Individual and median AC resistance readings for all the ECRs. Individual and average AC resistance readings for the black (uncoated) rebars tested. Individual and median AC resistance ratios for all the ECRs tested. A listing of the number and percentage of samples with AC resistance ratios in excess of 2,000, and the number and percentage of samples with AC resistance ratios in excess of 300.

Note: A sample blank data sheet is attached.

Field Epoxy Coated Rebar Resistance Ratio Testing w/ Copper Probes

Job: _____

Date: _____

Tests by: _____

Air Temperature: _____

Coating: _____

ECR Test No.	Bar Size No.	Measured AC Resistance, ohms	Calculated AC Resistance Ratio	Visual Observations
1				
2				
3				
4				
5				
6				
7				
8				
9				
10				
11				
12				
13				
14				
15				
16				
17				
18				
19				
20				

Note: Visual Observation is Optional. Code = NVD - No Visible Damage; VD - Visible Damage

Probe Size: 4-inch or 12-inch (circle one)

Black #5 Bar Controls: AC Resistance, ohms

Test #1 _____ Test #2 _____ Test #3 _____

Average of 3 Black Bar Controls = _____ ohms

Comments: _____

Summary of Results: Median AC Resistance Ratio: _____

Number and Percentage with Ratios > 2,000: Number = _____; Percent = _____

Number and Percentage with Ratios > 300: Number = _____; Percent = _____

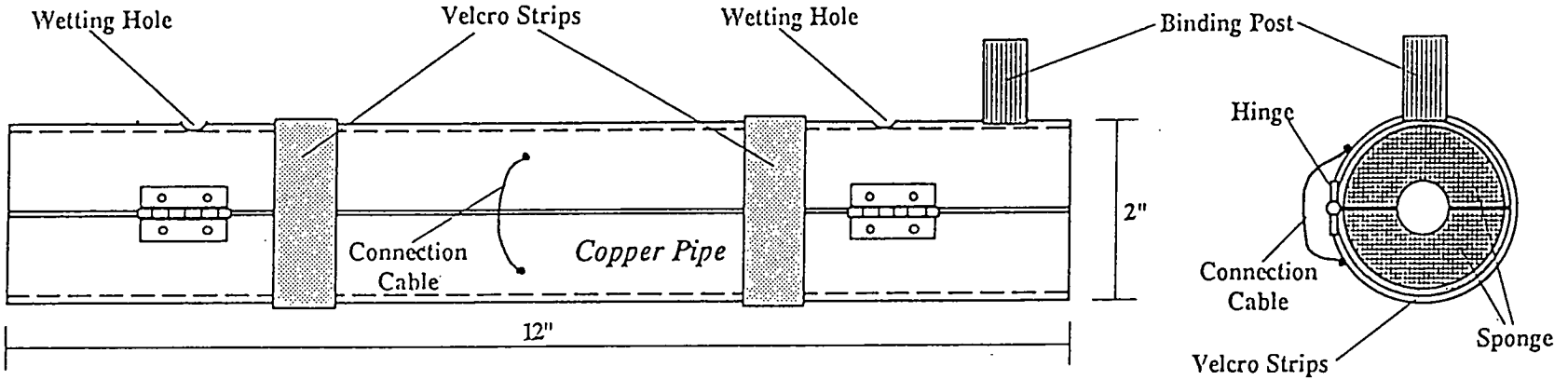

12-inch AC Resistance Probe

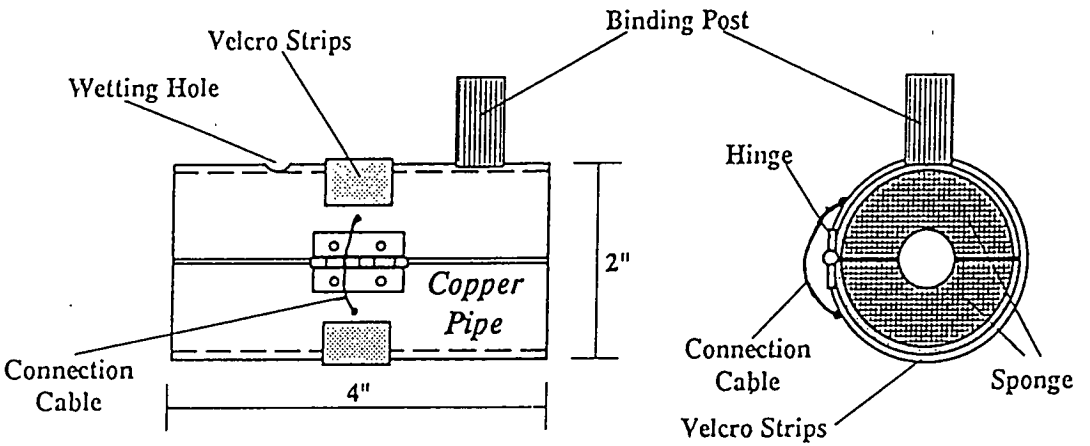

4-inch AC Resistance Probe

Figure 1. Probe Schematic

Attachment 2

PROCEDURE FOR ACCEPTANCE TESTING OF EPOXY COATED REINFORCING STEEL FOR COATING BREAKS PRIOR TO CONCRETE PLACEMENT, USING A MODIFIED HOLIDAY DETECTOR

1. SCOPE

1.1 This test method describes an electrical test procedure for rapidly determining the coating quality with respect to coating breaks, of epoxy-coated reinforcing steel (ECR) in the field using a commercially available holiday detector which has been modified by lowering the detection level from 80,000 to 2,000 ohms. The method is applicable to both bent and straight bars.

1.2 The values stated in inch-pound units are to be regarded as standard. The SI units in parentheses are provided for information.

2. REFERENCED DOCUMENTS

2.1 NCHRP 10-37 Final Report, "Performance of Epoxy Coated Reinforcing Steel in Highway Bridges, Appendix D: Jobsite Quality Control of Coating Breaks".

3. SIGNIFICANCE AND USE

3.1 This test method provides a reliable means of rapidly evaluating the quality of epoxy coating reinforcing steel (rebar) before concrete placement.

3.2 All tests performed upon a statistically significant sampling shall **not** indicate an audible "beep" response when the appropriate probe and the detector contact the test epoxy coated reinforcing bar. Compliance with this requirement does not in itself ensure that adequate long-term performance in a corrosive environment can be expected from the ECR represented by the testing. Other tests are also necessary. However, if an audible response is obtained, there is a good probability that the test rebar will perform poorly in a corrosive environment.

4. APPARATUS

4.1 *Test Probes* - The test probes shall be constructed as shown in Figure 1 and Figure D-2 of the report referenced in 2.1. For straight bars, a 4-inch probe constructed from split copper pipe with sponges shall be used. For bent bars, a 2-inch wide (5 cm) by 2-inch (5 cm) thick by 6-inch (15 cm) long sponge shall be attached to the nonmetallic wand provided by the manufacturer of the detector. The sponges used shall be pure cellulose sponge or its equivalent.

4.2 *Leadwire and Resistors* - A 3-foot length of #18 AWG insulated copper leadwire resistors (1/4 watt or larger, plus or minus 10 percent accuracy) as follows: 1,500 ohm; 2,200 ohm; and 3,300 ohm.

4.3 *Holiday Detector* - An 80,000 ohm portable holiday detector with ground lead and nonmetallic wand with leadwire, Tinker Rasor Model M-1™ (P.O. Box 281, San Gabriel, California 91778; Phone: 818-287-5259) or its equivalent shall be obtained and modified as follows. Remove the top cover and locate screw adjustment on the circuit board potentiometer (only one screw adjustment exists on the circuit board). Connect the leads (section 4.2 leadwire and detector ground lead) to the detector and to a 2,200 ohm resistor. An audible "beep" will begin. Slowly adjust the screw until the "beeping" ceases. Remove the 2,200 ohm resistor and insert a 1,500 ohm resistor. The detector should "beep". If so, proceed. If not, readjust the screw until a beeping sound is heard. Remove the 1,500 ohm resistor, and insert a 3,300 ohm resistor. The detector should not beep. If it does, repeat the adjustment procedure.

4.4 *Grounding Device* - Two needle-nosed vise grips or equivalent for attaching the detector ground lead to the reinforcing steel (through the epoxy coating).

5. REAGENTS AND MATERIALS

5.1 *Wetting Solution* - Soapy water having an electrical resistivity of 70 to 90 ohm-cm at 73°F (23°C). This solution can be made by adding 100 grams of Cascade™ powdered dishwasher detergent (or equivalent) to 1 gallon (3.8 liters) of tap water.

5.2 *Epoxy Patching Material* - Two component field liquid patching material compatible with the epoxy coating on the reinforcing steel and inert in concrete, as recommended by the coating manufacturer.

6. TEST SAMPLES

6.1 ECR for this coating break test shall be sampled randomly using an applicable standard method.

6.2 Forty (40) or more ECR locations shall be tested for each batch of ECR presented. Unless otherwise defined, 35 tests shall be performed on straight bar and 5 tests shall be performed in the bend areas of bent bars.

7. TEST PROCEDURES

Straight Bars:

7.1 Completely saturate the probe sponges by immersing them in a container filled with the wetting solution specified in Section 5.1. Remove the sponges and place one inside each probe half without compressing them.

7.2 For each test, randomly select a location on the test ECR (between crossing bars if the ECRs are already tied-in-place). Place the lower half of the open probe on the underside of the ECR at the test location. Ensure that the sponge in the probe

is in complete contact with the ECR to be tested, and that the ECR is centered in the probe sponge.

7.3 Close the probe and tighten it with the Velcro™ strips, allowing excess wetting solution to drain away from the test bar.

7.4 Ensure that the ECR surface on both sides of the probe is dry.

7.5 Attach needle-nosed vise grips to the test ECR at least two inches (5 cm) away from the probe. Use sufficient pressure to ensure that the epoxy coating is penetrated and the vise grip directly contact the steel beneath the coating. If in doubt, install a second vise grip on the same bar and connect one detector lead to each vise grip. Proper installation results in the detector "beeping".

Note: Only one vise grip connection is required per bar. Thus if more than one location per bar is tested, the vise grip can remain in place for all tests on that bar.

7.6 Connect the ground lead from the detector to the vise grip and the other lead to the binding post on the probe for 10 seconds. Record whether or not the detector "beeps".

7.7 Remove the vise grip and patch the epoxy coating using the patching material specified in Section 5.2 in accordance with the manufacturer's instructions. Use a mirror to ensure that the patching is adequate on the back side of bars which are tied-in-place.

7.8 Repeat the above steps on all other ECRs.

Note: Totally resaturate the sponges between each test.

Bent Bars:

7.1 Attach a 2-inch (5 cm) wide by 2-inch (5 cm) thick by 6-inch (15 cm) long sponge to the nonmetallic wand in the manner shown in Figure 1. Immerse the sponge in wetting solution and then squeeze it to one-half size to remove excess water.

7.2 For each test, randomly select a location on the bent portion of the test ECR. Attach the vise grip to the test ECR at least two inches (5 cm) away from the area (and above the test area if the bend is vertical). Use sufficient pressure to ensure the epoxy coating is penetrated and the vise grip directly contacts the steel beneath the coating. If in doubt, install a second vise grip on the same bar and connect one detector lead to each vise grip. Proper installation results in the detector "beeping".

Note: Only one vise grip connection is required per bar. Thus if more than one location per bar is tested, the vise grip can remain in place for all tests on that bar.

7.3 Connect the ground lead from the detector to the vise grip and the wand lead to the detector.

7.4 Wrap the sponge tightly around the bent bar at the test location, being careful that excess water does not run onto the bar below the test area. Hold the sponge tightly in place for 10 seconds ensuring that the entire surface of the bar beneath the sponge is in contact with the sponge. Remove the sponge and record whether or not the detector "beeped".

7.5 Remove the vise grip and patch the epoxy coating using the patch materials specified in Section 4.2 in accordance with the manufacturer's instructions. Use a mirror to ensure that the patching is adequate on the back side of bars which are tied-in-place.

7.6 Repeat the above steps on all other ECRs.

8. REPORTING REQUIREMENTS

8.1 The report shall include:

8.1.1 *Temperature* - The estimated air temperature at the time of the measurements shall be reported.

8.1.2 *Results* - Bar size and shape (straight of bent) at each test location. Documentation of whether or not an audible "beep" was recorded at each of the forty (40) test locations. The percentage of test locations at which audible "beeps" were recorded.

Note: A sample blank data sheet is attached.

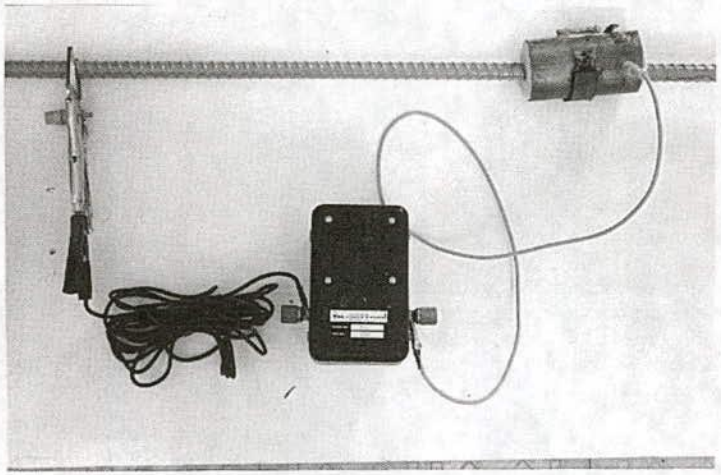

Test Setup for Straight Bars.

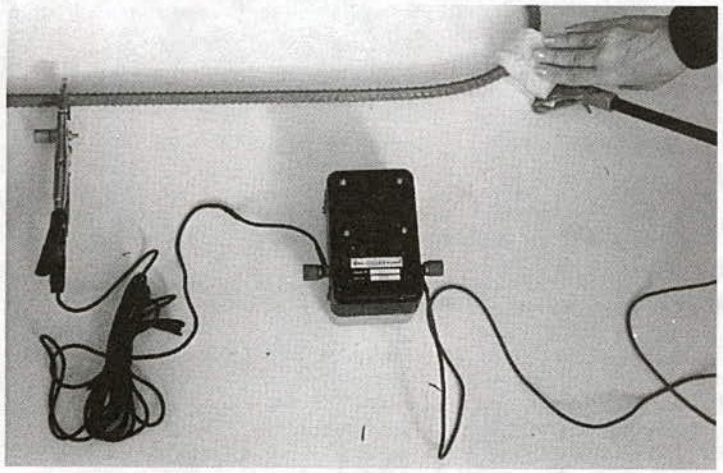

Test Setup for Bent Bars.

Figure 1. Test Equipment and Setup.

Epoxy Coated Rebar: Field Coating Break Detection using a 2,000 ohm Electrical Detector

Job: _____

Date: _____

Tests by: _____

Air Temperature: _____

Coating: _____

ECR Test No.	Bar Size & Shape	Detector "Beeps" Yes or No		ECR Test No.	Bar Size & Shape	Detector "Beeps" Yes or No
1				21		
2				22		
3				23		
4				24		
5				25		
6				26		
7				27		
8				28		
9				29		
10				30		
11				31		
12				32		
13				33		
14				34		
15				35		
16				36		
17				37		
18				38		
19				39		
20				40		

Summary of Results:

Percentage of Test Locations Where Detector "Beeped": _____

APPENDIX E

MAGNETOMETER FEASIBILITY STUDY

OBJECTIVES

The scope of the present work involved determining the feasibility of using multivector magnetometers to detect breakdown of ECR. Because development of this technique, as applied to epoxy-coated reinforcing steel in concrete, is in the research stage, the present investigators have worked closely with personnel at Johns Hopkins University Applied Physics Laboratory (JHU-APL) because of their expertise using this technology. Work to-date has been limited to laboratory size specimens where the geometry and ECR condition were controlled. However, locating deteriorated ECR in existing structures and predicting the condition of the ECR will require an effort in terms of time and funding that is beyond the scope of the present program.

SPECIMEN PREPARATION

Epoxy-Coated Rebars Used for the Study

Two seven-foot job site epoxy-coated rebars provided by New York Department of Transportation were used. The epoxy powder was Scotchkote 213, and the rebars were coated and accepted on June 6, 1990. These rebars were delivered to the project job site on July 3, 1990, and stayed on site until October 15, 1990. During the on site exposure the rebars were moved around several times by dragging across the ground for a distance of about 75 feet. They were placed on wood timbers from 7/3/90 to 10/10/90 and then on the ground for five days before they were shipped to KCC INC. The rebars were received by KCC INC on November 12, 1990, and stored in the KCC INC lab until they were sectioned into eight 21-inch-long pieces (four from each bar) for the present study on December 2, 1991. All eight 21-inch-long rebars were fully characterized for holidays, bare areas, mashed areas and pencil hardness with the results being presented in Table E-1.

The eight rebars were divided into four groups (1-4, as listed in Table E-1) with different macroscopic defects created as follows:

1. Epoxy-coated rebars without intentional macroscopic defects.
2. Epoxy-coated rebars with intentional 1/4-inch-diameter defects spaced five inches apart. One defect was introduced at the top, side and bottom of the rebar with the first defect being four inches from the specimen end.
3. Epoxy-coated rebars with intentional 1/2-inch-diameter defects spaced five inches apart. The location of the defects was the same as for the 1/4-inch ones.
4. Epoxy-coated rebars the same as in Group 3 but pre-corroded as the anode in the KCC INC Accelerated Corrosion Test.

Table E-1. ECR Characterization Data Summary.

Group Number	Bar Code	Holiday # per foot	Bare Area # per foot	Mashed Area # per foot	Pencil[1] Hardness
1	6C	0	9	9	F
	7B	0	12	64	F
2	6A	0	27	75	HB
	7A	0	21	64	F
3	7C	0	29	32	HB
	7D	0	15	3	F
4	6B	0	32	5	HB
	6D	0	20	4	HB

[1]Softest to Hardest Scale: 6B < 5B < 4B < 3B < 2B < B < HB < F < H < 2H < 3H < 4H < 5H < 6H < 7H < 8H < 9H

It was anticipated that the influence of the defects in Table E-1 upon the magnetometer results would be negligible compared to the intentional, macroscopic ones.

Specimen Design and Preparation. Eight 6"x8"x18" concrete specimens were cast (two for each group). Each specimen contained one epoxy-coated rebar at the top and one black steel bar at the bottom. The details of the design are shown in Figure E-1.

Concrete with the following mix design was used for casting the specimens:

w:c = 0.55

Cement: 588 lbs/cu. yd. Water: 323 lbs/cu. yd.

Sand: 1170 lbs/cu. yd. Stone: 1786 lbs/cu. yd.

For the top lift (3.5 inches deep) of the specimens, 23.45 lbs $CaCl_2/yd^3$ of concrete was added to give a chloride content of 15 lbs/cu. yd. of concrete. A rotary drum mixer with a capacity of one cubic foot was used to prepare the concrete. The actual fresh concrete slump achieved with this mix design ranged from seven to nine inches. The specimens were demolded after 24 hours of wet burlap curing and then cured in a fog room for 28 days. The AC resistance between the rebars was then measured for each specimen, and resistors were installed between the two rebars. The size of the resistors was from 5 to 10 percent of the measured AC resistance.

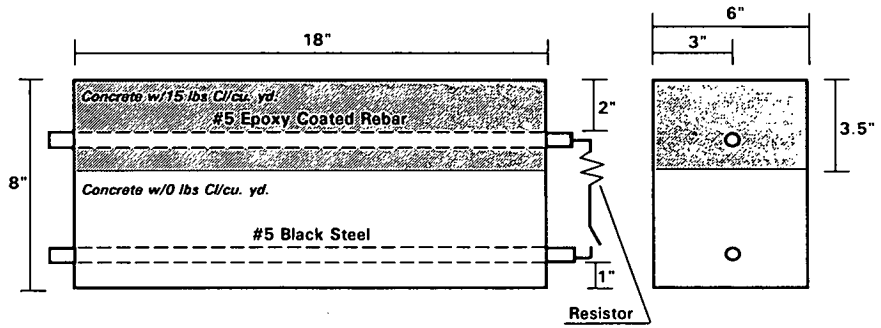

Figure E-1. Specimen Configuration for Magnetometer Study.

Preliminary Test

At the age of 29 and 32 days (one and four days after coupling the top and bottom rebar) the macrocell current, driving voltage, static potential and AC resistance were measured for all eight specimens. The results are presented in Table E-2. At 30 days (two days after the top and bottom rebars were coupled) one set of macrocell current data was collected on all eight specimens. The data are summarized in Figure E-2. After these tests all eight specimens were delivered on January 13, 1992 to APL-JHU for the magnetometer study. They were subsequently returned to KCC INC after the magnetometer measurements and placed on above-ground racks at the outdoor exposure facility in Sterling, VA.

Magnetometer Results

Experiments were performed at JHU-APL by Dr. Srinivasan using a two electrode AC impedance scan. All tests were conducted on the as-received slabs before exposure to external aqueous chloride environments. The procedure involved placing the magnetometer at one end of the specimen such that the "x" component of the magnetic field produced by the on-bar current (y-axis) was detected. A single frequency AC signal at an amplitude of 200 to 1000 mV was imposed upon the ECR with the lower bare rebar acting as a return electrode. After acquisition of the detector signal the magnetometer was moved one inch from the starting position, and

Table E-2. NCHRP 10-37 Corrosion Data Collected From the Specimens for Magnetometer Study - January 9, 1992 .

Specimen Code	Macrocell Current mA/sq.ft.	Driving Volt V	AC Resistance ohm	Static Potential, mV (CSE)										Temp. °F	Remark
				Epoxy Coated Rebar (Top)					Black Steel (Bottom)						
				1	2	3	4	Average	1	2	3	4	Average		
6C	0.0206	0.050	2201	-444	-442	-440	-435	-440	-170	-199	-196	-186	-188	70	No intentional defects
7B	0.3141	0.115	880	-500	-506	-509	-492	-502	-126	-126	-104	-86	-111	70	No intentional defects
6A	0.1434	0.033	387	-437	-451	-443	-433	-441	-219	-246	-232	-214	-228	70	Small Intentional defects
7A	0.3048	0.067	405	-484	-480	-475	-486	-481	-226	-183	-206	-187	-201	70	Small Intentional defects
7C	0.4319	0.049	180	-497	-529	-523	-525	-519	-179	-191	-178	-224	-193	70	Large intentional defects
7D	0.6698	0.094	242	-382	-402	-403	-399	-397	-155	-151	-179	-140	-156	70	Large intentional defects
6B	0.6275	0.031	167	-490	-511	-513	-511	-506	-232	-193	-200	-220	-211	70	Pre-corroded
6D	0.3314	0.024	211	-497	-507	-510	-520	-509	-197	-207	-218	-216	-210	70	Pre-corroded

NOTE: 1. The AC resistance is represented at 25°C.
2. The static potential was taken before installing the resistors.
3. The macrocell current, driving volt, AC resistance were taken 24 hours after installing the resistors.

Table E-2 (continued)

Specimen Code	Macrocell Current mA/sq.ft.	Driving Volt V	AC Resistance ohm	Static Potential, mV (CSE)										Temp. °F	Remark
				Epoxy Coated Rebar (Top)					Black Steel (Bottom)						
				1	2	3	4	Average	1	2	3	4	Average		
6C	0.0106														No intentional defects
7B	0.2273														No intentional defects
6A	0.1173														Small Intentional defects
7A	0.2591														Small Intentional defects
7C	0.4183														Large intentional defects
7D	0.5753														Large intentional defects
6B	0.7008														Pre-corroded
6D	0.3585														Pre-corroded

NOTE: The macrocell current was taken 48 hours after installing the resistors.

Table E-2 (continued)

Specimen Code	Macrocell Current mA/sq.ft.	Driving Volt V	AC Resistance ohm	Static Potential, mV (CSE)										Temp. °F	Remark
				Epoxy Coated Rebar (Top)					Black Steel (Bottom)						
				1	2	3	4	Average	1	2	3	4	Average		
6C	0.0125	0.018	2025	-162	-160	-129	-109	-140	-102	-99	-102	-123	-107	70	No intentional defects
7B	0.0183	0.018	1497	-138	-161	-164	-149	-153	-134	-143	-104	-122	-126	70	No intentional defects
6A	0.3211	0.062	396	-421	-431	-424	-409	-421	-294	-307	-343	-334	-320	70	Small Intentional defects
7A	0.2852	0.058	467	-369	-360	-356	-362	-362	-309	-275	-290	-283	-289	70	Small Intentional defects
7C	0.5025	0.051	198	-324	-359	-360	-344	-347	-364	-364	-372	-367	-367	70	Large intentional defects
7D	0.6568	0.079	238	-405	-414	-361	-386	-392	-334	-319	-350	-335	-335	70	Large intentional defects
6B	0.8271	0.052	194	-413	-418	-424	-449	-426	-380	-361	-370	-377	-372	70	Pre-corroded
6D	0.3884	0.031	229	-385	-377	-379	-383	-381	-294	-300	-325	-326	-311	70	Pre-corroded

NOTE: 1. The AC resistance is represented at 25°C.
2. The static potential was taken with the switches ON.
3. The macrocell current, driving volt, AC resistance were taken 3.5 days after installing the resistors.

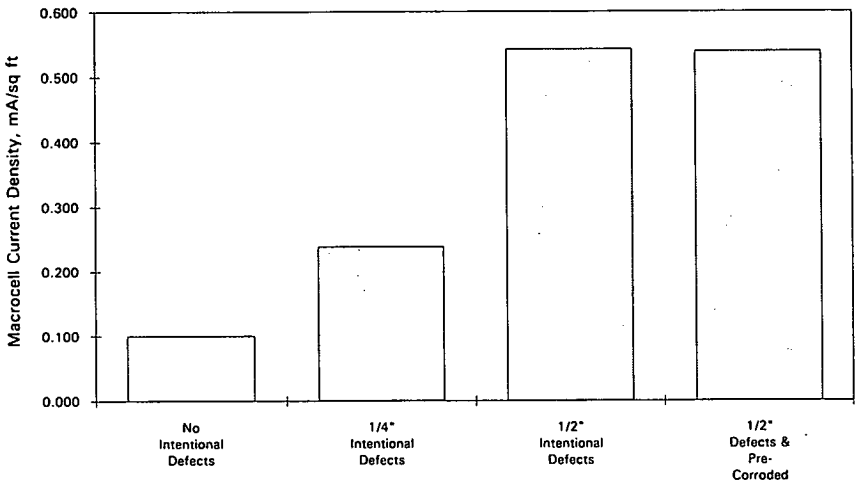

Figure E-2. Macrocell Current Data Summary.

the measurement was repeated. This process was continued until the entire length of the slab was mapped. Representative spectra are shown in Figures E-3 and E-4, and the actual data are listed in Tables E-3 and E-4. Impedance values for the ECR in slab 6C were an order of magnitude higher than for slab 6B. This was to be expected since the coating for specimen 6B had three intentional 1/2-inch-diameter defects. Although the impedance values for specimen 6C were higher, the relative magnitude was low compared to coating systems that exhibit excellent barrier protection. This indicated that some deterioration of the epoxy coating had occurred as expected because these bars were obtained from a jobsite. However, in the magnetometer configuration that was used the individual defects in slab 6B were not clearly identifiable. Because the magnetometer output signal was either low (just above the background noise levels) or changes in the detector output with position were subtle, it was difficult to identify with confidence the exact location of defects. However, on several scans a sudden, albeit small, change was observed that was indicative of a break in the coating. A scan made with an amplitude of 1000 mV produced higher current levels, which helped to improve the sensitivity of the detection system. Data collected over 11 inches showed two distinct, abrupt changes in the detector signal which corresponded to the location of two defects. Unfortunately, in an attempt to reproduce the test, the detected signals had decreased significantly making detection difficult. This behavior was probably caused by a passivation of the bare defect and

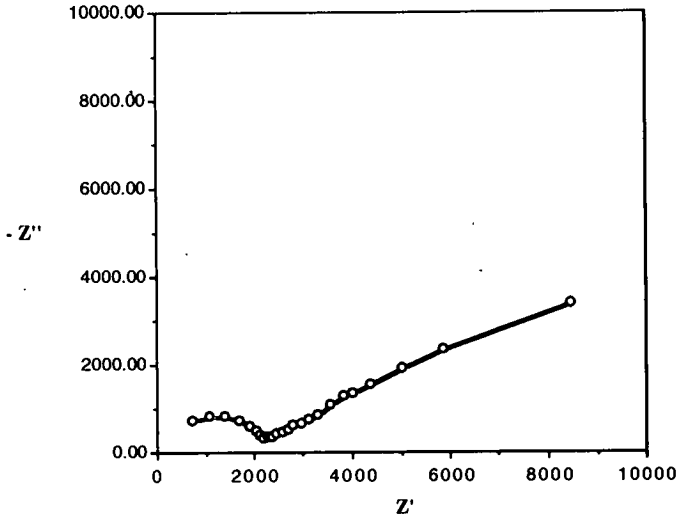

(i) Nyquist Plot

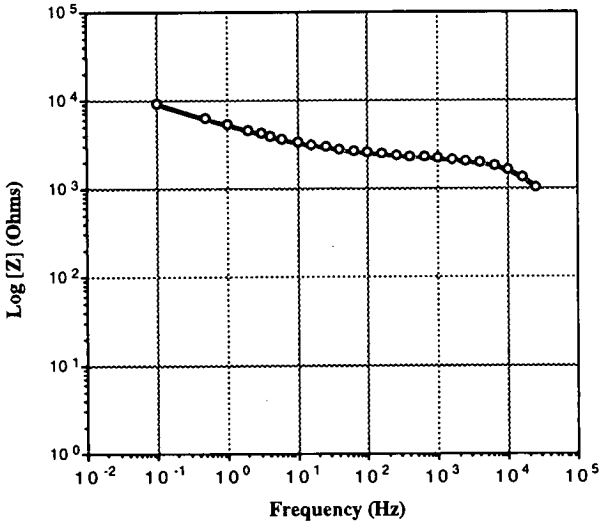

(ii) Bode Magnitude Plot

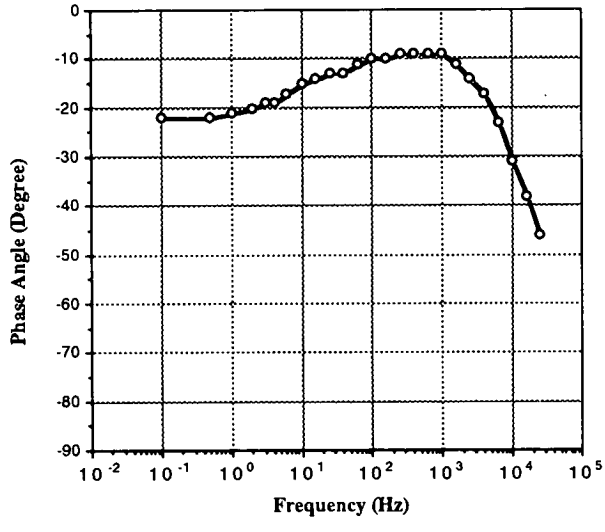

(iii) Bode Phase Angle Plot

Figure E-3. AC Impedance Plots for Specimen 6C, Epoxy Coated Rebar without Defects.

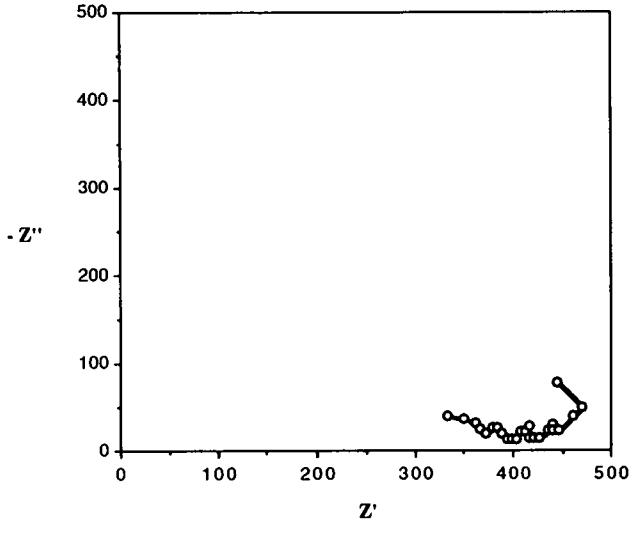

(i) Nyquist Plot

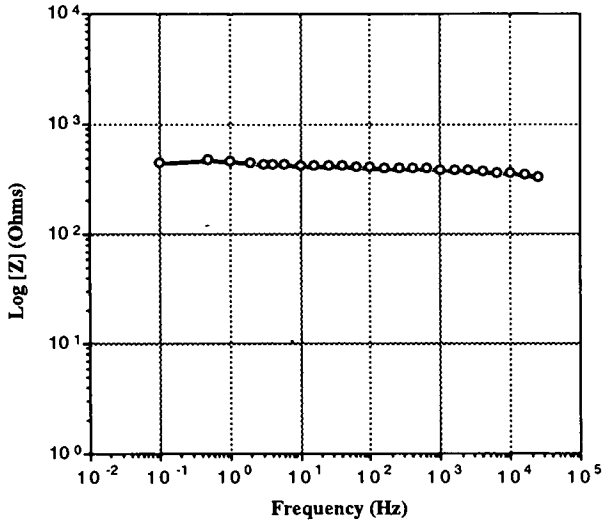

(ii) Bode Magnitude Plot

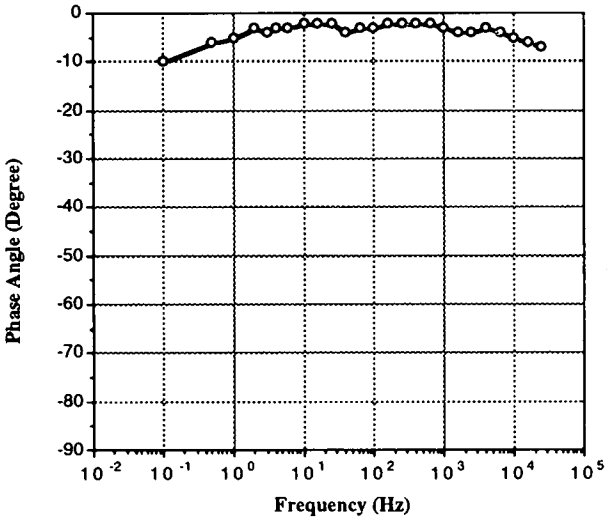

(iii) Bode Phase Angle Plot

Figure E-4. AC Impedance Plots for Specimen 6B, Epoxy Coated Rebar with Defects.

Table E-3. AC Impedance Data for Specimen 6B, Epoxy Coated Rebar with Defects.

6BEIS210 FREQUENCY	Z	PHASE	Z'	-Z''
0.10	451.86	-10	444.99	78.46
0.50	473.15	-6	470.56	49.46
1.00	462.38	-5	460.62	40.30
2.00	446.68	-3	446.07	23.38
3.00	441.57	-4	440.49	30.80
4.00	441.57	-3	440.97	23.11
6.00	436.52	-3	435.92	22.85
10.00	426.58	-2	426.32	14.89
16.00	421.70	-2	421.44	14.72
25.00	416.87	-2	416.62	14.55
40.00	416.87	-4	415.85	29.08
63.00	412.10	-3	411.53	21.57
100.00	407.38	-3	406.82	21.32
158.00	402.72	-2	402.47	14.05
251.00	398.11	-2	397.86	13.89
398.00	398.11	-2	397.86	13.89
631.00	393.55	-2	393.31	13.73
1000.00	389.05	-3	388.51	20.36
1585.00	384.59	-4	383.65	26.83
2512.00	380.19	-4	379.26	26.52
3981.00	371.54	-3	371.03	19.44
6310.00	367.28	-4	366.39	25.62
10000.00	363.08	-5	361.70	31.64
15849.00	350.75	-6	348.83	36.66
24999.00	334.97	-7	332.47	40.82

Table E-4. AC Impedance Data for Specimen 6C, Epoxy Coated Rebar without Defects.

6CEIS210 FREQUENCY	Z	PHASE	Z'	-Z''
0.10	9120.11	-22	8456.02	3416.45
0.50	6309.57	-22	5850.13	2363.61
1.00	5370.32	-21	5013.62	1924.55
2.00	4623.81	-20	4344.96	1581.44
3.00	4216.97	-19	3987.22	1372.91
4.00	4027.17	-19	3807.76	1311.12
6.00	3715.35	-17	3553.01	1086.26
10.00	3388.44	-15	3272.98	876.99
16.00	3198.90	-14	3103.87	773.88
25.00	3019.95	-13	2942.55	679.34
40.00	2851.02	-13	2777.95	641.34
63.00	2722.70	-11	2672.68	519.52
100.00	2600.16	-10	2560.66	451.51
158.00	2483.13	-10	2445.41	431.19
251.00	2398.83	-9	2369.30	375.26
398.00	2344.23	-9	2315.37	366.72
631.00	2290.87	-9	2262.66	358.37
1000.00	2213.09	-9	2185.85	346.20
1585.00	2162.72	-11	2122.98	412.67
2512.00	2089.30	-14	2027.24	505.45
3981.00	1995.28	-17	1908.08	583.36
6310.00	1862.09	-23	1714.06	727.58
10000.00	1640.59	-31	1406.26	844.97
15849.00	1364.58	-38	1075.31	840.12
24999.00	1035.14	-46	719.07	744.62

an associated increase in the impedance of the system, a decrease in the leakage current and weakening of the associated magnetic field.

Because of recent successes in applying this technique to locate coating breakdown in buried pipelines, Drs. Murphy and Srinivasan were confident that magnetometers could be used to locate individual defects in ECRs. In this regard, it is conceivable that individually coated rebars can be accurately mapped with magnetometers. Development of a reliable, sensitive system could provide the capability to predict the extent of deterioration of ECR in existing structures. However, implementation of this technique requires that direct electrical contact be made to the ECR. This is problematic for existing structures but can be obviated if provisions are made to ensure access to ECR on new constructs. The primary problem of clearly identifying coating defects involves optimizing the resolution of the magnetometer detection system. This is a function of the "take-off" distance (distance between the magnetometer pick-up coil and the ECR) and the diameter of the pick-up coil. In the present system the "take-off" distance is about five inches. Because the spatial resolution of the system is a function of the "take-off" distance, it is not possible to identify defects that are five inches or less apart. It must be recognized that this technique will not be able to detect holidays or areas of incipient breakdown but can only detect breakdowns once they have occurred. Resolution of the magnetometer system can be improved by reducing the "take-off" distance. This can be accomplished by physically placing the magnetometer closer to the concrete surface or reducing the concrete cover thickness, or both. Because the magnetometer is permanently mounted to a specially designed fixture, reducing the "take-off" distance by placing the magnetometer closer to the concrete surface was limited for the present experiments. An improved fixture could be designed to overcome this problem, however. A practical approach for continued research is to prepare several new specimen types for the specific purpose of improving system resolution and, at the same time, simplify the test. A possible specimen design that would accomplish this is shown in Figure E-5.

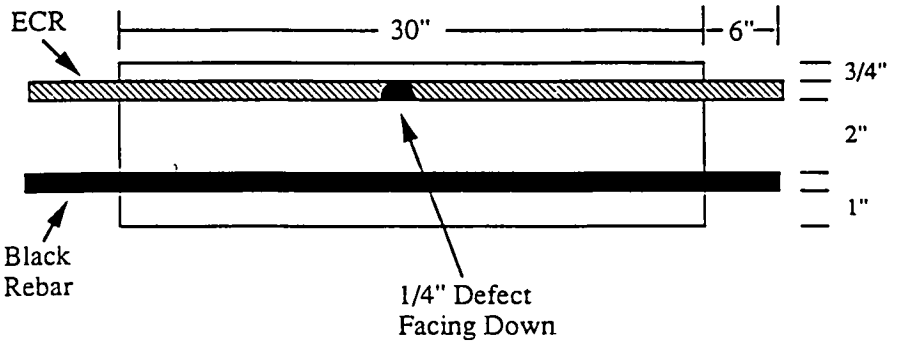

Figure E-5. New Test Specimen for Magnetometer Feasibility Study.

APPENDIX F

EPOXY COATED REBAR RECOMMENDED FORMS

1. General Core Information
2. Concrete and AC Resistance Results
3. Microscope Study Results
4. Accelerated Corrosion and Chemical Immersion Results

EPOXY COATED REBAR STUDY
INFORMATION FORM

PROJECT

SPECIMEN RECEIPT DETAILS

RECEIVED ON: _____
RECEIVED FROM: _____ CONTACT PERSON: _____
ADDRESS: _____ PHONE NUMBER: _____
_____
_____
ARRANGED BY: _____

SPECIMEN SOURCE DETAILS

STRUCTURE TYPE: _____ CONCRETE CONDITION (IN THE AREA OF CORE COLLECTED): _____
LOCATION OF STRUCTURE: _____
ENVIRON. EXPOS. TYPE: _____ CORROSION STATUS OF THE STRUCTURE: _____
STRUCTURE HIST. AVAILABLE: _____

CORE DETAILS

TOTAL NUMBER OF CORES RECEIVED: _____

LOG #	CORE LABEL	# TOP BARS	# BOT. BARS	DIAMETER inches	HEIGHT inches	CLEAR COVER	DESC. OF AREA OF CORE COLL.	DESCRIPTION OF CORE

EPOXY COATING PROPERTY & HISTORY DOCUMENTATION

BAR CODE	DEFORMATION PATTERN	BAR SIZE	COATING THICKNESS (mils) THICKNESS MEASUREMENT			AVERAGE	PENCIL HARDNESS	HOLIDAY	MASHED AREA	BARE AREA	VISUAL CONDITION
			OVERALL AVERAGE:								

EPOXY USED FOR COATING: _____ EPOXY CONDITION: _____
COATED BY: _____
AGE IN CONCRETE: _____

NOTES: _____
_____

FORM PROCESSED BY: _____ DATE: _____

KENNETH C. CLEAR, INC.
EPOXY COATED REBAR STUDY
INFORMATION FORM

PROJECT: C-SHRP

SPECIMEN RECEIPT DETAILS

RECEIVED ON: July 15, 1991
RECEIVED FROM: Nova Scotia Dept. of Trans. and Communications
ADDRESS: Stite 37, RR #1
Windsor Junction
Nova Scotia, B0N 2V0
ARRANGED BY: Bob Chojnacki
CONTACT PERSON: Steve Chiasson
PHONE NUMBER: (902) 861-1911

SPECIMEN SOURCE DETAILS

STRUCTURE TYPE: Bridge, Site 89-024
LOCATION OF STRUCTURE: Middle River Bridge, Hwy 104
ENVIRON. EXPOS. TYPE: North America, Heavy Salted
STRUCTURE HIST. AVAILABLE: Through Nova Scotia DOT
CONCRETE CONDITION (IN THE AREA OF CORE COLLECTED): Sound, No Delamination
CORROSION STATUS OF THE STRUCTURE: No corrosion induced damage.

CORE DETAILS

TOTAL NUMBER OF CORES RECEIVED: 6

KCC LOG #	CORE LABEL	# TOP BARS	# BOT. BARS	DIAMETER inches	HEIGHT inches	CLEAR COVER	DESC. OF AREA OF CORE COLL.	DESCRIPTION OF CORE
I-CSHRP-63	#1	1	0	4	3 1/2	3 1/2 in.	Cracked, Sound	Vertical crack - not thru rebar
I-CSHRP-64	#2	1	1	4	6	4 in.	Sound, Uncracked	Excellent
I-CSHRP-65	#3	1	0	4	6 1/2	4 in.	Cracked, Sound	Vertical crack through rebar
I-CSHRP-66	#4	1	0	4	6 7/8	4 in.	Sound, Uncracked	Excellent
I-CSHRP-67	#5	1	0	4	6	3 1/2 in.	Sound, Uncracked	Excellent
I-CSHRP-68	#6	1	0	4	6 1/2	3 in.	Cracked, Sound	Vertical crack - not thru rebar

EPOXY COATING PROPERTY & HISTORY DOCUMENTATION

BAR CODE	DEFORMATION PATTERN	BAR SIZE	COATING THICKNESS (mils) THICKNESS MEASUREMENT			AVERAGE	PENCIL HARDNESS	HOLIDAY	MASHED AREA	BARE AREA	VISUAL CONDITION
I-CSHRP-63	D 15 400	15M	12.1	12.8	11.6	12.2	H	0	3	0	No Corrosion
I-CSHRP-64	D 15 400	15M	11.1	10.6	10.1	10.6	H	0	5	0	No Corrosion
I-CSHRP-64B	D 15 400	15M	10.8	11.4	11.1	11.1	H	0	0	2	No Corrosion
I-CSHRP-65	D 15 400	15M	9.9	10.6	11.1	10.5	H	2	2	2	No Corrosion
I-CSHRP-66	D 15 400	15M	11.6	11.4	11.8	11.6	H	0	1	0	No Corrosion
I-CSHRP-67	D 15 400	15M	11.8	11.1	11.6	11.5	H	0	0	0	No Corrosion
I-CSHRP-68	D 15 400	15M	11.6	11.6	11.4	11.5	H	0	1	0	No Corrosion
			OVERALL AVERAGE:			11.3	H	0	2	1	

EPOXY USED FOR COATING: Scotchkote 213
COATED BY: (unknown)
AGE IN CONCRETE: 3 years
EPOXY CONDITION: All excellent

NOTES:

FORM PROCESSED BY: Qizhong Sheng
DATE: December 24, 1991

EPOXY COATED REBAR STUDY
CONCRETE & AC RESISTANCE TEST RESULTS

PROJECT

CORE PROPERTIES

LOG#	OVEN DRY WEIGHT g	WEIGHT IN WATER g	SATURATED WEIGHT g	DRY UNIT WEIGHT lbs/cu. yd.	MOISTURE ABSORPTION %	RAPID CHLORIDE PERMEABILITY		
						COULOMBS PASSED	RESISTIVITY ohm-cm	AGE

REBAR TRACE CHLORIDES

NUMBER OF SAMPLES COLLECTED: _____

LOG #	BAR #	TRACE pH	TOTAL CHLORIDE		WATER SOLUBLE CHLORIDE		TRACE CONDITION
			% CHLORIDE	LBS/CU. YD.	% CHLORIDE	LBS/CU. YD.	
		AVERAGE :					

BASE LINE CHLORIDE:

TOTAL CHLORIDE:
% CHLORIDE: _____
LBS/CU. YD.: _____

WATER SOLUBLE CHLORIDE:
% CHLORIDE: _____
LBS/CU. YD.: _____

SOURCE : _____

AC RESISTANCE TEST

LOG #	BAR #	DATE IN SOAK	TIME IN SOAK	DATE REM. FROM SOAK	TIME REM. FROM SOAK	HRS. OF SOAK	AC RESISTANCE, kohms/sq. ft.	
							0 HRS	72 HRS
						AVERAGE:		

EVALUATION: _____

KENNETH C. CLEAR, INC.
EPOXY COATED REBAR STUDY
CONCRETE & AC RESISTANCE TEST RESULTS

PROJECT: C-SHRP

CORE PROPERTIES

KCC LOG#	OVEN DRY WEIGHT g	WEIGHT IN WATER g	SATURATED WEIGHT g	DRY UNIT WEIGHT lbs/cu. yd.	MOISTURE ABSORPTION %	RAPID CHLORIDE PERMEABILITY		
						COULOMBS PASSED	RESISTIVITY ohm-cm	AGE
I-CSHRP-64	946.4	565.8	1034.5	3402	9.31%	4883	5628	3 YEARS
I-CSHRP-66	899.4	531.6	992.4	3288	10.34%	5964	4200	3 YEARS

REBAR TRACE CHLORIDES

NUMBER OF SAMPLES COLLECTED: 7

KCC LOG #	BAR #	TRACE pH	TOTAL CHLORIDE		WATER SOLUBLE CHLORIDE		TRACE CONDITION
			% CHLORIDE	LBS/CU. YD.	% CHLORIDE	LBS/CU. YD.	
I-CSHRP-63	I-CSHRP-63	10.0					Clean
I-CSHRP-64	I-CSHRP-64	10.0			0.0076	0.30	Clean
I-CSHRP-64	I-CSHRP-64B	10.0					Clean
I-CSHRP-65	I-CSHRP-65	10.0					Clean
I-CSHRP-66	I-CSHRP-66	10.0			0.0104	0.41	Clean
I-CSHRP-67	I-CSHRP-67	10.0					Clean
I-CSHRP-68	I-CSHRP-68	10.0					Clean
		AVERAGE :			0.0090	0.36	

BASE LINE CHLORIDE:

TOTAL CHLORIDE:
% CHLORIDE: _____
LBS/CU. YD.: _____

WATER SOLUBLE CHLORIDE:
% CHLORIDE: 0.0039
LBS/CU. YD.: 0.15

SOURCE : 6 1/8" FROM TOP OF THE CORE I-CSHRP-66.

AC RESISTANCE TEST

KCC LOG #	BAR #	DATE IN SOAK	TIME IN SOAK	DATE REM. FROM SOAK	TIME REM. FROM SOAK	HRS. OF SOAK	AC RESISTANCE, kohms/sq. ft.	
							0 HRS	72 HRS
I-CSHRP-63	5	Oct. 15, 91	1:30 PM	Oct. 18, 91	1:30 PM	72	21,206	661
I-CSHRP-64	5	Oct. 15, 91	1:30 PM	Oct. 18, 91	1:30 PM	72	> 42,800	7,004
I-CSHRP-65	5	Nov. 4, 91	12:15 PM	Nov. 7, 91	12:15 PM	72	> 42,800	> 42,800
I-CSHRP-66	5	Nov. 4, 91	12:15 PM	Nov. 7, 91	12:15 PM	72	603	99
						AVERAGE :	> 26,852	> 12,641

EVALUATION: _____

EPOXY COATED REBAR STUDY
MICROSCOPE STUDY RESULTS

PROJECT

EPOXY COATING PROPERTIES

LOG#	EPOXY COATING THICKNESS, mils				INTERFACIAL FOAM				THROUGH-FILM FOAM				UNDERFILM CONTAMINATION
	Individual Reading			AVE.	Individual Reading			AVE.	Individual Reading			AVE.	
I-CSHRP-67													

ANCHOR PATTERN

LOG#	REPLICATE TAPE METHOD, mils				PERTHOMETER METHOD, mils				SURFACE CONDITION
	Individual Reading			AVE.	Individual Reading			AVERAGE	
					-	-	-	-	

PHOTOGRAPHS

EVALUATION: _____

KENNETH C. CLEAR, INC.
EPOXY COATED REBAR STUDY
MICROSCOPE STUDY RESULTS

PROJECT : C-SHRP

EPOXY COATING PROPERTIES

KCC LOG#	EPOXY COATING THICKNESS, mils				INTERFACIAL FOAM				THROUGH-FILM FOAM				UNDERFILM CONTAMINATION
	Individual Reading			AVE.	Individual Reading			AVE.	Individual Reading			AVE.	
I-CSHRP-67	6.75	6.75	6.75	6.75	0	0	0	0	0	0	0	0	35%

ANCHOR PATTERN

KCC LOG#	REPLICATE TAPE METHOD, mils				PERTHOMETER METHOD, mils				SURFACE CONDITION
	Individual Reading			AVE.	Individual Reading			AVERAGE	
I-CSHRP-67	2.10	2.05	1.90	2.02	-	-	-	-	Clean

PHOTOGRAPHS

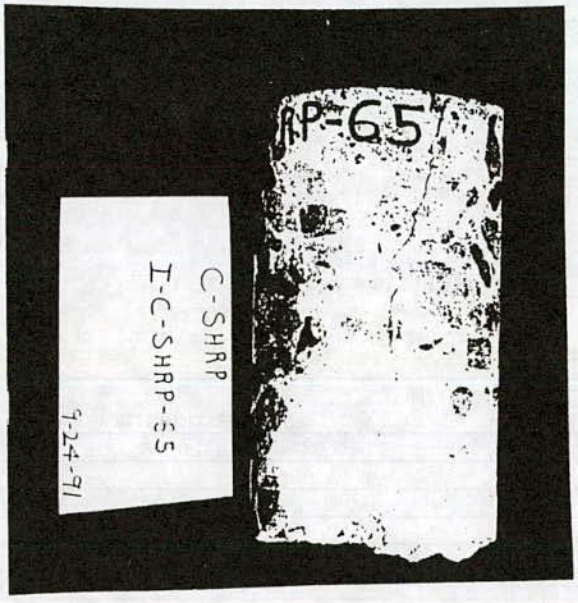

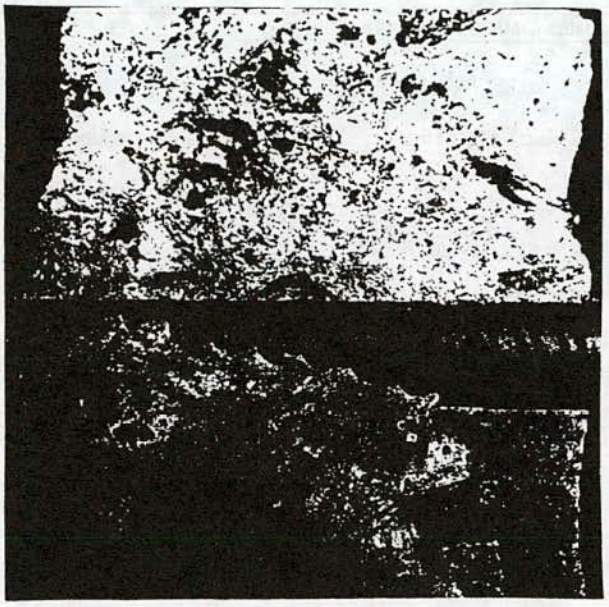

EVALUATION: _____

EPOXY COATED REBAR STUDY
ACCELERATED CORROSION AND CHEMICAL IMMERSION TEST RESULTS

PROJECT

ACCELERATED CORROSION TEST

ANODE REBAR #: _____ CATHODE REBAR #: _____

AC RESISTANCE: _____ ohms AT 0 MIN. _____ ohms AT 15 MIN. WITHOUT INTENTIONAL BARE AREA
_____ ohms AT 0 MIN. _____ ohms AT 15 MIN. WITH INTENTIONAL BARE AREA
_____ ohms AT THE END OF THE ACCELERATED CORROSION TEST

DRY KNIFE ADHESION: _____ FOR ANODE; _____ FOR CATHODE BEFORE TEST
_____ FOR ANODE; _____ FOR CATHODE A WEEK AFTER TEST

STATIC POTENTIAL: _____ FOR ANODE; _____ mV FOR CATHODE

ELAPSED DAYS	OUTPUT		INSTANT-OFF POTENTIAL, mV CSE		OBSERVATIONS
	VOLTAGE, V	CURRENT, mA	ANODE	CATHODE	

NOTE:

CHEMICAL IMMERSION TEST

LEFT REBAR #: _____ RIGHT REBAR #: _____

AC RESISTANCE: _____ ohms AT 0 MIN. _____ ohms AT 15 MIN. WITHOUT INTENTIONAL BARE AREA
_____ ohms AT 0 MIN. _____ ohms AT 15 MIN. WITH INTENTIONAL BARE AREA
_____ ohms AFTER CHEMICAL IMMERSION TEST

DRY KNIFE ADHESION: _____ FOR LEFT REBAR; _____ FOR RIGHT REBAR BEFORE TEST
_____ FOR LEFT REBAR; _____ FOR RIGHT REBAR A WEEK AFTER TEST

STATIC POTENTIAL: _____ mV FOR LEFT REBAR; _____ mV FOR RIGHT REBAR

ELAPSED DAYS	DRIVING VOLTAGE, V	MACROCELL CURRENT, mA	INSTANT-OFF POTENTIAL, mV CSE		OBSERVATIONS
			LEFT REBAR	RIGHT REBAR	

NOTE:

EVALUATION: _____
_____
_____

KENNETH C. CLEAR, INC.
EPOXY COATED REBAR STUDY
ACCELERATED CORROSION & CHEMICAL IMMERSION TEST RESULTS

PROJECT : C-SHRP

ACCELERATED CORROSION TEST

ANODE REBAR #: C-SHRP-63 CATHODE REBAR #: C-SHRP-64

AC RESISTANCE: 61 K ohms AT 0 MIN. 60 K ohms AT 15 MIN. WITHOUT INTENTIONAL BARE AREA
3 K ohms AT 0 MIN. 5.6 K ohms AT 15 MIN. WITH INTENTIONAL BARE AREA
6.1 K ohms AT THE END OF THE ACCELERATED CORROSION TEST

DRY KNIFE ADHESION: 1 FOR ANODE; 1 FOR CATHODE BEFORE TEST
1 FOR ANODE; 3 FOR CATHODE A WEEK AFTER TEST

STATIC POTENTIAL: -742 FOR ANODE; -539 mV FOR CATHODE

ELAPSED	OUTPUT		INSTANT-OFF POTENTIAL, mV CSE		
DAYS	VOLTAGE, V	CURRENT, mA	ANODE	CATHODE	OBSERVATIONS
0	2.01	0.05	254	-1163	no corrosion or H2 evolution
2	2.01	0.01	33	-1068	
3	2.01	0.03	-63	-1145	1 corroding spot on anode
4	2.01	0.03	60	-1147	
5	2.01	0.03	-276	-1133	1 more rust spot on anode, no H2 evolution
6	2.01	0.02	-286	-1132	
7	2.01	0.01	-156	-1082	

NOTE: ACT #34

CHEMICAL IMMERSION TEST

LEFT REBAR #: C-SHRP-65 RIGHT REBAR #: C-SHRP-66

AC RESISTANCE: > 1.1 M ohms AT 0 MIN. > 1.1 M ohms AT 15 MIN. WITHOUT INTENTIONAL BARE AREA
34 ohms AT 0 MIN. 35 ohms AT 15 MIN. WITH INTENTIONAL BARE AREA
48 ohms AFTER CHEMICAL IMMERSION TEST

DRY KNIFE ADHESION: 1 FOR LEFT REBAR 1 FOR RIGHT REBAR BEFORE TEST
5 FOR LEFT REBAR 5 FOR RIGHT REBAR A WEEK AFTER TEST

STATIC POTENTIAL: -552 mV FOR LEFT RE -572 mV FOR RIGHT REBAR

ELAPSED	DRIVING	MACROCELL	INSTANT-OFF POTENTIAL, mV CSE		
DAYS	VOLTAGE, V	CURRENT, mA	LEFT REBAR	RIGHT REBAR	OBSERVATIONS
1	.003	0.00	-627	-618	
4	.003	0.00	-667	-664	
8	.001	-0.01	-679	-677	
15	.001	0.00	-698	-696	2 rust spots on left bar, slight rust around bare area on right bar
20	.000	0.00	-702	-701	
28	.001	0.02	-697	-695	
36	.001	-0.01	-769	-768	significant rust inside bare area on left bar, 6 other rust spots
45	.000	-0.01	-790	-790	slight rust inside bare area on right bar, 1 other rust spot on bar

NOTE: CIT #18

EVALUATION:

APPENDIX G

TASK 4 - RESEARCH METHODOLOGY

MATERIALS

Coated reinforcing steel bars of varying lengths and representing four fusion epoxy powder coating types along with three modifications of one were obtained from eleven sources, eight domestic and three foreign, with each represented as conforming to appropriate industry standards. Specimens were identified according to source by a letter designation as **A, B, C, D, E, F, J, N, T** and **U**[1]. The reinforcing steel substrate types were classified according to the deformation design[2] as shown in Figure G-1. Table G-1 shows the corresponding classification for each source of ECR. Test specimens were cut into six-inch (15.2 cm) lengths using a power hacksaw. Special precautions were taken to ensure that the ECR specimens were not physically damaged during the cutting process by placing each bar in a Tygon® tube. Specimens for laboratory electrochemical testing were prepared by drilling and tapping a hole in one end so that a lead wire could be secured using a screw as shown by Figure G-2. Subsequent to cleaning, a thick, two-part epoxy coating (Epoweld®, Hardman Co.) was applied to both cut ends.

---

[1] There was insufficient quantity of material from one source to include it in a statistically significant evaluation, and only a few, preliminary tests were performed upon it. Consequently, it has not been listed.

[2] "Reinforcing Bar Testing", Second Edition, Concrete Reinforcing Steel Institute (CRSI), 1989.

Table G-1. Coated Reinforcing Steel Specimen Classification.

Deformation	Source
Cross	A, B, N
Inclined	C, D, E, F, T
Parallel	J, U

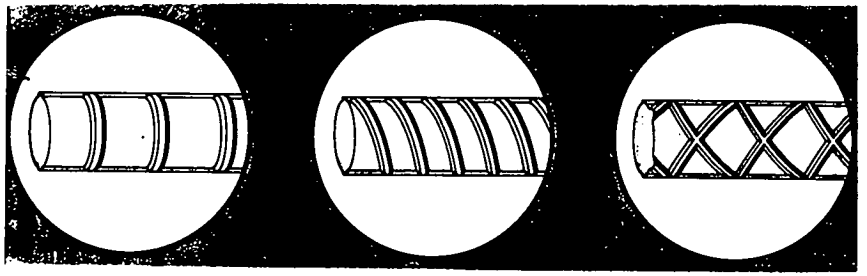

Figure G-1. Type of Deformation.

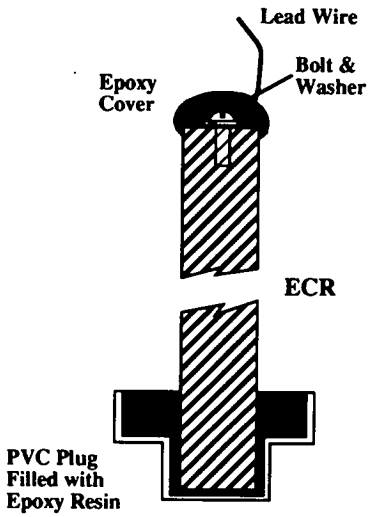

Figure G-2. Preparation of ECR Specimen.

COATING CHARACTERIZATION

All ECR specimens were characterized according to coating thickness, number of holidays, hardness and visual appearance prior to exposure testing.

Holiday detection was performed using a M-1 holiday detector (Tinker & Rasor, Inc.), which conformed to ASTM G62 (method A). Coating defects were identified and classified as one of four types, and typical examples were photographed using a WILD stereomicroscope.

Coating thickness measurements were made at various locations along the length of specimens using a Minitest 500 coating thickness tester. The average of three readings per location was recorded. Coating hardness measurements were performed according to ASTM D3363 using hardness pencils (Paul N. Gardner Co., Inc.) with a minimum of ten readings being obtained for each source.

Degree of cure was determined for each coating type by employing a solvent extraction technique (see Reference 2 in Appendix H). The solvent extraction test involved the following procedures:

- ECR specimens with a minimum length of two feet (0.61 m) were used for this test;
- coating samples were obtained by first dipping one foot (0.30 m) of the specimen into liquid nitrogen for one minute, placing the cold

bar into a bending machine, deforming to 180° to detach the coating and removing and collecting loose coating flakes from the substrate;

- coating samples were then stored in a labeled plastic bag and allowed to stabilize under ambient conditions for one week;
- the extraction thimble was weighed to the nearest 0.01 mg using a Metler analytical balance;
- the coating sample of about 0.5 grams or less was placed in the thimble and the two weighed together;
- both the coating samples and the glass thimble were handled with gloved hands;

the thimble with the sample was installed in a Soxhlet extraction tube;

- approximately **250 ml** of methylethylketone were added to a flask and placed in a heating mantle;
- the Soxhlet extraction apparatus was assembled;
- the temperature of the heating mantle was adjusted using a variable voltage power source until the solvent began to boil;
- the test was conducted for one week;
- upon completion of the test, the thimble containing the coating sample was removed from the Soxhlet apparatus and placed in an exhaust hood for one week;
- the thimble with the sample was then placed into an oven to dry at a temperature of 120°C for one hour;
- the heat was turned off and the thimble and sample were allowed to cool until the temperature reached 30°C;
- because the dried thimble and coating would continuously absorb moisture, the procedure was to complete the weighing as soon as possible after removal from the oven (usually within ten minutes); and the measured weight of the thimble and test sample were recorded and the weight loss was calculated. The final weight loss, when corrected for pigments and soluble additives, gives an accurate measure of cure.

ELECTROCHEMICAL IMPEDANCE SPECTROSCOPY

A schematic of the EIS instrumentation is illustrated in Figure G-3. The system consisted of a Schlumberger 1260 Gain Phase Analyzer and an EG&G Princeton Applied Research 273A potentiostat/galvanostat, both interfaced to an IBM PC compatible computer. Experiment control and data acquisition were based upon ZPLOT® (Scribner Associates); and data analysis utilized ZFIT® (Scribner Associates). EIS test parameters are listed in Table G-2.

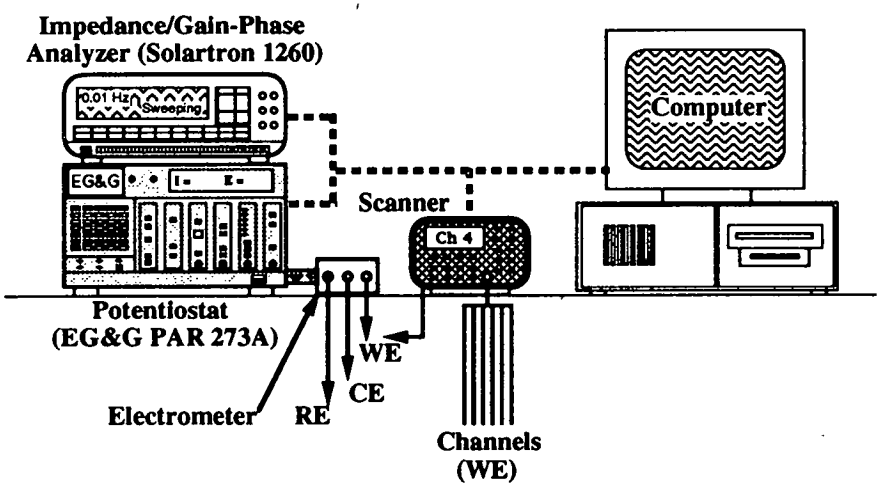

Figure G-3. Schematic Illustration of EIS Scanning Setup.

Table G-2. Electrochemical Impedance Spectroscopy Test Parameters.

Amplitude:	100 mV for ECR specimens 5-20 mV for black rebar
Wave Form:	single sine wave
Points/Decade:	10
Frequency Range:	65kHz → 10mHz (or 1 mHz)
Reference:	Ag/AgCl Ag/AgCl + capacitively coupled Pt wire for low conductivity environment
Auxiliary:	expanded commercially pure titanium or catalyzed titanium mesh

HOT WATER/EIS/ADHESION TESTING

Exposures in this category of tests involved placement of ECR specimens into individual cells containing the environment of interest, either distilled water or aqueous 3.5 weight percent (w/o) NaCl solution. These were positioned in an eight cell, controlled temperature water bath as shown by Figure G-4. Each cell consisted of an ECR specimen, catalyzed titanium (Elgard 210) mesh counter electrode and a Ag/AgCl reference electrode. The individual test cells were constructed so that the titanium counter electrode was placed around the inner circumference of the glass container and the reference placed between the counter and ECR specimen at about mid-specimen height. Approximately 5.5 inches (14 cm) of the specimen was immersed. Test duration was fourteen (14) days at a temperature of 80°C. Evaporative water loss from the cells was minimized by Plexiglas® covers, and water levels were monitored daily and distilled water added as necessary for replenishment. An initial EIS scan was performed at ambient temperature upon each specimen and then at 80°C after 1, 7 and 14 days immersion. Most scans were limited to two hours in order to avoid instability problems that might occur during the data acquisition period. This was especially problematic during the first twenty-four hours of immersion, during which time the electrochemical system underwent the most change. Instability problems, where these occurred, were characterized by discontinuities in the impedance diagrams in the low frequency range, usually below 1 Hz. At the conclusion of hot water testing (fourteen days) the ends of the ECR

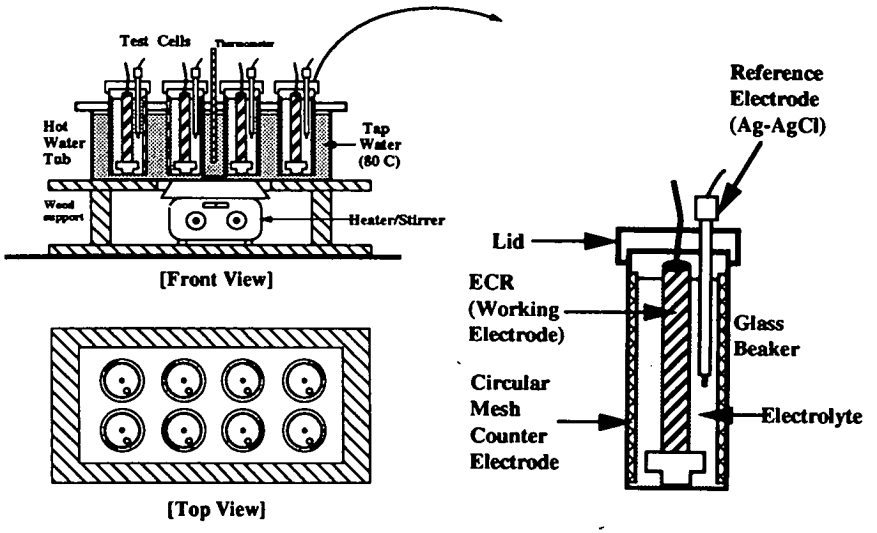

Figure G-4. Schematic of Hot Water Test Apparatus and Test Cell.

specimens were examined for signs of deterioration. Specimens with corrosion or deterioration at these locations were considered suspect and the EIS data for these disregarded.

Adhesion testing was conducted at various times after removal from the elevated temperature test environment. Three locations along the bar length were selected randomly per specimen, and a rasp was used to roughen the coating surface in order to provide maximum adhesion between the coating and the aluminum pull-stub. Roughened areas of the coating and the pull-stub were cleaned with ethanol, and a two-part structural epoxy adhesive (3M Scotch-Weld™, DP-460) was applied to the concave side of the pull-stub. This was then placed on the desired bar location using a specially designed alignment device. Particular attention was given to this step because improper alignment of the pull-stub could introduce bending moments which would invalidate the tensile-adhesion test. The alignment device also served to hold the pull-stub in place until the adhesive was sufficiently cured (approximately one-two minutes). Excess adhesive was removed from around the contact area. The adhesive was allowed to cure for twenty-four hours prior to testing, and the coating was then scored around the pull-stub so that bare metal was exposed. This last step was performed to isolate the coating test area and thereby eliminate any influence of cohesive forces which otherwise would be exerted during testing by the surrounding coating. Figure G-5 illustrates the adhesion test system schematically along with various aspects of the specimen and pull-stub. Note that different pull-stub

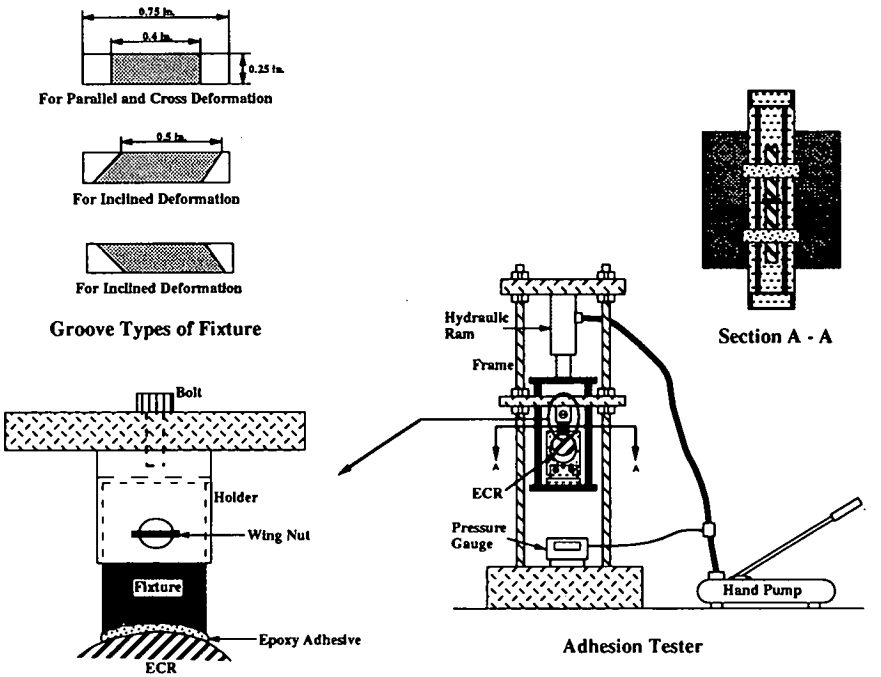

Figure G-5. Schematic of Adhesion Testing System.

geometries were employed according to the type of deformation pattern on the ECR being tested. The procedure for testing involved (1) alignment of specimen and pull-stub into the gripping device, (2) application of a tensile force to the specimen by engaging the pump lever of the hydraulic ram in a continuous, steady manner, and (3) recording the pressure at the time of detachment. The nominal adhesion strength was obtained by dividing the maximum applied force by the projected area of the concave surface of the aluminum pull-stub.

ATMOSPHERIC EXPOSURE

ECRs obtained from two North American sources (J and N) were exposed to natural weathering at the FAU outdoor test yard and to a natural marine atmospheric environment approximately 50 meters from the ocean. Half of each specimen set was exposed directly to ultraviolet radiation and the other half was sheltered to eliminate ultraviolet radiation exposure but exposed in such a manner that rain and/or the marine atmosphere had access to the specimens. The adhesion of these bars was tested before and after to hot water/EIS testing, and in addition some of the bars were incorporated into concrete slab specimens that were subjected to cyclic exposure tests.

CHEMICAL IMMERSION TESTS

In this category of experiments ECR specimens were exposed under ambient conditions to four test environments which included distilled water, aqueous 3.5 w/o NaCl solution, simulated concrete pore water and simulated concrete pore with addition of 3.44 w/o KCl. The simulated pore water solution was prepared using reagent grade chemicals and consisted of 2.63 w/o NaOH, 1.07 w/o KOH and 0.22 w/o $Ca(OH)_2$. Two ECR specimens per source were immersed in each environment. At approximately two-to three-month intervals, EIS scanning was performed and comparisons made to baseline data. The first round of EIS testing was performed in the immersion environment; however, subsequent testing also involved EIS testing in tap water.

ACCELERATED CORROSION TESTING (ACT)

Preliminary Tests

Baseline EIS scans were run in tap water for both anode and cathode ECR specimens. This was followed by the introduction of a 0.25 inch (0.63 cm) diameter holiday at mid-span of the cathode ECR specimen. All specimens were tested in the as-received condition and no attempt was made to coat bare areas and holidays that were present. ECR specimens were then placed in KCl containing simulated pore water (SP/Cl) and allowed to stabilize for about two hours. A schematic illustration of the ACT set-up is shown in Figure G-6. The open circuit potential (OCP) of the specimens was measured at the end of the two-hour stabilization period. A silver-silver chloride reference electrode and a high impedance voltmeter was used for these measurements. A two volt direct current (DC) perturbation was applied across

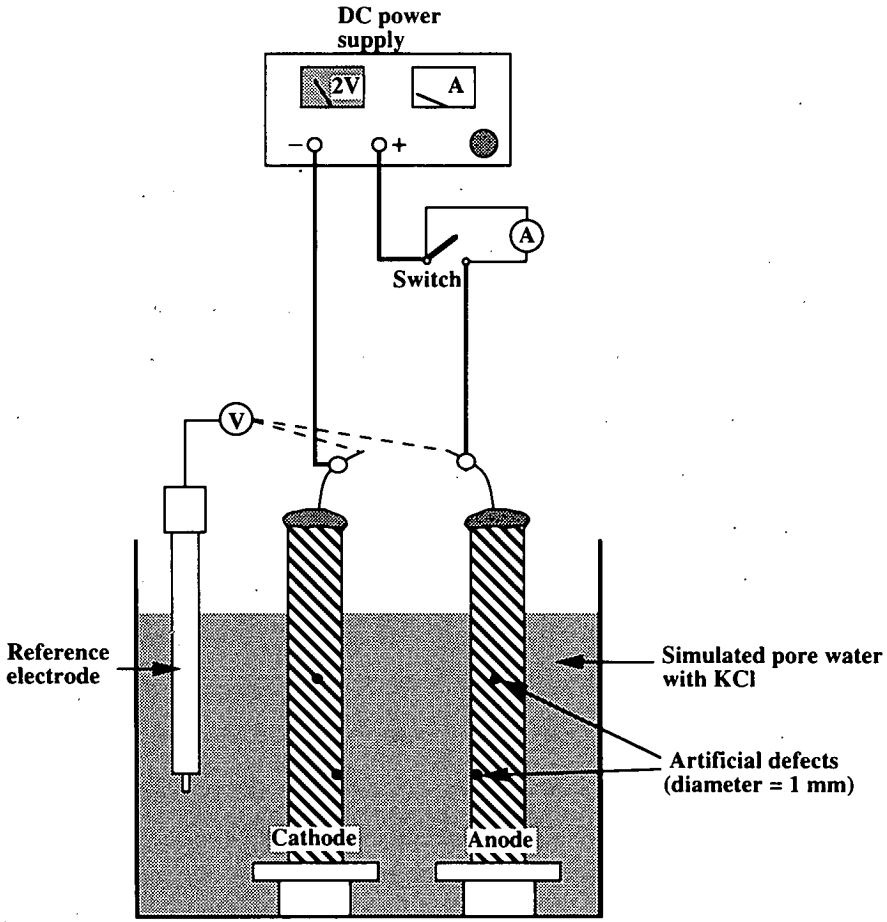

Figure G-6. Schematic of Accelerated Corrosion Test (ACT) Setup.

the anode and cathode using a DC power source. Once the proper voltage was maintained, the polarized potentials of the ECRs were measured. An ammeter was then connected across a switch which was placed in series between the positive terminal of the power supply and the anode. The switch was turned-off in order to monitor the current. If the current readings fluctuated, an average reading was taken over a few minutes. Periodic current measurements were made for fourteen days. The proper level of test solution was maintained daily by adding distilled water as needed. After measuring the 14th day current, the power supply was disconnected and specimens were kept in the test solution until their OCPs became stable, at which time the stabilized OCPs were recorded. Specimens were then examined for deterioration, poorly bonded coating was removed using a sharp utility knife and amount of delamination around the cathode and anode was measured. Selected specimens were photographs as deemed necessary. The relative degree of delamination on both electrodes was determined, as well as the number of rust spots and blisters. Blisters were opened and the pH was checked using indicator pH paper. After examination, the specimens were stored in a desiccator for future study.

Specimens with Controlled Defects

ECR specimens were first characterized by conducting a baseline EIS scan in distilled water. If the specimen was found to contain a defect, an attempt was made to locate this using a holiday detector. Defects were either patched with a two-part

epoxy or the ECR specimen was not used for further testing. EIS scans were obtained for repaired specimens to check for defects, and only those specimens exhibiting capacitive behavior were used. Once defect-free specimens were identified, two 1-mm-diameter intentional defects were introduced into both the anode and cathode. One defect was placed in a valley between lugs and one top of the rib. EIS scans were again obtained for both specimens to determine the decrease in impedance. The ACT test was then performed according to the procedure outlined in the previous section.

CONCRETE TEST SLABS

Concrete test slab dimensions were 14 by 13 by 7 inches (36 by 33 by 18 cm). Three black rebars were positioned in the bottom portion of the slab while two ECR specimens were incorporated into the top. All bars were #5 (0.625-inch (16-mm) nominal diameter), and the clear concrete cover was one inch (2.5 cm) in all cases. The slabs were designed so that the top lift (5 cm) contained 15 lbs Cl^- (8.91 kg/m^3), while the bottom five inches (13 cm) was cast with chloride-free concrete. The mix design was according to ASTM C109 (Table G-3). A schematic of the concrete test slab specimen is illustrated in Figure G-7. Eighty-eight test slabs were cast in October 1992 by K.C. Clear, Inc., in Sterling, VA, cured for thirty days, delivered to Florida Atlantic University and the molds removed in November 1992. Slabs were placed on elevated racks in the Department of Ocean Engineering test yard area

Table G-3. Concrete Mix for Test Slabs.

Cement	356.7 kg/m^3
Water	178.4 kg/m^3
Coarse Aggregate	910.3 kg/m^3
Sand	823.5 kg/m^3
Daravair, AEA	38.7 ml/m^3

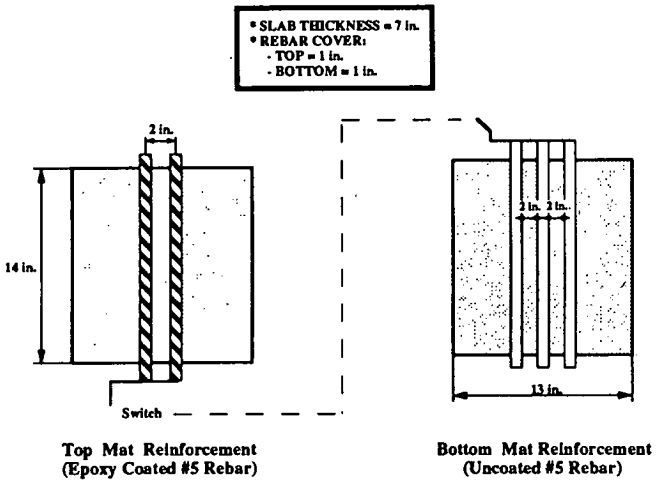

Figure G-7. Steel Reinforcement Arrangement of the Test Slabs.

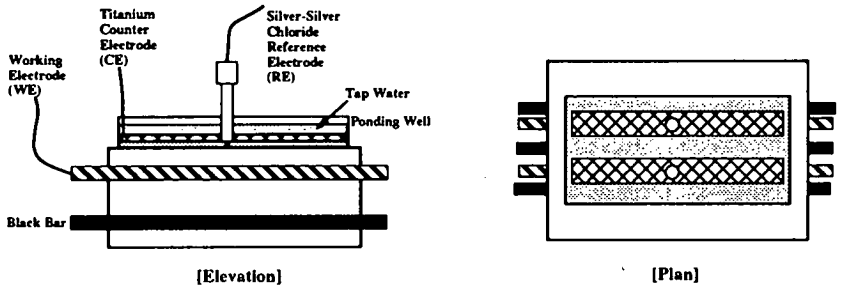

Figure G-8. Setup for EIS Scanning of Test Slabs.

which is approximately two miles (three km) inland from the ocean. An epoxy coating was applied to all sides and a tap water wet-dry ponding cycles program began in January 1993. Four exposure cycles were used including 1) continuous ponding, 2) three days wet and four days dry, 3) thirteen days dry and one day wet and 4) eleven days wet and three days dry. Bars in the bottom mat were shorted to one another and connected to ECRs in the top mat. Macrocell currents and open circuit potentials (OCPs) were measured, and EIS scans were conducted periodically during the subsequent nine months. A schematic of the arrangement for EIS is shown in Figure G-8.

APPENDIX H

RESULTS AND DISCUSSION

ECR SPECIMEN CHARACTERIZATION

Microscopic Examination

Examination of coatings using a stereomicroscope revealed that defects could be characterized according to appearance and location as belonging to one of four categories: bare areas (sites of mechanical damage), pin-holes, cracks or burrs. Representative photographs of three defect types are shown in Figures H-1 through H-3. Pin-hole type holidays were typically found at the base of cross-deformations (Figure H-1); crack type defects (Figure H-2) were generally located along lug bases but were also found in the valleys between deformations (lugs). Burr defects (Figure H-3), on the other hand, normally appeared as metal slivers penetrating through the coating from the substrate surface and occurred randomly along the bar length. Results of the holiday detection and visual inspection for each of the different bar sources are summarized in Table H-1. Data are not included for bars from C and T sources because the number of defects on these was judged to be excessive. C source specimens contained crack-like defects along the length of the lug and at some deformations, whereas T source specimens were severely damaged by mechanical action. Table H-1 shows that the number of defects and their type varied from source to source; and, as indicated, only bars from six of the 10 sources that were evaluated conformed to ASTM standards (*1*).

Holiday Measurements

Holiday detection was not able to identify all potential coating defect sites. For example, initial inspection of two U-source specimens showed no holidays prior to accelerated testing; however, after 24 hours of exposure to aqueous 3.5 w/o NaCl at 80°C, three holidays were detected on specimen U3 and one holiday on U4. Such holidays appeared to coincide with the presence of local rust spots, and examination with a stereomicroscope revealed coating cracks in these areas. Because moisture penetration increases with exposure time, sites predisposed for defect development were apparently not revealed during a pass with the holiday detection electrode and, therefore, only became apparent after moisture had penetrated the defect and electrical continuity established. In addition, holiday measurements could not identify thinly coated areas, although these are projected to be favored sites for detect formation. The various defect types could not be rated in terms of relative susceptibility to initiation

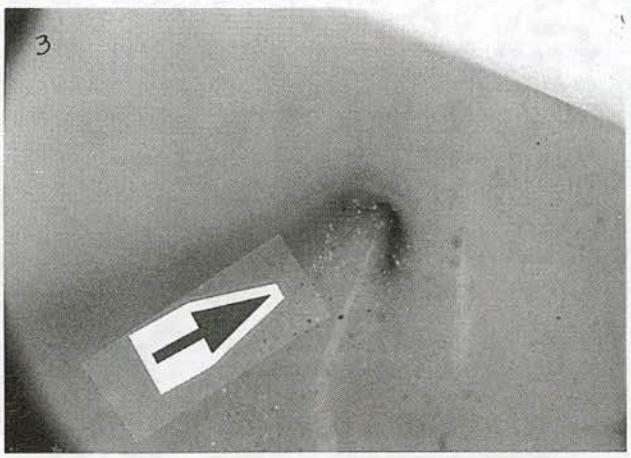

Figure H-1. A pin-hole at the base of cross deformation.

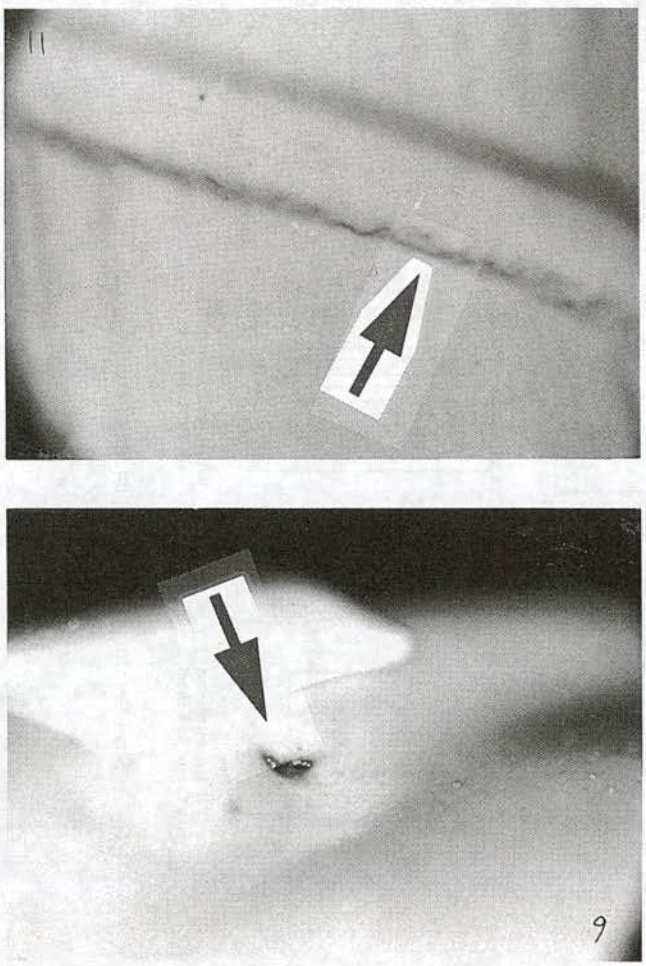

Figure H-2. (Top) Hairline crack along the base of a lug. (Bottom) Short crack at a valley.

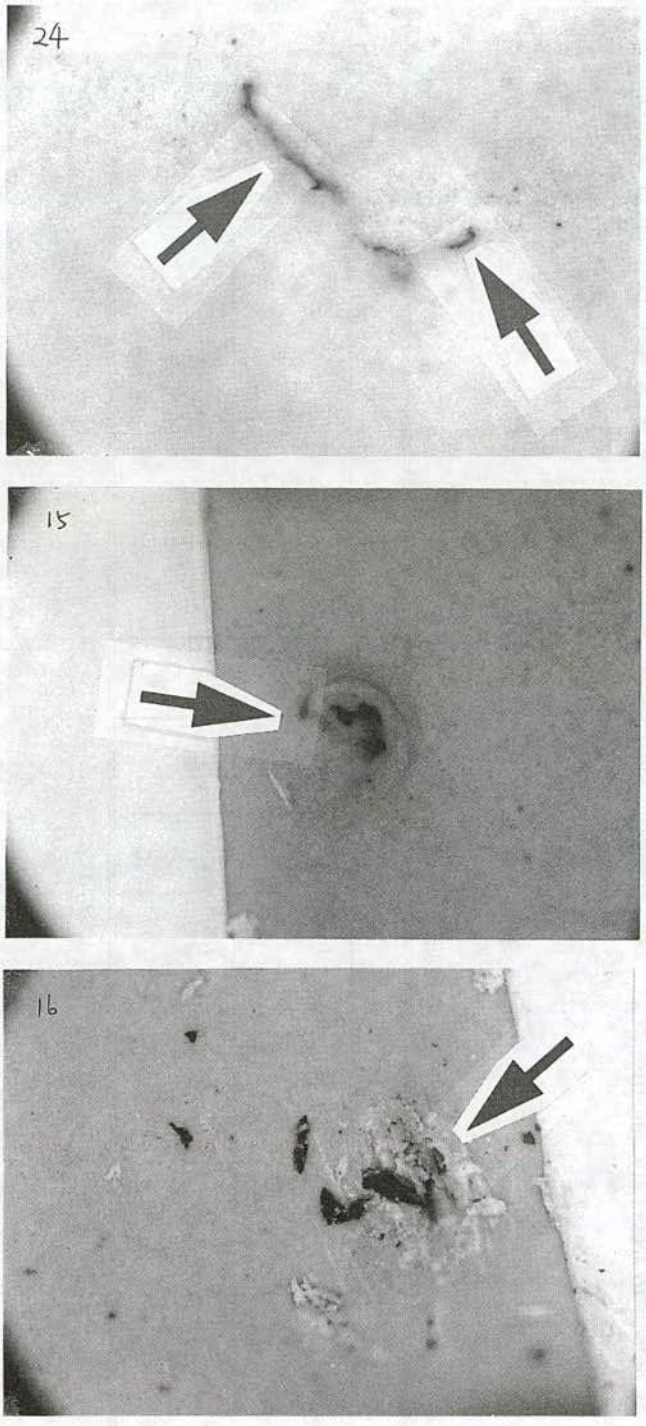

Figure H-3. (Top) Embedded burr at a valley. (Middle) Embedded burr at a valley. (Bottom) Metal burrs found beneath coating as shown in H-3(Middle).

of coating breakdown at these sites; however, post-exposure examination of specimens showed that corrosion sites were frequently located on or directly adjacent to deformations (lugs), including the raised markings used to identify the bar source. The above observations suggest that in-plant holiday detection using currently available commercial instrumentation and procedures is not sufficiently sensitive to identify all irregularities, which may eventually become holidays and sites of corrosion upon environmental exposure.

Coating Thickness Measurements

Results from coating thickness measurements made at various locations along the length and around the circumference of specimens are summarized in Table H-2. The first two columns show the average of readings made on the top of ribs and lugs (deformations) at the indicated sites on the specific bar type (see Figure H-4). Column three lists the average coating thickness for measurements made between deformations (valleys), and the last column shows values for areas adjacent to ribs. A list of all data collected and details on exact measurement locations are provided in Table H-3 and Figure H-5, respectively. From Table H-2 it can be seen that coatings were thicker on the top portion of lugs and ribs and thinnest in the valleys between deformations or close to the rib base. An average coating thickness ranking from thickest to thinnest is A, N > B, E, D > C, F, U > T, J. According to standard deviation values (Table H-3), it appears that ECR supplied by F and U sources, both of which were foreign, had the most uniform coating thickness. However, while the coating thickness between lugs (column 3, Table H-2) was within specification (minimum thickness 125 μm (5 mils) and maximum 300 μm (12 mils)) for coatings from all sources, 60 percent of the average top-of-rib thicknesses and 100 percent of the average top-of-lug thicknesses were greater than 300 μm. This does not mean that these bars are necessarily out of specification, however, since the above limits are not intended to apply specifically to lug and rib areas. The measurements do indicate that coating thickness varied, and it should be anticipated that the coating will be relatively brittle in high thickness locations and susceptible to relatively rapid corrodent ingress where it is thin.

Hardness Measurements

ECR specimens exhibited hardness values of B or HB with the exception of E- and F-source bars, which were slightly softer with a value of 2B. This lower hardness value for E-source specimens might have been predicted based on the solvent extraction test results, where E gave the highest weight loss. However, F-source specimens were similar to E specimens in hardness, but the coating in this case exhibited only moderate weight loss in the solvent extraction test. Moreover, the F-source specimen had a weight loss that was smaller than some specimens that exhibited higher hardness. It is apparent from these results that little or no correlation exists between hardness and weight loss. This lack of correlation may reflect the fact that for some coatings a large weight loss was related to pigment and additive content, rather than the extent of cure. Only the latter would strongly influence coating hardness.

Coating hardness alone is not expected to strongly influence corrosion protection; but a softer coating is expected to exhibit greater flexibility than a harder one, which might be important in long-term performance. Hardness measurements can provide some utility as a tool to evaluate changes in coating physical properties as a consequence of environmental exposure. For ex-

TABLE H-1. Coating defect types and numbers for various ECR sources

Types of Defects	A	B	C[1]	D	E	F	J	N	T[1]	U	NOTE
Mechanical Damage	5	5		14	2	2	7	19		1	
Cracks	2	5		0	2	0	1	7		4	
Burr	1	1		0	0	3	2	0		2	
Pin-hole	4	0		2	0	0	1	0		1	
Measured Length (m)	1.9	1.9	1.9	4.1	3.7	6.3	2.2	2.2	1.9	2.2	

[1] Specimens contain too many defects to accurately quantify.

Table H-1 (Summary)

Number of Defects/m

	A	B	D	E	F	J	N	U	C	T	NOTE
All possible defects	6.3	5.8	3.9	1.1	0.8	5.0	11.8	3.6	N/A	N/A	Inclusion of mechanical damage
Crack, Burr, Pin-hole	3.7	3.2	0.5	0.5	0.5	1.8	3.2	3.2	N/A	N/A	Quality parameter of coating plants

TABLE H-2. Average coating thickness at various locations

Units: μm

Bar Source	Top of Ribs[1]	Top of Lugs[2]	Valley Between Lugs[2]	Close to Rib Base[3]
A	401	372	271	279
B	451	351	254	262
C	263	354	206	-
D	271	402	249	157
E	262	386	277	218
F	318	328	290	147
J	307	397	198	218
N	337	424	302	221
T	205	328	234	145
U	311	318	262	249

NOTES: See Appendix, Figure 1A.

[1] Average of Measurement Position III and VII.
[2] Average of Measurement Position I, II, IV, V, VI and VIII.
[3] Average of Measurement Position III', III'', VII' and VII''.

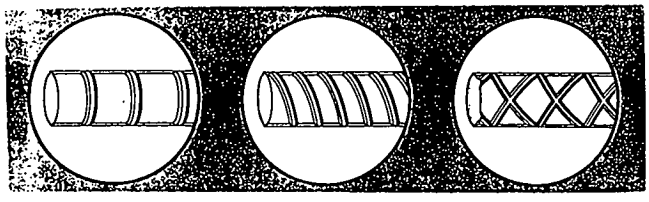

Figure H-4. Bar deformation patterns.

TABLE H-3. Coating thickness data and detailed locations

Source \ Location	I	II	III'	III	III''	IV	V	VI	VII''	VII	VII'	VIII
A	236 (24)	269 (28)	257 (25)	351 (36)	206 (20)	229 (23)	272 (25)	356 (33)	373 (20)	450 (28)	284 (10)	262 (31)
B	170 (13)	198 (13)	257 (15)	396 (13)	218 (23)	221 (15)	201 (8)	257 (20)	272 (23)	505 (33)	305 (15)	478 (28)
C	239 (8)	239 (13)	N/A	262 (36)	N/A	142 (20)	198 (10)	198 (13)	N/A	218 (18)	394 (20)	384 (51)
D	279 (18)	229 (8)	124 (15)	272 (10)	173 (25)	284 (20)	226 (41)	203 (10)	170 (8)	269 (20)	168 (13)	284 (13)
E	279 (18)	287 (23)	234 (23)	274 (23)	175 (13)	259 (20)	284 (20)	305 (23)	279 (25)	249 (15)	183 (10)	251 (18)
F	272 (8)	284 (13)	140 (31)	330 (10)	155 (15)	292 (10)	295 (8)	315 (13)	145 (15)	343 (13)	150 (5)	282 (10)
J	140 (8)	211 (15)	267 (30)	290 (20)	173 (15)	152 (10)	203 (15)	282 (18)	284 (28)	345 (31)	152 (15)	N/A
N	325 (10)	262 (18)	218 (18)	284 (33)	193 (5)	302 (23)	320 (10)	272 (23)	239 (18)	330 (38)	236 (31)	330 (38)
T	254 (13)	215 (20)	155 (15)	196 (18)	137 (13)	N/A	234 (13)	219 (8)	124 (15)	213 (15)	165 (13)	246 (15)
U	216 (5)	232 (8)	246 (13)	274 (10)	264 (13)	291 (13)	226 (15)	277 (5)	234 (8)	348 (20)	259 (10)	335 (28)

Note: Unit of thickness is μm and value in parenthesis is standard deviation.

ample, a detached coating from cathodic disbondment test specimens was typically harder than an intact one, which could be attributed to cation incorporation into the resin matrix, solubilization of plasticizers or continued cross-linking during exposure.

Degree of Coating Cure

Optimum long-term corrosion protection in service can only be realized if the coating is properly cured. Many coating properties vary as a function of degree of cure and application history. For example, coating properties such as flexibility and moisture resistance are a function of cross-linking density. Thus, a coating designed to resist moisture absorption often has poor flexibility. Alternately, those coatings formulated for high flexibility often possess poor moisture and chemical resistance. Therefore, a compromise in formulation (and application conditions) is needed to reach a balance of properties.

Traditionally the degree of coating cure is determined by measuring the change in glass transition temperature (T_g) between two successive DSC (differential scanning calorimetry) scans (delta T_g method). Procedures for this method can be found elsewhere (*2*). However, there are recognized problems in using the DSC technique to determine degree of coating cure. For example, a variation in scan rate will give different results and sometimes negative values are obtained for delta T_g (*2*). A potentially more accurate and reliable method of determining degree of cure is the solvent extraction test (*2*). The basic principle of this technique involves extracting unreacted components from

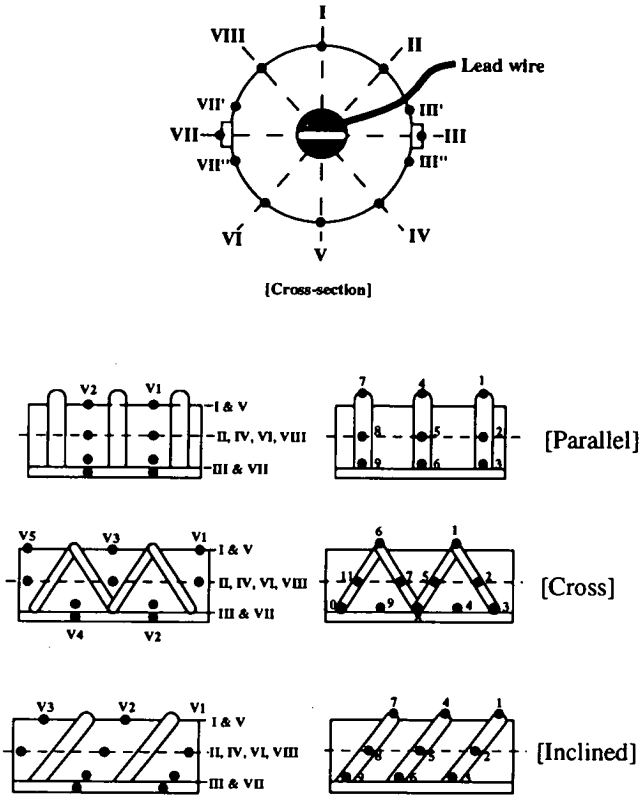

Figure H-5. Locations of coating thickness measurement.

the coating with hot methylethylketone (MEK). A fully cured coating will not exhibit weight loss, while unreacted components in a partially cured coating will be soluble in the MEK. The final weight loss, when corrected for pigment and soluble additive contents, provides a measure of the degree of coating cure.

Preliminary results from applying the solvent extraction technique are summarized in Figure 11 (CHAPTER 2). The apparent correlation between weight loss and ECR performance suggests that coatings with a higher degree of cross-linking should be less porous and, hence, more moisture resistant and less likely to experience premature deterioration than ones with fewer cross-links. Two coating sources, one from North America (E) and one foreign source (F), were designed for greater flexibility, which is often accomplished by reducing the extent of cross-linking or by the addition of plasticizers. These bars gave the highest weight losses, as should be anticipated, and these same ECR specimens exhibited intermediate to poor behavior in the hot water test. Coatings that gave the lowest weight losses (for example, A, B, D, and U) performed the best in hot water testing, chemical immersion and as exposed in concrete.

HOT WATER/EIS/ADHESION TESTING

Elevated Temperature Immersion

Initial accelerated corrosion testing involved exposure of randomly selected ECR specimens in the as received condition to distilled water at 80°C. Some of these specimens contained holidays, mashed or bare areas, while others had no detectable defects. Figures H-6 and H-7 present typical EIS data for specimens in each of these two categories at 0, 1, 7, and 14 days exposure. The plots shown in Figures H-6 and H-7 indicate that the most significant change in impedance occurred during the first day of exposure. One bare area was initially detected on Specimen N11 (Figure H-6a), and one rust spot was present after testing. For Specimen T12 (Figure H-6b) five indicator beeps (assumed to be holidays) were detected initially; and five rust spots, four coating cracks and in excess of 20 blisters existed after exposure. In these cases, where initial defects were present, the baseline impedance was low and typically characterized by the presence of a second time constant.[1] Conversely, in the absence of defects the baseline impedance was generally capacitive and high (Figure H-7). This distinction is consistent with the initial impedance depending upon the number and size of defects. As shown by Figure H-7, both B13 and J13 exhibited high impedance values and initial capacitive behavior. B13 displayed good behavior throughout the test as indicated by a single time constant and impedance values that remained above 3.3×10^8 Ohm-cm^2.[2] Alternately, the development of a defect in the case of J13 after 24 hours was evident by a sizeable drop in impedance and the presence of a second time constant centered at approximately 3 Hz.

A second round of testing involved specimens without defects as determined by visual inspection and holiday sensing with a requirement that ECR specimens also exhibit capacitive behavior in the initial EIS scan. Figures H-8 and H-9 present Bode plots for specimens without initially detectable defects from sources A, B, D, E, F, J, N, and U after 1 day of elevated temperature immersion in distilled water and aqueous 3.5 w/o NaCl, respectively. For both environments, B, D, N, F, and U retained relatively high impedance values, while A-source specimens showed intermediate behavior and E- and J-source specimens exhibited the lowest impedance. These results also show that greater separation of EIS data occurred in aqueous 3.5 w/o NaCl than in distilled water, suggesting that the former environment provided greater sensitivity to apparently subtle differences in coating properties. For example, while B10 gave high impedances throughout the distilled water test (Figure H-8), two other B-source specimens exposed to aqueous 3.5 w/o NaCl (Figure H-9) exhibited a spread of nearly 1.5 orders of magnitude in their impedances (that is, 2.1×10^9 Ohm · cm^2 for B13 versus 5.9×10^7 Ohm · cm^2 for B11); and with the exception of the A-, E- and F-specimen bars, all sources exhibited lower impedance in aqueous 3.5 w/o NaCl than in distilled water. Although 35 percent and 17 percent of the specimens exposed to distilled water and aqueous 3.5 w/o NaCl, respectively, revealed the development of holidays during the test, all specimens irrespective of source exhibited a decrease in imped-

[1]The presence of a second time constant at low frequencies (below about 10 Hz) generally indicates that corrosion is occurring at the substrate/coating interface or at the base of defects. (See Appendix B for more details.)

[2]The decrease in impedance was due to the development of conductive pores through the coating where the associated impedance is typically designated as the coating pore resistance (R_{po}). The R_{po} (actually $R_{po} + R_{ohmic}$) value can be obtained from the intersection of the frequency independent portion of the Bode magnitude plot with the ordinate. The R_{po} is often a good predictor of performance for many organic coating systems, where a decrease to values below about 10^6 Ohm · cm^2 is generally indicative of impending poor performance (*3*–5).

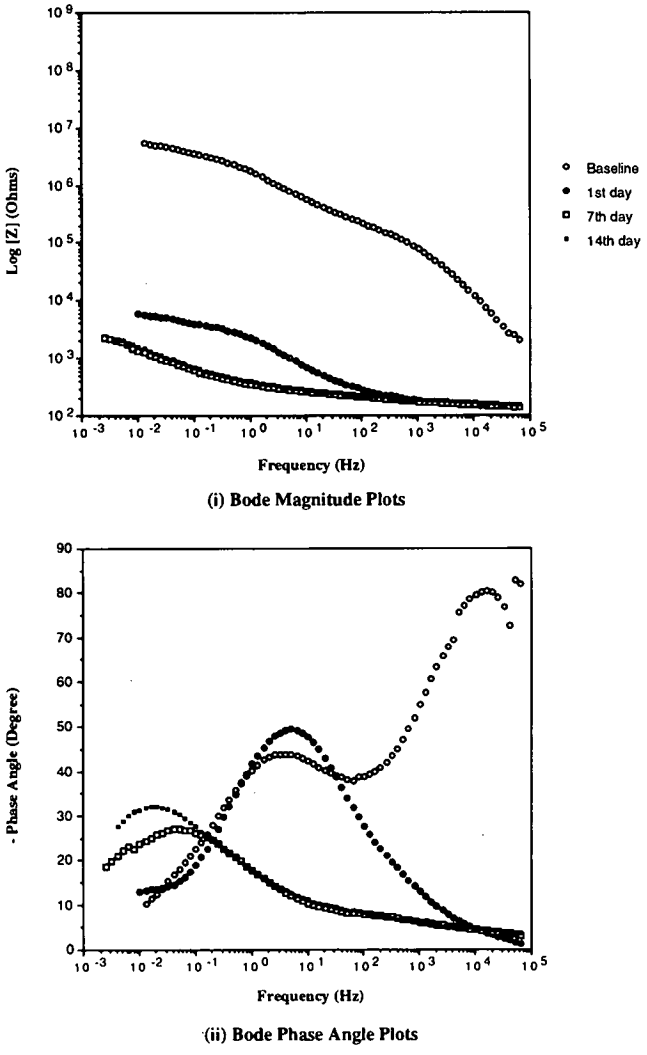

Figure H-6. (a) Bode plots for specimen N11 with one initial defect exposed to aqueous 3.5 w/o NaCl solution for 14 days at 80°C.

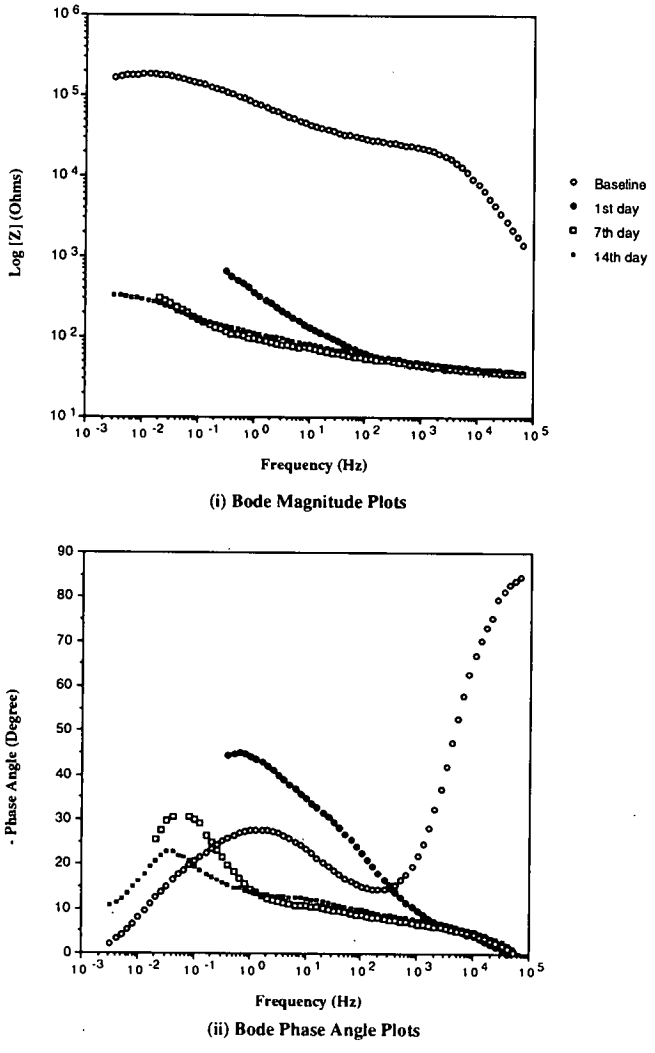

Figure H-6. (b) Bode plots for specimen T12 with five initial defects exposed to aqueous 3.5 w/o NaCl solution for 14 days at 80°C.

ance and a change from purely capacitive behavior to one with a parallel conducting path through the coating. In addition, U16 exposed to distilled water and A12, D11, and J13 exposed to aqueous 3.5 w/o NaCl blistered during the 14-day test. Consequently, the reduced impedance and protective capacity of these specimens must be attributed to a factor(s) other than conventionally detectable holidays and bare areas. The reduced impedance of specimens without detectable initial defects (and in the absence of developed defects over 14 days) is attributed to the establishment of conductive pores in the coating and to an associated reduction in R_{po}. This does not necessarily portend poor service performance but merely indicates that conductive pathways have developed; however, the presence of conductive pores is a precursor for localized coating breakdown. Further, the observation that significant impedance changes occurred during the initial day of exposure suggests that the HWT has utility as an in-plant quality control (QC) technique. Quantification of performance in such a test might involve measurement of impedance at one or several frequencies, which would simplify the QC procedure, decrease measurement time and reduce costs compared to conducting a complete EIS scan. (See section on Utility of HWT/EIS Adhesion in this Appendix for more details.)

It was also observed in the second round of testing that specimens J13 and J21 exhibited the poorest performance and showed the presence of a second time constant at low frequencies after 24 hours of immersion in aqueous 3.5 w/o NaCl (Figure H-9). The impedance of J13 continued to decrease over the 14-day test. This low impedance and the persistence of two time constants were due to the presence of a single (identifiable) holiday, which developed within 24 hours of immersion. However, by day 14 a sizeable increase in the impedance of J21 had occurred; and only one time constant was present (Figure H-10). Inspection of this specimen revealed the presence of three localized rust spots; however, holiday detection was unable to identify these as defect sites. The build-up of corrosion products within

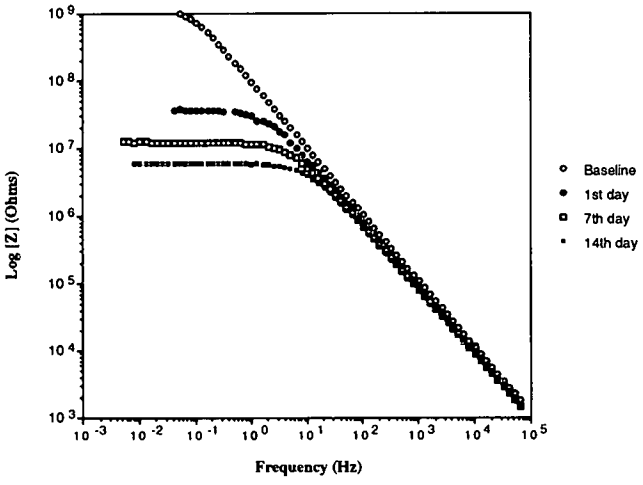

(i) Bode Magnitude Plots

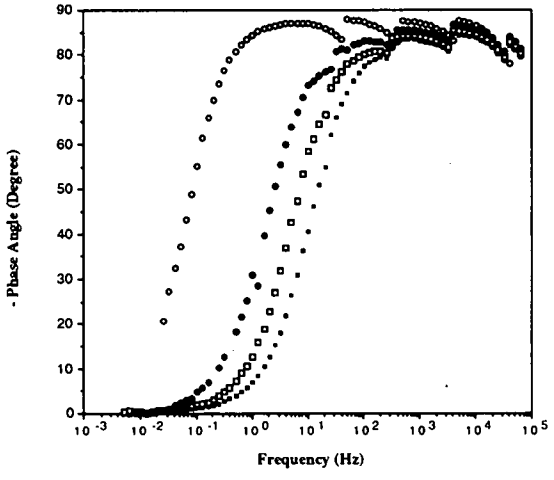

(ii) Bode Angle Plots

Figure H-7. (a) Typical impedance behavior of good ECR (B13) with zero defects before and during exposure to aqueous 3.5 w/o NaCl solution 80°C.

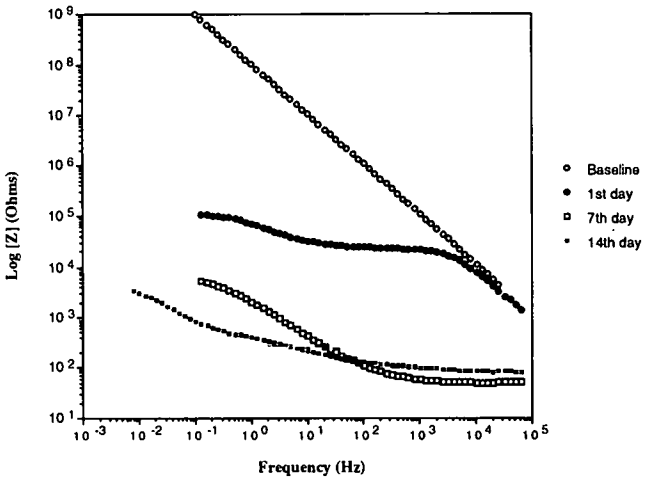

(i) Bode Magnitude Plots

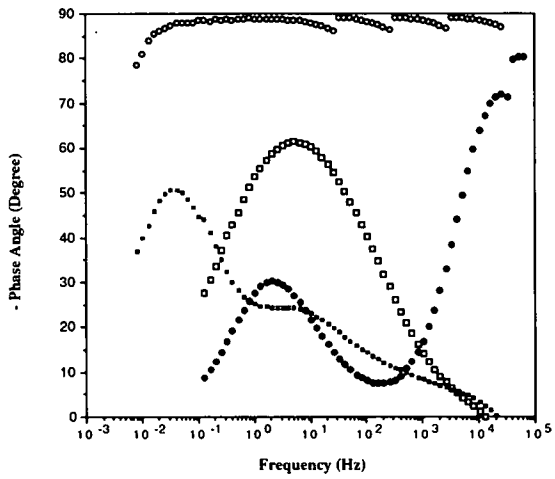

(ii) Bode Angle Plots

Figure H-7. (b) Bode plots for specimen 113 showing poor performance. This specimen was initially defect free; however, a single defect developed during exposure to aqueous 3.5 w/o NaCl solution for 14 days at 80°C.

holidays could account for the disappearance of the low frequency time constant and an increase in impedance. B11 also exhibited an increase in impedance over the course of the test. On the other hand, specimens D11, F1, F2, N12, U14, A11, A12, and B13 showed small impedance decreases between day 1 and day 14, while E1 and E3 showed no change. A summary of R_{po} values for these specimens as determined graphically from the Bode plots is provided in Table H-4.

Although no specimens developed a second time constant in distilled water by 24 hours, E5 and J15 showed a second time constant by day 14 (Figure H-11). Both developed a single holiday during the test. A12 also developed one holiday but did not exhibit a second time constant at low frequencies.[3] In comparison, specimens B10, D20, F3 and F5 showed no holidays or blisters over this period. Thus, it appears that some defect-free, high initial impedance ECR specimens maintained an acceptable degree of coating integrity during the 14-day exposure to distilled water, whereas others did not (Figure H-11). J15, E5, E2, and A21 gave the lowest R_{po} values after 14 days; however, the R_{po} values for E2, E5 (although E5 displayed a second time constant by day 14), and A21 remained essentially constant after day 1, whereas the R_{po} dropped an order of magnitude for J15. All other specimens including N9, B10, U16, F3, F5, and D20 exhibited a decrease in R_{po} of 1 to 2 orders of magnitude; however, none of the impedance values dropped below 10^6 Ohm·cm^2. A summary of R_{po} values for these specimens, as determined graphically from Bode plots, is provided in Table H-5.

Occurrence of defects for each specimen exposed to either distilled water or aqueous 3.5 w/o NaCl is summarized in Table H-6. The feature(s) of a specimen without initially detectable

[3]The absence of a second time constant in the frequency range examined indicated that the corrosion activity was low; hence, shifting the second time constant to frequencies below which could be practically measured. The presumed low corrosion activity is likely because distilled water is relatively unaggressive.

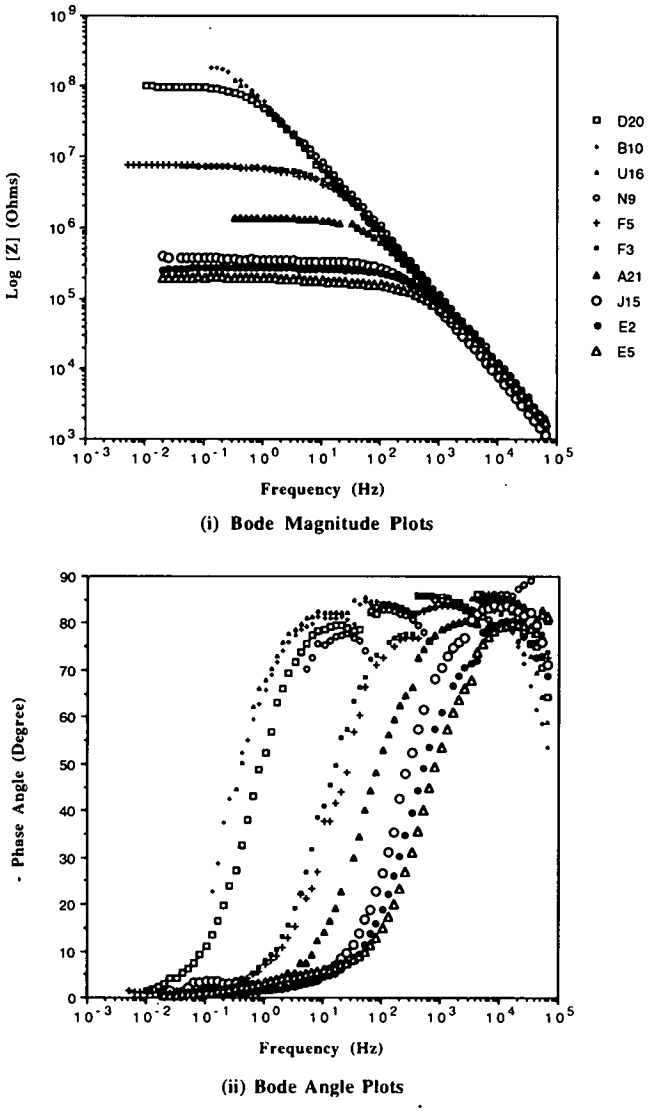

Figure H-8. Bode plots for defect-free specimens after 1 day in distilled water at 80°C (same as Figure 3 in Chapter 2).

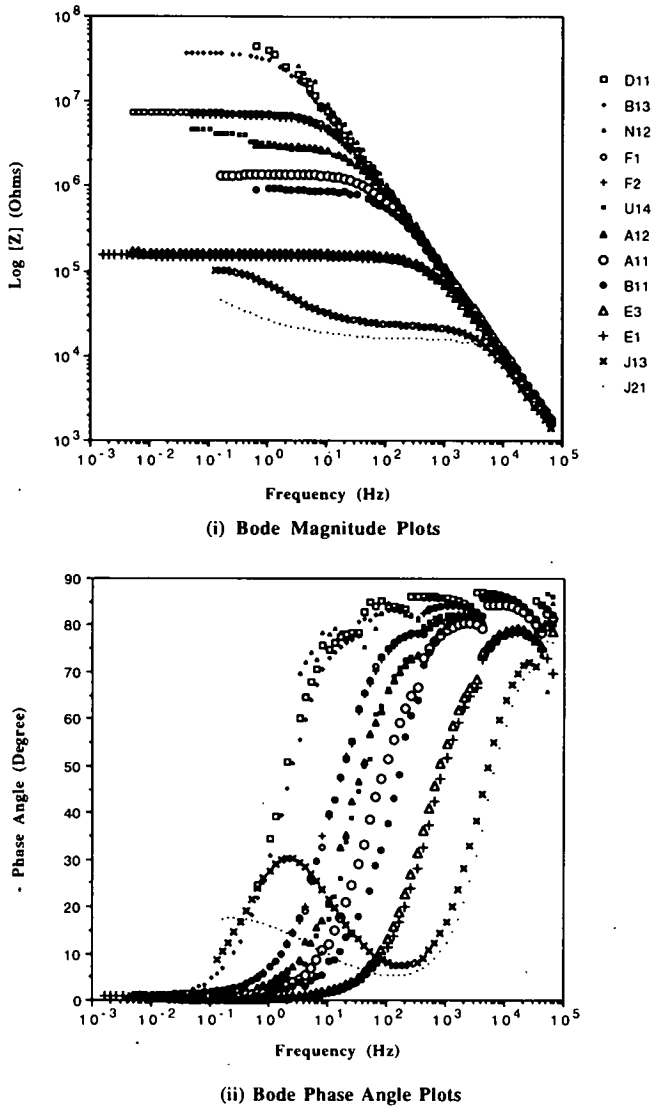

Figure H-9. Bode plots for defect-free specimens after 1 day in aqueous 3.5 w/o NaCl solution at 80°C.

defects which resulted in the coating remaining defect free and the ECR retaining relatively high impedance has not been identified. It must be anticipated, however, that because the probability of a significant defect being present increases with increasing bar length and size, impedance of specimens that performed well in the HWT may have been lower if the specimen surface area had been greater. The finding that no blisters occurred during the 14-day 80°C exposure for many specimens that were initially free of detectable defects, despite the fact that some of these developed defects during testing and would not be expected to provide long-term corrosion protection in service, indicated that a HWT coating qualification based on a blistering criterion alone is inadequate. It may be that processes responsible for blistering operate independently of those leading to a decrease in impedance and subsequent corrosion beneath coatings or at the base of holidays, or both; hence, the absence of blistering within the prescribed time of 7 days should not be a satisfactory condition for acceptance. No correlation was apparent between blister occurrence, defect development and impedance change and coating characterization parameters (thickness and hardness) to the extent that the latter were represented.

A third round of testing also involved using ECR specimens that were initially defect-free (that is, ones which exhibited capacitive behavior). However, before immersion into the elevated temperature bath, two intentional defects measuring 1 mm in diameter and spaced 2.5 cm apart were introduced into each coated specimen. One defect was placed in a valley between two lugs and the other on the top surface of the rib. EIS measurements were conducted immediately after the defects were introduced in tapwater and prior introduction into either distilled water or 3.5 w/o NaCl. The baseline EIS for A20 and D19 specimens captured two time constants and a decrease in R_{po} of four orders of magnitude as a consequence of introducing the two bare areas (Figure H-12); whereas the EIS data for B22, F14 and U20 showed only a single time constant. Impedance values decreased slightly for B22 and F14 and remained un-

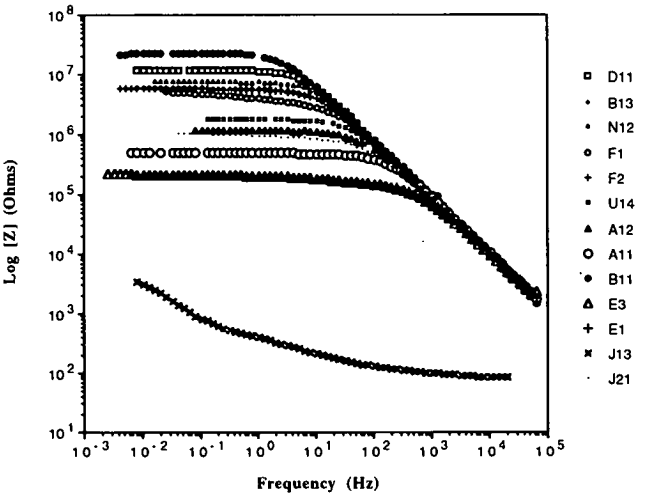

(i) Bode Magnitude Plots

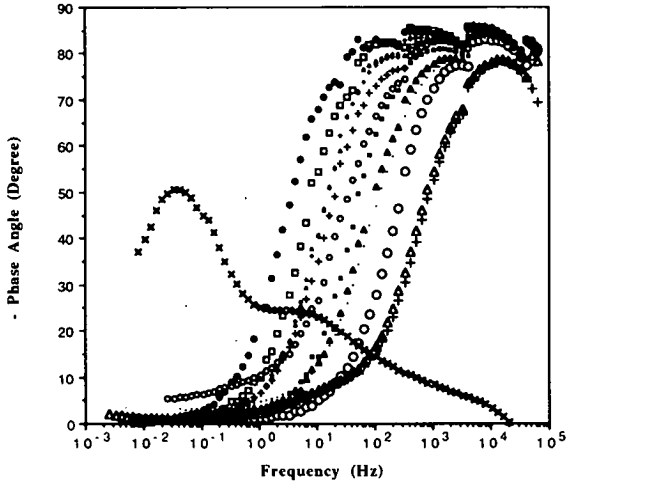

(ii) Bode Phase Angle Plots

Figure H-10. Bode plots for defect-free specimens after 14 days in aqueous 3.5 w/o NaCl solution at 80°C.

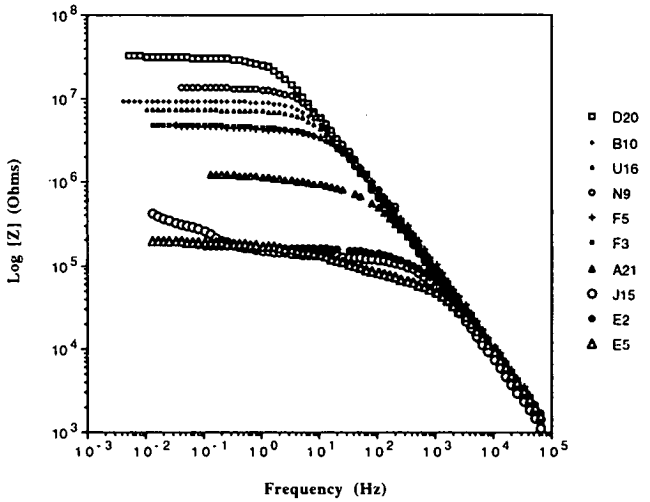

(i) Bode Magnitude Plots

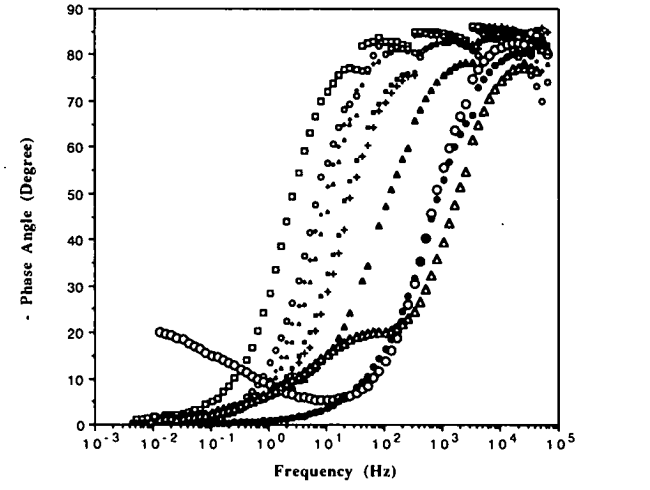

(ii) Bode Phase Angle Plots

Figure H-11. Bode plots for defect-free specimens after 14 days in distilled water at 80°C.

TABLE H-4. Coating pore resistance values for ECR specimens exposed to 3.5 w/o NaCl AT 80°C

Specimen	R_{po}, Ω·cm² 1 day	Time Constants 1 day	Time Constants 14 days	R_{po}, Ω·cm² 14 days
N12	5.4 X 10^8	-	1	4.9 X 10^8
D11	3.2 X 10^9	1	1	7.9 X 10^8
B13	2.5 X 10^9	1	1	3.9 X 10^8
F1	4.9 X 10^8	1	1	7.8 X 10^7
F2	4.5 X 10^8	1	1	3.8 X 10^8
U14	2.0 X 10^8	1	1	1.2 X 10^8
A12	2.1 X 10^8	1	1	5.5 X 10^7
A11	9.2 X 10^7	1	1	3.3 X 10^7
B11	5.8 X 10^7	1	1	1.5 X 10^8
E1	9.8 X 10^8	1	1	9.5 X 10^6
E3	1.0 X 10^7	1	1	9.7 X 10^6
J13[1]	1.7 X 10^8	2	2	< 7 X 10^3
J21	1.0 X 10^8	2	1	4.9 X 10^7

NOTE: [1] Pore resistance values for all specimens except J13 were determined from equivalent circuit model analysis utilizing a commercially available software package. The pore resistance for J13 was determined graphically from the Bode plot.

TABLE H-5. Coating pore resistance values for ECR specimens exposed to distilled water at 80°C

Specimen	R_{po}, Ω·cm² 1 day	# Time Constants 1 day	# Time Constants 14 days	R_{po}, Ω·cm² 14 days
B10	1.4 X 10^{10}	-	1	6.2 X 10^8
N9	2.9 X 10^9	-	1	9.1 X 10^8
U16	1.2 X 10^{10}	-	1	4.8 X 10^8
D20	6.5 X 10^9	1	1	2.0 X 10^9
F3	2.6 X 10^8	1	1	1.9 X 10^8
F5	2.6 X 10^8	1	1	2.4 X 10^8
A21	1.8 X 10^7	1	1	8.6 X 10^6
E2	1.3 X 10^7	1	1	4.8 X 10^6
J15	2.1 X 10^7	1	2	8.2 X 10^6
E5	9.8 X 10^6	1	2	3.5 X 10^6

NOTE: Pore resistance values for all specimens except J13 were determined from equivalent circuit model analysis utilizing a commercially available software package.

TABLE H-6. Summary of defect development during hot water testing

Specimen	DW Initial	DW 14 days	Specimen	NaCl Initial	NaCl 14 days
A9	3	2	A11	0	0
A10	3	4	A12	0	(B)
A21	0	1			
B9	1	1	B11	0	0
B10	0	0	B12	1	1
			B13	0	0
D9	0	0	D11	0	0
D10	0	0	D18	12	12(B)
D20	0	0			
E2	0	0	E1	0	0
E5	0	1	E3	0	0
F3	0	0	F1	0	0
F5	0	0	F2	0	0
J9	0	2	J11	2	2(B)
J10	0	2	J13	0	1
J15	0	0	J21	0	3(R)
N9	0	0	N11	1	1
N10	2	4(B)	N12	0	0
U9	1	2	U11	4	5
U10	1	1	U14	0	0
U16	0	0			

NOTE: (B) indicates the presence of blisters
(R) indicates that three rust spots were observed; however, holiday detection was unable to identify these as defect sites.

changed for U20 (Figures H-13 and H-14). After 24 hours in distilled water, the second time constant observed for A20 and D19 disappeared. In all cases, irrespective of ECR source, the impedance decreased by at least three orders of magnitude after 24 hours of immersion in hot distilled water. At 32 days of immersion, all specimens had nearly the same R_{po} values—with the exception of A20, which had a final R_{po} value that was about half of the other specimens. A summary of R_{po} for these specimens is provided in Table H-7. The disappearance of a clearly distinguishable low frequency time constant for A20 and D19 is not well understood at this time; however, this could have been caused by a shift in the second time constant to frequencies below 10 mHz. It should be noted, however, that at extended immersion times all specimens exhibited a sizeable decrease in R_{po} compared to their initial values. Attack at the base of the defects was minimal, although coating disbondment surrounding the defects was rather extensive in many cases and was greater for specimens exposed to distilled water compared to aqueous 3.5 w/o NaCl. For example, specimens A20, D19, F14, N13, and U20 exposed to distilled water gave an average disbondment area that was 44.5 percent of the total exposed area; conversely, specimens A16, B13, D13, F13, N22, and U18 exposed to aqueous 3.5 w/o NaCl gave an average disbondment area of 20 percent. There were two exceptions to this trend. Disbondment was greater for J and B specimens exposed to aqueous 3.5 w/o NaCl compared to companion specimens exposed to distilled water. Upon removal of the debonded coating a general pattern, as illustrated in Figure H-15, was observed which was characterized by relatively clean metal at the defect surrounded by a rust layer and an outer region of sizeable disbondment that was typically bright to dull gray in appearance. The observed morphology of deterioration represents a classic example of cathodic delamination (*6*). None of the specimens exposed to hot distilled water developed blisters during the more than 30 days of immersion.

The NaCl environment proved to be more aggressive than distilled water. The baseline EIS response for all specimens tested in this solution showed a second time constant that persisted throughout the course of the test (Figures H-16 through H-18. The R_{po} values decreased by about three-fours order of magnitude for A16, B13, D13 and U18 and by about two orders of magnitude for F13 (Table H-8). However, by day 32 all specimens had nearly identically shaped Bode plots and R_{po} values that ranged from 6.6×10^3 to 1.2×10^4 Ohm · cm^2. Blisters formed within 4 days on J12, D13, and B17 but were absent on the remaining specimens. Severe corrosion and coating disbondment around intentional defects were observed for all specimens. In general, attack in the defect was characterized by deep pitting and the build-up of voluminous corrosion products around the pit, which caused lifting of the coating, although cathodic disbondment in advance of anodic activity could have caused loss of coating adhesion. Beyond this region, an area of disbondment existed where the surface was bright in appearance. More specifically, three morphologies of coating breakdown were observed. These are illustrated by a series of schematic representations in Figure H-19. Type I morphology was exhibited by N22 and was characterized by a voluminous build-up of rust colored corrosion products beneath the coating immediately adjacent to the intentional holiday. Type II deterioration was exhibited by J12 and B17 and was characterized by a slight build-up of black corrosion products around the defect. Type III failure was exhibited by E15 and was characterized by a build-up of black corrosion products in the areas immediately adjacent to the defect, surrounded by a ring of light rusting. It is interesting to note that the type I morphology was most frequently exhibited by ECRs removed from the concrete test slabs.

Knife adhesion measurements were made on most specimens after 14 days of air drying. A summary of these results is presented in Table H-9. It was observed that the extent of adhesion loss was greatest for specimens exposed to distilled water, with the exception of B and J specimens where adhesion loss was more pronounced for companion specimens tested in aqueous 3.5 w/o NaCl.

It appears as though accelerated testing on ECR containing initial defects is not capable of distinguishing between good and poor coatings per se. This was confirmed by monitoring the impedance behavior of ECRs containing defects over extended immersion times at 80°C. Subtle differences between specimens of a particular source were evident within 24 hours of immersion; however, beyond 24 hours all specimens, irrespective of source, tended to exhibit similar impedance responses. It was observed that in the presence of defects all specimens were equally susceptible to attack at the base of holidays and subsequent coating disbondment adjacent to these sites.

Adhesion Testing

Observations made during continuous ponding of concrete test slabs containing ECRs (*7*) and work of Sagues (*8*) suggest that either wet adhesion loss or cathodic disbondment (or both) are major contributors to ECR failure. Hence, the development of a technique to measure coating adhesion was a major part of

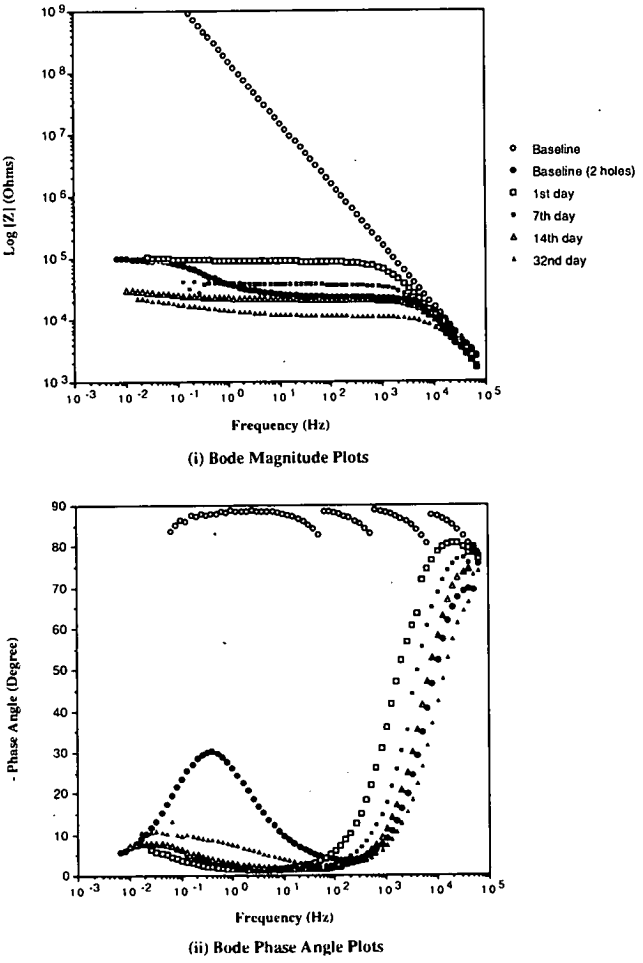

Figure H-12. (a) Bode plots for specimen A20 containing two artificial defects exposed to distilled water at 80°C.

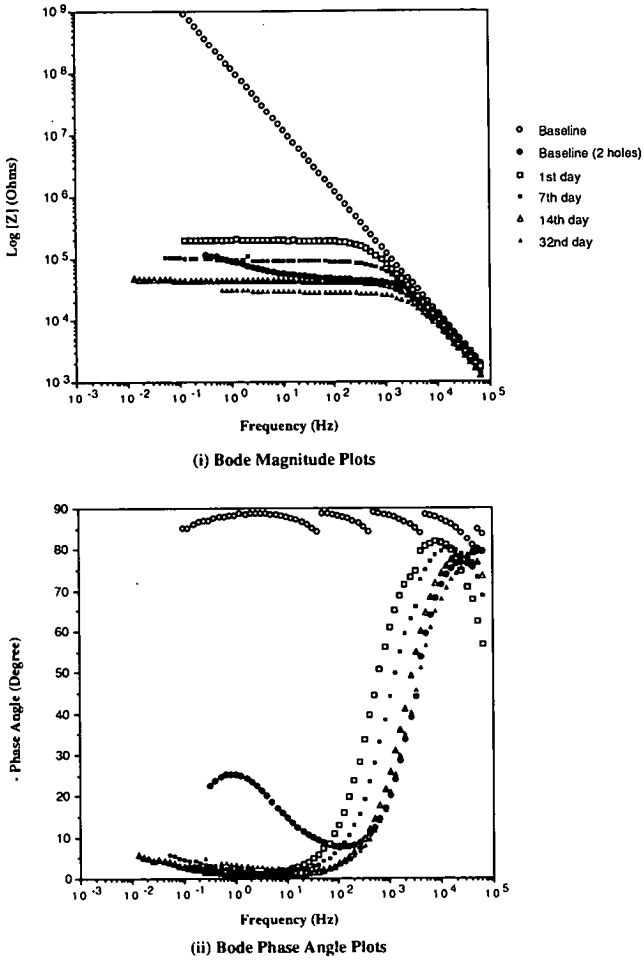

Figure H-12. (b) Bode plots for specimen D19 containing two artificial defects exposed to distilled water at 80°C.

this research effort. Although strong adhesion of a coating to a metal surface is not a prerequisite for good corrosion protection, in many situations a loss of adhesion leads to underfilm corrosion and makes the coating more susceptible to mechanical damage. A good coating has the ability to maintain its adhesion in the presence of defects and under various environmental exposure conditions; however, poor adhesion in the area of defects could ultimately lead to progressive underfilm corrosion. The ability to maintain adhesion in the presence of defects or under wet conditions should be an important factor in determining the durability of fusion bonded epoxy coatings. According to Funke (*9*), the most significant requirement for corrosion protection is good adhesion of the protective coating to the metal substrate; and because it is critical to maintain adhesion in the presence of water, a method to determine adhesion loss is important. The ability to maintain good adhesion in the presence of water is a function of the substrate, surface pretreatment, coating type, environment (including temperature), and to a lesser extent surface roughness (*10*).

Adhesion testing of virgin coatings resulted in either cohesive failure of the mounting adhesive or failure (adhesive) at the coating/adhesive interface. The load at which these failures occurred indicated that the initial adhesion of the coatings exceeded 9300 psi (62 MPa).

A generalized ranking for ECR specimens exposed to hot distilled water, irrespective of initial bar condition, according to adhesion (best to worst based on the average of the 1-, 14- and 21-day drying time values from Figure 10, Chapter 2) was T,C > U > B,D,J > A,E > F,N. Conversely, the ranking of ECR specimens according to results of EIS testing, again irrespective of bar condition, was B,U,N > D > F > A > J,E > T,C. Table H-10 compares the ECR rankings for the above, as well as for specimens removed from the concrete slab specimens after 10 months exposure. Thus, there is a general accord between the three tests (EIS, adhesion, and concrete slab exposure) but with some specific differences. Foremost is the high adhesion for the coating on the T and C source bars. Thus, the excessive defects present for T and C source specimens did not preclude good adhesion, at least in distilled water. Other factors contributing to differences are that adhesion varied with location on the specimen due to blisters and underfilm corrosion and that measurement area of a particular test was relatively small. However, the T-source bars performed poorly in the concrete slab exposure because of corrosion at and in association with coating defects.

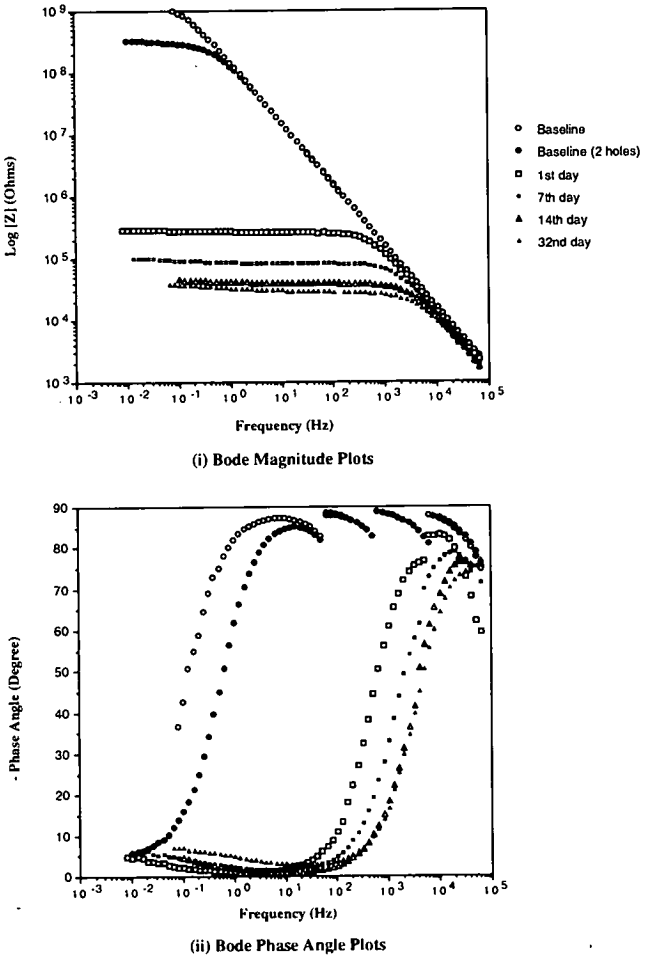

Figure H-13. (a) Bode plots for specimen B22 containing two artificial defects exposed to distilled water at 80°C.

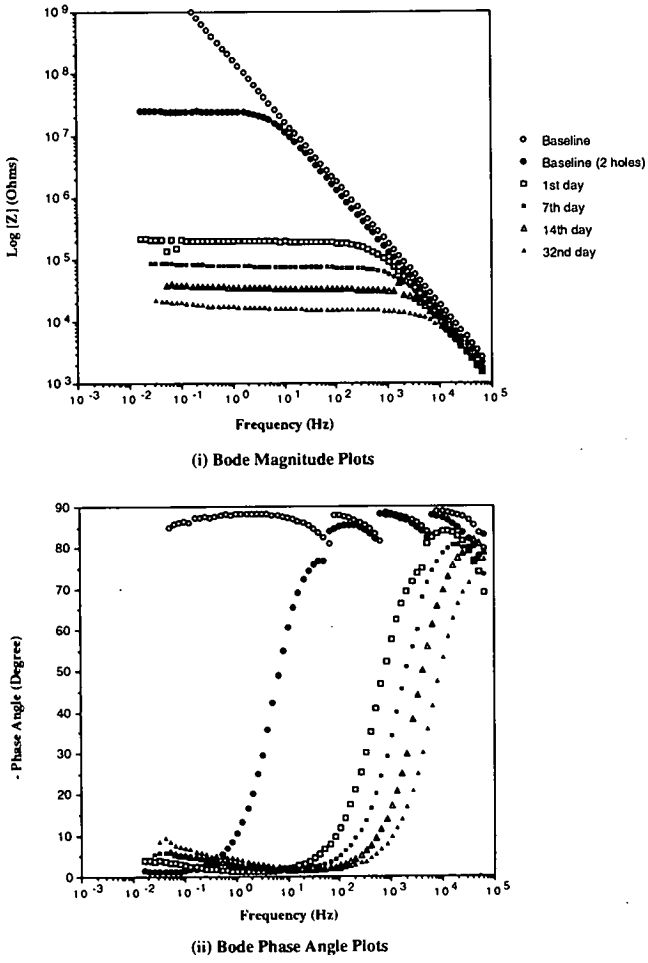

Figure H-13. (b) Bode plots for specimen F14 containing two artificial defects exposed to distilled water at 80°C.

Thus, while good wet adhesion is a desired ECR property, it is not sufficient, in and of itself, to ensure good performance when (excessive) defects are present.

As mentioned in the preceding section (Elevated Temperature Immersion), it was apparent from early EIS results on specimens containing natural defects and exposed to distilled water, where wet adhesion failures and blistering would be expected to be most severe due to high osmotic driving forces, that this environment might not be appropriate for accelerated testing. This was further supported by the fact that specimen types B, D, and U consistently gave the highest overall impedance values in distilled water but exhibited lower adhesion strengths than T and C source specimens, which had the poorest impedance responses in this environment. Conversely, it was observed that aqueous 3.5 w/o NaCl solution served as a better medium for distinguishing the difference between "good" ECR specimens and "poor" ECR specimens with regard to EIS. For example, after one day of drying, the highest adhesion values were obtained for sources B, D, and U (as was the case also for specimens containing no defects at the start of testing) and the lowest for C and T specimens, which proved to correlate better with EIS results (Figures H-6 and H-7). This observation suggests that hot water testing should be conducted in an aqueous chloride environment because chloride ions promote more underfilm attack compared to distilled water. These results, although still preliminary, indicate that the German hot water soak may not correlate well with ECR performance in more aggressive environments. In addition, for all specimens tested, little or no blistering of the epoxy coatings occurred during the 14 days of high temperature immersion. According to the German standard, these specimens would have passed the criterion of no blistering in 7–10 days of exposure to high temperature water; however, based on EIS and adhesion behavior poor performance would be anticipated for ECRs from several sources, for example, A, E and J.

A summary of adhesion test data after HWT and one day of drying for specimens containing no discernable initial defects is provided in Figure H-20. Adhesion values are reported for all sources with the exception of C and T sources which contained excessive holidays and were not included in this round of testing. It is apparent from Figure H-20 that distilled water was more effective than aqueous 3.5 w/o NaCl in promoting wet adhesion loss. This is consistent with the former electrolyte providing greater osmotic pressure and, hence, penetration of the coating compared to aqueous 3.5 w/o NaCl, as is generally recognized. A relative ranking of adhesion strength for defect-free specimens exposed to distilled water was U, B, D > J > A > E, F > N.

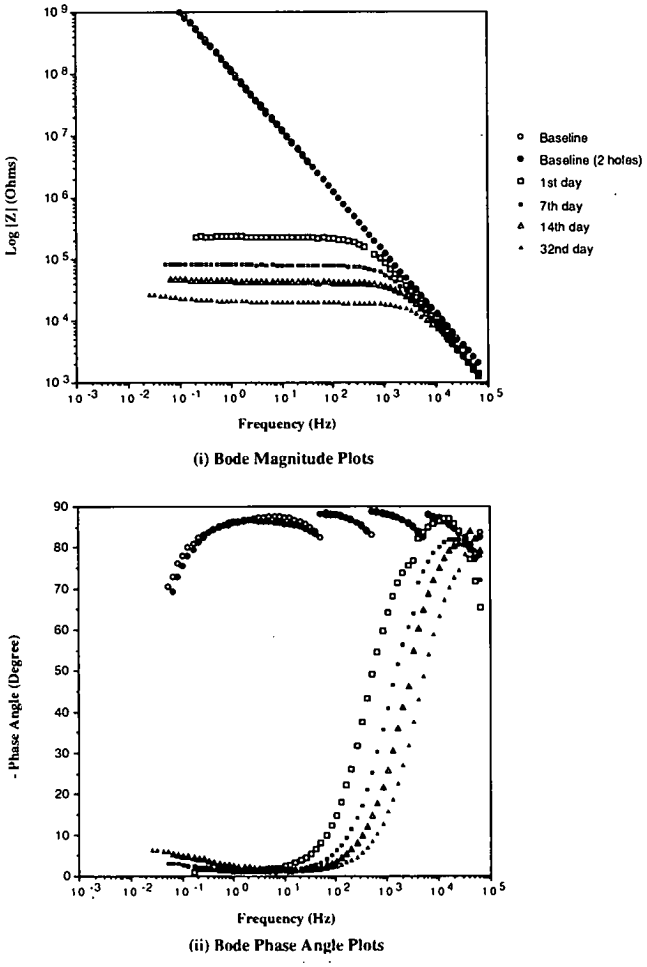

Figure H-14. Bode plots for specimen U20 containing two artificial defects exposed to distilled water at 80°C.

TABLE H-7. Coating pore resistance values for ECR specimens with intentional defects exposed to distilled water at 80°C

Specimen	# Time Constants Baseline	R_{po}, Ω·cm² Baseline	R_{po}, Ω·cm² 1 day	R_{po}, Ω·cm² 32 days
A20	2	1.4 X 10^{6}	6.6 X 10^{6}	6.6 X 10^{3}
B22	1	2.1 X 10^{10}	2.1 X 10^{7}	2.1 X 10^{6}
D19	2	3.1 X 10^{6}	1.3 X 10^{7}	2.1 X 10^{6}
F14	1	1.4 X 10^{9}	1.3 X 10^{7}	1.2 X 10^{6}
U20	1	> 6.6 X 10^{9}	1.6 X 10^{7}	1.2 X 10^{6}

This ranking did not correlate well, in general, with impedance results, where a ranking for this same environment was B, D, F, N, U > A > E, J. Thus, N specimens showed high impedance but the lowest adhesion; and J specimens exhibited low impedance but relatively high adhesion strength. Even though the J specimens used in this phase of testing contained no discernible defects initially, two of three specimens developed either detectable holidays or local rust spots during exposure. This behavior may reflect high susceptibility to coating breakdown in the presence of defects (holidays), which developed during elevated temperature exposure; however, occurrence of such defects did not necessarily compromise adhesion. The correlation between

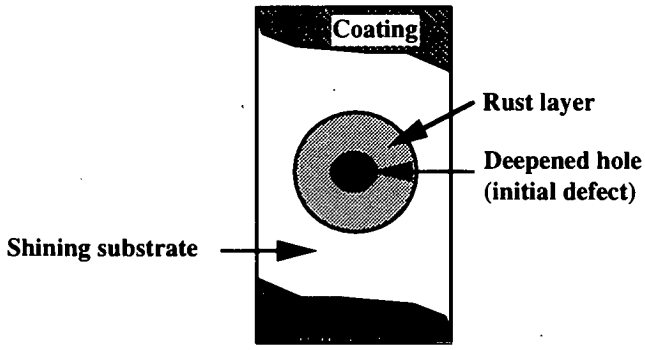

Figure H-15. Schematic of corrosion morphology near an artificial defect.

EIS response and adhesion was poor for specimens containing no detectable defects at the start of the test; however, it should be recognized that coatings possessing high impedance and exhibiting high wet adhesion strength offer the best probability of affording long-term protection. Loss of adhesion could set up conditions necessary for the development of a crevice-like environment that would eventually lead to severe underfilm attack, as has been observed in the examination of field failures (*11*). Therefore, a coating that resists adhesion loss, even in the presence of a defect, would intuitively be more resistant to underfilm corrosion.

In general, the coating/metal adhesion strength was observed to increase with extended drying time. A summary of the average adhesion strength for all sources, irrespective of initial bar condition, as a function of drying time is provided in Figures H-21 through H-23.

ATMOSPHERIC EXPOSURE

Two-Month Atmospheric Exposure

Four specimens in this category from each of the two exposure sites (marine and several km inland) were tested in distilled water and to aqueous 3.5 w/o NaCl at 80°C for 14 days. A summary of EIS data obtained during hot water testing for 2-month preweathered J and N specimens is given in Tables H-11 and H-12. Representative Bode (impedance) plots for selected bars are shown in Figures H-24 and H-25. Specimens FUCJ1, FCN1, BCJ1, and FCN2 (refer to Tables H-11 and H-12 for specimen designations) gave initially high impedance values (> 1 × 10^{8} Ohm · cm^{2} at 0.1 Hz), and after 14 days, the impedance values remained above 6.6 × 10^{7} Ohm · cm^{2}. These specimens showed no visible signs of deterioration. On the other hand, specimens FCJ1, FCN1, BUCN1, FCJ2, and FUCN2 showed visible signs of deterioration after HWT. In the latter case, baseline impedance values at 0.1 Hz ranged from 4 × 10^{7} to 1 × 10^{9} Ohm · cm^{2} but decreased to values below 1 × 10^{7} Ohm · cm^{2} during the first 24 hours of HWT; and by day 14 each of these specimens also showed the existence of a second time constant at low frequencies, which indicated that corrosion was occurring at the metal/coating interface. Three other specimens, FUCN1, BCN1, and FUCJ2, had intermediate behavior

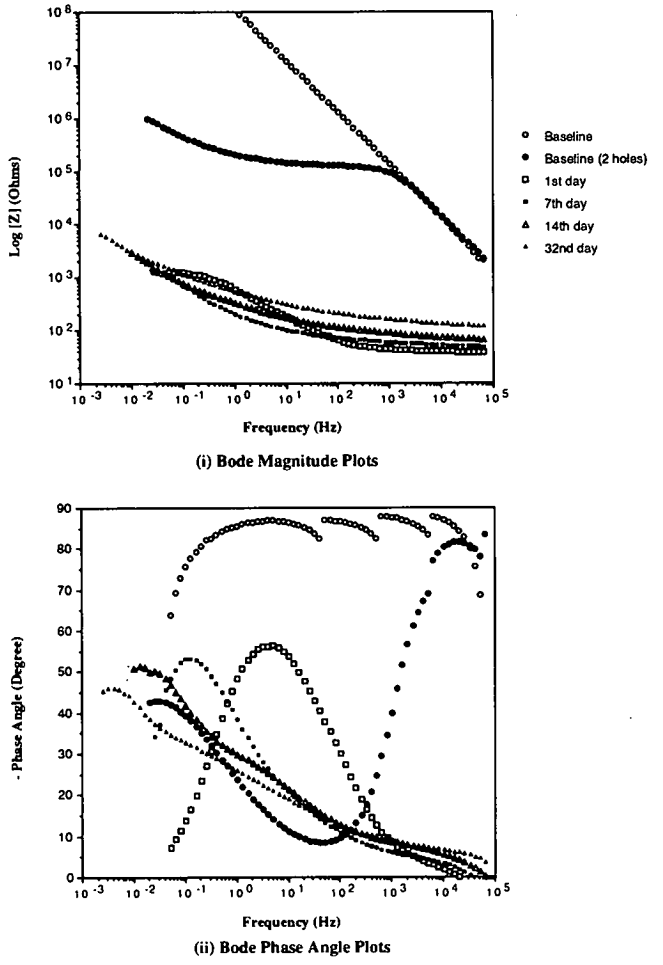

Figure H-16. (a) Bode plots for specimen A16 containing two artificial defects exposed to aqueous 3.5 w/o NaCl solution at 80°C.

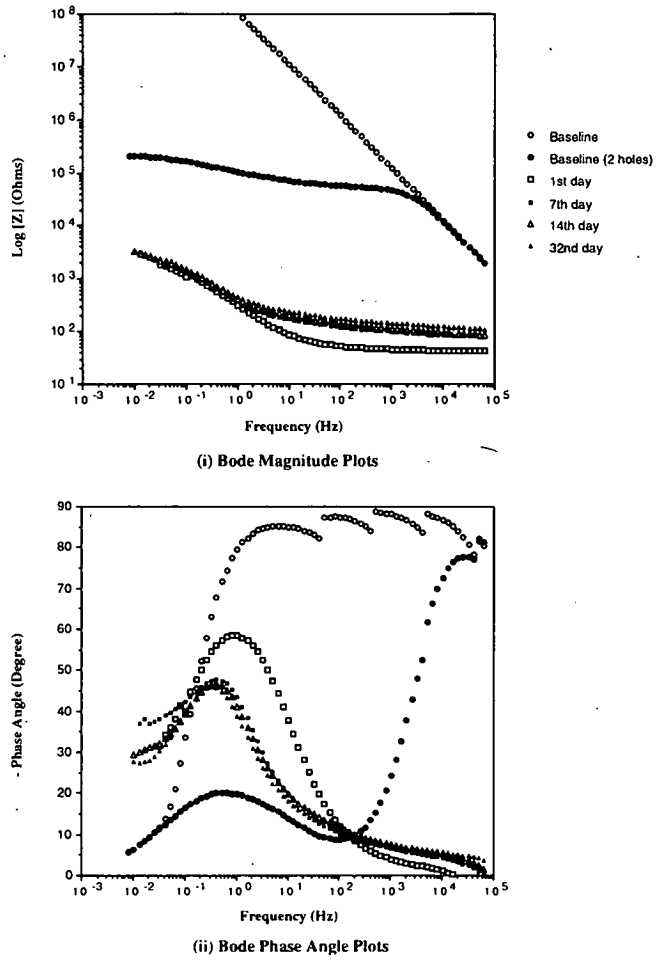

Figure H-16. (b) Bode plots for specimen B17 containing two artificial defects exposed to aqueous 3.5 w/o NaCl solution at 80°C.

in that each possessed initial high impedance values, i.e., > 10^9 Ohm · cm^2, and showed no visible signs of deterioration; however, after 14 days of high temperature immersion the impedance values of each specimen dropped below 10^7 Ohm · cm^2 and a second (low frequency) time constant developed. These results suggest that initially high impedance values did not ensure that good performance would be obtained during the 14 days of HWT exposure.

EIS measurements made during HWT were unable to clearly characterize ECR quality after 2 months of preweathering. This apparent lack of sensitivity could be related to an inability of EIS to detect wet adhesion loss or cathodic disbondment, particularly at early times of exposure. A summary of adhesion data for all bars exposed to either 80°C aqueous 3.5 w/o NaCl or distilled water is given in Figure H-26. Adhesion strength recovery was observed for 62.5 percent of the bars tested. In addition, adhesion strength was higher for J bars in comparison to N bars; for example, 87.5 percent and 75 percent of J bars showed higher adhesion strengths than N bars after drying times of 4 hours and 12 days, respectively. It appears that 2 months of atmospheric exposure—either covered or uncovered—did not adversely affect performance as characterized by adhesion strength and EIS testing. In addition, the marine exposure site was slightly more aggressive as indicated by lower adhesion strengths for ECRs exposed to this environment.

Four-Month Atmospheric Exposure

EIS scans on the 4-month preweathered specimens prior to hot water immersion revealed that eight specimens exhibited a second time constant, three exhibited one time constant, while only one specimen gave purely capacitive behavior. A summary of EIS data and a description of the visual appearance of the specimens are provided in Table H-13. Representative Bode (impedance) plots for selected bars are shown in Figures H-27 and H-28. From the available EIS data, it is obvious that the impedance magnitude decreased for all 4-month specimens during the 14-day test. In contrast to 2-month specimens, 4-month exposure to both environments resulted in no significant difference between the performance of J and N bars. Both specimen types show overall impedance values that were lower after 14 days of hot water immersion in comparison to 2-month preweathered specimens (compare Tables H-11 and H-12 for 2-

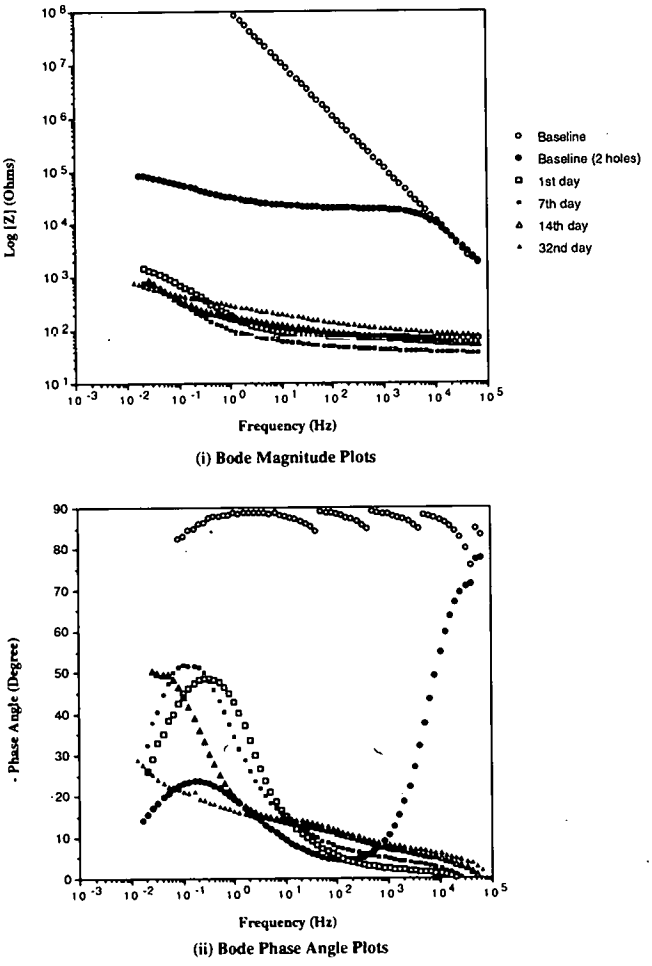

Figure H-17. (a) Bode plots for specimen D13 containing two artificial defects exposed to aqueous 3.5 w/o NaCl solution at 80°C.

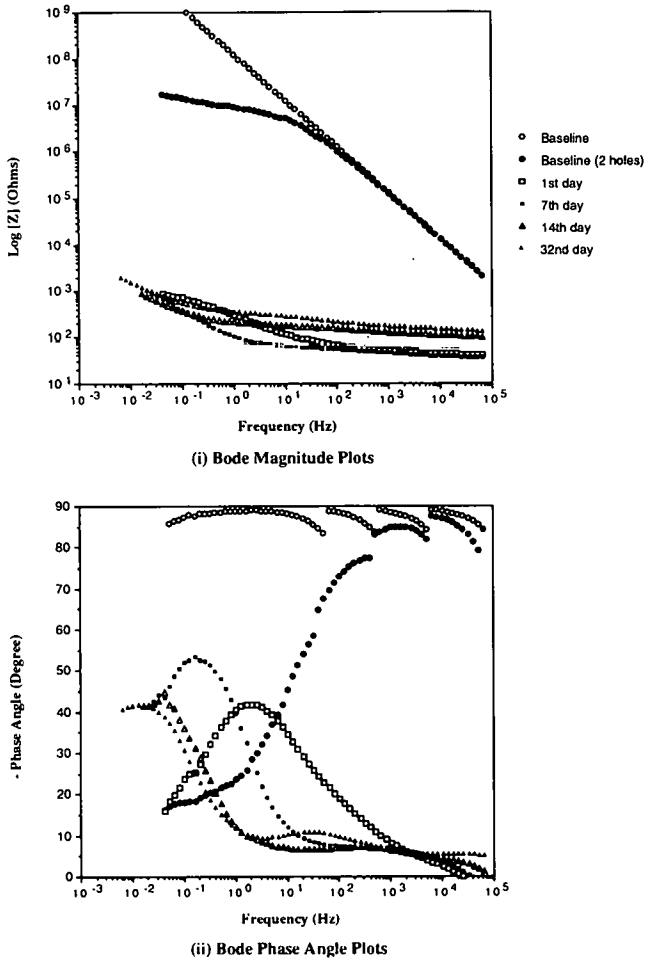

Figure H-17. (b) Bode plots for specimen F13 containing two artificial defects exposed to aqueous 3.5 w/o NaCl solution at 80°C.

month and Table H-13 for 4-month specimens) after identical EIS testing.

A summary of coating adhesion strength for 4-month specimens is provided in Figure H-29. It can be seen that J bars exhibited slightly better wet adhesion compared to N bars, which is similar to the trend described previously for 2-month specimens (Figure H-26). It appears that 4 months of preweathering eliminated any quality differences between the two sources as indicated by the nearly identical HWT impedance responses for the two sources. These impedance responses were lower than for non-weathered and 2-month preweathered specimens. A comparison between J and N bars exposed to 2 and 4 months of outdoor weathering was also made using EIS data obtained under ambient conditions in distilled water. A summary of the results is shown in Figure H-30, where mean impedance values at 0.1 Hz are used for comparison. From this figure, the 4-month exposure is shown to be more severe than the 2-month as indicated by lower impedance values of the former. Several of the 4-month preweathered specimens were examined after adhesion testing using a stereomicroscope, and it was found that the backside of the coating was contaminated and small amounts of coating residue and corrosion products covered the substrate surface.

EIS measurements were also made on concrete slabs containing both preweathered and non-weathered N- and J-source bars. These showed that 4 months of preweathering was detrimental as revealed by the lower impedance values for the former specimens. A comparison of initial macrocell current densities for the various sources embedded in salt-contaminated concrete is given in Figure H-31. The values plotted in this figure are the average of the average current density for all slabs of each of the four specific exposure (wet-dry cycle) types. From these data, it can be seen that 4-month preweathered N bar specimens had slightly lower macrocell current densities than the 4-month preweathered J bar ones. Conversely, J bars without preweathering had slightly lower macrocell current densities than N bars without preweathering. This provided further indications that extended preweathering eliminated any quality difference that might exist between ECR specimens from different sources (that is, those that were not preweathered).

From EIS, adhesion, and visual observations, it appears that ultraviolet radiation alone did not adversely affect performance;

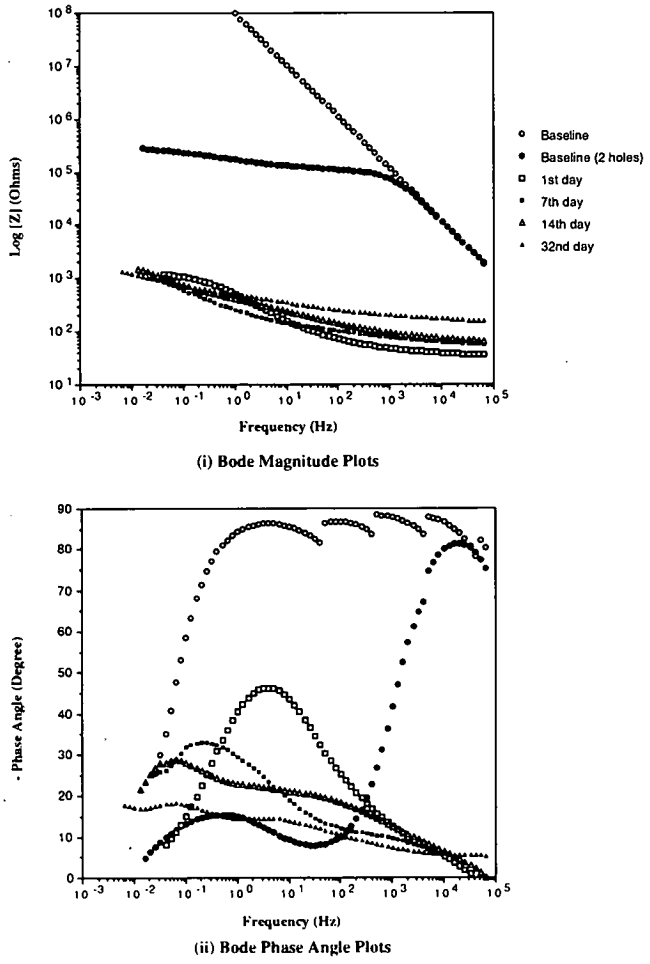

Figure H-18. Bode plots for specimen U18 containing two artificial defects exposed to aqueous 3.5 w/o NaCl solution at 80°C.

TABLE H-8. Coating pore resistance values for ECR specimens with intentional defects exposed to 3.5 w/o NaCl at 80°C

Specimen	# Time Constants Baseline	R_{po}, Ω·cm² Baseline	R_{po}, Ω·cm² 1 day	R_{po}, Ω·cm² 32 days
A16	2	1.0×10^7	3.3×10^5	1.0×10^4
B13	2	4.1×10^6	3.3×10^5	9.2×10^3
D13	2	1.4×10^6	3.7×10^5	6.6×10^3
F13	2	5.2×10^6	3.0×10^5	1.2×10^4
U18	2	6.6×10^4	2.5×10^5	1.2×10^4

for example, covered and uncovered specimens at both exposure sites exhibited nearly identical impedance responses. The reduction in impedance at 4 months was related more to the type of environment (inland versus marine) than to length of time exposed to ultraviolet radiation, at least within the limits of the present investigation. Based on EIS and adhesion data, it is predicted that J and N bars should perform similarly when exposed to salt contaminated concrete.

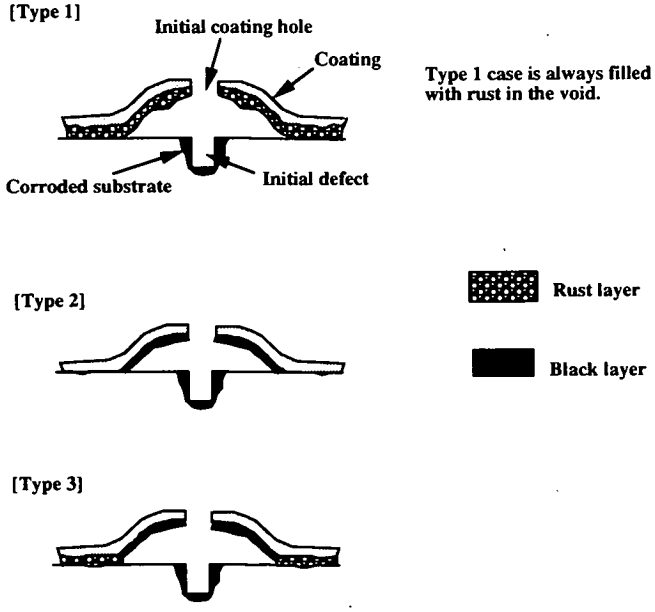

Figure H-19. Schematic of typical corrosion products found at artificial defects after hot water testing.

TABLE H-9. Qualitative summary of knife adhesion test results for ECR specimens containing defects and exposed to distilled water or 3.5 w/o NaCl for 32 days

Distilled Water	Degree of Disbondment	3.5 w/o NaCl
A20	>	A16
B22	<	B13
D19	>	D13
F14	≥	F13
N13	>	N22
J17	<	J12
U20	>	U18

ROOM TEMPERATURE IMMERSION IN AQUEOUS SOLUTIONS

Long-Term Exposure in Distilled Water

In this category of experiments, a J-source specimen was exposed to distilled water at room temperature for more than 500 days. EIS measurements were obtained at 0, 49, 100, 275, and 507 days. Bode plots are provided in Figure H-32. These scans show the existence of a second, low-frequency time constant by day 49, and it was visually apparent that a local rust spot had developed by day 100. Although initial screening of this specimen revealed no holidays, progressive breakdown of the coating had in any event occurred, even in the absence of added chlorides in the bulk solution. In comparison, a second time constant appeared within 24 hours for an initially defect-free J specimen exposed to aqueous 3.5 w/o NaCl in the accelerated test (80° C) but did not appear during the 14-day test when distilled water was used.

Aqueous Chemical Immersion

In this category of testing, ambient temperature exposures were performed on bars from the various sources in different

TABLE H-10. Comparison of ECR rankings according to bar source for impedance and adhesion tests and performance in concrete slabs

Ranking*	[Z] at 0.1 Hz after one day in DW HWT+	Adhesion after 14-day DW HWT+			Adhesion of Autopsied ECR
		1 day dried	14 days dried	21 days dried	
1	B, U, N	T	C, T	C	U
2		C, U		T	D
3			U	U	A
4	D	D	J	D, A, N	N
5	F	B	D		J (UV)
6	A	J	B, E		T
7	J	A, E, F		B	B, C, E, F data N/A
8	E		A, E	J	
9	C, T			E, F data N/A	
10		N	N		

* 1 best, 10 worst.

+ DW: distilled water

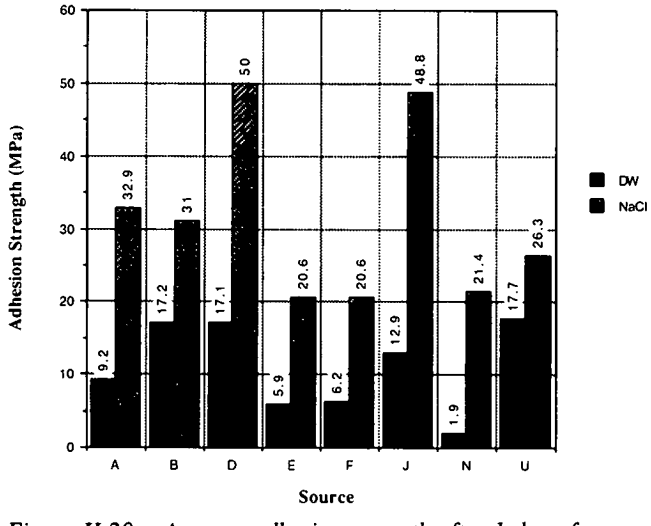

Figure H-20. Average adhesion strength after 1 day of drying for defect-free ECR specimens previously exposed for 14 days to either DW or aqueous 3.5 w/o NaCl solution to 80°C.

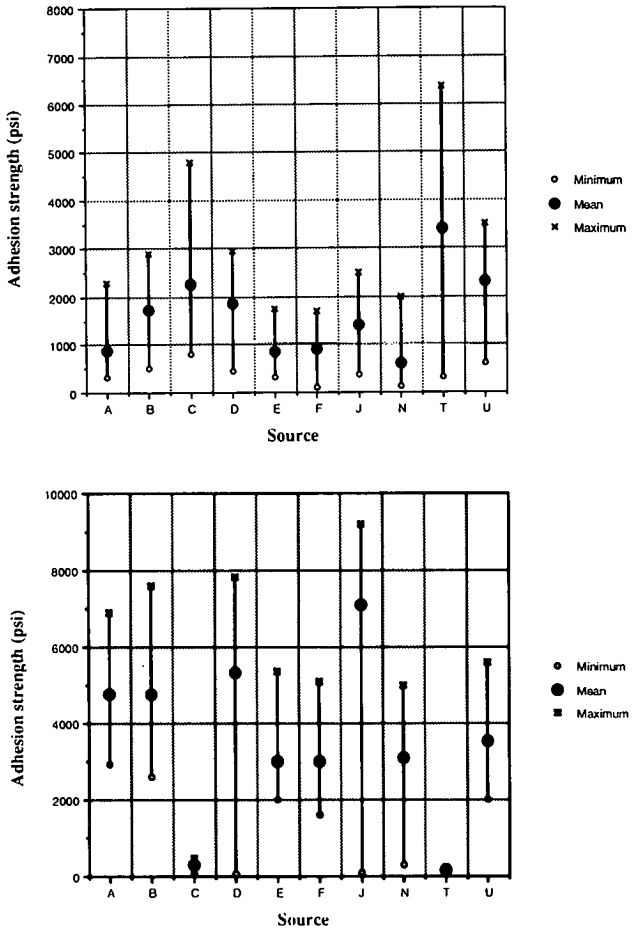

Figure H-21. (a) Adhesion strength after one day of drying for ECR specimens previously exposed to distilled water for 14 days at 80°C. (b) Adhesion strength after 1 day of drying for ECR specimens previously exposed to aqueous 3.5 w/o NaCl solution for 14 days at 80°C.

electrolytes, including distilled water (DW), aqueous 3.5 w/o NaCl (NaCl), synthetic pore water solution without chlorides (SP), and, last, synthetic pore water solution with 3.44 w/o KCl (SP/Cl). Coating quality was characterized initially and during exposure by EIS scans and by visual observations.

In general, three types of EIS response were observed for these specimens: (1) impedance remained unchanged (Figure H-33); (2) development of finite coating pore resistance from initially capacitive behavior (Figure H-34); and (3) development of a second time constant at low frequencies (Figure H-35). The development of a second time constant was consistent with occurrence of holidays or the appearance of localized rust spots. These responses were essentially the same as observed for ECR specimens exposed to the elevated temperature test environments; however, in the latter case, less than 24 hours was required, compared to 2 months or longer at ambient temperature for a significant impedance decrease. This correlation was noted only when capacitive behavior was observed prior to exposure testing, since no correlation was apparent between high and ambient temperature results when bare areas or holidays were initially present. However, it is the former case (no holidays or defects) that is important with regard to performance evaluation of coatings per se. For the case of ECR with no initially detectable defects, 1 day of hot water exposure was equivalent to 60–120 days at ambient temperature; and the EIS response or each was consistent with a common factor (progressive reduction

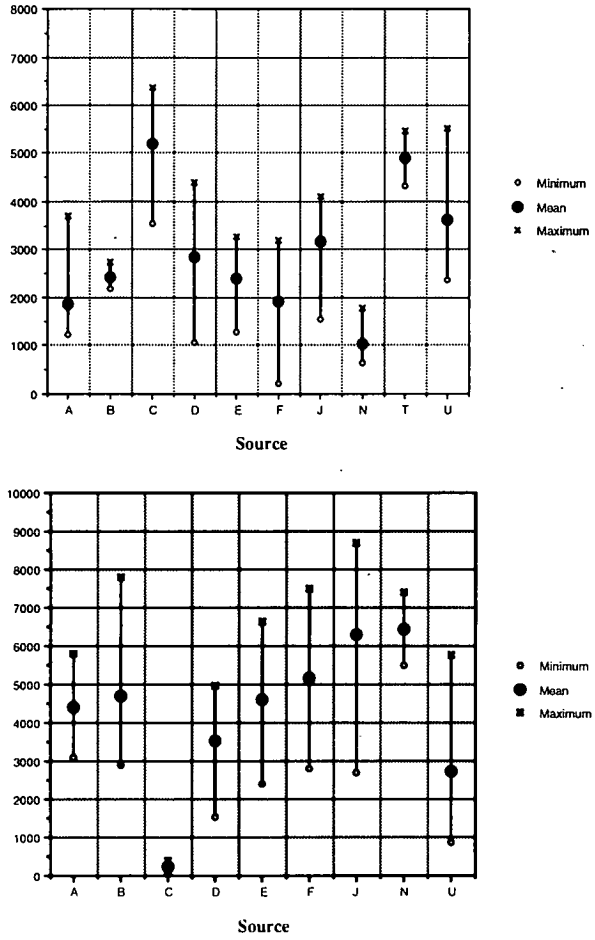

Figure H-22. (a) Adhesion strength after 14 days of drying for ECR specimens previously exposed to distilled water at 14 days at 80°C. (b) Adhesion strength after 14 days of drying for ECR specimens previously exposed to aqueous 3.5 w/o NaCl solution for 14 days at 80°C.

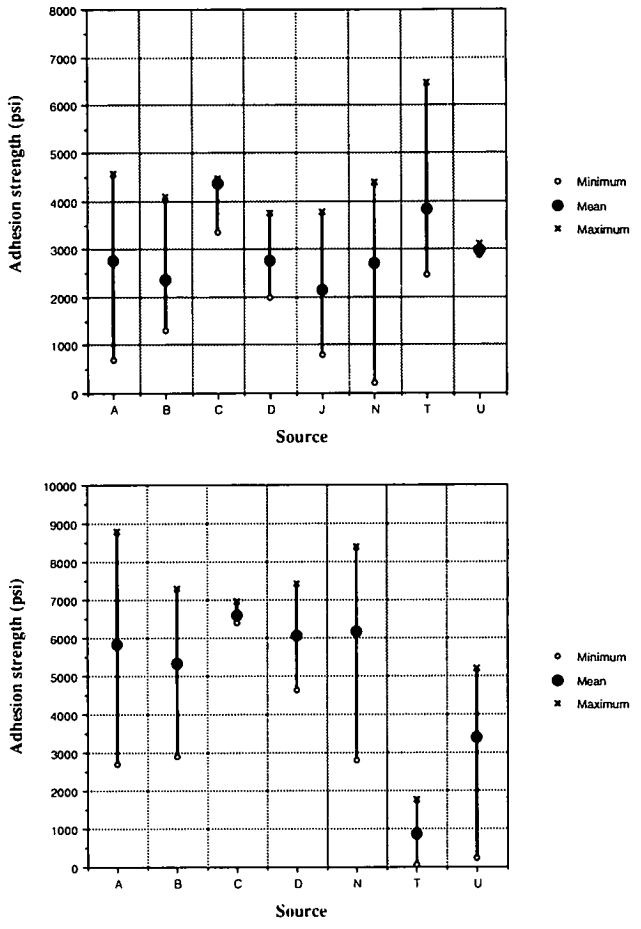

Figure H-23. (a) Adhesion strength after 21 days of drying for ECR specimens previously exposed to distilled water for 14 days at 80°C. (b) Adhesion strength after 21 days of drying for ECR specimens previously exposed to aqueous 3.5 w/o NaCl solution for 14 days at 80°C.

in pore resistance) being responsible for the impedance drop with time.

Figures H-36 through H-39 summarize results of the EIS scans for these various exposures as plots of initial (baseline) impedance versus the impedance at either 3 or 6 months for each of the above four electrolytes (both at 0.1 Hz). All baseline scans were performed either in tapwater (TW) or DW. Scans acquired during the exposures were either in TW or the particular exposure electrolyte (DW, NaCl, SP, or SP/Cl). This rather complex approach evolved as a consequence of determining that EIS scans in DW were not always as revealing as desired and were sometimes accompanied by experimental difficulties. The observation that the scan was electrolyte dependent also influenced the protocol that was ultimately adopted. No attempt was made in specimen selection and preparation to exclude ECR specimens that contained coating defects initially. Purely capacitive behavior upon initial exposure, which is indicative of an absence of conductive coating pathways and of defects, corresponded to an initial impedance (horizontal scale) near 10^9 Ohms (6.6×10^{10} Ohms · cm^2) as noted previously. According to this representation, the position of a particular 3- or 6-month datum point relative to the horizontal scale defined the initial impedance for a particular experiment. Thus, for cases where no impedance decrease occurred during the exposure, the data fell along the 45° slope line. Alternately, the further below this line a particular datum point is positioned, the greater the impedance

TABLE H-11. Summary of total impedance @ 0.1 Hz for 2-month preweathered specimens exposed to distilled water at 80°C

Specimen	Initial |Z| Ω·cm²	|Z| - Day 1 Ω·cm²	|Z| - Day 14 Ω·cm²	# Time Constants	# Rust/ Blister Sites
FUCJ1	6.6×10^{10}	N/A	1.3×10^{8}	1	–
FCJ1	1.3×10^{9}	5.9×10^{6}	3.3×10^{6}	2	4/0
FUCN1	3.3×10^{10}	N/A	3.9×10^{7}	2	–
FCN1	1.3×10^{8}	7.3×10^{6}	1.3×10^{6}	2	2/0
BUCJ1	1.3×10^{9}	N/A	6.6×10^{7}	1	–
BCJ1	5.9×10^{10}	N/A	1.9×10^{8}	1	–
BUCN1	3.9×10^{7}	3.2×10^{7}	2.6×10^{7}	2	2/0
BCN1	6.6×10^{10}	N/A	2.6×10^{7}	2	–

NOTE: FUC - FAU test yard uncovered; FC - FAU test yard covered; BUC - beach test site uncovered; BC - beach test site covered; N/A - not available because impedance response remained capacitive below 0.1 Hz.

TABLE H-12. Summary of total impedance @ 0.1 Hz for 2-month preweathered specimens exposed to 3.5 w/o NaCl at 80°C

Specimen	Initial |Z| Ω·cm²	|Z| - Day 1 Ω·cm²	|Z| - Day 14 Ω·cm²	# Time Constants	# Rust/ Blister Sites
FUCJ2	5.9 X 10^{10}	1.5 X 10^{7}	6.6 X 10^{7}	2	--
FCJ2	6.6 X 10^{7}	1.9 X 10^{5}	6.6 X 10^{4}	2	3/8
FUCN2	N/A	3.0 X 10^{5}	1.3 X 10^{5}	2	2/0
FCN2	6.6 X 10^{10}	N/A	N/A	1	--

NOTE: FUC - FAU test yard uncovered; FC - FAU test yard covered; BUC - beach test site uncovered; BC - beach test site covered; N/A - not available because impedance response remained capacitive below 0.1 Hz.

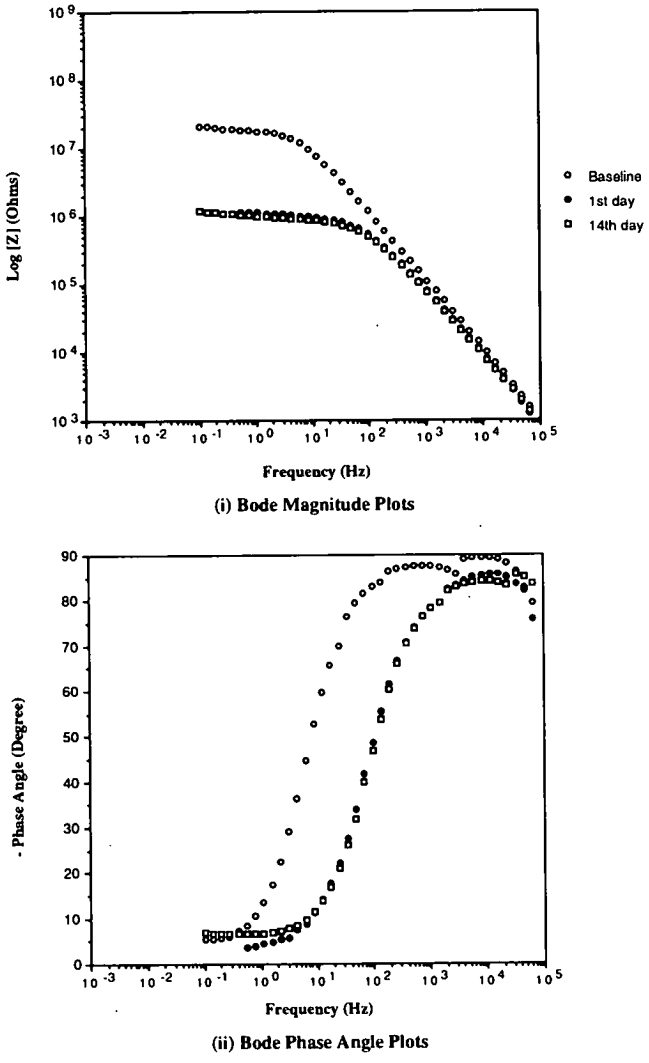

(i) Bode Magnitude Plots

(ii) Bode Phase Angle Plots

Figure H-24. (a) Bode plots for specimen BUCJ1 preweathered (uncovered) at the marine site for 2 months and tested in distilled water at 80°C.

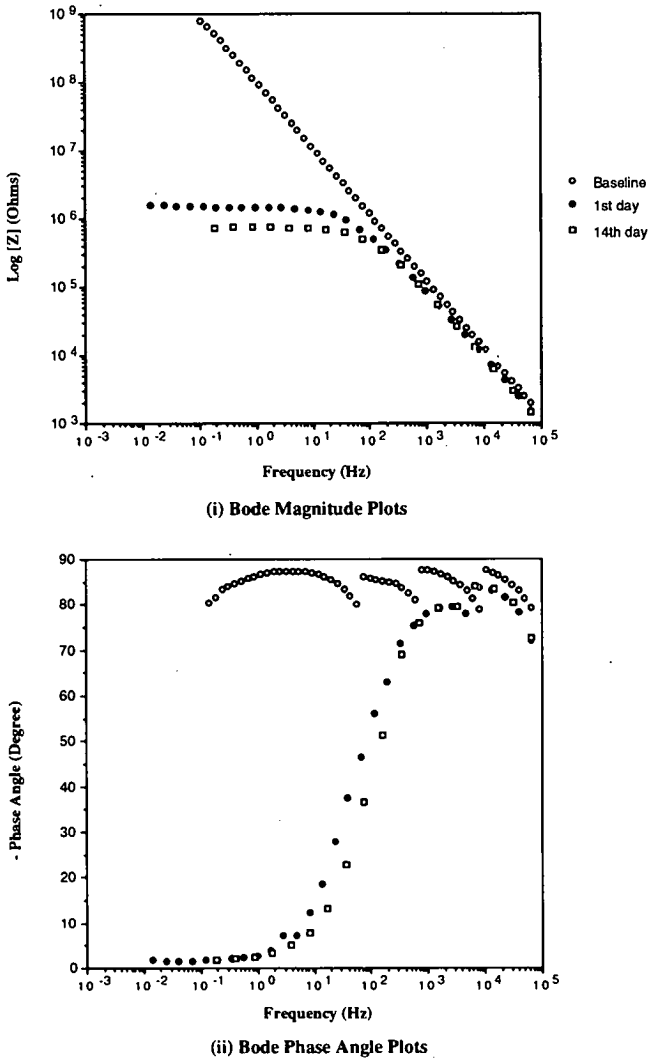

(i) Bode Magnitude Plots

(ii) Bode Phase Angle Plots

Figure H-24. (b) Bode plots for specimen BUCJ2 preweathered (uncovered) at the marine site for two months and tested in aqueous 3.5 w/o NaCl solution at 80°C.

decrease during the exposure; and the less likely it is the particular coating would provide long-term corrosion protection. Data points corresponding to relatively low values of baseline impedance contained initial defects. Also, the lower limit of performance is defined by the line of the lesser slope. The fact that this converged toward and intersected the 45° slope line indicates that the lower the baseline impedance the less the impedance decrease during the exposure. This does not necessarily mean that extensive, further coating deterioration did not occur, since impedance for such a specimen may have been dominated by that of the defect or bare area that was already present. This observation is consistent with the earlier projection that EIS scan changes with exposure duration may be of limited utility in assessing the quality of the coating per se for such bars, although the technique does, of course, reveal the presence of defects or of a highly conductive coating. In some cases, both 3- and 6-month data are presented for the same test, as indicated where data points for these two exposure times are positioned vertically with respect to one another. In other instances, data are present for only one of these times.

Caution must be exercised in projecting any influence of the electrolyte on EIS scan results in these CITs, since individual specimen-to-specimen variations could also have been a factor. Table H-14 summarizes the impedance data for each of the

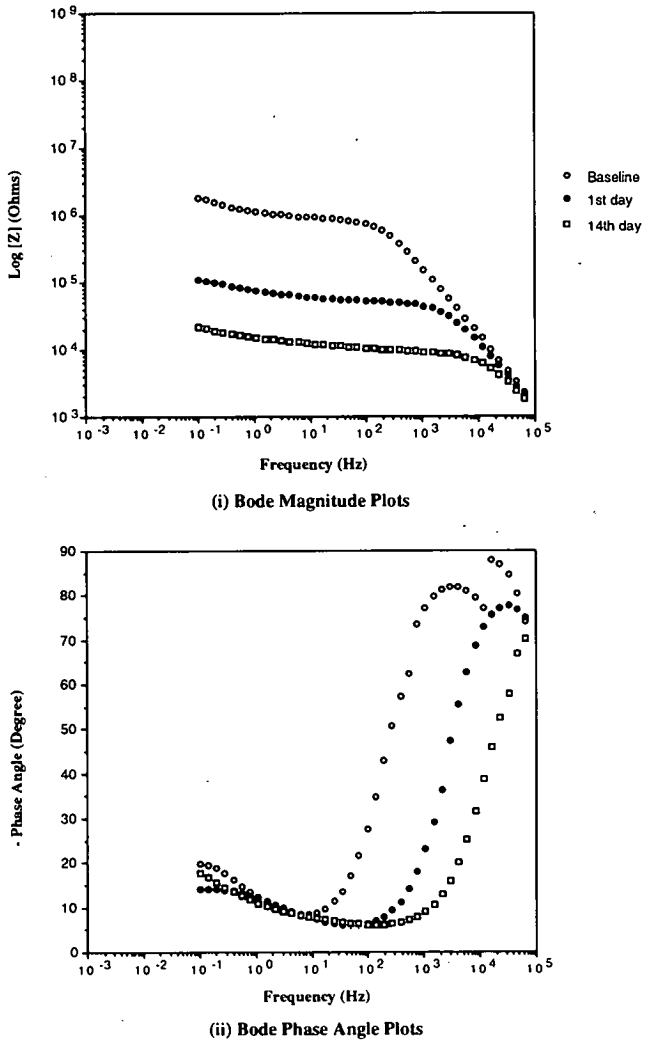

Figure H-25. (a) Bode plots for specimen FCN1 preweathered (covered) at inland site for 2 months and tested in distilled water at 80°C.

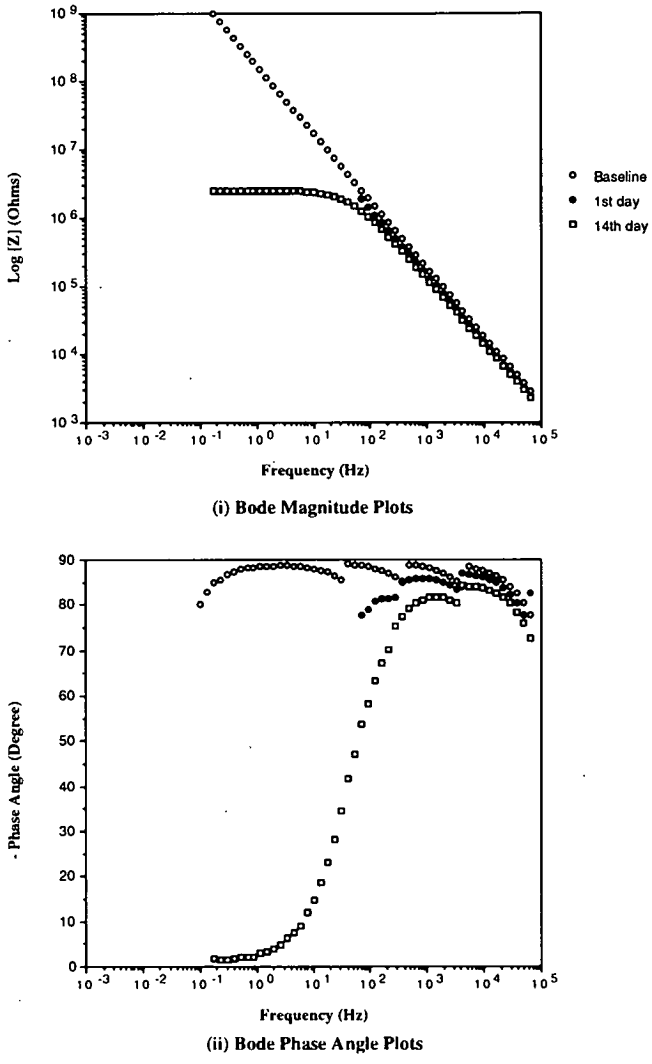

Figure H-25. (b) Bode plots for specimen FCN2 preweathered (covered) at inland site for 2 months and tested in aqueous 3.5 w/o NaCl solution at 80°C.

electrolytes according to, first, the fraction of specimens with initial impedance less than 10^8 Ohms (indicative either of conductive pathways or defects or both), second, the fraction exhibiting initially capacitive or near-capacitive behavior and, last, the fraction in the preceding category for which the impedance after either 3 or 6 months remained above 10^8 Ohms. For each of the electrolytes, approximately one-third of the specimens fell into the first category indicating, at best, less than ideal corrosion protection by the coating initially. This fraction should increase in proportion to ECR specimen surface area because of the enhanced probability of encountering a defect in a large specimen compared to a small. However, the fraction of specimens exhibiting initially capacitive or near-capacitive behavior was greater in DW (0.53) and NaCl (0.67) than for SP or SP/Cl (0.38 and 0.44, respectively), possibly indicating an influence of electrolyte upon impedance.[4] The same conclusion applied to the fraction of specimens with high final impedance (0.32 and 0.39, respectively, for the former environments and 0.17 and 0.06 for the latter). Thus, the synthetic pore water was more aggressive than the near neutral solutions, consistent with the generally recognized detrimental affect of OH^- on integrity of the coating-metal bond (*6,12*). Relatedly, the SP electrolyte with chlorides (SP/Cl) compromised purely capacitive behavior to the greatest extent in association with the influence of chlorides upon corrosion of steel. Because the latter two environments reflect conditions within concrete to a greater extent than the former two, it is appropriate that CIT and related tests employ SP type solutions; and this contributed to the decision to employ such an electrolyte for the ACT part of this program.

To further evaluate the influence of electrolyte composition, EIS scans during the course of the various exposures were performed in TW as well as the specific exposure electrolyte. A solution influence was particularly apparent for specimens exhibiting low impedance, as illustrated by the experiment depicted in Figure H-40. Here the initial EIS scan for one ECR specimen

[4] This projection is complicated by the fact that some of these specimens were inherently capacitive initially, whereas for others holidays were patched such that capacitive behavior resulted.

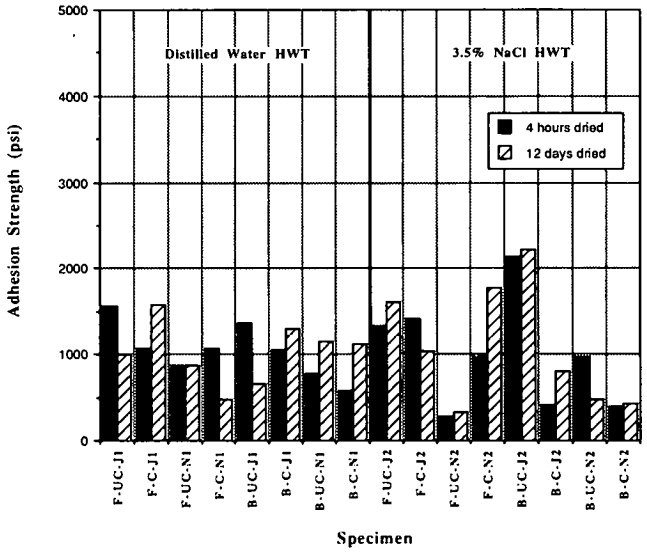

Figure H-26. Average adhesion strengths of 2-month preweathered specimens after hot water testing.

showed purely capacitive behavior in both TW and SP. Three 1 mm^2 defects were then introduced into the coating. Subsequent scans were performed sequentially after brief periods (less than 30 mins) in TW and SP, 100 hours in SP and, finally, after 2 hours in TW. The data in Figure H-40 indicate that some information regarding coating capacitance and pore resistance was discernable at frequencies above 1 kHz when the EIS scan was in TW; however, in the SP environment only information about the defect (presumably at its base) was revealed. This dependence of EIS response on the nature of the test electrolyte was observed only for ECR specimens with defects. Additional experiments are required to further examine this behavior.

ACCELERATED CORROSION TESTING

Results of Preliminary Testing

As expected, the magnitude of currents across anode and cathode ECRs was related to the degree of coating damage (that is, initial impedance of the ECRs), especially the anodic one. The impedance of the cathode was low due to the presence of the artificial defect. Figures H-41a and H-42a present baseline impedance data for two illustrative anode specimens (A15 and B14), where initial impedance for the former was high relative to that for the latter. Current during the ACT was noted to be correspondingly lower for A15 than for B14. Visual inspection after 14 days of ACT revealed that the condition of B14 was much worse than that of A15 (Figure H-43). This was reflected in EIS scanning after the test where A15 maintained a higher impedance than B14 as shown in Figures H-41b and H-42b. The size of delaminated areas on the companion cathodes was related to the magnitude of current as well. Coating disbondment around the 0.25 in. (6.3 mm) hole was more significant with B source ECR (B16) than the A source bar (A18). Plots of current against time for A- and B-source specimens used in ACT are shown in Figure H-44.

T-source specimens, which had the highest density of coating damage in the as-received condition, performed poorly in the ACT as reflected by high currents. Both T-source specimen anodes (T15 and T17, respectively) developed a number of localized rust spots in accordance with the density of coating defects. On the other hand, delaminated areas on the companion cathodes (T16 and T18) differed in that coating disbondment on T16 (paired with T15) was much more significant than that exhibited by T18 (Figure H-45). The current against time plots for both anode-cathode sets are given in Figure H-44.

Results for ECRs Containing Intentional Defects

After running four sets of preliminary ACTs, it was decided that, instead of employing ECRs in the as-received condition, it would be better to conduct these tests using specimens with the same initial condition. This followed from the realization that it was difficult to compare the performance of ECRs from the 10 sources with different initial number and size of defects. Therefore, subsequent experiments involved using ECRs with the same initial condition. This was accomplished by introducing two small artificial defects into both the anode and cathode. All other detectable defects were patched prior to the ACT using a two-part epoxy resin. A summary of results from this round of ACT is shown in Figure H-46 as a plot of current versus time for specimens from each source, except for A, B, and T sources, which were tested only in the preliminary portion of ACT. In addition, C-source specimens were not included in this round of ACT because these bars contained excessive coating cracks at the base of deformations, as noted previously.

There seemed to be no definitive relationship between the magnitude of current and the degree of delamination. Thus, ECRs exhibiting the highest currents were not necessarily the ones with the largest degree of disbondment. Source F specimens suffered the most extensive delamination, but this was not apparent from the current measurements. On the other hand, E-source specimens exhibited less delamination compared to D-source ECRs even though the currents associated with E-source bars were higher than D ones. The order of delamination (large to small) at the cathode was F > N > D > J > E > U. For the anode this was F > J > N > E > D > U. Note that this does not agree with the rankings of sources based upon the EIS *or* adhesion measurements or with ECR performance in the salt contaminated concrete slabs.

CONCRETE SLAB TESTS

Figures H-47 through H-49 present plots of macrocell current as a function of ECR corrosion potential (uncoupled from the bottom mat black bars) after 10 months ponding according to three of the wet-dry cycles. These indicate that the coating on the ECRs that had experienced prior atmospheric exposure for 4 months (legend designation "UV") was the least protective (high current and relatively active corrosion potential); however, some non-atmospherically exposed bars as well were corroding. In this regard, examples are apparent where the macrocell current for T-source specimens was within one order-of-magnitude of that for the bare bars. It is anticipated that with continued exposure corrosion potentials for bars, which had initial defects and

TABLE H-13. Magnitude of total impedance @ 0.1 Hz and visual observations for 4-month preweathered ECRs exposed to 14 days of hot water immersion.

4 Month UV Specimens												
	HWT Specimen in DW						HWT Specimen in 3.5% NaCl					
	4BUCN1	4BUCJ2	4FUCJ2	4BCJ2	4FCN1	4FUCN2	4BCJ1	4FUCN1	4BUCN2	4BUCJ1	4FUCJ1	4FCN2
Initial |Z| $\Omega \cdot cm^2$	$4.2x10^8$	$4.2x10^9$	$1.3x10^9$	$5.2x10^8$	$4.2x10^8$	$2.1x10^8$	$1.0x10^9$	$2.1x10^9$	$2.6x10^8$	$4.2x10^{10}$	$4.2x10^9$	$1.3x10^9$
|Z|-Day 1 $\Omega \cdot cm^2$	$4.4x10^7$	$2.0x10^7$	$5.7x10^7$	$7.3x10^7$	$9.2x10^7$	N/A	N/A	$7.9x10^5$	$3.8x10^5$	$2.7x10^7$	$5.7x10^5$	N/A
|Z|-Day 14 $\Omega \cdot cm^2$	$6.6x10^6$	$2.6x10^6$	$8.3x10^5$	$5.2x10^6$	$4.1x10^7$	$4.1x10^7$	$1.0x10^5$	$1.6x10^6$ (10th day)	$2.1x10^5$	$4.2x10^6$	$1.0x10^5$	$2.6x10^5$
# Time Constants	1	1	2	1	1	1	2	-	3	1	2	2
# Rust/ Blister Sites	0/0	0/0	0/0	0/0	0/0	0/0	1/0	0/0	2/0	0/0	1/10	1/0
# T.C. before HWT	2	1	2	1	2	2	2	2	2	1	1	2

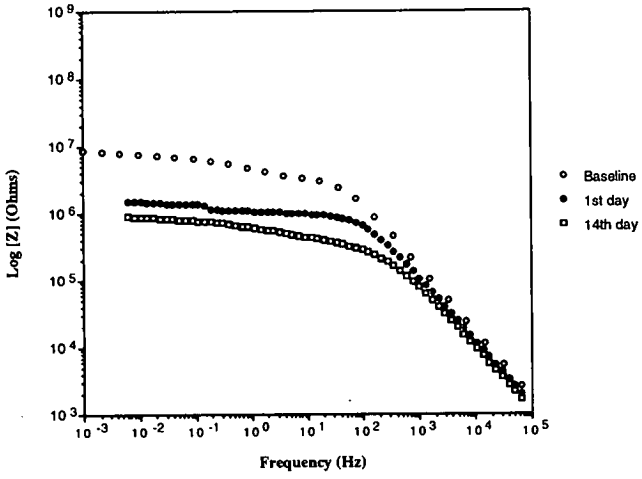

(i) Bode Magnitude Plots

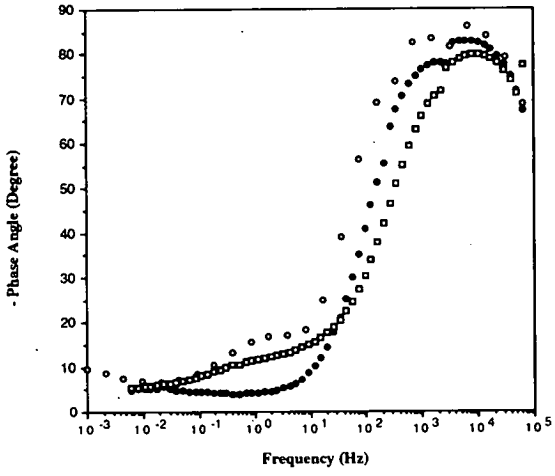

(ii) Bode Phase Angle Plots

Figure H-27. (a) Bode plots for specimen 4FCN1 preweathered (covered) at inland site for 4 months and tested in distilled water at 80°C.

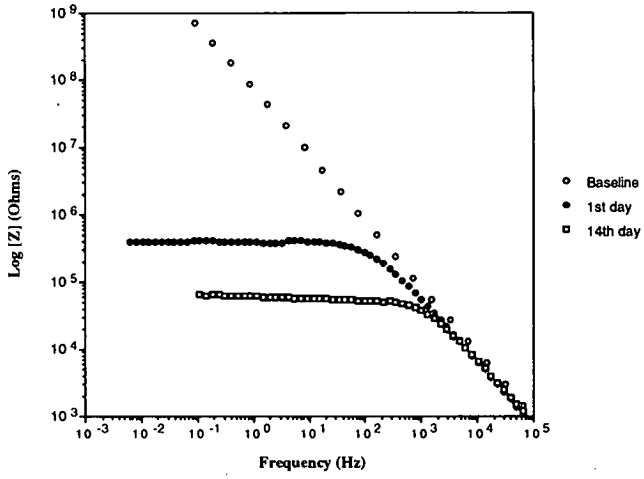

(i) Bode Magnitude Plots

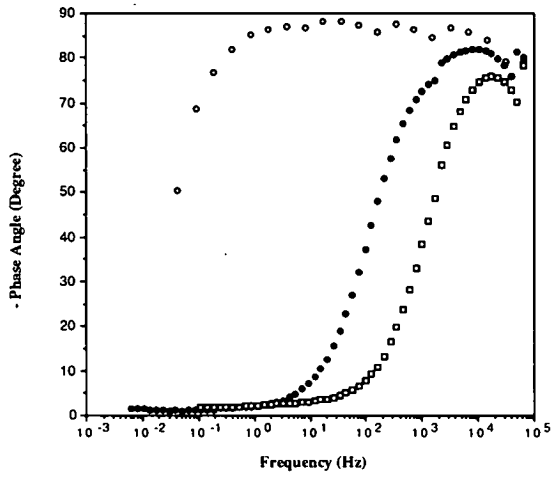

(ii) Bode Phase Angle Plots

Figure H-27. (b) Bode plots for specimen 4BUCJ1 preweathered (uncovered) at marine site for 4 months and tested in aqueous 3.5 w/o NaCl solution at 80°C.

which develop defects will progressively become more negative and that current for these will increase; however, it must be recognized that this current is the macrocell current between the ECR and bare bars only and not what develops from underfilm microcells. Alternately, other ECR specimens maintained relatively positive potentials and low macrocell current for the exposure duration to-date. This is exemplified by data points at the left axis for which no coating defects or macrocell current were detected. These were arbitrarily assigned a current of 0.0001 μA so that they could be represented on the semilogrithmic plots.

Correspondingly, Figures H-50 through H-52 present the same data as in Figures H-47 through H-49 but with macrocell current normalized (current divided by percentage of coating area that was damaged) according to the measured coating defect area prior to manufacturing the concrete specimens. By this representation the normalized (localized) ECR current for some bars approached and even exceeded that of the bare bars. However, the bare bar data as reported here have not been normalized. If this were done, then these data points would be displaced to the left by two orders of magnitude. Not accounted for in this representation is the probability that additional defects developed with time in some cases (as observed in HWT and CITs) which would lower the normalized current value. Alternately, underfilm corrosion at defect sites was discussed in Chapter 2 as an important facet of ECR corrosion failure; and it is entirely possible that microcell and well as macrocell action was concurring here.

While the data in Figures H-47 through H-52 appear to indicate an influence of the wet-dry cycle that was employed for these exposures, close examination experiments (one ponding cycle) but not another. For example, a number of J- and N-source atmospherically exposed bars were used in the D ponding exposure and exhibited active potentials and high macrocell currents; but no such specimens were present in the B exposure slabs. It is concluded that to-date no influence of the type of wet-dry cycle employed is apparent.

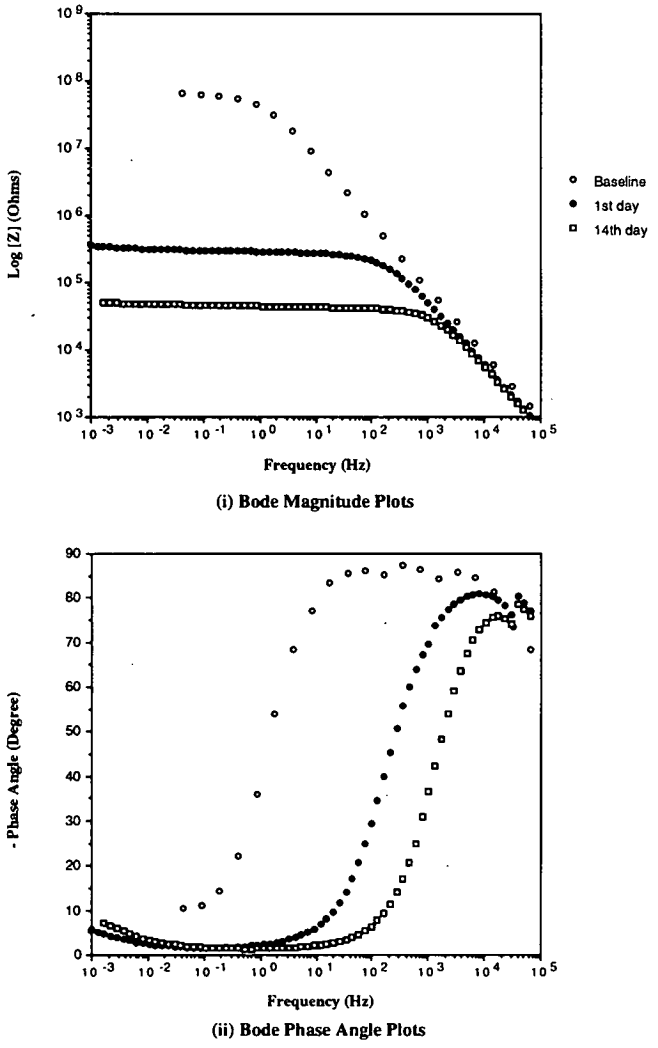

Figure H-28. (a) Bode plots for specimen 4BUCJ2 preweathered (uncovered) at marine site for 4 months and tested in distilled water at 80°C.

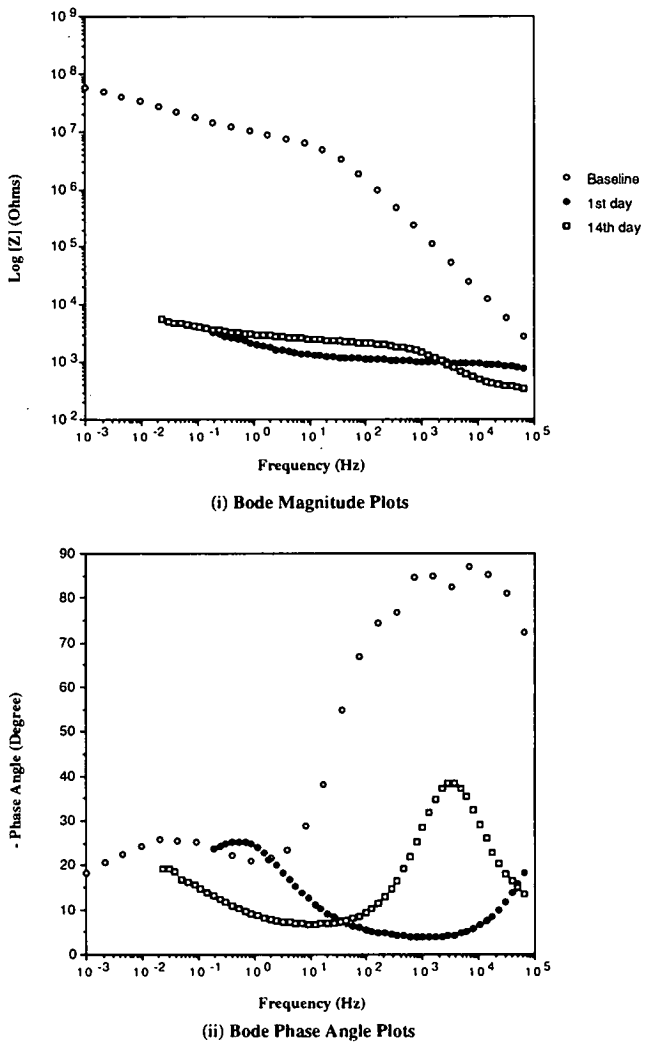

Figure H-28. (b) Bode plots for specimen 4FUCN2 preweathered (uncovered) at inland site for 4 months and tested in aqueous 3.5 w/o NaCl solution at 80°C.

EIS scans were performed on 72 ECRs embedded in 32 concrete test slabs at 0, 4, 6, and 8 months of exposure to various wet-dry cycles. Of the 72 ECRs examined after 4 months, 54 showed an overall reduction in impedance and the existence of a second-time constant. The remaining ECRs showed a slight to moderate impedance increase. This latter observation is not well understood at this time; however, some possibilities include a build-up of corrosion products that blocked active corrosion sites or deactivation of corrosion sites due to changes in the local concrete environment (or both).

At 8 months of exposure, the impedance response was such that the Bode plots could be classified as corresponding to either "good," "intermediate," or "poor" coating protectiveness. Representative Bode plots for each type are shown in Figures H-53 to H-55. ECR source specimens and the frequency of occurrence (number given in parentheses) that gave the highest impedance values (that is, $|Z|$ @ 0.1 Hz > 5×10^7 Ohm·cm^2) included the following: A (7), D (5), J (4), J-UV[5] (3), N (2), N-UV (6) and U (12). ECR source specimens exhibiting intermediate impedance behavior (that is, $3 \times 10^5 < |Z| < 5 \times 17^7$ Ohm · cm^2) and their frequency of occurrence were A (8), D (14), J (13), J-UV (8), N (11), N-UV (10), T (9) and U (6). ECR source specimens that exhibited the lowest impedance values ($|Z| < 3 \times 10^5$ Ohm · cm^2) and their frequency of occurrence included the following: J-UV (1) and T (9).

A total of eight slabs were autopsied at 10 months and the extracted ECRs examined for deterioration. Specimen 30R (A-source bar) exhibited impedances greater than 5×10^7 Ohm · cm^2 and showed no signs of deterioration. Conversely, specimens 28LF (J-UV-source bar) and 56L (T-source bar) were severely corroded and had the lowest impedance values. The following extracted specimens belong to the intermediate group with regard to their impedance response: 30L (A-source bar), 49L/49R (D-source bars), 4L/4R (N-source bars), 56R (T-source bar), and 70L/70R (U-source bars). Specimens in this group exhibited some form of deterioration that ranged from a few pin-holes to moderate rusting in localized areas. For exam-

[5]Preweathered for four months.

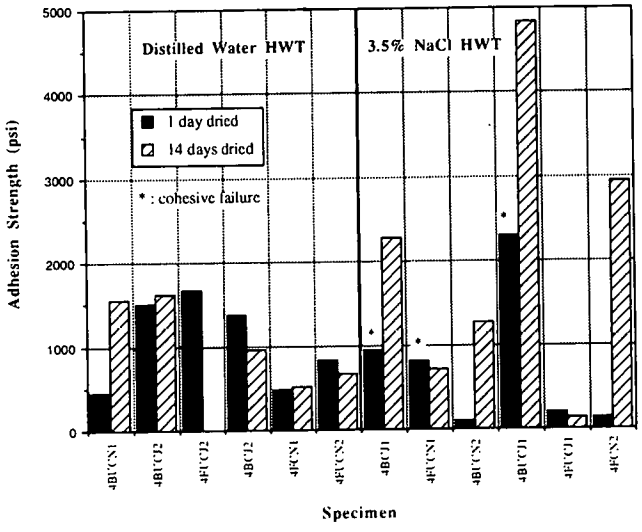

Figure H-29. Average adhesion strengths of 4-month preweathered specimens after hot water testing.

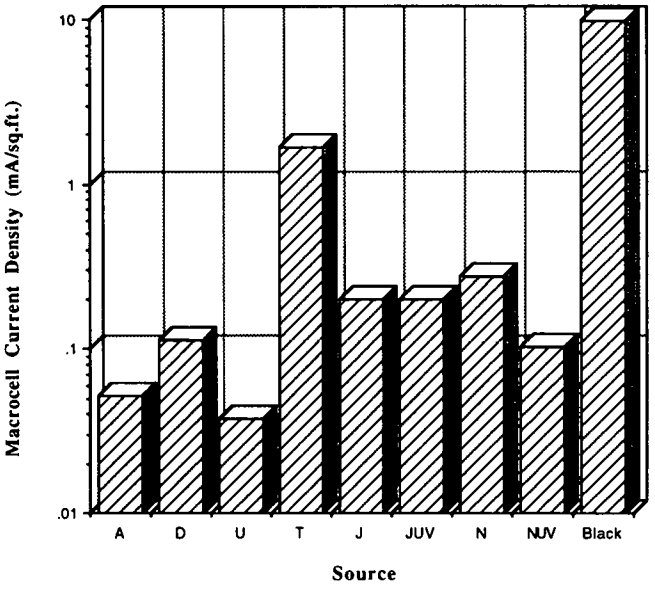

Figure H-31. Summary of initial macrocell current densities for concrete slab specimens as a function of ECR source.

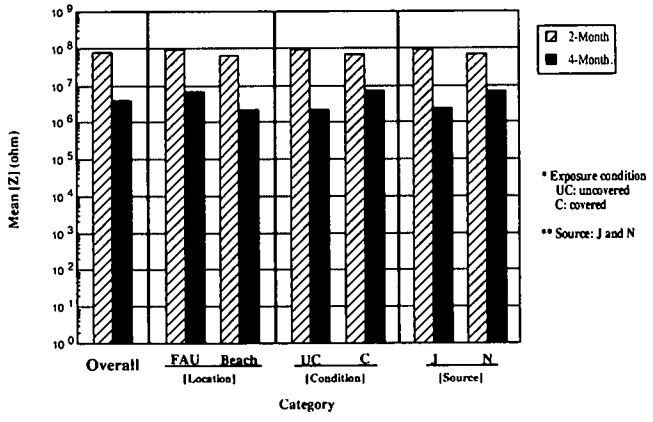

Figure H-30. Comparison of initial mean [Z] at 0.1 Hz between 2- and 4-month preweathered specimens before hot water testing.

ple, 30L (A-source bar) and 70L (U-source bar) exhibited minimal disbondment near a pin-hole and coating crack, respectively. Most ECRs, irrespective of source or exposure condition, that experienced localized coating breakdown exhibited relatively extensive disbondment. Coating adhesion loss was apparently caused by a combination of underfilm corrosion and cathodic delamination.

In general, EIS and visual observations conformed to the trends that were apparent in the accelerated testing and ambient aqueous solution exposure facets of the program. However, some differences between accelerated testing and concrete slab testing were observed. For example, blisters that formed during HWT were filled with high alkaline solutions with pH values of approximately 13; whereas, pH of the solution beneath disbonded and blistered coatings on ECR in concrete was approximately 2. Also, the observed impedances, which reflect the relative deterioration of the embedded ECRs, correlated with changes in the OCP. This is exemplified by comparison of OCPs for these same specimens as shown in Figure H-56. ECR specimen 50L (Figure H-53) exhibited one of the highest impedances, most noble (positive) OCP values and zero macrocell current after 8 months of exposure. Subsequent to the initial exposure period the OCPs for specimens 16L and 56L, where ECRs embedded in these slabs exhibited significantly lower impedance values compared to 50L, were more negative; and the respective macrocell currents after eight months were 0.16 μA and 30 μA. It is considered that general correlations are apparent between results from the different types of tests.

IN-PLANT QUALITY CONTROL TESTING

The quality of fusion bonded epoxy coatings is dependent on a number of parameters, for example, substrate cleanliness, surface profile of the rebar, epoxy powder handling, degree of coating cure, and size and density of holidays. The last of these (holidays) is regarded as *a* principal factor controlling ECR performance in salt contaminated concrete. However, each of these parameters is important both individually and interactively and can strongly influence the extent of ECR degradation. Most coating failures, with the possible exception of mechanical damage, can be attributed to the influence of one or more of these parameters on the active failure mechanism. To ensure that a sound epoxy coating is applied, it is necessary to provide strict quality control (QC) standards at all stages of fabrication, handling, storage and placement. Improving QC standards is the primary goal of efforts such as the CRSI voluntary plant certification program and of the efforts to revise and improve existing specifications (see CHAPTER 4 and APPENDIX A). Two shortcomings of present ECR technology are inadequacies associated with in-plant testing and inspection of ECRs at the jobsite after placement. Unfortunately, only a few parameters can be evaluated by on-line monitors, while several important QC tests, such

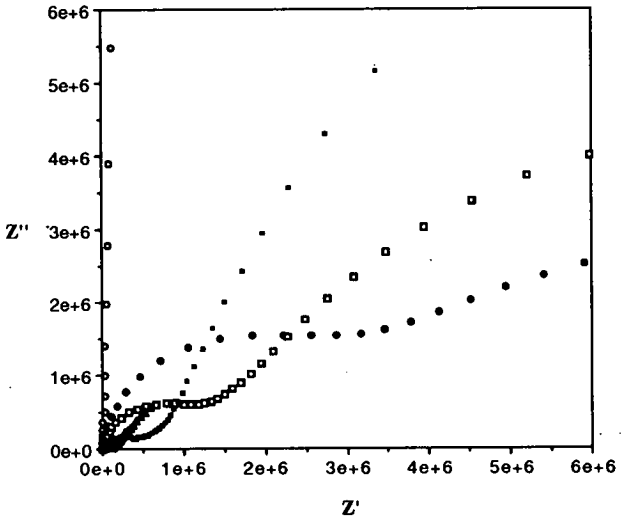

(i) Nyquist Plots

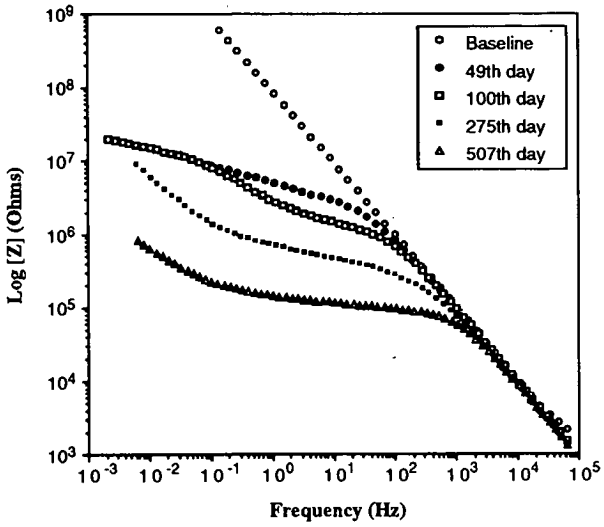

(ii) Bode Magnitude Plots

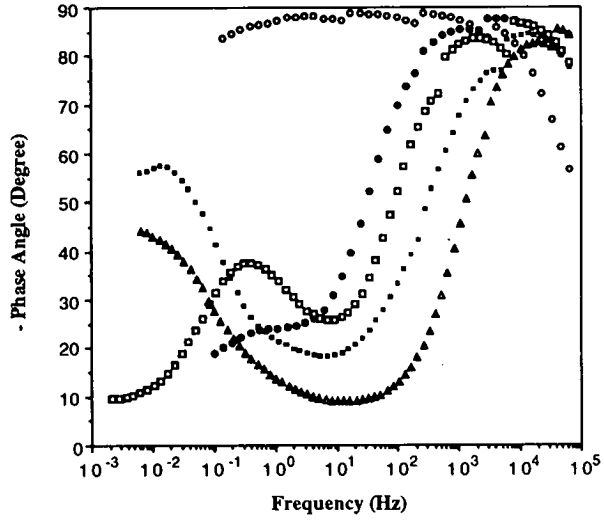

(iii) Bode Phase Angle Plots

Figure H-32. Nyquist and bode plots for J-source ECR exposed to distilled water for 500 days at room temperature.

as the proposed 24-hour HW/EIS test (see section on Utility of HW/EIS/Adhesion Test), can be conducted on coated bars before they are shipped to the job site. However, as emphasized in CHAPTERS 2 to 4, ECR failure invariably stems from underfilm corrosion; and so specified values of the above parameters are relevant only as they contribute to inhibiting this attack and if satisfactory long-term corrosion protection in salt contaminated concrete results. Thus, the key factors that must be addressed in coating and bar quality control are 1) reduction of conductive pathways through the coating and 2) coating debonding in association with corrosion at defects. It is within this context that the following discussion of the various ECR parameters must be viewed.

Coating Thickness

Measurement of coating thickness can be a useful quality control check that is readily implemented. For a coating thickness protocol to be effective it must ensure that specifications for coating thickness uniformity and minimum coating thickness are met. The major drawback with this qualification test is the inability to perform thickness measurements along the entire length of each coated bar. Thus, the effectiveness of this test relies on random sampling so that adequate statistics can be compiled above a given production run. In addition, there are differences between specifications with regard to what is an acceptable coating thickness and statistics of the thickness distri-

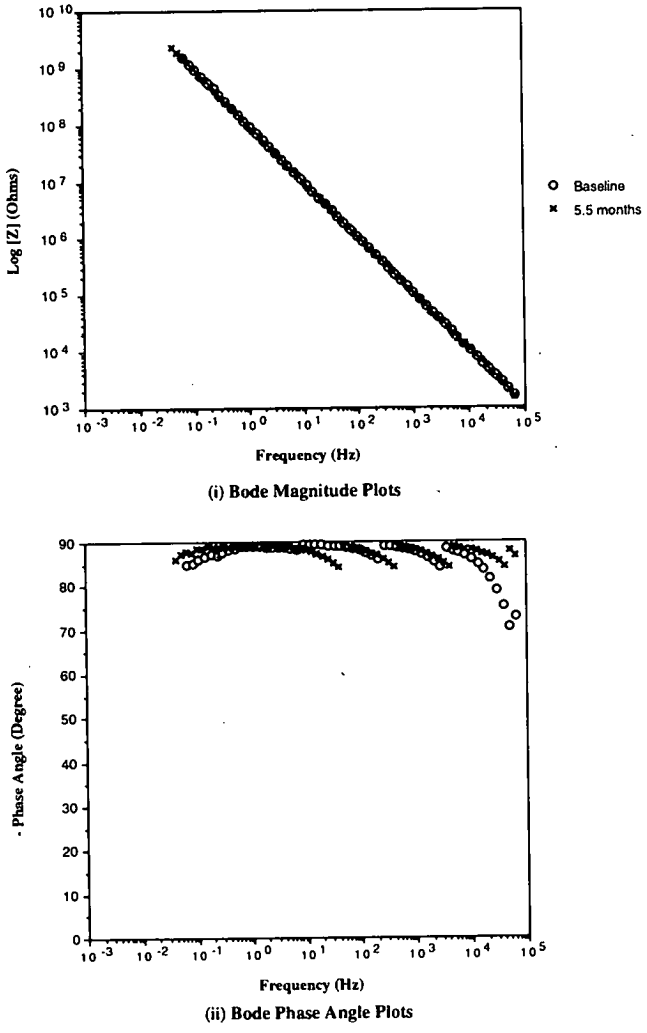

Figure H-33. Bode plots for specimen B7 exposed to aqueous 3.5 w/o NaCl solution for 5 1/2 months at room temperature.

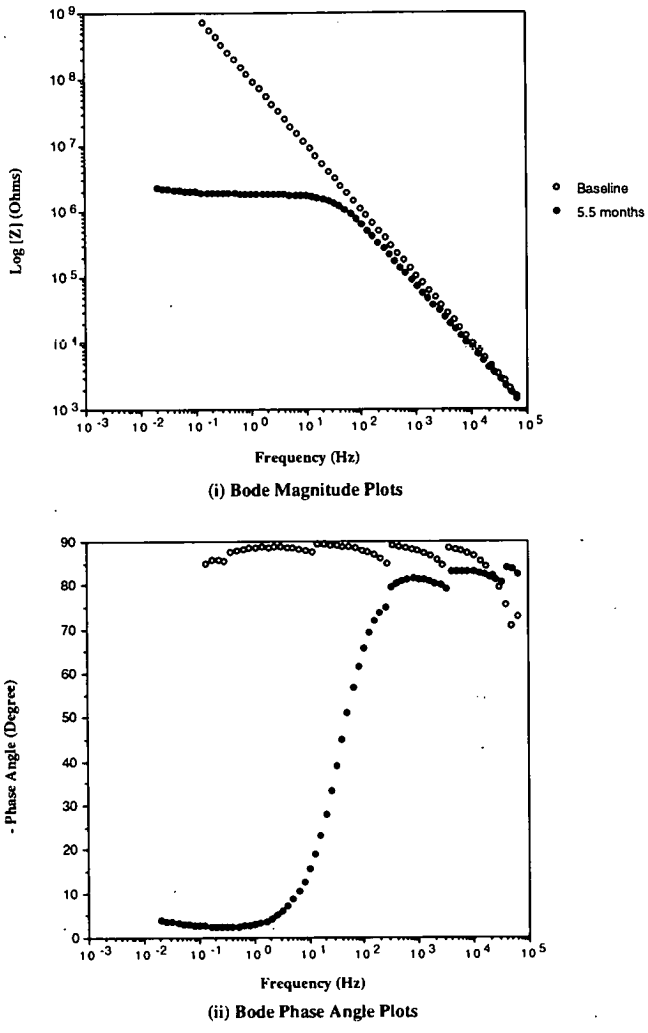

Figure H-34. Bode plots for specimen D6 exposed to simulated pore water solution (without KCl) for 5 1/2 months at room temperature.

bution. Also, no strong correlation has been established between coating thickness and performance in service. Inadequate attention has probably been focused upon the fact that coating thickness is often below specification at the base and along edges of deformations, and so these sites could be particularly susceptible to breakdown in corrosive service. One of the presently investigated foreign source ECRs had particularly uniform coating thickness, probably because these bars contained fewer deformations per bar length and the deformations had larger radii than is normally the case.

Holidays

Coating holidays are defects that can sometimes be detected using portable or on-line DC detectors, which provide an audible signal when a holiday is encountered. The procedure involves connecting the bar to one lead from a 67.5 volt tester and the other to a moist sponge or water stream. When a break in the film is encountered the circuit is completed and either an audible signal is emitted or a mechanical system marks the spot. Because bar performance is expected to vary inversely with the number and size of holidays, detection of these defects is an important QC check. Similar to the situation for coating thickness, holidays can strongly influence performance. However, ECR that has been handled and packaged for transport to job sites, unloaded and stored at job sites and, finally, placed in forms for concreting typically experiences additional mechanical damage and holiday development; and occurrence of such damage at these stages must be monitored and controlled.

Degree of Cure

Coating uniformity is controlled by the degree of cure and has been measured by use of thermal analysis techniques such as differential scanning calorimetry. At present these techniques require expensive equipment and generally cannot be employed easily in production facilities. Conversely, the solvent extraction technique (see section on Degree of Coating Cure in the ECR

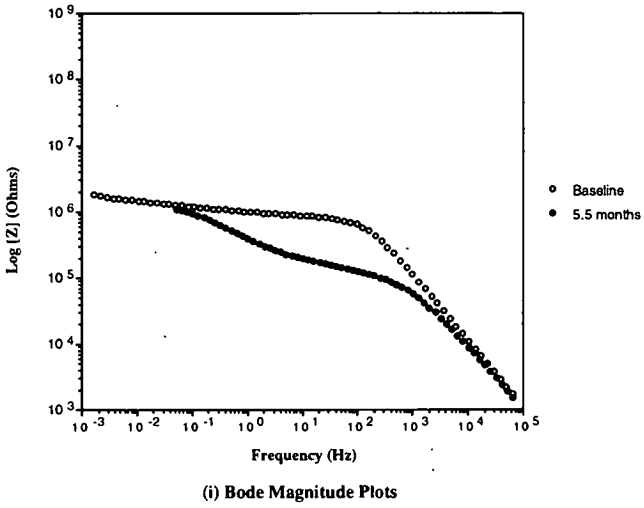

Figure H-35. Bode plots for specimen N2 exposed to simulated pore water solution (without KCl) for 5 1/2 months at room temperature (two rust spots are present).

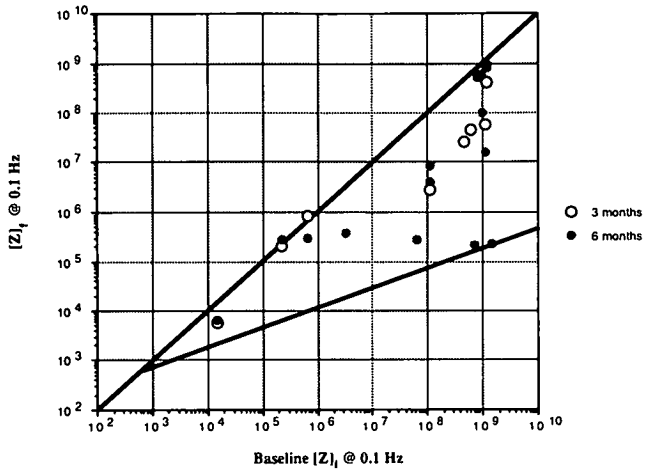

Figure H-36. Change of impedance at 0.1 Hz for all specimen sources exposed to distilled water at room temperature.

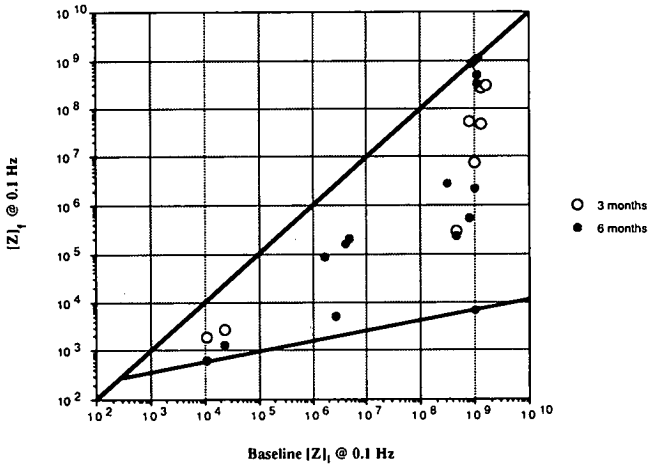

Figure H-37. Change of impedance at 0.1 Hz for all specimen sources exposed to aqueous 3.5 w/o NaCl solution at room temperature.

Specimen Characterization section of this Appendix) is an expensive, easy-to-run procedure and is potentially more reliable than thermal analysis (*2*). Unfortunately these techniques are invasive and require that a piece of the coating be removed from the bar for testing, but development of a simple QC test to determine the extent of coating cure is potentially important in light of an apparent correlation to performance (see CHAPTERS 2 and 3). The correlation of state-of-cure and ECR performance is not completely understood and additional characterization in this area is strongly recommended.

Coating Adhesion

Loss of epoxy coating adhesion has been documented and is recognized to play an important role in the progression of ECR deterioration. Although improved wet adhesion might slow the deterioration process by making the formation of local environments conducive (that is, of low pH) for accelerated underfilm corrosion more difficult, the determination of (wet) adhesion strength per se is unlikely to provide insight into the long-term performance of ECR. This is especially true in the absence of additional comprehensive research, which yields improved understanding regarding this parameter. The utility of hot water and adhesion testing was described in CHAPTERS 2 and 3; and additional discussion is provided subsequently.

Underfilm Contamination

Underfilm contamination occurs because of dust, dirt, chlorides, or blast cleaning remnants on the bar at the time of coating application. This factor can be evaluated in the plant prior to coating using special adhesive tapes, visual standards and chloride tests or on coated bars by removing a coating chip and microscopically examining the underside. Procedures for the

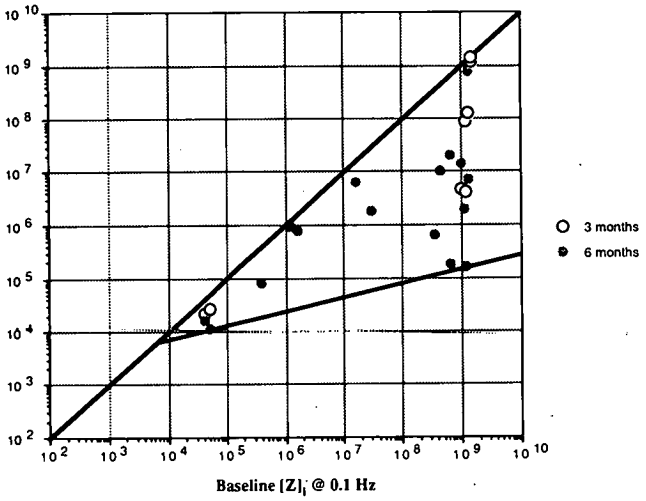

Figure H-38. Change of impedance at 0.1 Hz for all specimen sources exposed to SP solution without KCl at room temperature.

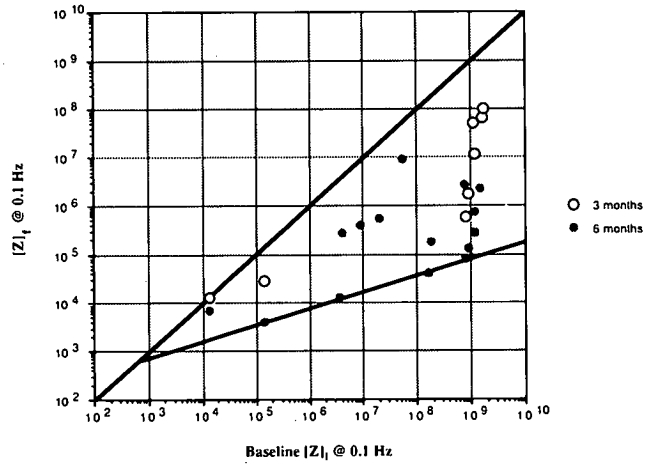

Figure H-39. Change of impedance at 0.1 Hz for all specimen sources exposed to SP solution with KCl at room temperature.

TABLE H-14. Summary of aqueous chemical immersion impedance data

Test Solution	Fraction with $[Z]_i < 10^8\ \Omega$	Fraction with $[Z]_i \gtrsim 10^9\ \Omega$	Fraction with $[Z]_f > 10^8\ \Omega$
Distilled Water	6/ 19 (0.32)	10/ 19 (0.53)	6/ 19 (0.32)
3.5 % NaCl	6/ 18 (0.33)	12/ 18 (0.67)	7/ 18 (0.39)
Simulated Pore Water	8/ 24 (0.33)	9/ 24 (0.38)	4/ 24 (0.17)
Simulated Pore Water with KCl	7/ 16 (0.44)	7/ 16 (0.44)	1/ 16 (0.06)

former are defined in the CRSI certification program (*13*) and for the latter by the C-SHRP report (*11*). Obviously, underfilm contamination is important to coating adhesion because in contaminated areas the coating will bond to the contaminants rather than to the steel substrate. Also, osmotic transport of water through the coating may be enhanced; and locally aggressive corrosion cells may be set up.

Degree of Voids

The presence of voids within the coating and particularly at the coating/metal interface provides sites where water can collect. The localization of voids at the coating/metal interface increases the chance of premature breakdown because these may serve as corrosion initiation sites or lead to poor wet adhesion, or both. Alternatively, the time required for sufficient water and reactants to collect at this interface may decrease in the presence of voids. As noted in APPENDIX A, however, ECR within marine concrete test piles exposed by the Florida DOT exhibited no signs of coating deterioration or corrosion after 9 years, and the coating of these bars was reported to contain excessive foam. Hence, some aspect(s) of foam may interrelate to other factors which can enhance performance. Unfortunately, no technique other than the percent foam determination is presently available to accurately measure the concentration of voids in a coating. Hence, it is unlikely that such a technique will be available for on-line in-plant use in the near future. Development of a new technique would require a major research effort. Although the number and size of voids in a coating may strongly influence coating performance, characterization outside of a laboratory setting is impractical.

Oxygen, Water, and Ionic Permeabilities

Although the permeability rates of oxygen, water, and ionic species through a coating are important factors with respect to degradation, they are inherently difficult to quantify and vary considerably based on the environment and quality of the concrete. Even more difficult is measuring these properties on attached coatings outside of a laboratory setting. All protective organic coatings used commercially will permit the transport of these species; and it is well recognized that if the access of moisture, oxygen, and ionic species to a metal could be eliminated, then corrosion would be inhibited. There is, however, no real prospect to accomplish this through the use of a protective organic coatings alone. Although controlling the environment, including the quality of the concrete, is possible so that rates at which moisture, chlorides and oxygen reach the ECR are retarded, in the absence of this control ECR performance is likely to be dominated by the size and number of coating defects. Hence, measuring the transport rate of these species through attached epoxy coatings provides no practical information about coating quality in terms of long-term performance, unless perhaps defect-free coatings can be employed. It is desirable, however, to ensure proper coating application so that the permeability of corrosion and debonding facilitating reactants through the coating itself is low, because in the presence of underfilm contamination and coating defects the resulting ECR is unlikely to perform satisfactorily in long-term, salt contaminated concrete

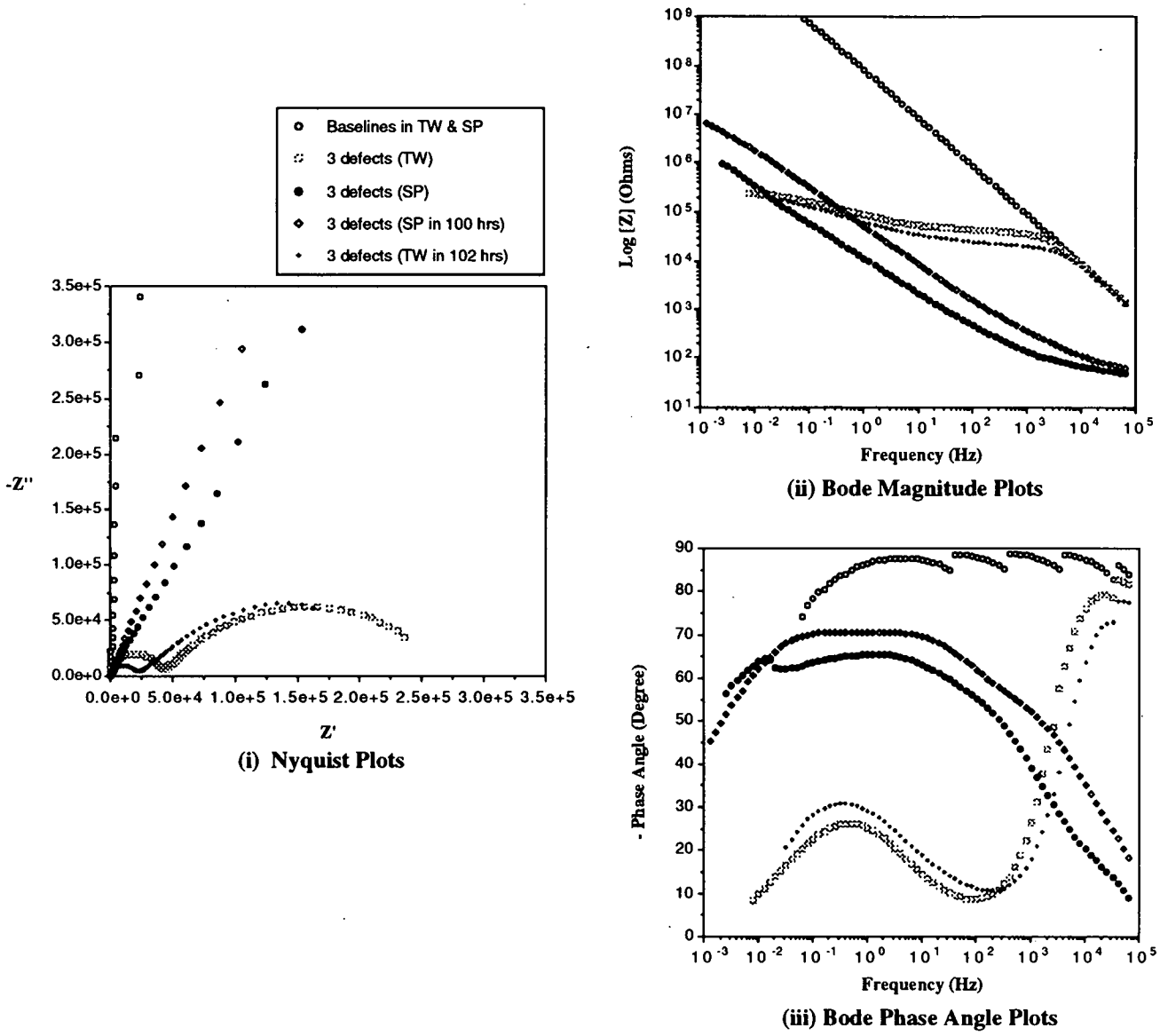

Figure H-40. Nyquist and bode plots as a function of test environment for an ECR specimen with intentional defects. Initial baseline data is for a specimen exposed to tap water. Specimen was then exposed to simulated pore water solution (without KCl) with subsequent EIS scans conducted in both environments at various time.

service. As such, low oxygen, water, and ionic permeabilities are necessary, but not sufficient, coating attributes.

Moisture Content

Moisture content of a coating, particularly the amount of water located at the coating/metal interface, is important in establishing a pathway for corrodents through the coating and in the development of a local environment beneath the coating that supports corrosion activity. The measurement of moisture content can be accomplished either gravimetrically or by EIS. Each of these is relatively easy to employ at in-plant settings; however, data at ambient exposure can only be obtained after weeks or months of sample exposure to an aqueous environment. As noted above, it is the moisture content at the coating/metal interface that is the most important factor. In this regard, hot water exposure combined with EIS may have special utility because the former accelerates water uptake by the coating and the latter can identify electrochemical activity at the metal/coating interface.

Cathodic and Anodic Delamination

Cathodic and anodic delamination are accepted mechanisms of organic coating failure and may play an important role in ECR failures. The ACT (Accelerated Corrosion Test) used by KCC INC (*14*) and the Resistance to Applied Voltage test in the ASTM (*15*) and AASHTO (*16*) ECR specification annex

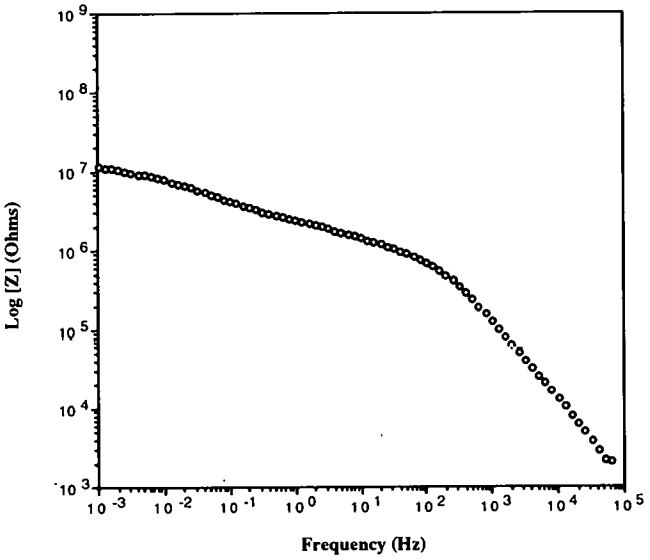

(i) Bode Magnitude Plot

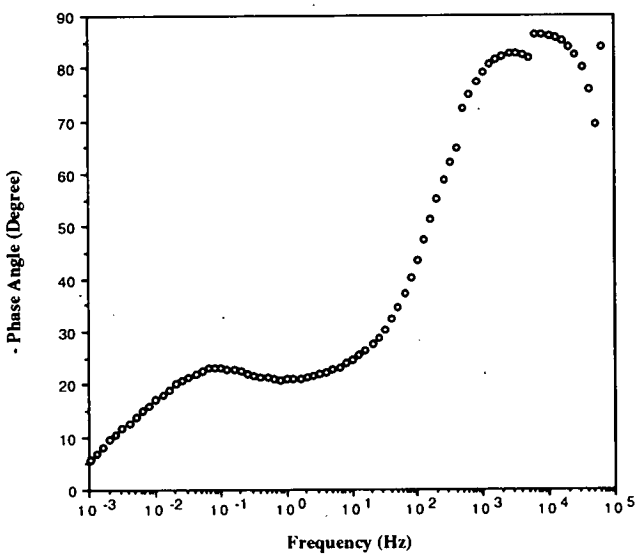

(ii) Bode Phase Angle Plot

Figure H-41. (a) Initial EIS scan for A15 before ACT.

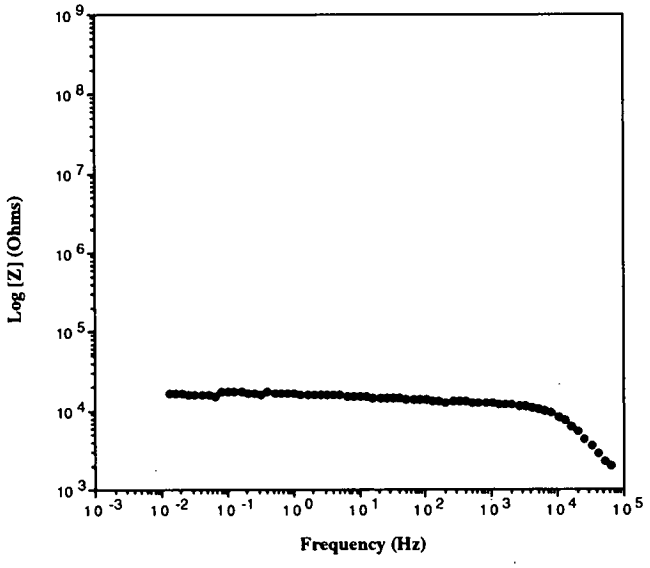

(i) Bode Magnitude Plot

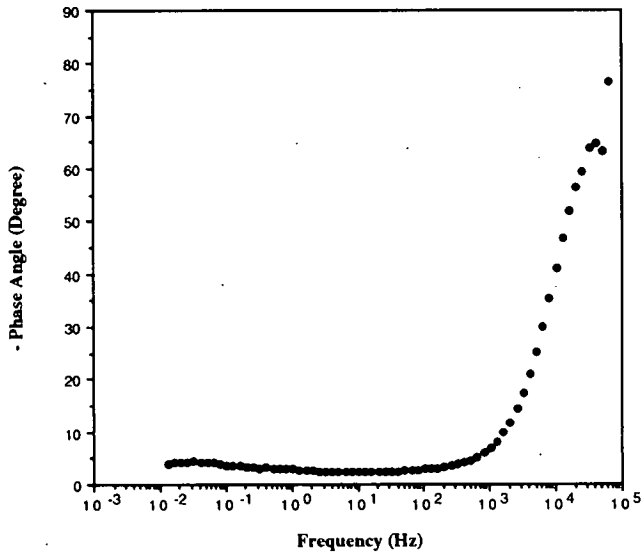

(ii) Bode Phase Angle Plot

Figure H-41. (b) EIS scan of A15 after 14-day ACT.

use two ECRs and define the influence of both cathodic and anodic disbondment. However, use of these or similar tests as an in-plant screening technique to predict long-term performance is not well established. Although determination of cathodic and anodic delamination tendency may be worthwhile, meaningful tests may take several weeks to months to complete. Consequently, the usefulness of these parameters as a QC check is limited. In addition, the present research team is unaware of data that correlate short-term cathodic and anodic delamination test results with long-term coating performance. Although this test is common to the ECR industry, it appears to be inappropriate because failures caused by the ACT are not representative of in-service behavior. In this regard the ACT can only provide data upon which a qualitative comparison can be made between ECR specimens, but the results do not permit prediction of future performance (see CHAPTER 2). It may be that some combination of short-term cathodic delamination and hot-water immersion tests will provide the necessary characterization. This should be the subject of further investigation.

Utility of HWT/EIS/Adhesion

One of the goals of this research was to develop a more reliable, easy to implement and interpret quality control (QC) testing for in-plant use. The German hot water test in its present format requires a lengthy immersion time and this aspect invalidates its use as a practical in-plant QC procedure. Because the

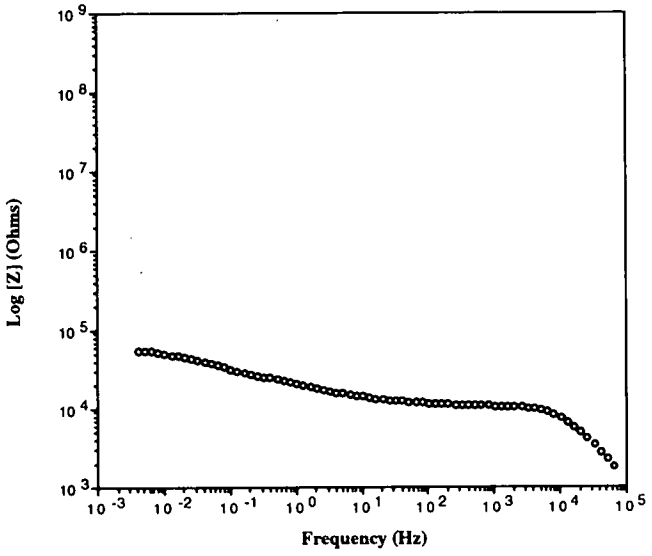

(i) Bode Magnitude Plot

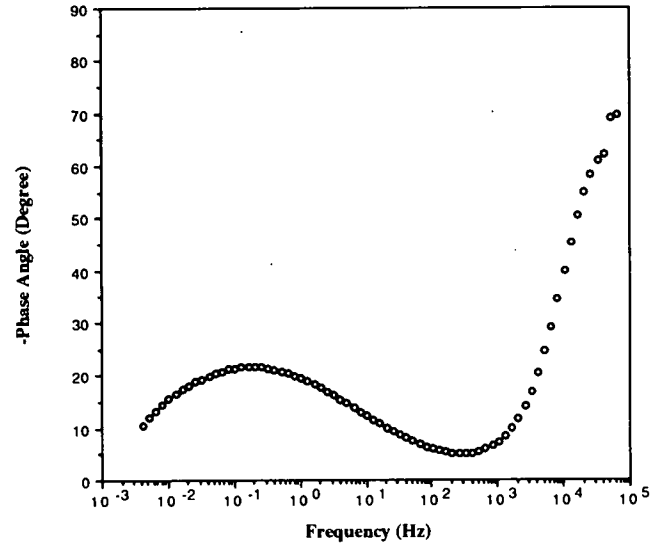

(ii) Bode Phase Angle Plot

Figure H-42. (a) Initial EIS scan of B14 before ACT.

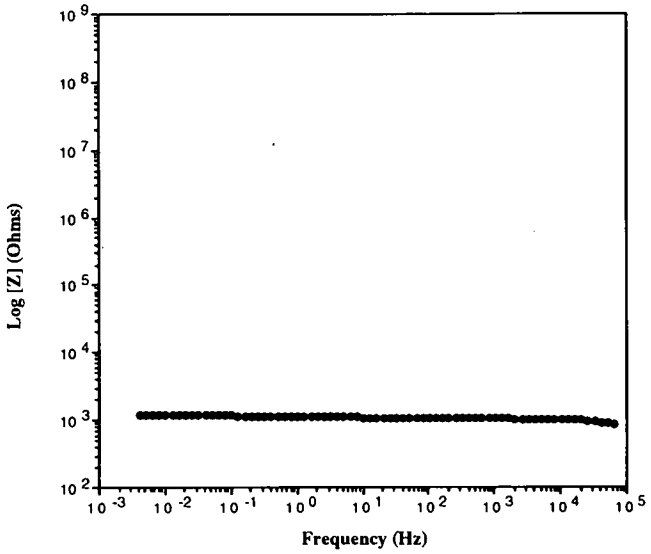

(i) Bode Magnitude Plot

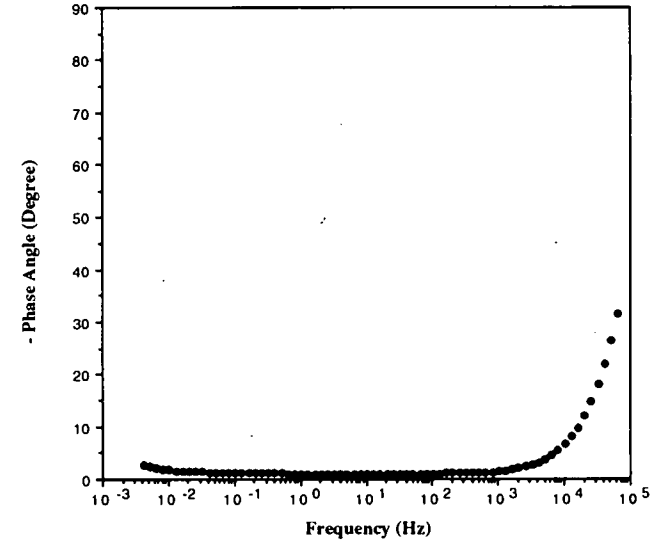

(ii) Bode Phase Angle Plot

Figure H-42. (b) EIS scan of B14 after 14-day ACT.

most significant change in impedance response occurs within 24 hours after ECR immersion in hot distilled water or aqueous 3.5 w/o NaCl solution, it appears likely that a hot water soak that incorporates impedance measurements can provide useful information in a single day. Other evidence suggests that more discriminating EIS measurements result when aqueous NaCl solutions are used. Under ideal circumstances, accelerated testing increases the rate of a reaction but does not alter the basic mechanisms when compared to ambient conditions. It is recognized that temperatures above the T_g will change the properties of the epoxy coating; hence, an accelerated test must be conducted 10°C or more below this temperature. The testing temperature chosen in this work was 80°C, which was at least 20–30°C below the T_g of these fusion bonded epoxy coatings based on limited differential scanning calorimetry measurements. In sufficient numbers or size, defects dominate the impedance response of a coated metal; and, therefore, the utility of EIS as an integral component in a QC test is limited to defect-free ECR specimens. It is under the latter situation that EIS is best able to discriminate a "good" from a "bad" coating in the short term. This was demonstrated by the copious EIS data collected on ECR specimens exposed to elevated aqueous environments (see section on Elevated Temperature immersion in this APPENDIX).

In addition to running periodic EIS scans on ECRs exposed to the elevated temperature environments, post immersion adhesion tests were conducted. Although adhesion loss plays an important role in the mechanism of epoxy coating failures in concrete, adhesion measurement assumes a lesser role compared to EIS

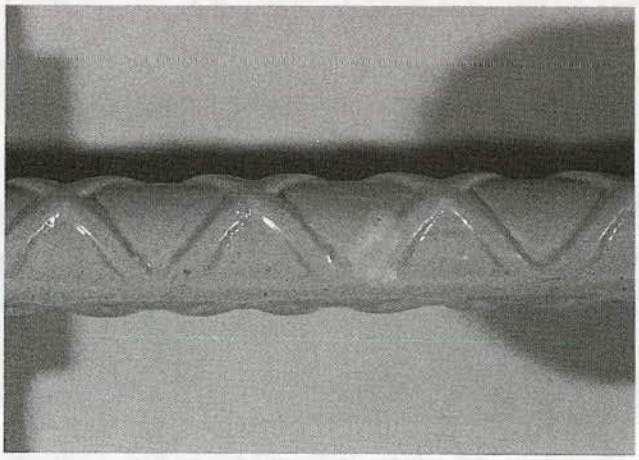

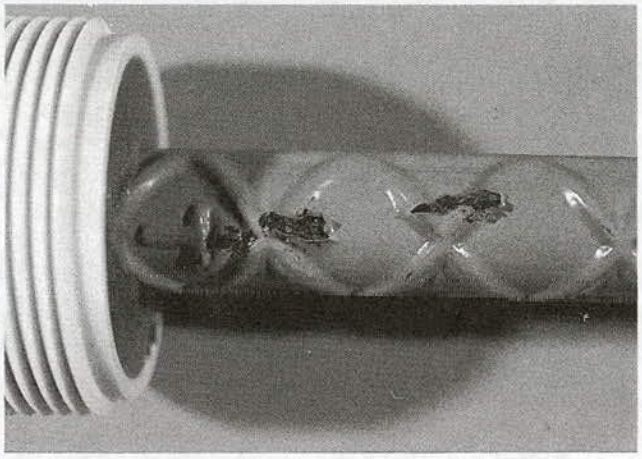

Figure H-43. (Top) Photograph of A15 after ACT. (Bottom) Photograph of B14 after ACT.

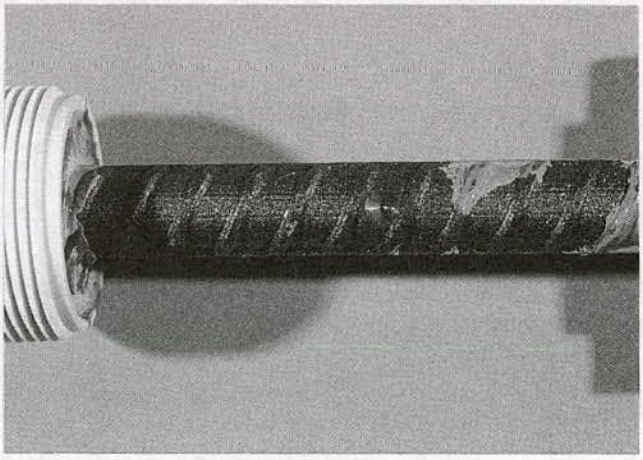

Figure H-45. Photograph of T18 after ACT.

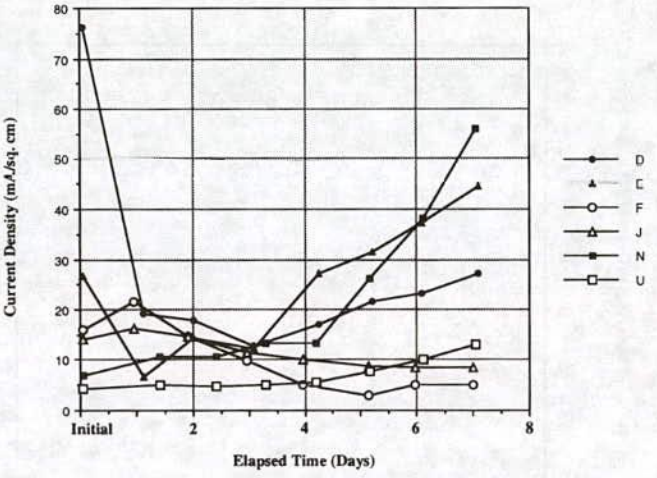

Figure H-46. Results of ACT with ECRs containing same size defects.

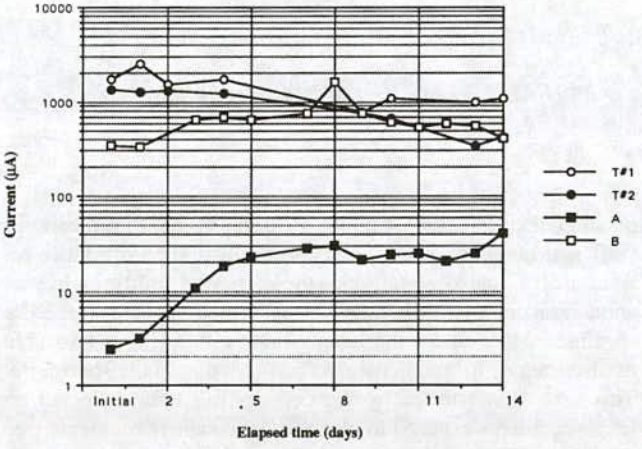

Figure H-44. Results of preliminary ACTs for three defect-containing ECR source bars.

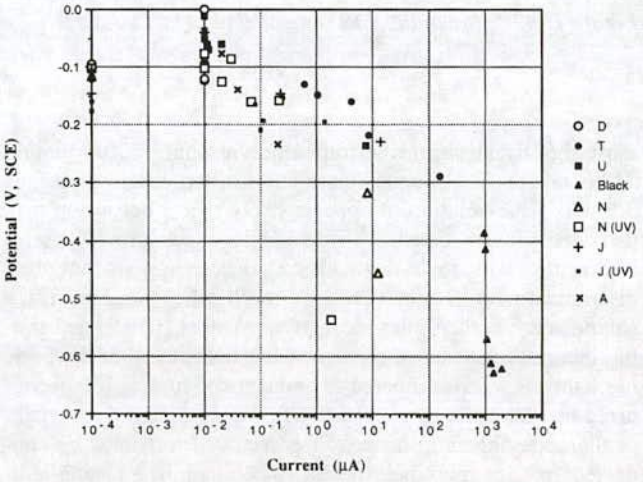

Figure H-47. Potential versus current of uncoupled condition ('A' Exposure).

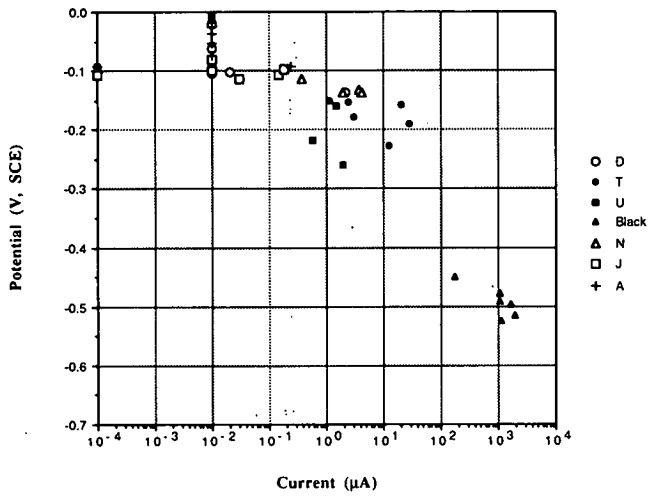

Figure H-48. Potential versus current of uncoupled condition ('B' Exposure).

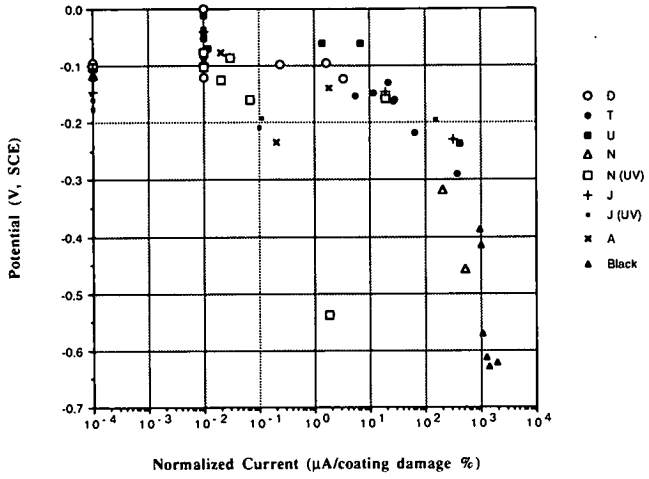

Figure H-50. Normalized current versus potential of uncoupled condition ('A' Exposure).

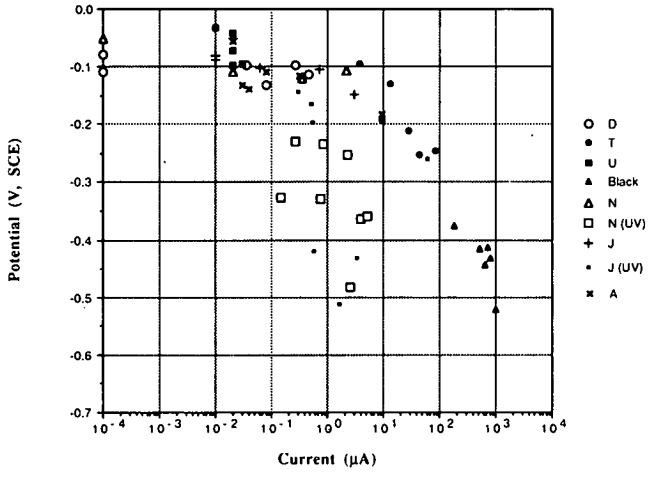

Figure H-49. Potential versus current of uncoupled condition ('D' Exposure).

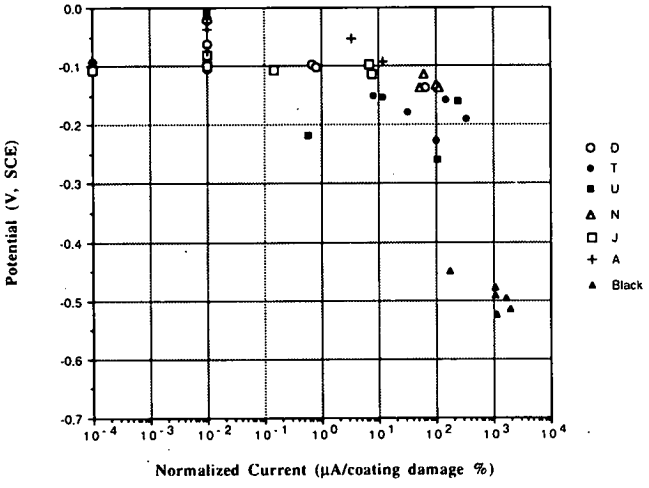

Figure H-51. Normalized current versus potential of uncoupled condition ('B' Exposure).

in distinguishing between "good" and "bad" ECRs. There is a fundamental lack of knowledge on what constitutes a minimum standard of adhesion after environmental exposure and how this correlates to long-term performance. In addition, the present work indicates that only a moderate correlation exists between adhesion and the electrochemical behavior as characterized by EIS. Therefore, unless a correlation between adhesion strength and performance can be established, it should not be considered for inclusion in a QC protocol, particularly in view of the fact that single frequency impedance measurements, as discussed subsequently, are relatively simple and expedient compared to adhesion measurements.

The EIS technique as employed in this research would be problematic with regard to in-plant use. The equipment is expensive, and a broad frequency scan would require a minimum of several hours to run. It would be desirable to develop a user friendly system that employs a single frequency measurement similar to that pioneered by Bacon, Smith and Rugg (*3*). Although single frequency measurements cannot provide details about electrochemical mechanisms or insight into the selection of an equivalent circuit analog, they can be used as a method for making comparisons amongst a number of coated metal specimens having different characteristics. A single frequency must be empirically correlated with other techniques such as gravimetric moisture absorption measurements or visual observations in order to gain mechanistic information on protective coating deterioration. Precedence in the form of an ASTM standard (*17*) has been established for use of a single frequency test for evaluating the quality of sealing porous, anodized aluminum films. More recently, Walter (*18*) examined the utility of using a single frequency impedance measurement to monitor the performance of painted metals and concluded, based on comparisons with wide frequency measurements, that a single frequency impedance measurement can be used to monitor protective coat-

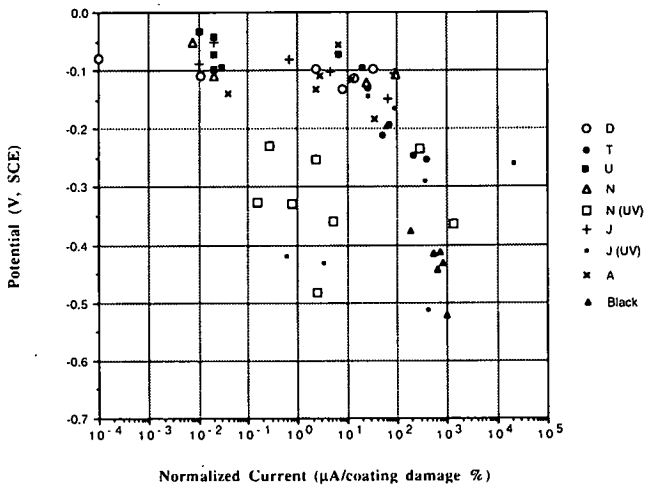

Figure H-52. Normalized current versus potential of uncoupled condition ('D' Exposure).

ing degradation. In addition to Walter's work, Mansfeld and Kendig (*19*) used a damage function, defined as

$$D = \log \left\{ \frac{Z_o}{Z_t} \right\}_{.0.1\text{Hz}} \qquad [1]$$

where Z_o is the initial impedance and Z_t is the impedance at a specific time of exposure (both impedance values being obtained at 0.1 Hz), in order to evaluate the corrosion resistance of anodized aluminum coatings. The data in Figures H-8 and H-9 and Tables H-4 and H-5 indicate that the impedance changes that occurred at 0.1 Hz upon HWT exposure were appropriate as well for the present evaluation. A plot of the damage function, *D*, as defined by equation [1], against time of exposure to either distilled water or aqueous 3.5 w/o NaCl at 80°C for the various defect-free ECRs is given in Figure H-57. In most cases, *D* increased with time as would be anticipated for specimen impedance values that decrease with exposure. Conversely, several specimens exhibited a decrease in *D* with time which reflected impedances that increase with exposure. Specimens that were judged to afford good protection exhibited low *D* values and small changes in *D* over the duration of the test. The applicability of using such a damage function to rank coated specimens would require establishing a valid threshold value that could serve as a pass/fail criterion.

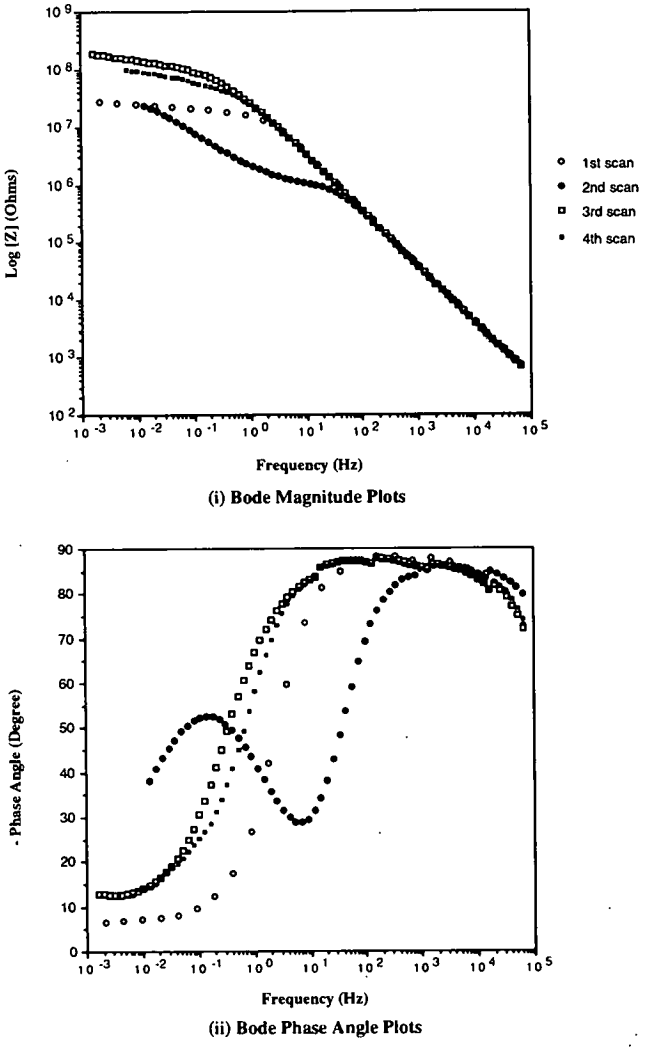

Figure H-53. Bode plots for slab specimen 50L (D Source) exhibiting high overall impedances during 8 months of exposure.

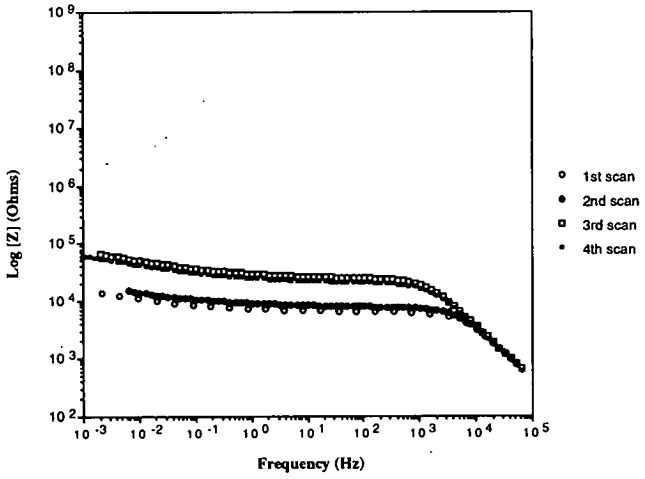

(i) Bode Magnitude Plots

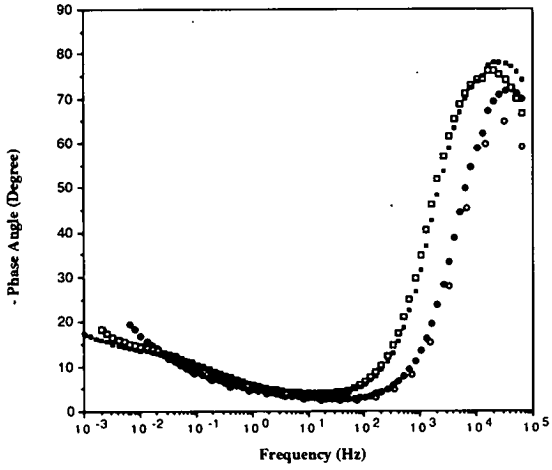

(ii) Bode Phase Angle Plots

Figure H-54. Bode plots for slab specimen 16L (J Source) exhibiting intermediate impedances during 8 months of exposure.

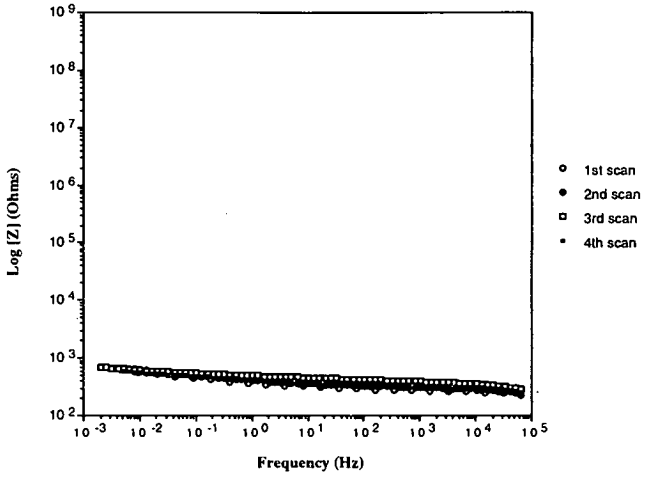

(i) Bode Magnitude Plots

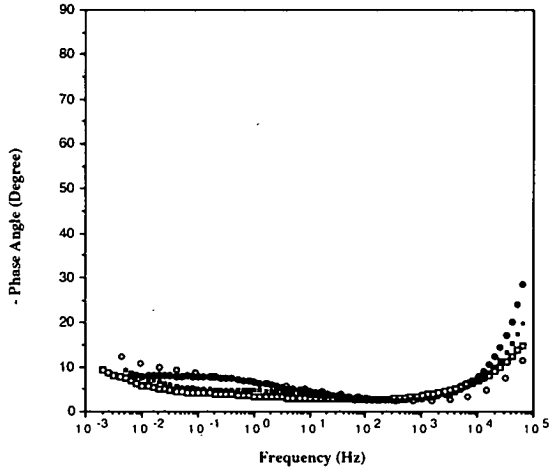

(ii) Bode Phase Angle Plots

Figure H-55. Bode plots for slab specimen 56L (T Source) exhibiting low overall impedances during 8 months of exposure.

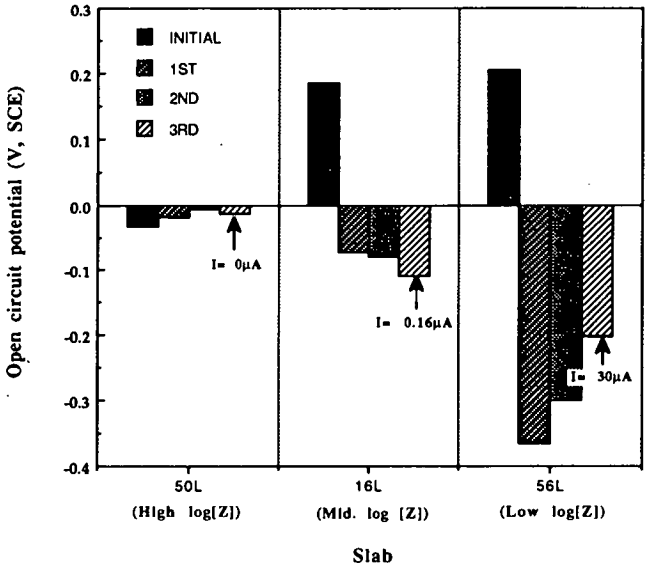

Figure H-56. OCP values for ECR specimens 50L, 16L and 56L at time of EIS scans (also included are macro-cell current values).

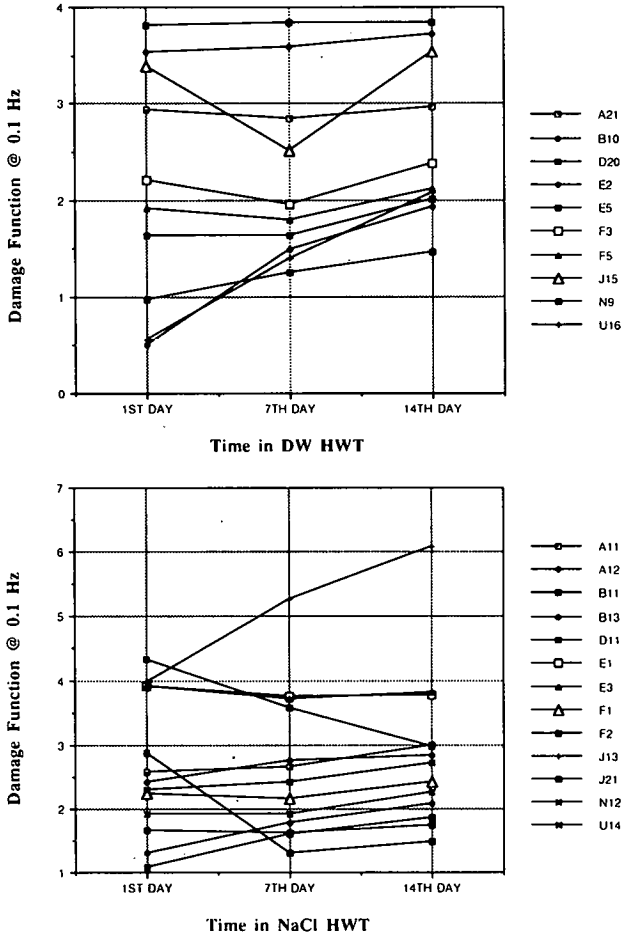

Figure H-57. (a) Change of damage function for defect-free ECRs in DW HWT. (b) Change of damage function for defect-free ECRs in NaCl HWT.

BIBLIOGRAPHY

1. AMERICAN SOCIETY OF TESTING MATERIALS, *ASTM A775/A775M-86* and *D3963,* Philadelphia PA.
2. NEAL, D., "Fusion-Bonded Epoxy Coatings — Cure and Glass Transition Temperatures," *MP* 32(2), 49 (1993).
3. BACON, R.C., SMITH, J.J., AND RUGG, F.M., *Ind. Eng. Chem.* 40(1), 161 (1948).
4. LEIDHEISER, JR., H., "Electrical and Electrochemical Measurements as Predictors of Corrosion at Metal-Organic Interface," *Corrosion Control by Coatings,* ed. H. Leidheiser, Science Press, Princeton, NJ (1978), p. 143.
5. SCULLY, J.R., *J. Electrochem. Soc.* 136(4), 979 (1989).
6. LEIDHEISER, JR., H., *J. Adhesion Sci. Tech.* 11(1), 79 (1987).
7. CLEAR, K., "Effectiveness of Epoxy-Coated Reinforcing Steel," Final Report, Concrete Reinforcing Steel Institute, Schaumberg, IL (by K.C. Clear, Inc.) (Dec. 1991).
8. SAGUES, A., "Mechanism of Corrosion of Epoxy-Coated Reinforcing Steel in Concrete," *Report No. FL/DOT/RMC/0543-3296,* Florida Department of Transportation, Gainesville, FL (April 1991).
9. FUNKE, W., "Blistering of Paint Films," *Corrosion Control by Organic Coatings,* ed. H. Leidheiser, Jr., NACE International, Houston, TX (1981).
10. LEIDHEISER, H., JR. and FUNKE, W. *J. Oil Colour Chem. Assoc.* 70(5), 121 (1987).
11. CLEAR, K.C., "Effectiveness of Epoxy-Coated Reinforcing Steel," Final C-SHRP Report (Oct. 1992).
12. LEIDHEISER, H., JR., *Corrosion* 38(7), 374 (1982).
13. "Concrete Reinforcing Steel Institute Certification Program," T.L. Neff, P.E. Administrator, (June 1991).
14. CLEAR, K.C., "Effectiveness of Epoxy Coated Reinforcing Steel," Final Report, Canadian Strategic Highway Research Program, Ottawa, Canada (Oct. 1992).
15. AMERICAN SOCIETY FOR TESTING MATERIALS, Standard Specification for "Epoxy-Coated Reinforcing Steel Bars," *ASTM A775M-86,* ASTM Annual Book of Standards, Philadelphia, PA.
16. Standard Specification M284-86 for Epoxy Coated Reinforcing Bars, American Association of State Highway and Transportation Officials, Washington, D.C. (1986).
17. Standard Specification for "Measurement of Impedance of Anodic Coatings on Aluminum," ASTM B547-80, ASTM Annual Book of Standards, American Society for Testing and Materials, Philadelphia, PA.
18. WALTER, G.W., *Corr. Sci.* 30(6/7), 617 (1990).
19. MANSFELD, F. and KENDIG, M., *Corrosion,* 41(8), 490 (1985).

THE TRANSPORTATION RESEARCH BOARD is a unit of the National Research Council, which serves the National Academy of Sciences and the National Academy of Engineering. It evolved in 1974 from the Highway Research Board which was established in 1920. The TRB incorporates all former HRB activities and also performs additional functions under a broader scope involving all modes of transportation and the interactions of transportation with society. The Board's purpose is to stimulate research concerning the nature and performance of transportation systems, to disseminate information that the research produces, and to encourage the application of appropriate research findings. The Board's program is carried out by more than 270 committees, task forces, and panels composed of more than 3,300 administrators, engineers, social scientists, attorneys, educators, and others concerned with transportation; they serve without compensation. The program is supported by state transportation and highway departments, the modal administrations of the U.S. Department of Transportation, the Association of American Railroads, the National Highway Traffic Safety Administration, and other organizations and individuals interested in the development of transportation.

The National Academy of Sciences is a private, nonprofit, self-perpetuating society of distinguished scholars engaged in scientific and engineering research, dedicated to the furtherance of science and technology and to their use for the general welfare. Upon the authority of the charter granted to it by the Congress in 1863, the Academy has a mandate that requires it to advise the federal government on scientific and technical matters. Dr. Bruce M. Alberts is president of the National Academy of Sciences.

The National Academy of Engineering was established in 1964, under the charter of the National Academy of Sciences, as a parallel organization of outstanding engineers. It is autonomous in its administration and in the selection of its members, sharing with the National Academy of Sciences the responsibility for advising the federal government. The National Academy of Engineering also sponsors engineering programs aimed at meeting national needs, encourages education and research and recognizes the superior achievements of engineers. Dr. Robert M. White is president of the National Academy of Engineering.

The Institute of Medicine was established in 1970 by the National Academy of Sciences to secure the services of eminent members of appropriate professions in the examination of policy matters pertaining to the health of the public. The Institute acts under the responsibility given to the National Academy of Sciences by its congressional charter to be an adviser to the federal government and, upon its own initiative, to identify issues of medical care, research, and education. Dr. Kenneth I. Shine is president of the Institute of Medicine.

The National Research Council was organized by the National Academy of Sciences in 1916 to associate the broad community of science and technology with the Academy's purpose of furthering knowledge and advising the federal government. Functioning in accordance with general policies determined by the Academy, the Council has become the principal operating agency of both the National Academy of Sciences and the National Academy of Engineering in providing services to the government, the public, and the scientific and engineering communities. The Council is administered jointly by both Academies and the Institute of Medicine. Dr. Bruce M. Alberts and Dr. Robert M. White are chairman and vice chairman, respectively, of the National Research Council.

Transportation Research Board
National Research Council
2101 Constitution Avenue, N.W.
Washington, D.C. 20418

ADDRESS CORRECTION REQUESTED

000021-02
Materials Engineer
Idaho DOT
P O Box 7129
Boise ID 83707-1129